R82-06

LINKED HYDRODYNAMIC AND BIOGEOCHEMICAL MODELS OF WATER QUALITY IN SHALLOW LAKES

TC171
.M41
.H99
no. 268

MIT LIBRARIES
3 9080 00314 8472

Peter Shanahan

and

Donald R.F. Harleman

RALPH M. PARSONS LABORATORY

AQUATIC SCIENCE AND ENVIRONMENTAL ENGINEERING

Report Number 268

Prepared under the support of the

National Science Foundation

Water Resources and Environmental Engineering Program

March 1982

MIT

DEPARTMENT
OF
CIVIL
ENGINEERING

SCHOOL OF ENGINEERING
MASSACHUSETTS INSTITUTE OF TECHNOLOGY
Cambridge, Massachusetts 02139

MITLibraries

77 Massachusetts Avenue
Cambridge, MA 02139
http://libraries.mit.edu/ask

DISCLAIMER NOTICE

Due to the condition of the original material, there are unavoidable flaws in this reproduction. We have made every effort possible to provide you with the best copy available.

Thank you.

Some pages in the original document contain text that is illegible.

R82-06

LINKED HYDRODYNAMIC AND BIOGEOCHEMICAL MODELS OF WATER QUALITY IN SHALLOW LAKES

by

Peter Shanahan

and

Donald R.F. Harleman

RALPH M. PARSONS LABORATORY

AQUATIC SCIENCE AND ENVIRONMENTAL ENGINEERING

Report Number 268

Prepared under the support of the

National Science Foundation

Water Resources and Environmental Engineering Program

March 1982

M.I.T. LIBRARIES
JUL 2 7 1982
RECEIVED

ABSTRACT

Approaches to lake water quality modeling are critically examined with particular attention to the formulation of water quality transport as the link between hydrodynamics and biogeochemical reaction. A linked water quality model for shallow lakes includes three major components: a biogeochemical reaction component, a lake hydrodynamics component and a water quality transport component. State-of-the-art modeling approaches for each component are reviewed, and a synopsis of phosphorus dynamics in shallow lakes is given. For the water quality transport component, review of the literature shows two significantly different approaches to water transport: a lumped component approach based upon multiple fully-mixed boxes, and a continuum approach employing the finite difference method to approximate the continuous governing equations. The multiple-box model is shown in an analysis of the kindred fully-mixed tanks-in-series conceptual reactor model to create an excessive implicit dispersion due to its formulation. This leads to a model in which the model mass transport is not closely related to the properties of the physical system being modeled. Rather, dispersive transport in the model is shown to depend heavily upon the model formulation -- the model transport parameters thus cannot be specified from hydrodynamic data but must be found by calibration. In direct contrast, the finite difference model maintains a far closer approximation to the physical system and permits direct specification of water quality transport from the actual lake hydrodynamics.

To support these arguments, a computer program incorporating both a multiple-box model and an alternative one-dimensional finite difference model is developed and applied to Lake Balaton in Hungary. The biogeochemical component of both models is a four component phosphorus-phytoplankton interaction model originally proposed by van Straten (1980). Hydrodynamic information is supplied to the one-dimensional finite difference model by linkage to a transient two-dimensional single-layer model of wind-driven circulation. A one-dimensional dispersion coefficient is computed from the two-dimensional velocity field using a method based upon that of Fischer (1966, 1969) and Holley, Harleman and Fischer (1970), but proceeding from the assumption that advection rather than turbulent diffusion dominates lateral mixing. The finite difference model developed for Lake Balaton consists of forty grids and is used to simulate a representative period from early spring to late summer. The results are contrasted with those produced by a four-box model of the lake using long-term average advection and calibrated dispersive exchange flows. The finite difference model is found to lead to a predicted behavior more similar to that observed in field data collected from Lake Balaton. Experimentation with the models is conducted to examine the behavior of the lake and the dominant factors leading to that behavior.

C741223

ACKNOWLEDGEMENTS

Support for this study was provided by the United States National Science Foundation under Grant Number CEE-7906125. In addition, the International Institute of Applied Systems Analysis (IIASA) of Laxenburg, Austria supplied living expenses and financial support for Peter Shanahan during a two-month residence at IIASA.

Dr. László Somlyódy, the leader of the Lake Balaton Case Study at IIASA, supplied most of the data employed in the model application to Lake Balaton and furnished countless helpful suggestions and insights. Prof. K. D. Stolzenbach, Dr. E. Eric Adams, Prof. Harry H. Hemond, Prof. Ole S. Madsen, Prof. Frank E. Perkins, and Dr. Ming-Pin Wang supplied advice and suggestions during the course of the research and in reviewing drafts of this report.

This text was prepared using the IBM Document Composition Facility installed on the MIT Information Processing Center IBM 370/168 computer and IBM 6670 laser printer. Ms. Suzanne Shanahan entered the text and typed the figures and tables with care and precision. She and Ms. Carole Soloman typed the equations into the text, and Ms. Soloman aided in preparing and publishing the technical report. Ms. Patricia Dixon assisted in the administration of the research project and in numerous other ways. All computations and computer graphics were done with the MIT Information Processing Center IBM 370/168.

TABLE OF CONTENTS

LIST OF TABLES

LIST OF FIGURES

1 INTRODUCTION

1.1 Background of the Study

The deterioration of lake water quality is being faced throughout the world. Increasing population and development, and changing agricultural practices have created pressures from which few water bodies escape. And, although society can take steps to prevent or correct water quality degradation, such actions are invariably costly and prior knowledge of their effectiveness is often impossible. The people and agencies charged with planning water quality control thus face a very difficult set of problems indeed. Not only must they develop methods and strategies to control water pollution, but they must also forecast the cost and effectiveness of these strategies to guarantee that the controls used insure the best water quality at the least expense.

Mathematical computer models of water quality have arisen in response to the needs of water pollution control planning. Clearly, society cannot afford to test expensive control strategies by trial and error; a less costly means to develop and evaluate control alternatives is required. Water quality models contribute in two ways. First, by describing the physical, biological and chemical processes affecting water quality, models increase understanding and suggest control methods. And secondly, predictive models can forecast future water quality and permit trials of possible strategies at very reasonable expense. Accurate and efficient water quality models can thus play a valuable role in the management of environmental water quality.

Here we report on a program of research to develop and apply mathematical computer models of water quality in a particular, important environment: the shallow freshwater lake. Although shallow lakes as large as our application lake, Lake Balaton in Hungary, are rare, small shallow lakes and ponds are perhaps the most common of water bodies. Relatively little attention has been paid in the past to the special problems of modeling such environments and even less attention has been directed to the particular interest of our research: the influence of hydrodynamics upon shallow lake water quality, and the proper linkage of hydrodynamic transport models with biogeochemical water quality models.

Our attention to the linkage of hydrodynamic models and biogeochemical water quality models addresses a weakness in current water quality modeling practice. This weakness arises when the modeler fails to consider the dominant length and time scales of the lake processes of interest. The complete water quality model must match these dominant scales in its representation of both hydrodynamics and biological dynamics. This is seldom done in practice. As a result, one finds highly sophisticated models of lake water quality chemistry and biology compromised by inadequate, or even inaccurate, models of water motion and mass transport. Similarly, there are models which attempt to determine hydrodynamics and mass transport with high accuracy, but then simply lump all biochemical transformations into a single first-order loss term. In this report we seek to demonstrate the necessity to consider both hydrodynamics and biochemistry in a compatible and even-handed fashion.

Our hypothesis is that the proper linkage of hydrodynamic and biogeochemical models will create a more accurate and complete picture of lake water quality dynamics.

1.2 Summary

Shallow Lake Water Quality Modeling

In Chapter 2 we briefly review water quality modeling for shallow lakes, first supplying background on the processes which govern shallow lake water quality dynamics and then reviewing a number of models typical of current practice. Our specific goal in water quality modeling is to chart the course of eutrophication and to determine water quality management schemes which can slow or reverse eutrophication.

In virtually all lakes, algal biomass, which is the most prominent manifestation of eutrophication, is limited in growth by an insufficiency of the nutrient phosphorus. Although phosphorus is found in numerous particulate and dissolved forms in water, orthophosphate is the primary form readily utilized by algae. Modeling efforts thus concentrate on the possible pathways to orthophosphate. In shallow bodies of water there is a net loss of phosphorus to the sediments, but episodic release of sedimentary orthophosphate is probably an important, though intermittent, exception. Such releases are episodic in shallow water since orthophosphate is chemically bound to the sediments under the aerobic conditions which typically prevail. On those occasions when the water overlying the sediment becomes anoxic, or when the sediments are physically disturbed, orthophosphate release can occur. Another source of utilizable phosphorus is that which enters the lake from the surrounding drainage basin. Human activity becomes an important factor here since sewage inflow and runoff from agricultural and urban areas can all be rich in utilizable phosphorus. The task of the eutrophication model is thus to trace the pathways of phosphorus from these external and internal sources to the growth of algae and eventually to the departure of phosphorus from the active biological system.

In most engineering studies, such as this one, a biogeochemical water quality model is employed. Such a model is founded on the principle of conservation of mass of the element or elements of interest. In lake eutrophication, our interest is in phosphorus and the proper formulation of its cycle in the lake environment. In Chapter 2, four alternative phosphorus biogeochemical models developed specifically for shallow lakes are presented. Differences in the models are due largely to the number of phosphorus forms included as model compartments and the consequent complexity of the mathematical formulation and parameter requirements.

We also point out in Chapter 2 that the spatial resolution of the model is an important factor, though it has been given minor attention in most previous modeling investigations. Most models have employed simple model spatial structures -- often hypothesizing the lake as a single, homogeneous tank, or at best two or a few such tanks. However, as we will show in the results of this study, the choice of the model spatial structure is a matter of considerable subtlety which greatly influences the model's ability to properly include hydrodynamic transport as an influence relative to biogeochemical processes.

In a review of spatial structure and mass transport in lake water quality models we find widely varying practices. Two different premises in model construction are identified: the finite difference model which seeks to approximate the continuous mass conservation equation, and the box model in which an integral expression of mass conservation is made for each of one or more discrete volume elements. The first is essentially a continuum approach, while the second is a lumped parameter approach.

Differences in the averaging of time and space are largely responsible for the different approaches to water quality modeling in general and to mass transport in particular. All transport models depend upon a more-or-less arbitrary separation of advection from diffusion or dispersion. The separation is effected by averaging over time and space -- the resulting mean motion is defined as advection while all residual transport becomes diffusion or dispersion. If the degree of averaging in space is over fewer than three dimensions, a finite difference model is employed. Three-dimensional averaging, either over the entire lake or over large lake segments, leads to the box model approach.

We continue our analysis of transport modeling with a review of a number of state-of-the-art lake water quality models. There is little consensus in current practice on a single "best" modeling approach -- both finite difference and multiple-box formulations are employed commonly. Most unfortunate is the failure of the literature to critically examine and contrast the different modeling approaches. Even in research programs employing both finite difference models and box models, there are no definitive comparisons or recommendations.

Our examination of model spatial structure and mass transport concludes with a theoretical analysis. The analysis concentrates on a critical review of multiple-box models, studying their properties through analytical solutions for conceptual reactor models. A comparison of the tanks-in-series reactor, as the analog of the box model, and the dispersed flow reactor, corresponding to the continuum model, indicates the representation of dispersive transport to be a weakness in the box models. Unlike the continuum models, the box models carry large implicit dispersion in their formulation. This dispersion is unrelated to the real mixing properties of the physical system and thus must be treated as an empirical model parameter, typically found by calibration. In contrast, in a well formulated continuum model, dispersion is a specified input which may be directly determined from the observed properties of the actual lake.

Lake Circulation Modeling

The discussion above has suggested the potentially major role of hydrodynamics in lake water quality, so in Chapter 3 we include a review of the state of the art in lake circulation modeling. Our goal in this review is to supply the background needed to select an appropriate hydrodynamic model component to be used in concert with a biogeochemical model of lake water quality.

The review of lake circulation modeling proceeds along three subject lines: an overview of the common modeling approaches, an examination of the limitations imposed by typical model assumptions, and a look at the important parameters to be employed as model input.

The numerous approaches to circulation modeling all seek to solve the equations of momentum and continuity in some simplified form. We may classify these models according to their temporal variation -- either transient or steady state -- and according to their spatial representation. Spatial representation falls into two broad categories: simplified models of less than two dimensions, and true circulation models of two or three dimensions. There are three major groups within this latter category: single-layer models, which assume a vertically homogeneous lake; multi-layer models, which presume the lake to be divisible in two or more essentially homogeneous layers; and, the Ekman models, which neglect certain forces and accelerations in order to partially solve the problem by analytical methods.

Simplifying assumptions and approximations are a necessary part of any circulation model, and are quite acceptable where conditions permit. A number of assumptions in wide use are examined, and we state conditions under which the assumptions are appropriate. Investigated are the shallow water assumptions, neglect of convective acceleration, neglect of horizontal shear transport, and the rigid-lid assumption. All of the approximation criteria, however, include the very important caveat that they may be inapplicable in nearshore or other local regions where bathymetry changes abruptly.

Circulation models also depend upon the selection of values and formulae for various input parameters. Particularly important parameters are the vertical eddy viscosity and the stresses at the water surface and bottom. The eddy viscosity, though it significantly impacts the velocity profiles predicted by a model, is a subject of considerable disagreement in the literature. Many representations of this parameter as a function of depth have been proposed, but there is virtually no information with which to identify a superior alternative. There is greater coherence in the literature addressing the stress produced by wind on the water surface. The formulae of Wu (1969) are found to be widely accepted, although preliminary results by some researchers indicate that these formulae may not be accurate in very shallow water. Bottom stress is represented using a greater variety of methods than surface stress, though this is due more to computational constraints than to a lack of understanding or agreement. Though it is less true for the bottom stress as a parameter than for the surface stress or vertical viscosity, we can nevertheless make the following summary observation: although the form and value of these parameters significantly affect model results, selection of parameters is made difficult by the lack of unified theory or adequate experimental data. Thus, the model results inevitably reflect the considerable uncertainty of these parameters.

Lake Balaton

Following the review of the literature of circulation modeling, the

report turns in Chapter 4 to a description of the application lake, Lake Balaton. Balaton is a large, but unusually shallow lake (3.2 meters deep, on average, and 75 kilometers long). Hydrologic flows into and out of the lake are minor compared to the dominating wind-driven flows and seiching. Wind-driven flows are influential due to the lake's shallowness, however their complexity defies a simple generalization of their dynamics. Non-uniformities in wind speed and direction, as well as the boundaries of the lake shoreline, influence horizontal flow patterns. The vertical flow profile is shown by field measurements to be non-uniform and highly transient. Superimposed upon this motion is a very prominent seiche, with both longitudinal and transverse modes as well as various secondary modes. Comprehensive field studies by Hungarian scientists over more than a decade have defined the characteristics of Lake Balaton's seiche in some detail. The shallowness of the lake significantly influences the longitudinal seiche by lengthening its period and causing it to damp out after a few cycles.

Water in Lake Balaton is generally of high quality, although elevated biomass levels and blue-green algae are creating problems in Keszthely Bay. The lake is a hardwater lake with high pH, alkalinity, calcium and magnesium. Dissolved oxygen is rarely low, as a consequence of the constant wind mixing throughout the shallow depth. A high suspended sediment concentration is also caused by the wind action.

Phosphorus is believed to be the nutrient which limits algal growth, however its behavior in the lake is not satisfactorily understood. The dominance of calcium carbonate in the lake's chemistry should lead to nearly complete removal of orthophosphate from the lake, preventing substantial algal growth. However, growth does occur and different sources and controls of orthophosphate may govern. The character and origin of possible orthophosphate sources in Lake Balaton is an area of current research and experimentation.

It is clear, nevertheless, that nutrient loading from outside the lake is a major factor in phosphorus availability. The concentration of nutrient inflows at the lake's western end, particularly the Zala River inflow, leads to strong longitudinal gradients of phosphorus along the lake. A recent study published by IIASA (Jolankai and Somlyody, 1981) has quantified the nutrient loads into the lake according to their origin and location.

Linked Water Quality Model Development

In Chapter 5 we describe the linked water quality model developed for this study with a particular emphasis on the use of a rational and systematic procedure to define the capabilities and characteristics needed in the model. The procedure followed is, first, to prescribe the goals and purposes of modeling the lake; second, to identify the length and time scales of the major physical and biochemical processes in the lake; and, third, to design the model components for consistency with the time and length scales of the processes of interest and with the available observation data from the lake. This model identification process for Lake Balaton indicates a model able to identify variations in algal abundance along the lake over time periods of a few weeks. Consequently, a transient

one-dimensional water quality model is proposed as an appropriate model. Further analysis leads to the selection of a transient two-dimensional (single-layer) wind-driven circulation model as the model's hydrodynamic component and a simplified four-compartment model of the phosphorus cycle as the biogeochemical component.

The water quality transport model establishes the basic structure of the model. The transport model solves the equations of mass conservation for a set of water quality constituents subject to advection, dispersion, reaction, and inflow and outflow. The model links the results of the hydrodynamic and biogeochemical components as inputs for its solution of the equations. The mass transport equations are formulated in both of two alternative forms: a finite difference continuum model and a multiple-box model. The availability of two approaches permits comparisons, as well as a critical evaluation of the multiple-box model which is common in current lake water quality modeling practice.

The hydrodynamic component of the water quality model is a horizontal two-dimensional model of wind-driven circulation. The model solves the linearized equations of motion subject to non-linear bottom stress and wind surface stress. Determined are the histories of water surface elevation and of depth-integrated velocity in the two horizontal directions. The equations are solved using an explicit finite difference method. Output from this component is used to specify one-dimensional advection and dispersion to the water quality transport model.

The biogeochemical component is drawn from the SIMBAL model, developed by van Straten (1980) and made available by IIASA. The model simulates the transient interactions of four species of phosphorus: two algal populations (with different temperature tolerance), a pool of dissolved inorganic phosphorus and another of detrital phosphorus. The transient influences of external phosphorus loads, water temperature and solar radiation are included as well. Output from this model component determines the reaction and nutrient input terms of the water quality transport equations.

Determination of the hydrodynamic inputs to be employed in the linked water quality model is discussed next. The conclusions of the discussion are that it is impossible, but fortunately unnecessary, to determine the small-scale movement caused by seiche transport. The excursion of the seiche is too small to be modeled correctly, but it is also too small to be an important influence upon the water quality. Elimination of advective motion leaves dispersion due to wind-driven circulation as the important mechanism linking water quality and hydrodynamics. A new method, appropriate to the lake environment, is developed to compute dispersive transport from the velocity distributions predicted by the hydrodynamic component. The method is a technique similar to those developed by Fischer (1966,1969) for open-channel flow, but rederived from the differing assumption that secondary currents dominate lateral mixing in the lake environment.

Simulation of Lake Balaton

In Chapter 6 we report on simulations of Lake Balaton which evaluate the influences on the lake's water quality and compare alternative model formulations. Considered first is the behavior predicted by the continuum model employing a finite difference grid of forty increments. We compare models based on hydrologic flow alone, models using the dispersion coefficient computed by the method of Chapter 5, and models using fixed dispersion coefficients. The results show that behavior most similar to that observed in the lake is produced by the model employing the computed dispersion coefficient. This conclusion is drawn from the general character of the observed Lake Balaton data. These data are insufficient to verify the model in a rigorous fashion, but the conclusions are nevertheless well-supported by the data available. Simulations employing constant values of the dispersion coefficient in time and space show that a coefficient of 1 m^2/s gives fair agreement with the results of models using the spatially and temporally varying computed dispersion coefficient.

Additional simulations show that the dominant influence upon Balaton's water quality is the spatial distribution of inflowing nutrient loads. The hydrodynamic and biogeochemical components hold roughly equal influence upon the predictions, at a lesser but still important level below the nutrient load distribution. The results thus indicate that calibration of the biogeochemical component is less a determinant of the model results than has generally been supposed. The results further support our contention that model hydrodynamics is an important influence upon water quality and should be duly accounted for in model development and calibration.

Finally, the results of the continuous forty-grid model are compared with the four-box model. The four-box model without exchange flow is found to include greater dispersion than the forty-grid model. Exchange flows, which would add additional dispersion, should thus not be considered. The four-box model is also found, not surprisingly, to lose all detail in the spatial concentration distribution. In summary, the four-box model results are approximate and tend toward underprediction.

Closing Remarks

Chapter 7 reports the major conclusions and recommendations drawn from the results of this research. Our primary conclusion is that the multiple-box model is an inferior alternative to the continuum approach embodied by the finite difference model. The multiple-box model fails because its formulation implicitly adds unintended dispersion to the model mass transport and divorces the model parameters from the geometry and physics of the prototype lake. As a consequence, model design must depend heavily on calibration to specify mass transport. In contrast, the finite difference model avoids these pitfalls caused by excessive spatial averaging. The finite difference approach maintains a good approximation to the continuum of the actual lake, thus permitting direct specification of model transport from the observed or simulated lake hydrodynamics. This insures that mass transport will be found independently of the model biogeochemistry, avoiding the pitfalls faced by some modelers when they

attempt to calibrate both hydrodynamic transport and biogeochemical rate constants simultaneously.

Our recommendations for design of water quality models is presented in a reanalysis of the length and time scales governing the model behavior. This repeats the analysis which began Chapter 5, but it is done in much greater detail and accuracy, and with specific attention to the modeling assumptions made in development of the hydrodynamic linkage. The analysis finds that the model formulation is sound, with good consistency between its various components. The analysis is further generalized to examine other modeling regimes feasible for Lake Balaton and to indicate directions for the application of such analyses to lake modeling problems in general. Finally, we draw upon the analysis as a guide for the design of a field data collection program to support water quality modeling.

Besides our general investigation of approaches to lake modeling, we devoted considerable effort in this study to the specific case of Lake Balaton. The clearest of our findings concerning Lake Balaton is that the observed water quality of the lake is most directly the result of the spatial distribution of the incoming phosphorus load. The resulting phosphorus distribution in the lake is substantially altered by biogeochemical reaction, long-term advection and dispersive mixing -- all acting with more-or-less the same degree of influence. A remarkably minor determinant of the lake's observed water quality was judged to be the advective influence of the seiche. The dispersion caused by seiche advection is important however.

Finally, we close with recommendations for future research. Our suggestions are to work further with the Lake Balaton finite difference model to continue investigating the influences of the biogeochemical and hydrodynamic transport components. To this end, recalibration of the biogeochemical model is proposed as well as refinement of the model loading inputs. Other suggestions are to gather further data from the lake to construct a model component for water-sediment phosphorus interaction and, on a different front, to independently and critically examine the determination of the dispersion coefficient developed in this study.

2 WATER QUALITY MODELS FOR SHALLOW LAKES

2.1 Introduction - The Purpose of Lake Water Quality Models

Lake water quality models have many applications; however, in this research we are specifically concerned with predicting the lake's trophic state. The trophic state of a lake is a reflection of the availability of nutrients for the growth of algae. Lakes range from oligotrophic (nutrient poor -- literally, "poorly fed") to eutrophic (nutrient rich -- "well fed"). Typically, they begin as oligotrophic and, over geologic time, become progressively more and more eutrophic. The speed of this transition, if allowed to proceed naturally, depends upon the quantity of organic matter supplied to the lake by its drainage basin and the nutrients recycled within the lake itself.

The process described above, proceeding imperceptively through geologic time, would hardly seem sufficiently worrisome to provoke computer modeling to predict its course. However, the lake's natural course can be greatly accelerated by man's activities. The discharge of sewage and other wastes to the lake, as well as rainfall runoff from urban areas, feedlots and fertilized agricultural lands, can introduce far more nutrients than natural processes. The resulting acceleration of the lake's nutrient enrichment hastens the arrival of the eutrophic condition, a process sometimes called cultural eutrophication.

The effects of nutrient enrichment engender the concern over eutrophication. The overabundance of nutrients leads to rapid algae growth -- often of species which render the lake unattractive for swimming and other recreational activities. Further, too rapid growth of algae may cause severe depletion of life-sustaining oxygen in the water column. The subsequent decay of dead algae leads to offensive odors and otherwise unpleasant recreational conditions. As well, taste and odor imparted to the water may taint the lake as a water supply. Concern over such effects, rather than over nutrient enrichment per se, has led H.F. Hemond to suggest as a practical working definition of eutrophication, "any biomass level that people object to."

Whatever definition one employs, the goals for eutrophication modeling are clear. What is desired is a means to predict the course of the lake's algal population under nutrient introduction regimes likely in the future. In particular, we would like the ability to foresee probable algal blooms -- the rapid, nearly uncontrolled, growth of algae. With such a model as a tool, control schemes to correct the lake's course may be proposed and evaluated. It is this ability to anticipate the likely behavior of the lake under different water quality management programs that is the key potential of water quality models.

In the sections to follow, we address the formulation of a model component to describe water quality dynamics, including eutrophication, in terms of the biogeochemical cycling of phosphorus.

2.2 Phosphorus in Shallow Lakes

The remarks of the previous section emphasize the importance of nutrients in determining the lake's water quality. Although phytoplankton require many chemical elements for growth and life processes, the major nutrient elements are phosphorus, nitrogen and carbon. On average, plant tissue contains these three elements in the ratio of one part (by weight) phosphorus to seven parts nitrogen to forty parts carbon (Wetzel, 1975). This ratio must be roughly preserved in the plant's nutrient needs as well. According to Liebig's Law of the Minimum, the growth of an organism will be limited by that nutrient which is least relative to the organism's needs; in most lakes this is the element phosphorus (Wetzel, 1975). Accordingly, most water quality models simulate the availability and cycling of phosphorus in order to determine the behavior of the lake ecosystem over time. In this section, we will present a short review of phosphorus in aquatic habitats and particularly the shallow lake.

2.2.1 Forms of Phosphorus in Lake Water

The analysis of phosphorus is made difficult by problems of measurement (Wang, 1981). The chemically identifiable fractions of phosphorus in water do not necessarily reflect the forms of phosphorus important in biological cycling. Further, the measurement techniques have been shown prone to error, and thus the quantities of phosphorus in the various fractions are often inaccurately reported. Despite these difficulties, we may construct a reasonably coherent picture of the phosphorus forms in natural water.

Phosphorus is found in both particulate and dissolved forms in lakes (Wetzel, 1975). The particulate or sestonic phosphorus includes organisms, phosphorus minerals and phosphorus carried by organic particulates. Orthophosphate (PO_4^{3-}), polyphosphates and organic colloids are the usual dissolved forms. We will examine these particulate and dissolved sub-groups in turn below, before proceeding to a description of their transformations in the phosphorus cycle.

The organisms included in particulate phosphorus are primarily phytoplankton, with zooplankton and bacteria to a lesser extent. Phosphorus is a key element in the organic compounds functional in the photosynthetic and metabolic processes of the phytoplankton. It is found in the nucleic acids, DNA and RNA, in the energy transporting nucleotides, ATP and ADP, and in numerous other organic compounds of lower molecular weight. These various organic compounds within phytoplankton account for most of the particulate phosphorus found as organisms.

The mineral forms of phosphorus common in lakes are the apatites -- calcium phosphate hydroxides. The primary form is hydroxylapatite, $Ca_5(PO_4)_3OH$, a relatively insoluble compound. Also included in the min-

eral particulate forms are those inorganics to which phosphorus will adsorb. The major adsorbers are calcium carbonates, iron and aluminum compounds, and clays. At high pH, calcium carbonates have high adsorption capacity for phosphorus (Lijklema, 1980). In hardwater lakes, where calcium carbonate precipitates as a result of biological activity, adsorbed phosphorus will co-precipitate in substantial quantities as well (Otsuki and Wetzel, 1972). Iron and aluminum hydroxides and clay compounds are also important adsorbers of phosphorus; however, their influence is felt most at lower pH.

The third particulate fraction is that phosphorus associated with non-living organic matter -- either adsorbed onto dead organic particulates or as a constituent of the particles. All living material contains organic phosphorus and thus any organism is a potential source of particulate organic phosphorus. Typically, it is one of the more substantial phosphorus fractions in lake water.

Though a very small part of the total phosphorus in a lake, orthophosphate generates considerable interest. Orthophosphate, or dissolved inorganic phosphorus, is the form most readily available for uptake and use by phytoplankton. Its invariably low concentration in lake water reflects the rapidity and completeness of algal uptake. Orthophosphates are the product of such natural processes as weathering and dissolution of phosphorus-bearing rocks and soil, and biological processes within the lake. Other sources include agricultural fertilizers and domestic sewage. Under the usual pH conditions in lakes, it appears as the ionic forms HPO_4^{2-} and $H_2PO_4^-$ associated with phosphoric acid, H_3PO_4.

The second dissolved phosphorus form, condensed polyphosphate, is the result of biological activity or synthetic man-made compounds, particularly detergents. Polyphosphates are broken down by biological activity to eventually yield orthophosphate. Though slow compared to other biological phosphorus reactions, these reactions are sufficiently fast to significantly affect nutrient availability. Time scales for polyphosphate degradation are on the order of days to weeks (Stumm and Morgan, 1970).

Dissolved organic phosphorus includes both dissolved and colloidal forms produced by biological growth. The exact chemical character of these high molecular weight compounds is largely unknown, though they constitute roughly one-fourth the total phosphorus in typical lake waters (Stumm and Morgan, 1970).

2.2.2 Phosphorus Transformations in Shallow Lakes

A review of the literature of phosphorus in lakes reveals a number of phosphorus transformations which can produce orthophosphate, the biologically important form. In this section we will examine major transformation pathways associated with algal growth processes and with the exchange of phosphorus between the sediments and the water column.

Phytoplankton Growth and Phosphorus

The existence of radioactive phosphorus isotopes, ^{32}P and ^{33}P, has made it possible to study the transformations of phosphorus between its biologically important forms in tracer experiments with laboratory cultures. Unfortunately, the difficulties mentioned earlier in accurately measuring the different forms of phosphorus prevent these techniques from being as fruitful as they would were the fractions more reliably measured. Nevertheless, the experimental results have identified important aspects of phosphorus movements in lake water.

Particularly illuminating are Lean's findings (1973), which are also discussed by Wetzel (1975). From tracer experiments, Lean deduced at least four major compartments of biologically important phosphorus. (See Figure 2.1.) The major pathway found by Lean can be followed in sequence around the cycle. First, there is uptake of orthophosphate by the particulate fraction. Lean feels that the particulates include at least two sub-fractions: one, presumably algae, is actively involved in cycling phosphorus, while the other does not participate. The particulate phase excretes or releases a minor amount of orthophosphate and a greater quantity of low molecular weight dissolved organic phosphorus. A small portion of this low molecular weight phosphorus is directly hydrolysed to orthophosphate. The majority follows a longer route, first binding to colloidal phosphorus in a condensation reaction. This reaction apparently displaces orthophosphate from the colloid to start the cycle over again. A small portion of the colloidal phosphorus is continuously lost from the cycle to particulates unavailable for biological use. These eventually settle from the water column, as does a portion of the particulate fraction.

The most striking aspect of this cycle is its rapidity. Lean found, after injecting isotope-labeled orthophosphate into the culture, that only two minutes were required before radioactive phosphorus appeared in the colloidal fraction. Fast cycling was verified in lake field studies as well. Such rapid turnover has important implications for the ultimate fate of phosphorus in lakes. As pointed out by Golterman (1973), a small fractional loss from a rapidly repeating cycle can lead to substantial removal over the course of a year.

Water-Sediment Interactions and Phosphorus

In most aerobic, and thus shallow, lakes there is a net transport of phosphorus to the sediments (Wetzel, 1975). Phosphorus reaches the sediments via the settling of particulates -- both the organic and inorganic particulate forms described above are important sources. The phosphorus returns to the water column in a number of ways according to the physical, chemical and biological character of the lake.

Usually, the concentration of dissolved phosphorus, and particularly orthophosphate, is much higher in the interstitial water of the sediments than in the overlying lake water. The orthophosphate concentration changes continuously from a low value at the sediment surface to high concentrations a few centimeters into the sediments. In the sediments, orthophosphate in solution in the interstitial water is usually in saturation

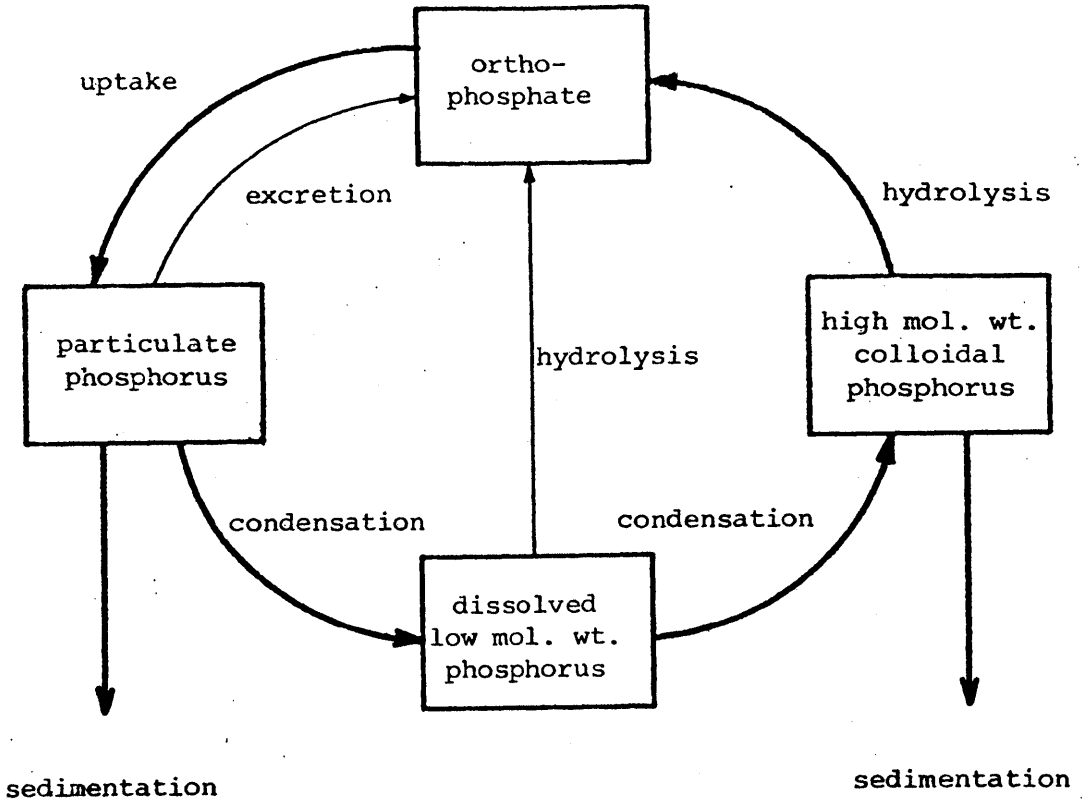

Figure 2.1

Biological movements of phosphorus according to Lean (1975)

equilibrium with the mineral forms of phosphorus, according to Stumm and Stumm-Zollinger (1972). They report interstitial orthophosphate concentrations up to 10.5 mg/ℓ -- as many as one thousand times greater than typical lake water orthophosphate concentrations. Sedimentary phosphorus is also suppied by the decay of organic matter which has settled to the sediment surface. As a result of the accumulation of these phosphorus inflows, the sediments hold an enormous store of phosphorus in most lakes. Release of sedimentary phosphorus is thus a major factor in the ability of a lake to recover from eutrophication. Unfortunately, it is an uncertain factor.

Mechanisms causing the release of sedimentary phosphorus depend mainly upon physical and chemical processes. We will examine two important routes for phosphorus release in lakes: the diffusion processes which occur when the sediments are undisturbed and the phosphorus releases which accompany the mixing and resuspension of sediment.

The proximity of very different orthophosphate concentrations within and without the sediments leads to diffusive transfer driven by steep concentration gradients. Diffusion within the sediment interstitial water is necessarily a slow process, but may nevertheless cause substantial

phosphorus transfer (Stumm and Stumm-Zollinger, 1972). The effectiveness of this transfer is controlled by the chemistry of the sediments (Wetzel, 1975 and Lijklema, 1980). In shallow lakes, the water column is usually completely aerobic and oxygen will diffuse into the sediments to a few centimeters. This oxygen microzone has significantly different chemistry than the lower sediments. Most importantly, reduced iron diffusing from below into the microzone will be oxidized into insoluble iron hydroxide -- a compound with very high adsorption capacity for phosphorus. Thus, the oxidized microzone acts as a very effective phosphorus trap, virtually sealing off the sediments from active exchange with the lake water.

Under certain conditions -- namely, when the oxidized microzone does not interpose -- diffusion can be an important phosphorus release mechanism. In stratified eutrophic lakes, anoxic conditions occur in the hypolimnion every summer. Eventually, the sediments become anoxic and reduced, the absorption capacity is greatly diminished, and phosphorus is released. Anoxia may occur in shallow, unstratified lakes on those occasions when extreme algal growth and decay exhaust all available oxygen and impede oxygen introduction at the lake surface. These rare conditions occur only in highly eutrophied shallow lakes. Also possible in shallow lakes is the physical disturbance of the sediments to below the microzone. This will expose the reduced sediments to the water column and lead to phosphorus release for a period of time.

Physical disturbance of the sediments is an important mechanism in shallow lakes. Frequently, strong winds cause the water column to mix down to the sediments, and the consequent disruption of the surface sediments can lead to release of phosphorus. The mechanism of this interaction involves both physical and chemical processes. The physical agent is the shear stress exerted on the lake bottom by currents and wave action, causing sediment particles and organic matter to become suspended in the water column. For the suspended sediment, this leads to a change in chemical conditions -- often a substantial change. Usually, the interstitial water of the sediments will have lower pH, but higher orthophosphate concentration than the overlying water. Thus, when particulates with phosphorus bound to aluminum or iron are resuspended, the increase in pH will cause orthophosphate to be released.

Resuspended calcium carbonate, on the other hand, will absorb more orthophosphate at the higher pH of the lake water. But, the transport from the high orthophosphate concentration of the sediments to the lower concentration in the water column has the reverse influence, causing the release of orthophosphate. Either process may prevail, so that the behavior of resuspended calcium carbonate sediments must be determined experimentally for any particular lake (Lijklema, 1980).

Other Biological Processes and Phosphorus

Research by many different workers, summarized by Wetzel (1975), suggests that zooplankton, bacteria and aquatic macrophytes may all enter into the cycling of phosphorus. Zooplankton, for example, ingest phosphorus with phytoplankton and other seston, but then excrete it as

orthophosphate and other forms. The significance of zooplankton as an orthophosphate source relative to other sources is as yet undecided, however.

As with phytoplankton, aquatic plants require phosphorus as an essential nutrient. Thus, as the plants grow during the spring and summer, they acquire and store phosphorus. This phosphorus is rapidly returned to the lake after the plant has died and decayed (Wetzel, 1975).

An interesting possible influence of plant life on the limnetic phosphorus cycle is the potential ability of macrophytes to transport significant quantities of orthophosphate from the sediments to the lake water. McRoy et al. (1972) have conducted careful studies of eelgrass in a coastal marine environment and shown that the macrophytes absorb significantly more orthophosphate from the sediments than the lake water. Subsequent excretion to the water effected a net phosphorus transport from the sediments to the water column. Though McRoy's findings are for a marine ecosystem, similar pathways are likely in freshwater bodies -- a conjecture strongly supported by Wallsten's (1980) studies in a shallow Swedish lake. The significance of macrophyte nutrient pumping relative to other possible phosphorus regenerative mechanisms in shallow lakes is entirely unknown, however.

2.3 Models of Shallow Lake Water Quality

2.3.1 Classification of Models

Following Quinlan (1975), we may identify three basic approaches to modeling aquatic ecosystems. First is the biodemographic model, which uses the individual or species as a fundamental unit. Such a model will, for example, bookkeep cell numbers based upon a mathematical formulation of the cell life cycle.

A second approach to water quality ecology is via the bioenergetic model. These models, which quantify the ecosystem in terms of energy or power, trace the flow, storage and loss of energy within the ecosystem. A formulation of the conservation of energy will govern such models.

The third approach is the most common in engineering applications and will be used in this study. This is the biogeochemical model, a model based on the conservation of mass of one or more key elements. In lakes, the elements of most interest are the nutrients -- carbon, nitrogen and particularly phosphorus; biomass and dissolved oxygen may be modeled as well. These models attempt to duplicate the cycling of elements within the waterbody, at least to the extent that the cycles are known. The elements are quantified in terms of concentration within the lake water, for example phosphorus in mg/ℓ.

Regardless of the approach employed, we may cite some guiding principles to be observed in model formulation (Najarian and Harleman, 1975). First is the stipulation that mass be conserved for all elements considered. Implications of this requirement are the use of consistent units for all element compartments and the careful bookkeeping of all element transformations. The second fundamental principle is causality -- that the transformations between the forms of phosphorus be determined by the interacting components and by environmental influences upon the element system. Application of this principle is limited by our knowledge of the transformation processes and by the inability to capture all detail in practical computation.

2.3.2 Water Quality Model Structure

There are two major aspects to the structure of lake water quality models: the representation of the phosphorus cycle and the spatial resolution of phosphorus distribution. The phosphorus cycle is represented in the model as various different forms of phosphorus between which transfers of matter occur. The phosphorus forms employed are known as state variables, or sometimes compartments. The transfers between the forms are due to chemical or biological transformations which are formulated in the model as reaction equations. Typically, a biogeochemical model formulates the phosphorus cycle via the trophic levels of the ecosystem. For example, one model compartment may represent zooplankton phosphorus, which feeds upon phytoplankton phosphorus, which in turn uptakes dissolved inorganic phosphorus, and so on. This model formulation is based upon experimentation with laboratory cultures and can draw upon laboratory results as a guide in parameter specification.

To decide the spatial resolution desired for the water quality model is to decide the associated hydrodynamic transport model -- the two issues are inseparable. The alternative spatial structures for lake models (both deep and shallow) are summarized in Figure 2.2. Most water quality models to date have tended to use the simpler structures - modeling the lake as a single fully-mixed tank (known as a one-box model) or as two such tanks. The two-box model is often used in deep stratified lakes with one box to represent the epilimnion and one for the hypolimnion. More sophisticated models are less common, but do exist, particularly for the vertical structure of stratified lakes. For the problem at hand, shallow lakes, there is very little vertical structure in the actual lake and the horizontal spatial resolution is of greatest interest. We will further explore the model variations from Figure 2.2 in this and the next chapter in the contexts of modeling transport and circulation.

In the following sections we review a selection of biogeochemical and water quality transport model alternatives from the literature. Discussed are models pertinent to shallow lake modeling in general, and to Lake Balaton in particular.

Temporal Representation

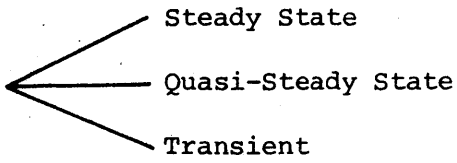

Spatial Representation

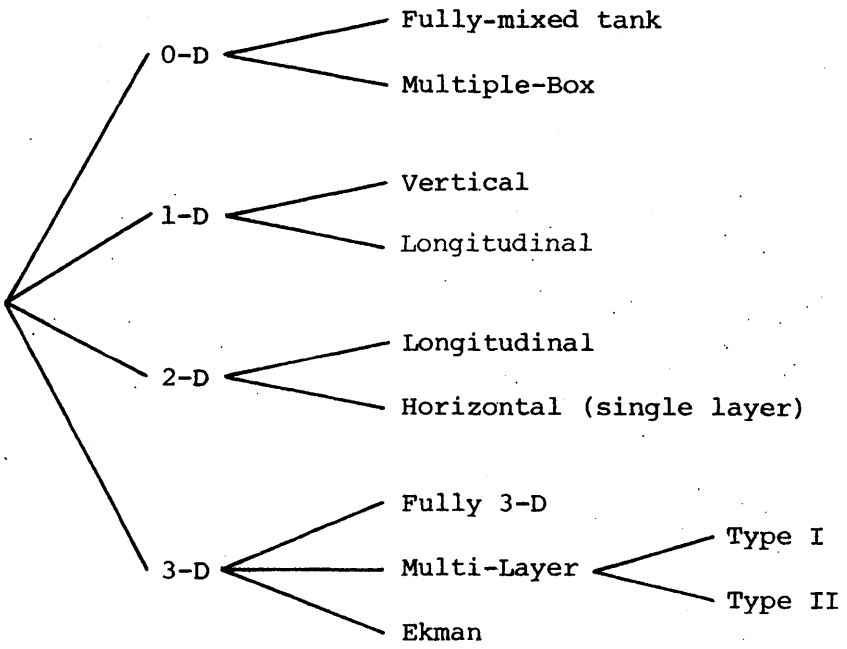

Figure 2.2

Lake model alternatives

2.4 Models of Phosphorus Biogeochemistry

2.4.1 Review of Selected Models

A limited number of phosphorus models specifically for shallow lakes have been proposed. In this section we will review three models developed for Lake Balaton in Hungary drawing upon the original references as well as a similar review by van Straten and Somlyódy (1980). At the close of this section, we will briefly report another shallow lake model from the literature to illustrate a higher trophic level model formulation.

BEM

The earliest model of Lake Balaton was developed by the Balaton Ecological Modelers Group of the Hungarian Academy of Sciences (Herodek and Csáki, 1980, Csáki and Kutas, 1980 and Kutas and Herodek, 1980). This model is a mixed biomass and nutrient model rather than a model of the phosphorus cycle alone. It considers seven compartments. Three of these track biomass: one compartment each for winter and summer algal species and one for bacteria (decomposers). Biomass components are measured in mg dry weight of biomass (algal or bacterial) per liter. Nutrient compartments include orthophosphate, nitrate and dead organic matter (detritus). The seventh model compartment is the sediment phosphorus store.

Two main transformation pathways are modeled: the primary production of algal biomass and the decomposition of detritus by bacteria. (See Figure 2.3.) Primary production is the growth of algae which accompanies the uptake of the nutrients nitrate and orthophosphate. It is modeled as a function of algal biomass and temperature subject to limitation by nutrient and light availability. Nutrient limitation is fashioned as a Monod kinetic process for each of the two nutrients. A geometrically weighted average of the three limiting factors, the two nutrients and light, is taken to control primary production.

Detritus in the model is the product of algal and bacterial mortality. It is recycled to the nutrients nitrate and orthophosphate by the growth process of the bacteria. Bacterial uptake of detritus is modeled as a function of temperature, bacterial biomass and detrital concentration, the last quantity in a Monod-type expression. The decomposition process, which includes excretion of the elemental nutrients as well as respiration, is a function of temperature and bacterial biomass. Conversion from mass of detritus to bacterial biomass, and thence to nutrient biomass, is accomplished assuming fixed nitrogen and phosphorus proportions in the detritus and by taking nitrate and orthophosphate production to be fixed fractions of decomposition.

Other pathways of the model are the loss of orthophosphate to the sediments by co-precipitation with calcium carbonate formed during algal primary production. A sediment release function reintroduces a part of the sedimentary phosphorus back into the water column as a temperature dependent first order process.

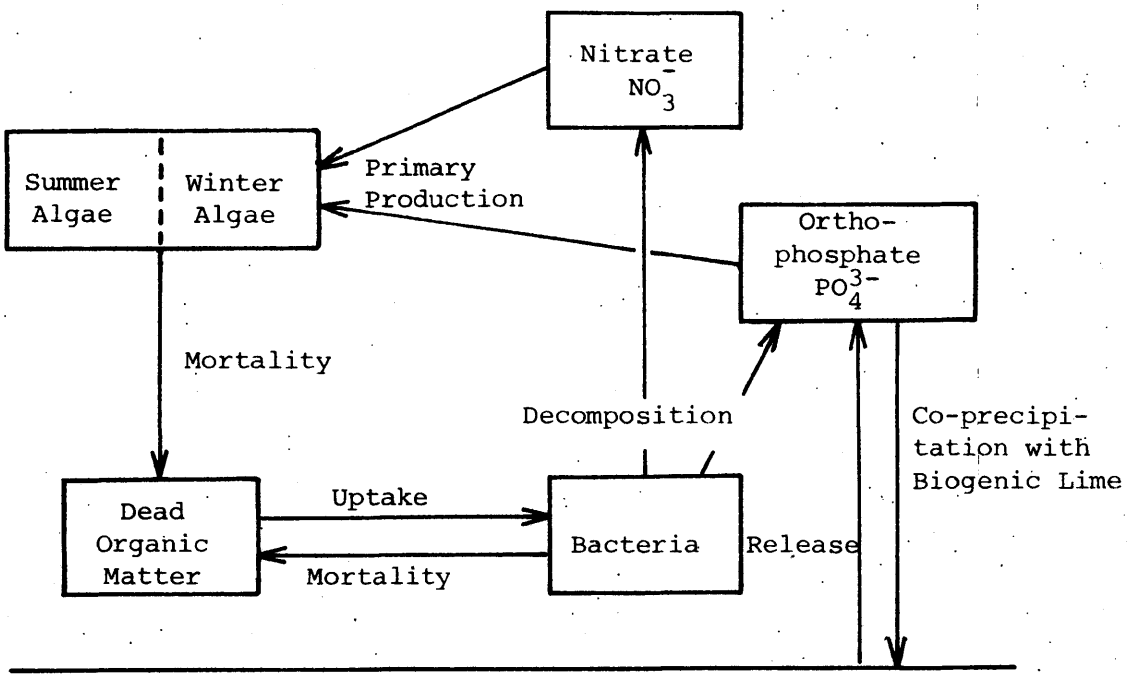

a) Biomass and nutrient compartments

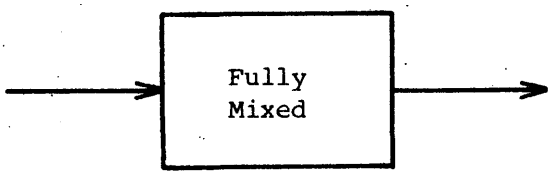

b) Hydrodynamic model

Figure 2.3

BEM Phosphorus Model

The model hydrodynamics are simple: a single fully mixed tank is considered. This formulation has been employed to model single basins of Lake Balaton in separate simulations.

BALSECT

The model BALSECT (standing for Balaton Sector Model) was developed at IIASA by Leonov (1980a, 1980b). The theoretical model includes eight phosphorus components in addition to dissolved oxygen (Figure 2.4a). The phosphorus components are dissolved inorganic phosphorus (orthophosphate), dissolved organic phosphorus and non-living particulate phosphorus (detritus) in both the water and the sediments. In the water alone are compartments for phytoplankton and bacterial phosphorus. The lake is modeled hydrodynamically as four fully-mixed basins (Figure 2.4b) -- a division of the lake originating in hydrologic studies discussed in Section 4.2.1. Solids and water continuity are maintained between the basins using monthly average inflows and outflows.

Phosphorus is cycled in the water column by biologically mediated reactions. Algae consume dissolved inorganic phosphorus at an uptake rate determined by a Monod dependence on the nutrient concentration, and further controlled by temperature and light. The algae in turn produce dissolved organic phosphorus by excretion and non-living particulate phosphorus by mortality. Mortality is taken to be inversely proportional to the uptake rate by a Monod-type relation, thus making excretion a very complex function of the nutrient concentration in the water. The dependency of excretion and mortality on the uptake rate is an unusual and complex formulation for models of this type.

Bacteria mediate the mineralization of dissolved organic phosphorus. Uptake of dissolved organic phosphorus is modeled by Monod kinetics including temperature dependency. Excretion of orthophosphate (dissolved inorganic phosphorus) and mortality to the particulate compartment are formulated in analagous relations to those used for algae. Finally, particulate phosphorus is assumed to decompose to dissolved organic form in a temperature dependent reaction.

The water column components interact with simultaneously reacting components in the sediments. Phosphorus enters the sediment via settling of non-living particulates. Once in the sediments, it is assumed to decompose to, first, dissolved organic phosphorus and then to dissolved inorganic phosphorus, both steps proceeding by temperature dependent first-order decay. A portion of the dissolved organic phosphorus is lost to permanently unreactive forms in the sediments. Sedimentary phosphorus re-enters the water by first-order release of dissolved inorganic phosphorus. This model of the sedimentary phosphorus cycle has yet to be implemented in simulations of Lake Balaton due to a lack of calibration data. In its place, first order settling to and release from the sediments has been employed.

SIMBAL

Another model from IIASA is SIMBAL, the simple Balaton model, devel-

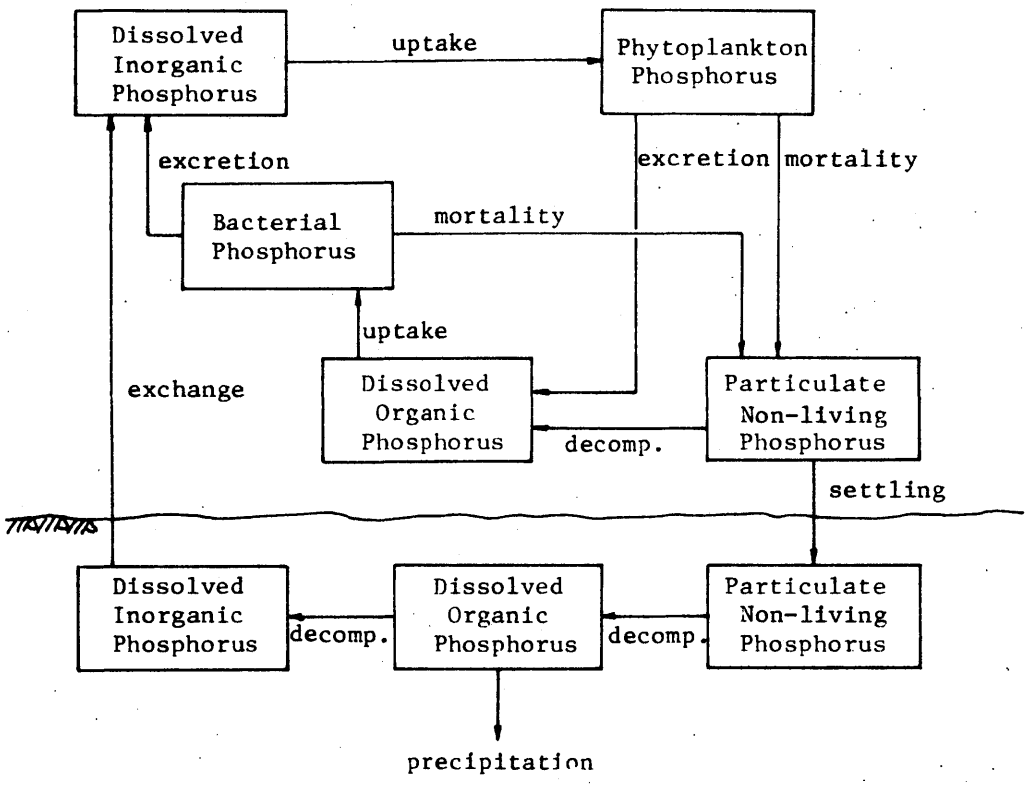

a) Phosphorus component cylces

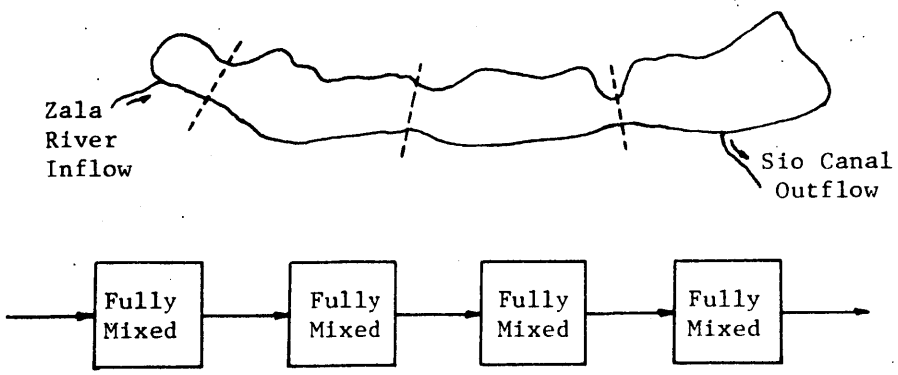

b) Hydrodynamic model

Figure 2.4

BALSECT Phosphorus Model

oped by van Straten (1980) using the BEM model as a basis. This model is of interest for its means of development as much as for the model itself. It is, in fact, a second, more elaborate formulation of a previous model found lacking in its ability to reproduce observations from the lake. Rejection of the first model was the outcome of a formalized procedure to evaluate model performance given incomplete and imperfect measurements from the field.

van Straten's procedure explicitly accounts for the various uncertainties facing the model -- the large uncertainty in observation data and in forcing function input data -- as well as the incomplete knowledge of the system behavior and thus model formulation. He allows for these factors by first defining an acceptable range of model results for historical periods, based on the incomplete and uncertain observation data for those periods. Then, for a given model formulation, bounds are placed on the possible values of the model parameters. With these definitions, a Monte Carlo simulation is performed, selecting parameter values randomly from within the defined bounds and recording those parameter combinations which yield model results within the acceptable response range.

van Straten's first model, shown as Model I in Figure 2.5, was unable to produce any response within the acceptable range. Model I is a simplified representation of the phosphorus cycle. It omits bacteria from explicit formulation, capturing the effect of bacterial behavior through a strong dependence on temperature for the mineralization term. In addition, the detritus compartment combines both dissolved organic and particulate organic phosphorus. Interaction with the sediment is included through first-order sedimentation of detrital phosphorus and biogenic precipitation of dissolved inorganic phosphorus, and through a temperature dependent release of dissolved inorganic phosphorus from the sediments. The model includes two algal compartments for summer and winter species, a distinction captured through different temperature dependencies. Algal growth is limited by the orthophosphate concentration via a Monod relation, and by light availability. Growth is also formulated to include temperature dependence, as is algal mortality.

As stated, Model I was unable to reproduce the observed lake behavior within the permitted range, a failure due to overpredicted dissolved inorganic phosphorus increases at the end of the algal growing periods. To correct this error, van Straten hypothesized another mechanism at work to remove the excess orthophosphate: a process of continuous adsorption and desorption with suspended sediment in the water column. This process was added to create Model II, also shown in Figure 2.5. The flux of phosphorus to or from the sorbed state is assumed proportional to the difference in lake orthophosphate concentration above or below a specified equilibrium level. This level is a model parameter, varied with location in the lake. Inclusion of the adsorption-desorption mechanism eliminates the problems of Model I, and Model II was able to make reasonable simulations of the lake's behavior.

The hydrophysical model employed in SIMBAL is based upon the same longitudinal four-box structure used in the other Balaton models. van Straten adds one feature, however, in an attempt to capture the dynamic

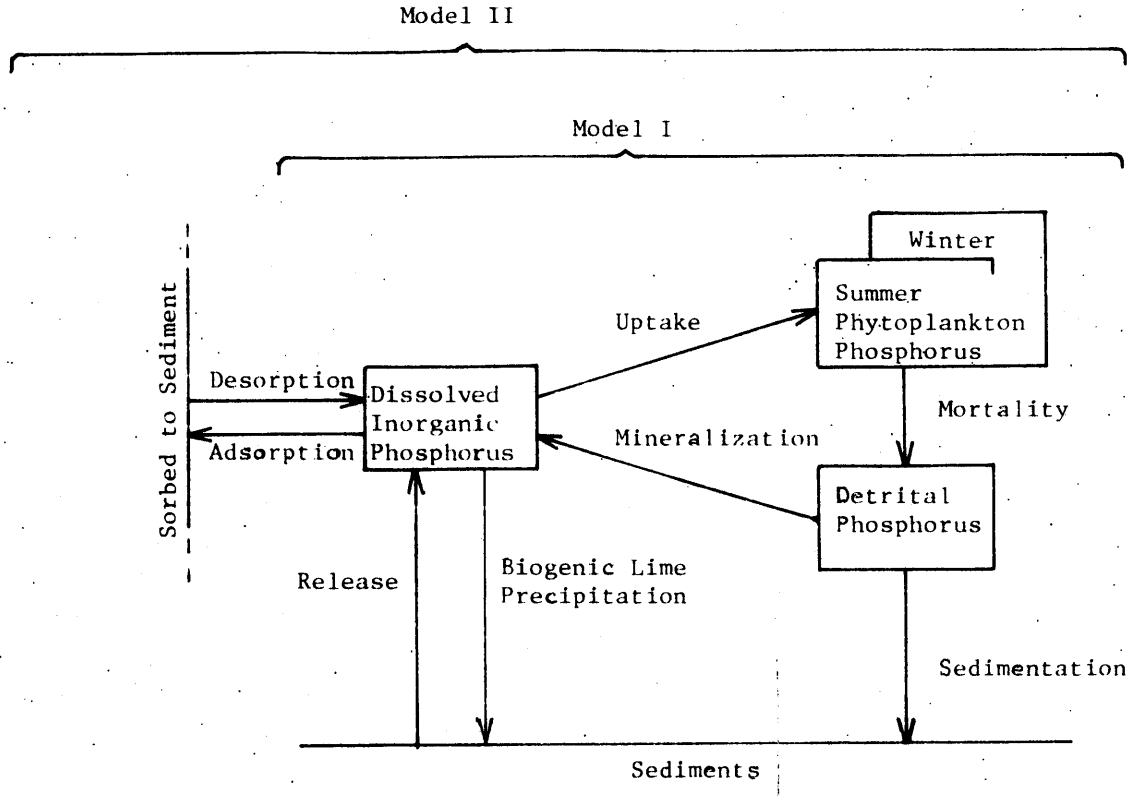

(a) Phosphorus Cycle Compartments

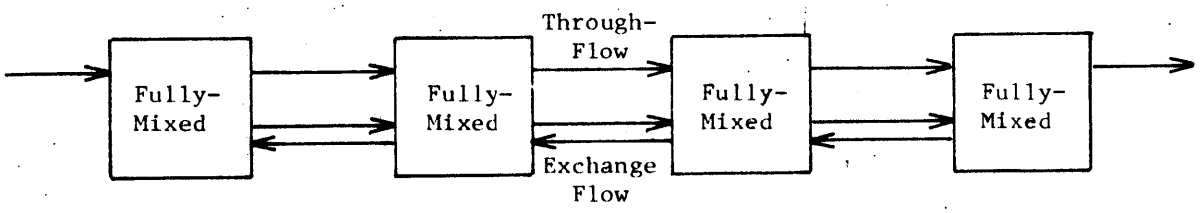

(b) Hydrodynamic Model

Figure 2.5

SIMBAL Phosphorus Model

character of Lake Balaton's water motion. He terms this a return velocity, though it might more appropriately be called an exchange flow since it represents equal but opposite flows between two adjacent boxes. The return velocity is taken as constant in both time and space. van Straten finds estimation of the other parameters to be sensitive to the value of the exchange flow -- a finding which reinforces our contention, stated in Chapter 1, that water quality models must pay careful heed to both hydrodynamics and biogeochemistry.

Jørgensen's Model

Since the Lake Balaton models include relatively few trophic levels, it is instructive to look at Jørgensen's model, developed to model small shallow lakes in Denmark (Jørgensen, 1976 and 1978). As can be seen in Figure 2.6, Jørgensen includes the higher fish and zooplankton trophic levels, in addition to phytoplankton. Grazing rates are all defined using Monod-type relations.

Jørgensen's representation of phytoplankton dynamics is a significant departure from the models above. He formulates phosphorus uptake by phytoplankton as a two-stage process, differentiating between the uptake as a function of lake water nutrient concentration, and the cell growth, governed by the phytoplankton internal cell nutrient concentration. Such a formulation is effective in modeling luxury uptake by cells during short periods of high ambient concentration. In the model, the rapid luxury uptake realistically leads to a slower, long term growth of the phytoplankton population. This representation is better able to model the response to transient release of sediment nutrients than a model without a lag factor between uptake and growth.

Jørgensen's model also includes a complex submodel of water-sediment interaction (Jørgensen et al., 1975). Phosphorus enters the sediment via first-order settling of detritus and phytoplankton from the water column. It enters into the sediment compartment labelled "exchangeable phosphorus," which we take to consist of the particulate organic form. This in turn is degraded to "interstitial phosphorus," presumably dissolved orthophosphate. The degradation reaction is a temperature dependent first-order decay. Release of the interstitial phosphorus to the water column is proportional to the concentration difference in orthophosphate between the interstitial and lake water, modulated by a temperature dependence.

2.4.2 Conclusions

Use of water quality models for prediction requires that they first be calibrated and verified. It is safe to presume that any of the biogeochemical models presented can be calibrated to match the measurements taken in Lake Balaton. The models include sufficient parameters to allow wide ranges in their response, and the field data for calibration include only nine stations along the lake sampled biweekly. With few data and many parameters, calibration is easily possible. This has been demonstrated to varying degrees of accuracy with the Balaton models and is fair to assume for Jørgensen's model as well.

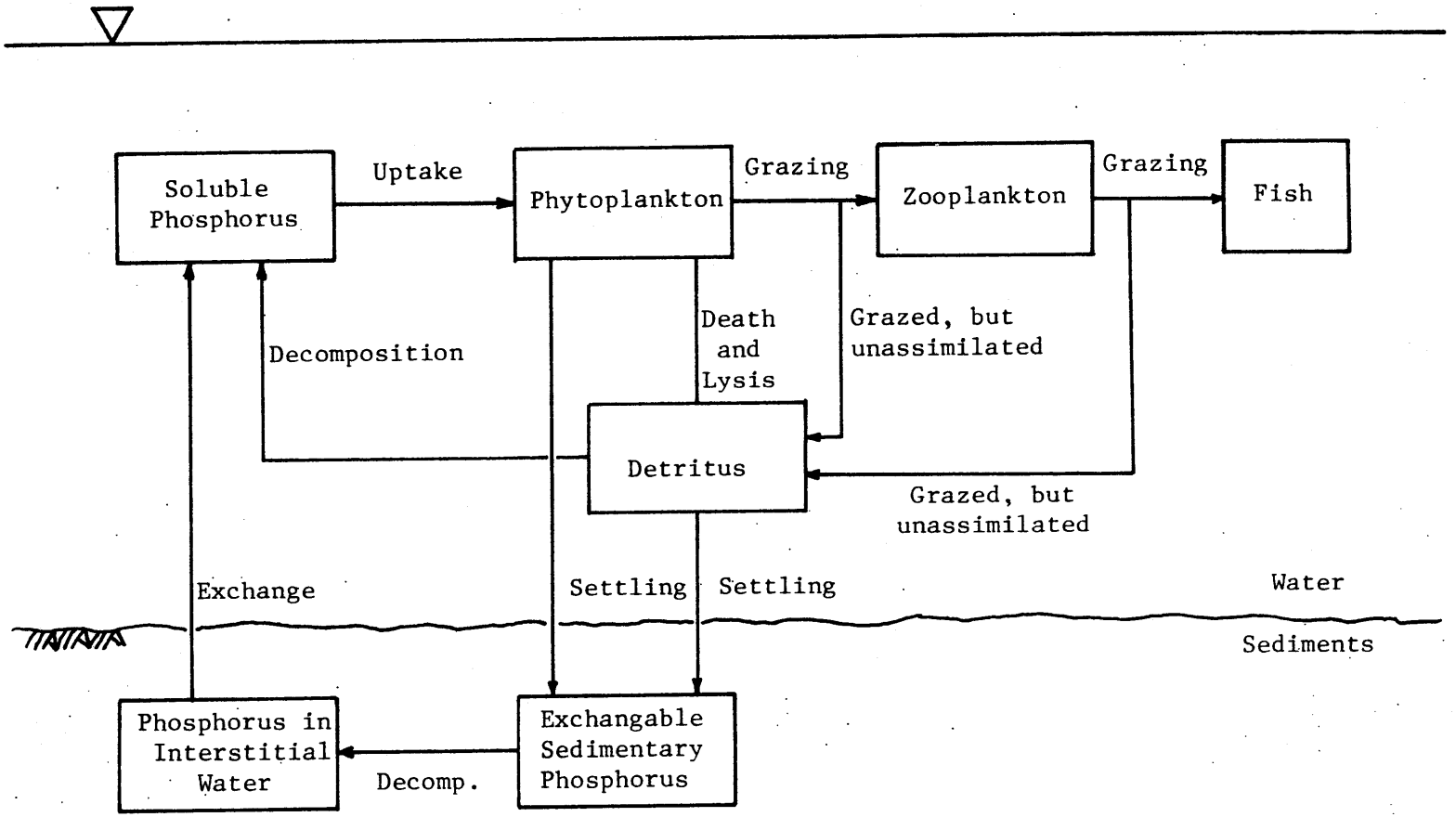

Figure 2.6 Phosphorus Cycles in Jørgensen's Model (1976, 1978)

Thus, the models are probably similar in their ability to produce behavior near that observed in the lake. Differences between the models arise from their complexity and their choice of emphasis. Emphasis is best placed, in our opinion, upon the sediment-water interaction relation. Ultimately, it is the fate of the sedimentary phosphorus stores which will determine the lake's response to water quality management programs. Continued phosphorus release from the sediments will lead to slow recovery from eutrophication despite significant decreases in the external phosphorus inputs. The sediments are thus the critical factor controlling the shallow lake's eventual trophic state.

Model complexity increases with the number of state variables and reaction terms. And, as complexity grows, so grow the number of model parameters and the quantity of data required for calibration. The number of state variables, for example, is a good indicator of the amount of calibration information needed. Jørgensen (personal communication) suggests that the number of data needed grow roughly as the square of the number of model parameters. In Table 2.1, we show a census of state variables and parameters for the four models examined. Of the parameters shown, only about one-fourth need be considered essential to the model calibration process; the other, non-essential, parameters may be defined from the literature or exhibit minor influence upon the model results. According to Jørgensen's criterion for model calibration data requirements, the SIMBAL model needs but half the data of the other models. Even still, SIMBAL's calibration requirement approaches or exceeds the availability of directly measured quantities in the Balaton data base. Adequate calibration is thus a limitation on all of the Balaton models.

Although the problems of calibration seem great, the problems of verification are, if anything, greater. So far, the Balaton models have not been verified in the sense that calibration parameters developed in simulations of one year have been employed to successfully simulate a second year. This, however, is the crucial test of a model's predictive ability and an absolute requirement if the model is to be accepted as a predictive tool. Indeed, Simons and Lam (1980) have pointed out that the model cannot be considered a predictor of long-term eutrophication until it has been verified in continuous simulations lasting at least as long as the lake's hydraulic residence time. For Lake Balaton, this means the model results must be compared with field observations over a duration of about a decade. There are not sufficient data for such a task, but even if there were, it is unlikely that the present models would be verified over such a long time period, judging from Simons' and Lam's results in a similar test for Lake Ontario.

To conclude, we find that biogeochemical modeling is in its infancy. The problems of calibration, verification and even model formulation must still be grappled with before such models grow into routinely used tools for prediction.

Table 2.1

Number of state variables and parameters for phosphorus cycle models

	BALSECT	BEM	SIMBAL	Jørgensen
State variables	8	6	4	7
Model parameters - total	30	33	22	30
Rate Constants	15	12	9	12
Nutrient limitation factor constants	1	3	1	5
Light limitation factor constants	3	3	2	3
Temperature dependency constants	11	12	9	5
Phosphorus content conversion factors	0	3	0	4
Assumed constant concentrations	0	0	1	1
Factors to convert model output to measures quantities	1	0	3	0

2.5 Models of Water Quality Transport

As stated earlier, the spatial structure of the model necessarily implies a formulation of hydrodynamic transport to accompany the model biogeochemistry. The selection of the proper spatial detail, and consequently the hydrodynamic transport model, is a problem of considerable subtlety which is only beginning to be addressed by water quality modelers. Since a major emphasis of this research is upon just this issue, we will return to it in later chapters for more detailed discussion in the context of our application lake. As background to that discussion, this section gives a review of modeling techniques applied to hydrodynamic transport in lake water quality models.

A large number of lake eutrophication models presume that the lake can be modeled as a fully-mixed tank with spatially uniform concentration. While such models can be appropriate and useful for small shallow lakes with short hydraulic residence times, they simplistically represent larger or deeper lakes in which significant concentration variations exist. In deep lakes, vertical temperature stratification leads to significantly different properties above and below the steep temperature gradients of the thermocline. To capture these differences, models with two or more vertical layers have been developed. The concentrations of biochemical constituents within each layer are determined by accounting for the reactions within the layers and the transport of matter between the layers. Biogeochemical models of deep lakes are thoroughly reviewed by Wang (1981).

Modeling the vertical dimension of deep lakes is of only peripheral interest to our study of shallow lakes. However, the practices of modeling horizontal variations in large lakes are essentially the same for shallow lakes and deep lakes. Large shallow lakes are far fewer than deep lakes, so modeling examples of spatial transport in shallow lakes are rare. Lake Balaton is without doubt the most intensively modeled large shallow lake, but the Balaton models supply only a restricted range of transport model alternatives. In the remainder of this section we will review a selection of lake models representative of different approaches to modeling horizontal transport. The review considers the formulation of model transport assuming the circulation information necessary to quantify transport is given. A review of mathematical models to determine lake circulation is included later as Chapter 3.

2.5.1 Governing Equations

The equation of mass conservation for a dissolved or suspended constituent within the lake water is:

$$\frac{\partial c}{\partial t} = -u\frac{\partial c}{\partial x} - v\frac{\partial c}{\partial y} - w\frac{\partial c}{\partial z} + \frac{\partial}{\partial x}\left(\varepsilon_x\frac{\partial c}{\partial x}\right) + \frac{\partial}{\partial y}\left(\varepsilon_y\frac{\partial c}{\partial y}\right) + \frac{\partial}{\partial z}\left(\varepsilon_z\frac{\partial c}{\partial z}\right) + s \qquad (2.1)$$

where

x, y	are the horizontal direction components,
z	is the vertical direction component,
t	is time,
c	is the constituent concentration,
u, v, w	are the fluid velocity components in the x, y and z directions respectively,
ε	is the turbulent diffusion coefficient in the direction indicated by its subscript, and
s	represents the rate of net addition of constituent mass per unit volume due to external and internal sources and sinks.

This equation states that the change in concentration with time is equal to the change due to advective transport (represented by the first three terms on the right-hand side), due to diffusive transport (the next three terms) and due to sources and sinks (the last term, s). Included in the sources and sinks term are the addition and subtraction of mass due to biogeochemical reaction.

Boundary conditions to Equation 2.1 are generally simple. Flux boundary conditions apply at the lake bottom and water surface, and at the lake periphery -- most often the flux is zero.

Equation 2.1 is the basis of all lake water quality models, albeit with extensive simplification in some models. In the discussions to follow we pay particular attention to two basic approaches to solving Equation 2.1. The first is the multiple-box model, in which the lake is divided into a set of completely mixed volume elements. Concentration is determined in each element by simple mass balance -- essentially the integral of Equation 2.1 over the element volume. This results in an ordinary differential equation for each element k:

$$V_k\frac{dc_k}{dt} = \sum_j\left[Q_{jk}c_j + \frac{\varepsilon_{jk}A_{jk}}{\ell_{jk}}(c_j - c_k)\right] + S_k \qquad (2.2)$$

where

V_k	is the volume of element k,
c_k	is the concentration in element k,
Q_{jk}	is the advective flow from element j to k,
ε_{jk}	is the diffusion coefficient between elements j and k,

A_{jk} is the interfacial area between elements j and k,

S_k is the sum of all sources and sinks within element k, and

ℓ_{jk} is the distance between the centroids of elements j and k.

In some derivations, an exchange flow, X_{jk}, is introduced to replace the quantity $\varepsilon_{jk}A_{jk}/\ell_{jk}$ which has the units of a flow. In the discussion to follow we will refer to models of the type in Equation 2.2 as multiple-box models (or finite section models after Thomann (1972)).

Implicit in the construction of the multiple-box model is the requirement that Equation 2.1 be reduced to a zero-dimensional version by averaging over all three spatial dimensions. In zero-dimensional models, concentration can no longer be considered a continuous function of space; it is a discrete function over relatively large integrated volume elements.

Alternatives to this model are to retain the three-dimensional dependence of Equation 2.1 or to employ less extensive averaging, retaining one or two-dimensional dependence. This permits Equation 2.1 to be solved by a fundamentally different approach in which the continuous dependence of mass concentration upon at least one spatial dimension is modeled. For these models, one employs the finite difference method to construct an approximate representation of the equation (Leendertse, 1971). Application of the finite difference method results in a difference equation which is directly analogous to the original differential equation. The difference equation is, in essence, a continuum approach which seeks to approximate the continuous governing equation at finite intervals. As such, it differs conceptually from the integral approach of the multiple-box model. We will return to this distinction in detailed discussions in later chapters.

2.5.2 Transport in Water Quality Models

Two types of transport are included in Equation 2.1: advective transport due to organized large-scale motion and diffusive transport due to small scale turbulent fluctuation. The first type of motion is captured in the fluid velocities u, v and w, while the second type of motion is represented via the turbulent diffusion coefficients, ε_x, ε_y and ε_z. The separation of motion into two such components is arbitrary to the extent that it depends upon the time and length scales assumed to represent advection. In the limit of infinitely short length and time scales, all motion will be represented as advection, and turbulent diffusion will disappear.

The representation of turbulent transport using diffusion coefficients is an imperfect, but highly successful, approximation made by analogy with Fick's Law of molecular diffusion. Formally, turbulent transport is the residual transport which remains after averaging the extremely transient field of velocity and concentration over a short but finite time period. The time period implicit in Equation 2.1 is no longer than a few of minutes. If considerably longer periods are used -- for example the inertial period or seiche period of the lake -- the subdivision of advective and diffusive motion will be much different and the diffusion coefficient will change accordingly. The modified coefficient resulting from longer averaging periods is sometimes termed the effective diffusion coefficient. The question of temporal averaging arises frequently in modeling tidal estuaries; it is discussed further in that context by Harleman (1971) and Hinwood and Wallis (1975).

Models based upon the time periods above, though covering a broad range, all fall within the category of transient models in Figure 2.2a. Time periods on the order of weeks or months can be modeled as quasi-steady -- that is, as a series of steady-state conditions under the assumption that the lake has had sufficient time to reach a new equilibrium within each time period. Still longer time periods, over one or more years, can be modeled as steady. The effective diffusion coefficients for these models will again differ from those appropriate for shorter time periods.

Just as temporal averaging creates turbulent diffusive transport, spatial averaging also leads to an apparent transport known as dispersion. Dispersion arises from spatial nonuniformities in velocity and concentration over the dimension or dimensions of averaging. As with turbulent diffusion, dispersive transport is usually assumed to adhere to Fickian diffusion relations. Thus, dispersive transport is taken as the product of the concentration gradient and a dispersion coefficient, D.

Just as different effective diffusion coefficients result from different time averaging periods, the dispersion coefficient will vary according to the dimension removed by spatial averaging. In Figure 2.2b, a number of spatial averaging regimes are identified. Two-dimensional models are created by averaging vertically over the depth or laterally over the width of the lake. The dispersion coefficients appropriate to laterally averaged models will in general be very different than those for vertically averaged. One-dimensional models are created for long shallow lakes by averaging vertically over the cross section and for deep lakes by averaging horizontally. Complete averaging over all three dimensions gives rise to zero-dimensional models -- fully-mixed tanks -- in which internal dispersive transports are no longer considered.

Dispersive transport must also be considered in models which are produced by subdividing the lake into discrete spatial intervals. The multiple-box model, for example, averages over the spatial nonuniformities in the distributions of velocity and concentration along and within the box boundaries. The consequences of this particular type of spatial averaging upon the selection of the dispersion coefficient have not been systematically addressed in the literature. Typically, an empirical

approach is practiced, determining the dispersion coefficient by calibration of the model results. In some versions of this model, the dispersion coefficient is not directly employed but a dispersive transport is specified as an exchange flow, the equal exchange of mass between adjacent boxes as defined above following Equation 2.2.

More attention has been paid to the dispersion due to the spatial averaging implicit in a fixed grid finite difference model. The analysis is appropriate to horizontally two-dimensional single or multi-layer models -- these models fall within both the two-dimensional and three-dimensional categories in Figure 2.2. For these models, the concept of a sub-grid-scale turbulent transport has been developed assuming horizontally isotropic turbulence which is a function of the length scale (grid spacing) considered. The transport is represented by what is known as a sub-grid-scale turbulent diffusion or dispersion coefficient. The hypothesis of this method is that the diffusion coefficient can successfully capture motion occurring on length scales less than the grid size. A theoretical basis is established to support this hypothesis (Deardroff, 1971), however the appropriate value of the dispersion coefficient as a function of grid size is not determined by the theory. In practice, the coefficient is determined empirically from field data as presented, for example, by Murthy and Okubo (1977).

The variety of transport modeling alternatives defies easy or comprehensive generalization. The models clearly share one common trait: they are all statements of the conservation of mass. However, making that statement is complicated by the fact that motion is a continuous spectrum in space and time. Any difference in the model in characterizing space or time thus necessarily affects the nature of the conservation of mass statement. Formally, the statement arises by averaging Equation 2.1 over time or space or both, and differences in the periods of averaging are seen in the advective transport and diffusive or dispersive transport. In the following section, we review how some prominent lake models treat the problem of characterizing transport. The influence of spatial averaging is more pronounced in these lake models and we emphasize that aspect of model formulation in our review.

2.5.3 Review of Selected Models

In this review we examine some of the more well-known models of water quality in large lakes. Our emphasis is on spatial detail and hydrodynamic transport, however we will indicate the models' biogeochemical formulations as well. The order of presentation will be from spatially simple to complex, beginning with multiple-box models.

DiToro and Matystik (1980) and DiToro and Connolly (1980) have recently published models of Lake Huron and Lake Erie. The models are similar in their treatment and determination of transport, although they differ in their biogeochemical formulation. The Lake Erie biogeochemical model is more complex, using fifteen compartments to model the dissolved oxygen, phosphorus, nitrogen and silicon cycles. The Lake Huron model considers only the phosphorus and nitrogen cycles, requiring eight model compartments. The emphasis of both models is upon the biogeochemical

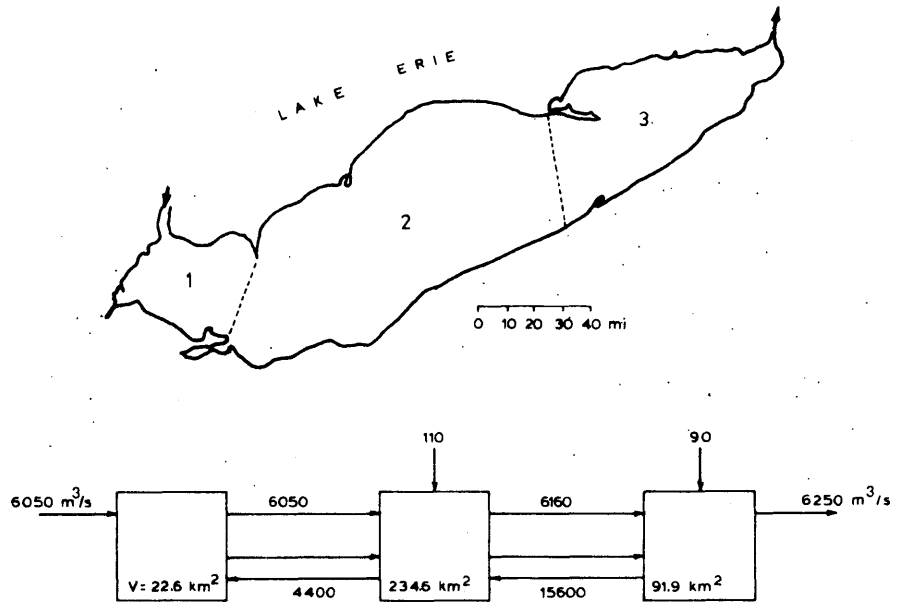

Figure 2.7

DiToro and Connolly (1981) multiple-box Lake Erie model

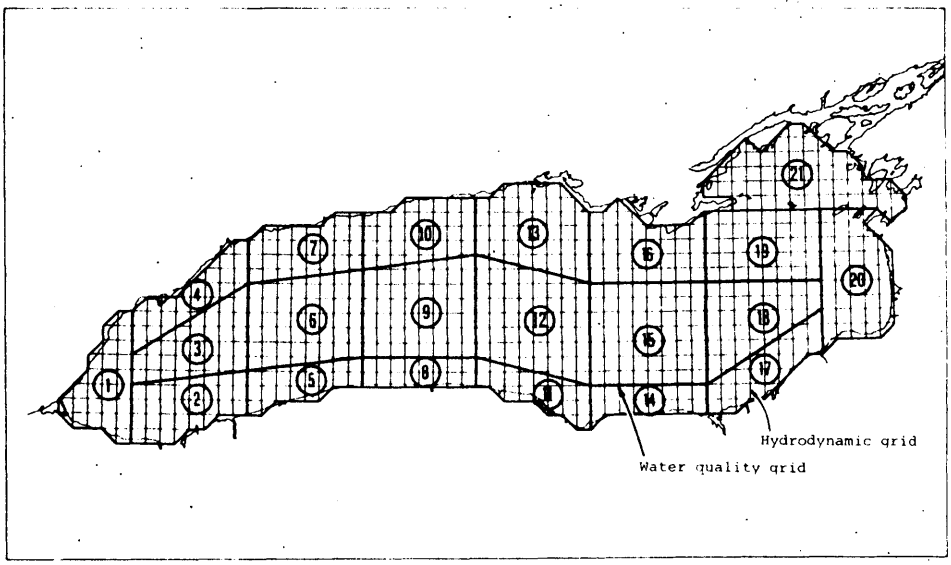

Figure 2.8

CCIW Lake Ontario model

kinetics, and sophisticated formulations are developed to model the element cycles. A computational time step of one-half day is used for both models.

Simple spatial structures and transport models accompany the complex biogeochemical kinetics in DiToro et al.'s models. The models are of the multiple-box type. Both lakes are modeled as three horizontal segments -- in two vertical layers in the Lake Huron model and in three layers in the Lake Erie model. In both models, horizontal advection, which is confined to the surface layers, is determined by flow budgets based on long-term observed hydrology. The advective transport is thus steady, reflecting the net rate of transport through the lakes over periods of some years. The diffusive transport is determined by calibration against observed temperature and chlorinity in Lake Huron, but against only temperature in Lake Erie. The segmentation and calibrated flows for Lake Erie are shown in Figure 2.7.

Somewhat greater complexity is found in the three-dimensional multiple-box models used by a number of researchers including Thomann et al. (1975 and 1979), Chen et al. (1975 and 1979), and Richardson (1976). The Thomann model, LAKE3, consists of a total of sixty-seven finite segments arranged into five layers. The horizontal subdivision varies from twenty-six segments in each of the upper layers, to ten, three and two segments as one proceeds downwards through the three lower layers.

Thomann et al. devote considerable effort to model calibration and verification in their study published in 1979. As a result of their calibration efforts, they changed the model biogeochemical structure from that originally proposed in 1975. Initially a ten compartment model of the nitrogen and phosphorus cycles was employed; however, this was replaced by an eleven compartment model incorporating silicon as well.

Thomann et al. depended largely upon field data to specify transport in the model. Advective flows were given for winter and summer conditions as best estimates based on field observations, using published mathematical circulation model results as an additional guide. Sensitivity to advective transport was tested and found small for reduction of transport by a factor of ten. Dispersion coefficients were found by calibration using temperature as a tracer.

The Thomann model is very similar to DiToro's models, but extends the analysis to two horizontal dimensions with greater spatial detail. The element cycles are modeled similarly in both models, and the treatment and determination of transport is essentially the same. For transport, both use an ad hoc procedure to specify advection and dispersion. The transports are treated as steady or quasi-steady, and determined in an approximate fashion from available field data and steady-state circulation model results. Horizontal dispersion is generally held constant, with the exception that Thomann assumes dispersion between nearshore and offshore regions to drop to zero from mid-April to the end of May as a consequence of the thermal bar effect. Thomann uses a computational time step of about two hours.

The model developed by Chen et al. (1975 and 1979) is more complex than that of Thomann et al., yet it is based upon generally similar principles. The model is a multiple-box type, segmenting the lake into forty-one horizontal boxes extending over eight layers. The biogeochemical model includes thirty-nine compartments and considers the phosphorus, nitrogen, silicon and carbon cycles as well as pH and inert tracer substances. The computation time step is one day. The transport model departs from the procedures used in the models reviewed previously -- rather than using calibrated steady or quasi-steady flows, Chen et al. employ simulation results from a numerical circulation model to specify flow between the boxes. The authors do not, however, state the procedures followed to specify dispersion.

Richardson (1976) constructed a model of Saginaw Bay in Lake Huron along the same lines as Thomann's model, but including only a single conservative substance, chloride. Richardson's paper is a narrative description of the steps followed in first setting and then modifying the model transports to achieve a calibration with field observations. The most striking aspect of this procedure is the degree of improvisation and extrapolation of observations necessary to arrive at transport quantities. Richardson first poses a steady transport regime based on published observations. This is calibrated to duplicate observed concentrations when assuming steady conditions, but the calibration subsequently fails in attempts to reproduce transient observations. This leads to a two-season transport specification hypothesized from observations of a spring thermal bar effect. Although the final model results are a fair match to field data, the procedure begs many questions: Can the calibrated transport be unique? Can the calibration be used successfully for any year of observation? Is there a more direct, less empirical means to quantifying transport for the model?

All of the preceding models were of the multiple-box or finite section type. The alternative formulation, the finite difference model, has been employed by fewer researchers, most notably Simons, Lam and others at the Canadian Center for Inland Waters (CCIW). Other examples of finite difference models are given by Paul et al. (1979).

The CCIW model, with variations, has been applied to Lake Ontario (Boyce et al., 1979 and Simons, 1976), Lake Erie (Lam and Jaquet, 1976 and Lam and Simons, 1976) and Lake Superior (Lam and Halfon, 1978). The models share some common features. For all, a multi-layer circulation model was employed to determine the advective transport. The circulation model employed a finite difference method on a square mesh grid. The grid size ranged from 5 km on Lake Ontario, to 6.67 km on Lake Erie, to 10 km on Lake Superior. The results from the circulation simulations were averaged over time for Lake Ontario (over the inertial period, seventeen hours) and Lake Erie (one day) prior to use in the water quality simulations.

The treatment of spatial discretization varies considerably in the water quality components developed to model the different lakes. In Lake Erie, coincident finite difference grids were employed for both circulation and water quality so that the advective flux from the circulation model could

be used as transport in the water quality model with no modification for spatial differences. However, the circulation model output was, as mentioned above, averaged in time to remove transient oscillations. The diffusive transport was defined from the concept of sub-grid-scale turbulence. Both the circulation and water quality models employed a single layer formulation for most of the simulation year, using a two layer model only during summer stratification.

The basic water quality transport model for Lake Erie was employed to model both chloride (Lam and Simons, 1976) and phosphorus (Lam and Jaquet, 1976). Chloride is conservative and thus requires but a single model component. It was simulated with a six-hour computation time step; the results were compared with extensive field data and verified. Also, the sensitivity to the sub-grid-scale turbulent diffusion coefficient was tested and found moderate -- coefficients in the range 25 to 75 m^2/s proved satisfactory. The chloride model served as the foundation for a two-component phosphorus model. The phosphorus model considered transport, settling and resuspension/regeneration to be the major mechanisms controlling total phosphorus, with simulation results revealing transport to be dominant. Only the period after the autumn overturn (the single-layer situation) was modeled for phosphorus; reasonably good agreement with field data was achieved. The computation time step used in the chloride model was doubled in the phosphorus model, to twelve hours.

In Lake Superior, Lam and Halfon (1978) used an approach slightly different from that followed in the Lake Erie model. The water quality model of Superior employed a grid size of 20 km, twice that in the linked hydrodynamic model. Vertically, a four-layer model was used for both water quality and hydrodynamics. Horizontal advective transports in the water quality model were determined by appropriately summing the circulation computed in the hydrodynamic simulation. Diffusion was defined from the grid size following the sub-grid-scale diffusion concept. The biochemical component of the water quality model was the two-species phosphorus model used for Lake Erie. The model was exercised in three different modes: in the first, a one-box (spatially uniform) model was run; in the second, the 20 km grid model was run; and in the third, the grid model was run, but without considering transport. All three predicted similar lake-wide average concentrations. However, the multiple-box model with transport showed important nearshore-offshore differences in phosphorus concentration which were corroborated by field data. Neglect of transport led to significant departures from the spatial patterns observed in the field.

CCIW's most recent modeling effort is the study of Lake Ontario. The horizontal discretization used for Lake Ontario is a dramatic departure from the two previous lake models. As shown in Figure 2.8, the water quality model was not based upon a regular mesh, but rather, upon irregular segments. The published description of horizontal transport is a bit sketchy, particularly for the determination of diffusive transport. Advection was found by summing the hydrodynamic model results (spatially interpolated where necessary) over the faces of the water quality segments. Diffusive transport could be computed in either of two ways,

according to Boyce et al. (1979). Equal but opposite exchange flows between the segments could be found by calibration or computed from sub-grid-scale diffusion coefficients. The description by Simons (1976) implies the latter was used, however no procedural details are given. The model employs a four-layer vertical structure, computing vertical diffusive transport as a function of density stability. The transport model was verified in simulations of temperature prior to modeling phosphorus.

The Lake Ontario model version reported by Simons (1976) included a complex biochemical model based on the previously described Thomann et al. (1975) formulation. Simons made no changes in Thomann's model, except to use a longer computational time step, one-half day. The three situations tested with the Lake Superior model were once again compared: a one-box model, a spatially discretized model, and a discretized model without transport. The findings were similar to those given earlier -- the inclusion of spatial detail improved the agreement with observations, but was not necessary to capture the lake-wide average behavior.

The Lake Ontario project summary (Boyce et al., 1979) is frustratingly inconclusive. The work reported earlier by Simons is only referenced in the summary although results from a simpler two-component phosphorus model are discussed. Despite many years of experience in modeling the Great Lakes with different approaches to biochemical simulation and in the treatment of transport and spatial discretization, the authors offer no conclusions or recommendations. Their closing remarks simply state that more work is necessary on individual model components before lake models can be fruitful. Unfortunately, their failure to completely report their findings from the different model formulations prevents us from drawing firm conclusions, although it is clear that spatial discretization is necessary if it is desired to predict more than simply the lake-wide response.

Similarly inconclusive is the report by Paul et al. (1979). From a number of lake modeling efforts discussed in Paul's report, the most pertinent to this review is the study of Lake Baikal in the U.S.S.R. Lake Baikal was modeled using a three-dimensional finite difference model as well as a multiple-box model consisting of fourteen boxes. The three-dimensional model was based upon a finite difference solution on a 15 km by 7.8 km horizontal grid. Advective transport for the finite difference model was determined in a 3-D hydrodynamic circulation model with a coincident grid; diffusive transport was based upon sub-grid-scale diffusion. A single conservative substance was modeled. The fourteen-segment model employed a much simpler approach. The segments were more or less arbitrarily specified, and long-term transport between the segments was found from the mean current pattern in an approximate fashion. Unfortunately, no results from the fourteen-segment model are given and thus it is impossible to compare results from the two modeling approaches. The report therefore offers no conclusions or recommendations as to the preferred water quality modeling technique -- a finite difference model or a multiple-box model.

2.5.4 Analysis of Mass Transport Formulations

The preceding review of the state-of-the-art in modeling water quality in large lakes reveals widely varying approaches in the treatment of transport and spatial structure. We believe mass transport and spatial structure to be a fundamental issue in lake water quality modeling and particularly in coupled hydrodynamic and biogeochemical models. In this section we will present a theoretical analysis of hydrodynamic transport in the water quality model and examine aspects of that theory in lake models. The theory and illustrations will examine the differences between box models and finite difference models.

Multiple-box and finite difference models have been used in many different applications, however previous researchers have offered no conclusions as to the preferable formulation. As an approximation of the continuous differential equations, the finite difference models should offer greater detail and accuracy. Yet, multiple-box models are in wide use with an apparently reasonable degree of success. What, then, is the fundamental distinction between finite difference models and box models in their ability to capture water quality transport and reaction?

Conceptual Reactor Models

To begin to answer this question we can look upon the lake as a simple reactor vessel similar to the engineered vessels used in wastewater treatment or chemical engineering. In those fields a number of conceptual models have been developed to represent the flow and mixing characteristics of the reactors. The fully-mixed tank presented in Section 2.4.1 is one such model. For Lake Balaton, two other conceptual models are of interest: the tanks-in-series reactor and the dispersed flow reactor. For simplicity, our analysis will be directed to models of one-dimensional transport. However, our conclusions are of wider validity and generally apply to three and two-dimensional modeling as well as one-dimensional.

Before examining the tanks-in-series and dispersed flow models, it is useful to discuss the most fundamental models, the fully-mixed tank and the plug flow reactor (shown schematically in Figure 2.9). These models are the end points in a continuous spectrum of models and their flow and mixing characteristics bracket all others. Such characteristics are conveniently determined by the concentration seen in the reactor outflow in response to a pulse injection of conservative, unreactive tracer entering with the inflow to the reactor. The fully-mixed tank instantaneously and completely mixes the injected mass throughout the reactor. The tracer is thus immediately observed in the outflow and slowly decreases in concentration as it is diluted with fresh, tracer-free inflow. The concentration response is:

$$\frac{c}{c_0} = e^{-t/t^*} \qquad (2.3)$$

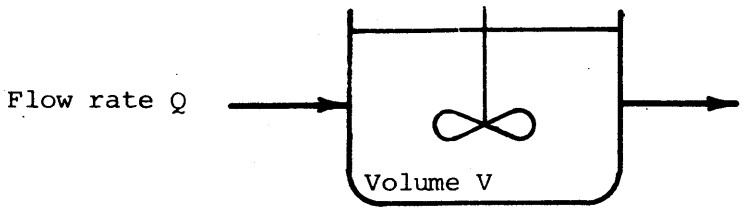

a. Single fully-mixed tank

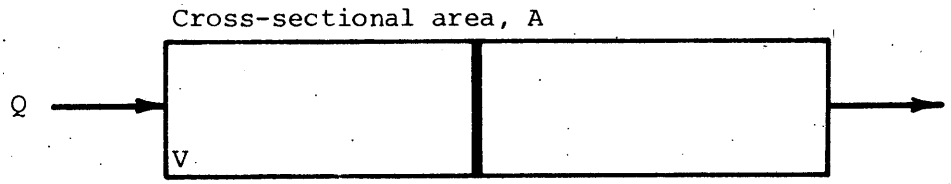

b. Plug flow reactor

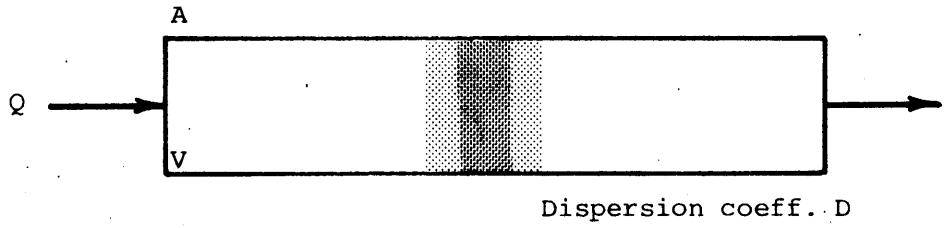

c. Dispersed flow reactor

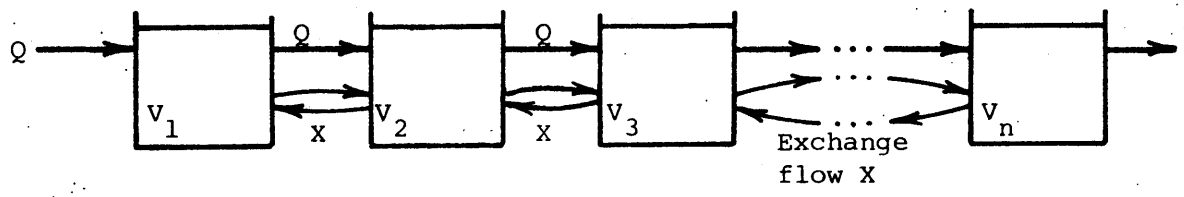

d. Tanks-in-series with exchange flow

Figure 2.9

Conceptual models of reactor vessels

where
- c is the outflow concentration,
- M is the mass of injected tracer,
- V is the tank volume (constant in time),
- t is the time since tracer injection,
- t^* is the tank residence time, given by Q/V,
- Q is the flow into and out of the tank (constant in time), and
- c_o is the reference concentration, defined as M/V.

While the fully-mixed tank is based on the premise of infinitely strong mixing, the plug flow reactor supposes no mixing to occur at all. A tracer injection entering the plug flow tank simply travels through the tank as a plug, exiting the tank unaltered after the time to traverse the tank. Its concentration response is:

$$\frac{c}{c_0} = \begin{cases} \infty & t = t^* \\ 0 & \text{otherwise} \end{cases} \qquad (2.4)$$

The concentration is infinite since undiluted tracer has that concentration by definition.

The dispersed flow reactor gives a response falling between the plug flow and fully-mixed limits; it is a reactor which includes mixing, but not the infinite mixing of the fully-mixed tank (Figure 2.9). The mathematical basis of the model is the one-dimensional advective-dispersion equation.

$$A \frac{\partial c}{\partial t} + UA \frac{\partial c}{\partial x} = A \frac{\partial}{\partial x} \left(D \frac{\partial c}{\partial x}\right) \qquad (2.5)$$

where
- U is the cross-sectionally averaged advective velocity,
- A is the cross section area, and
- D is the one-dimensional dispersion coefficient.

In this simplified version of the equation, the substance of interest is assumed conservative with no loss or gain of mass, and the cross-sectional area and average velocity are assumed constant with x. This model shares the governing equation and is thus the conceptual equivalent of the one-dimensional lake water quality model. For a reactor of finite volume this equation must be solved with the boundary conditions that the total flux at $x = 0$ is zero after the pulse injection ($t > 0$):

$$Qc - AD \frac{\partial c}{\partial x} = 0 \qquad \text{at } x = 0 \tag{2.6a}$$

and that the dispersive flux at the end of the reactor is zero:

$$AD \frac{\partial c}{\partial x} = 0 \qquad \text{at } x = L \tag{2.6b}$$

where D is the dispersion coefficient,
A is the tank cross-sectional area, and
L is the tank length.

(In many analyses, the second boundary condition is improperly replaced by the condition that $c = 0$ at $x = \infty$, leading to an incorrect solution for a finite tank.) The solution of Equation 2.5 with boundary conditions 2.6 for a pulse tracer input is given by Thomas and McKee (1944):

$$\frac{c}{c_0} = 2 \sum_{n=1}^{\infty} \frac{\mu_n (Pe/2 \sin \mu_n + \mu_n \cos \mu_n)}{\left[(Pe/2)^2 + \mu_n^2 + Pe\right]}$$

$$\exp\left\{\frac{Pe}{2} - \left[\frac{(Pe/2)^2 + \mu_n^2}{Pe}\right]\frac{t}{t^*}\right\} \tag{2.7}$$

The nth root, μ_n, in this equation is defined by the implicit relation:

$$\cot \mu_n = \frac{1}{2}\left[\frac{\mu_n}{Pe/2} - \frac{Pe/2}{\mu_n}\right] \tag{2.8}$$

Pe is the Peclet Number, the dimensionless ratio of advection (through-flow) to dispersion (mixing); it is defined as:

$$Pe = \frac{QL}{AD} \tag{2.9}$$

The Peclet Number is a convenient measure of the reactor's dispersive character. In the limit that dispersion becomes infinite -- the fully-mixed tank -- the Peclet Number is 0. As the dispersion vanishes and the reactor approaches plug flow, the Peclet Number becomes infinite. The response of the dispersed flow reactor, as given by Equation 2.7, is shown in Figure 2.10 for a range of Peclet Numbers.

The tanks-in-series model is the conceptual equivalent of the multiple-box lake model. Shown schematically in Figure 2.9, the model consists of a series of tanks with through-flow entering the first tank, passing from the first tank to the second, and so forth until it exits the last tank. The model may be made more complex by including equal but opposite exchange flows between neighboring tanks, or by considering tanks of unequal volumes. For the simplest configuration, n equal volume tanks with no exchange flow, the response to a pulse injection is given as:

$$\frac{c}{c_o} = \frac{n}{(n-1)!}\left(\frac{t}{t^*}\right)^{n-1} \exp\left(-\frac{t}{t^*}\right) \qquad (2.10)$$

where
- c is the concentration in the outflow of the nth tank,
- V is the volume of an individual tank, and
- t^* is the residence time of one tank, equal to V/Q, and
- c_o is the reference concentration, equal to M/nV.

Equation 2.10 is plotted for various values of n in Figure 2.11. For n equal to 1, the response is obviously that of a single fully-mixed tank. Less obvious is the response as n becomes infinite -- in that case the series behaves as the plug flow reactor. In the intermediate range of n, the tanks-in-series model implicitly includes a degree of mixing; this can be seen by comparing tanks-in-series responses with those of dispersed flow reactors.

The addition of exchange flows between tanks-in-series has the effect of increasing mixing. The equation for this model cannot be solved analytically; however numerical solutions are given by Tuan et al. (1980). Solutions for equal volume tanks-in-series are shown in Figure 2.12 for various values of the exchange ratio, α, defined as:

$$\alpha = \frac{X}{Q}$$

where X is a constant exchange flow between all tanks.

As can be seen, in the limit that α becomes infinite, the concentration response approaches the fully-mixed tank.

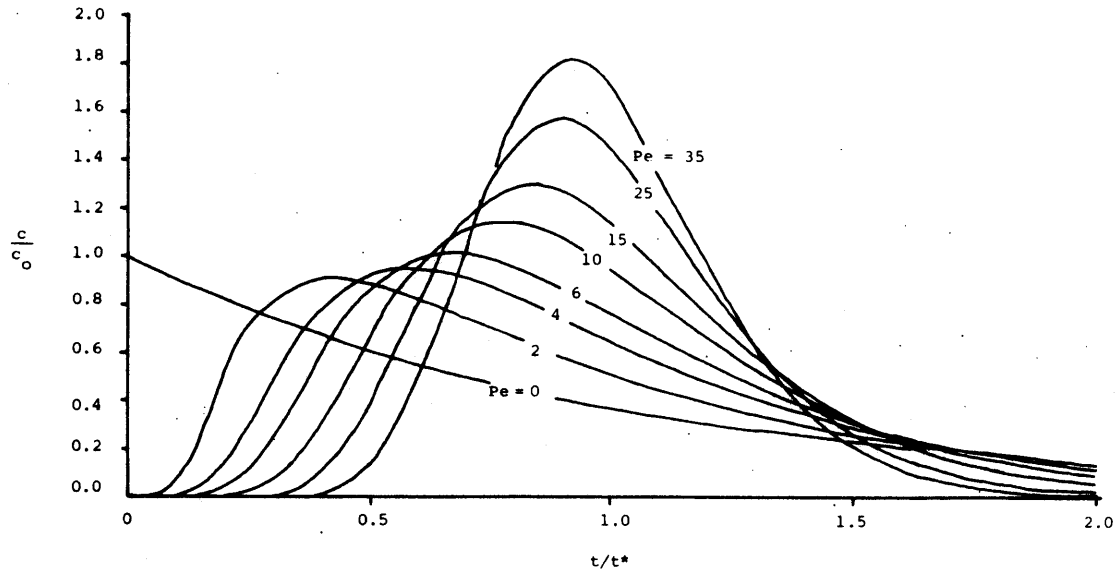

Figure 2.10

Response of dispersed flow reactor to pulse input
as a function of Peclet Number, Pe

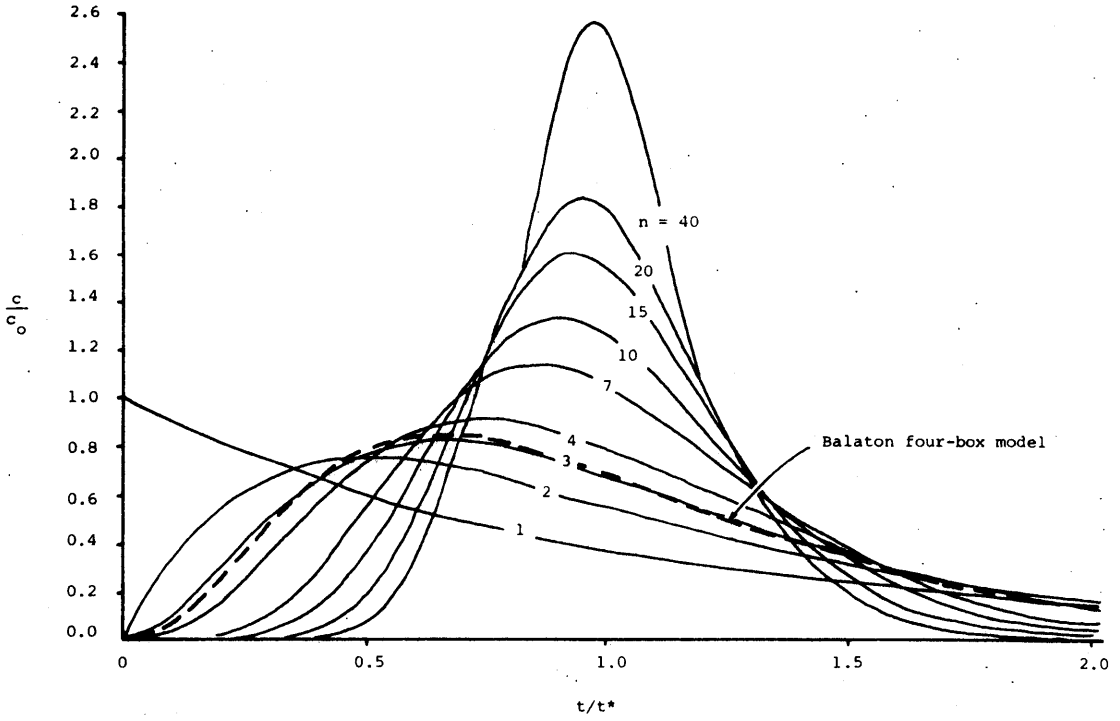

Figure 2.11

Response of fully mixed tanks-in-series to pulse input
as a function of number of tanks, n

The effect of unequal tank volumes is a function of the relative tank sizes and the number of tanks, and must be treated on a case-by-case basis. The solution can be derived, for tanks without exchange flow, by repeated application of the unit impulse response for a single tank (Thomann, 1972):

$$u(t) = \frac{1}{V} \exp\left(-\frac{t}{t^*}\right) \qquad (2.11)$$

The response of fully-mixed tank number i in a series of tanks is the convolution of the unit impulse response with the mass inflow:

$$c_i(t) = \int_0^t M_i(\tau)\, u_i(t-\tau)\, d\tau \qquad (2.12)$$

where $M_i(t)$ is the mass inflow to tank i as a function of time,
$u_i(t)$ is the unit impulse response based on the volume and residence time of tank i, and
c_i is the concentration response of tank i.

For the first tank in a series $M_1(t)$ is the impulse input, and Equation 2.12 yields the solution in Equation 2.3. For the ith tank, $M_i(t) = QC_{i-1}(t)$, so that the solution to the complete series can be built by proceeding stepwise through the tanks. For example, for four unequal tanks-in-series the solution is:

$$\frac{c}{c_o} = (1+r_2+r_3+r_4)\left\{\frac{1}{(1-r_2)(1-r_3)(1-r_4)} \exp\left(-\frac{t}{t^*}\right) + \right.$$

$$\frac{r_2^2}{(r_2-1)(r_2-r_3)(r_2-r_4)} \exp\left(-\frac{t}{r_2 t^*}\right) +$$

$$\frac{r_3^2}{(r_3-1)(r_3-r_2)(r_3-r_4)} \exp\left(-\frac{t}{r_3 t^*}\right) +$$

$$\frac{r_3^2}{(r_4-1)(r_4-r_2)(r_4-r_3)} \exp\left(-\frac{t}{r_4 t^*}\right) \Bigg\} \qquad (2.13)$$

where c_o is the reference concentration based on the total series volume, equal to $M/(V_1+V_2+V_3+V_4)$,

t^* is the residence time based on tank 1, equal to V_1/Q, and

r_i is the volume ratio of tank i to tank 1, equal to V_i/V_1.

The response of this model using the volume ratios of the four Lake Balaton basins is shown as the dashed line in Figure 2.11. The volume of Basin I is much smaller than the other, more nearly equal basins, so that the total Balaton response is nearly that for three equal tanks-in-series.

Relating Dispersed Flow Reactors and Tanks-in-Series

The similarity of the dispersed flow and tanks-in-series reactor responses is apparent in Figures 2.10 and 2.11, and the reactor characteristics have been related by a number of researchers. Determining the variance of the concentration with time as an analytical expression of dispersion, Levenspeil and Bischoff (1963) found the following relation between the number of tanks, n, and the dispersed flow reactor Peclet Number, Pe:

$$\frac{1}{n} = \frac{2}{Pe^2}(Pe - 1 + e^{-Pe}) \qquad (2.14)$$

For large n and Pe this approaches $Pe = 2n-1 \simeq 2n$. This relation neglects the influence of exchange flow in the tanks-in-series reactor, however. We can isolate the influence of the exchange flow upon the tanks-in-series Peclet Number by using the following relation between exchange flow and the dispersion coefficient:

$$X = \frac{DA}{\Delta x}$$

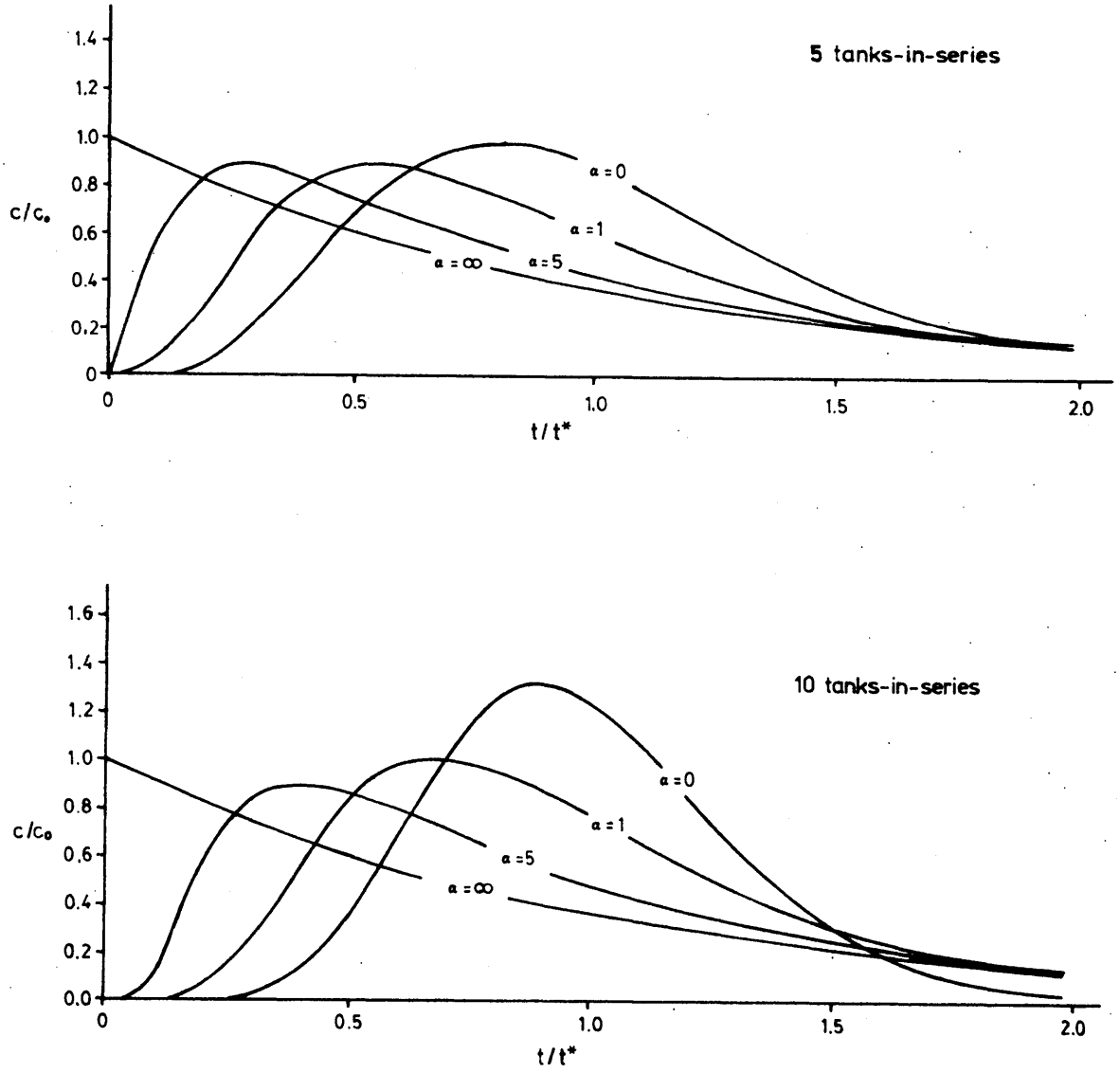

Figure 2.12

Response of fully mixed tanks-in-series
with exchange flow to pulse input

(This relation is derived below as Equation 5.14). Substituting $L = n\Delta x$ for n equal tanks, and employing the definition of the Peclet Number, $Pe = QL/AD$, we find the Peclet Number due only to exchange flow for the tanks-in-series model:

$$Pe' = n\frac{Q}{X} = \frac{n}{\alpha} \qquad (2.15)$$

We thus have two Peclet Numbers, one implicit in the number of tanks (which for large n is approximately $Pe \approx 2n$) and one due to exchange flow ($Pe' = n/\alpha$). The combined influence of these two effects is:

$$Pe'' = \frac{1}{\frac{1}{Pe} + \frac{1}{Pe'}} = \frac{2n}{2\alpha + 1} \qquad (2.16)$$

This relation agrees with that given by Zvirin and Shinnar (1976). The influence of the exchange flow can be seen to decrease the tanks-in-series Peclet Number by a factor of $2\alpha+1$. There are two asymptotes for Equation 2.16:

$$Pe'' = Pe \quad \text{for } Pe' \gg Pe \quad (\alpha \ll \tfrac{1}{2})$$

$$Pe'' = Pe' \quad \text{for } Pe \gg Pe' \quad (\alpha \gg \tfrac{1}{2})$$

Let us return for a moment to the tanks-in-series model without exchange flow and consider the limit of large n. In this limit, the tank length, Δx, becomes small and the model approaches a finite difference approximation of the differential equation for mass transport. Such approximations are known to include so-called numerical or artificial dispersion, an apparent dispersion arising from truncation errors in the finite difference equation (Bella and Grenney, 1970). A typical difference formulation is given as Equation 5.10 (in Figure 5.3). For Equation 5.10 the numerical dispersion in grid i, presuming $U = Q/A$ to be constant, is:

$$D_n = (\gamma_i + \gamma_{i+1} - 1)\frac{U\Delta x}{2} - \frac{U^2\Delta t}{2} \qquad (2.17)$$

The second term arises from truncation error in the approximation of the time derivative. The first term is a function of the spatial weighting coefficents, γ_i and γ_{i+1}. It occurs when upstream or downstream differencing is used for the advective term; or to be more precise, it is due to the truncation error in the spatial derivative because these differencing schemes are only first-order accurate in Δx. If the second-order accurate central difference is used ($\gamma_i = \gamma_{i+1} = 1/2$), this contribution to artificial dispersion disappears. In the multiple box model, $\gamma_i = \gamma_{i+1} = 1$ for flow from upstream to downstream. The numerical dispersion due to advective error alone is then:

$$D_a = \frac{U\Delta x}{2}$$

Using $\Delta x = L/n$ and rearranging we find:

$$\frac{UL}{D_a} = Pe = 2n$$

This says, for large n, that the numerical dispersion due to off-centered finite differences is equal to the implicit dispersion of the tanks-in-series model. Thus, the tanks-in-series implicit dispersion is, in a sense, numerical dispersion. However, it should be clear from Equation 2.14 that for small n, factors other than finite difference truncation error come into play. We will thus continue to distinguish between implicit dispersion, a factor in multiple-box models with a few tanks, and numerical dispersion, the error seen in finite difference models with large n. This distinction is subtle, but important.

Magnitude is an important aspect of the distinction between the implicit dispersion of the tanks-in-series model and the numerical dispersion in finite difference approximations of dispersed flow. In a well-constructed finite difference model, the numerical dispersion will be small and will be dominated by the dispersion specified through the model dispersion or diffusion parameter. In a tanks-in-series model, however, the implicit

dispersion is large. It is a major determinant of the model behavior; in fact, in the absence of exchange flows it is the only dispersion in the model. Application of the tanks-in-series model to chemical engineering or water treatment problems employs the implicit dispersion as a surrogate for the actual dispersion of the reactor. That is, the number of tanks n is chosen to produce an effluent response similar to that observed from the physical system; as such, the number of tanks is a calibration parameter. An equivalent procedure would be to enter Equation 2.16 with the Peclet Number, Pe, of the system to be modeled, and choose n and α to achieve an equivalent dispersion in a tanks-in-series model. Stefan and Demetracopoulos (1981) use this philosophy to apply a tanks-in-series model (without exchange) to riverine transport, however we know of no similar treatment of n as a calibration parameter in lake or reservoir modeling.

2.5.5 Conclusions for Lake Model Formulation

The preceding analysis of conceptual reactor models is important to lake water quality modeling in two ways: it allows direct comparison of the hydrodynamic properties of the multiple-box and finite difference models, and most important, it points out the implicit dispersion contained in multiple-box models. This implicit dispersion is the fundamental distinction between the box (or finite section) models and the finite difference models, aside from the obvious difference of spatial resolution in the model results. The consequence of the implicit dispersion is diminished control over the mixing characteristics of the multiple-box water quality model. Control exists in the continuum model through explicit diffusion or dispersion parameters which the modeler specifies. In contrast, the box model without exchange flow permits no specification of dispersion other than that hidden within the selected number of tanks. Even if an exchange flow is specified, it must significantly exceed the through-flow if it is to dominate the dispersion implicit in the number of tanks. If the exchange flow is less, as will often be the case, the lake must be subdivided into tanks so as to achieve the desired dispersion, rather than making a subdivision based on lake bathymetry or the desire for predictions at particular locations.

A corollary to the arguments of the preceding paragraph is the problem which arises when a box model is formulated with no consideration for its implicit dispersion. This, unfortunately, appears to be the usual practice in multiple-box models for lake water quality where box boundaries are typically chosen based only on lake geometry. In this case, unless the implicit dispersion is fortuitously near that of the actual lake, the resulting model bears little resemblance to the system is purports to model.

Ignorance of the implicit dispersion can also lead to error in specifying exchange flows for a multiple-box model. Clearly, the hydrodynamic characteristics of box models are not uniquely related to those of the physical system -- a fact which must be realized in model design and parameter estimation. Particularly when unequal boxes with varying exchange and through-flows are used, the box model exchange flow cannot be specified directly from field data or circulation model results.

Some modelers imply that field data or circulation model results can be used to specify the exchange flows. However, this is simply not accurate: there is no well-founded method to relate the observed flow history or velocity distribution to the model exchange flow. To see this, consider the implications of the relation between the exchange flow, X, and the dispersion coefficient, D, for one-dimensional transport:

$$X = \frac{DA}{\Delta x}$$

According to this, the exchange flow and the dispersion coefficient do not have a unique relation based only on the properties of the physical system: the model parameter Δx intervenes. Given that D and A are properties of the physical system, it is clear that X cannot be found independently of the model formulation. One cannot, for example, determine the velocity distribution in a cross section of the lake, find the mean velocity in that section, and then sum the positive deviations from the mean to get an exchange flow. Although this deviation flow, and the equal but opposite flow due to negative deviations, are clearly involved with mixing in the lake, they cannot be related to the multiple-box exchange flow, X, in any straightforward manner.

The only available route to determination of exchange flows or dispersion coefficients in the multiple-box models is calibration. Calibration is acceptable under certain conditions. For example, calibration against a conservative tracer is a sound procedure if sufficient data are available. Nonconservative tracers, such as temperature, are far less suitable, however. If the interreacting variables of the water quality model are used rather than independent tracers, the calibration procedure becomes rapidly unworkable. A transport calibration performed through the biogeochemical model only compounds the already difficult problem of calibrating biogeochemical rate constants by adding hydrodynamic parameters as well. Such a procedure confuses biogeochemical with hydrodynamic influences and generally obscures the character of the model. A far more attractive alternative is a model in which hydrodynamic parameters can be determined directly from hydrodynamic data, either field data or circulation model simulations, independently of the model biogeochemistry.

In summary, our analysis of conceptual reactor models has found current lake modeling practice based on multiple-box models to have serious inadequacies. Two major failings are evident. First, the multiple-box models carry within their formulation a substantial degree of implicit dispersion governed by the number of boxes in the model. This dispersion is usually not properly considered when multiple-box models are constructed. Second, a parameter which can be purposely varied to control mixing in the model is the exchange flow -- however there is no rigorous means to determine exchange flows from lake hydrodynamics. These failings greatly impede the modeler seeking rational model design. He has available only two parameters to control the model dispersion. One is the number of boxes, n, which he would prefer to fix from the lake's

geometrical characteristics. Second is the exchange flow, which can only be found properly by calibration against field measurements of a conservative tracer. In current practice, the modeler rarely appreciates the subtle influence of these parameters upon mixing in the model. Consequently, their effects are ignored and an erroneous or inappropriate model is employed.

3 LAKE CIRCULATION MODELING

3.1 Introduction

The circulation of water within a lake or reservoir is a major determinant of the lake's water quality behavior. Too often, this influence is treated inadequately in models of lake water quality, which tend to employ simple box models and long-term average flows. In later chapters, we will develop a water quality model which includes a more sophisticated hydrodynamic component. As background to the development of that model, this chapter presents an overview of lake circulation modeling.

Two major classes of motion, horizontal and vertical, will be dealt with in the discussion to follow. Horizontal circulations are those due predominately to the travel of water from the inflow points of the lake to the outflows, or arising from the force of wind upon the water surface. Vertical circulations arise from the differences in water density in a stratified lake and are produced when various agents disrupt the normally stable stratification. Mixing by the wind, inflows of high or low density water, and heating or cooling at the water surface are typical agents.

Excluded from this chapter are a number of types of water motion which do not involve the large scale travel of water masses. Surface waves are the major class of these omitted smaller scale processes. The discussion to follow is general, however, in the sense that models appropriate to both deep and shallow lakes, rather than just shallow, are presented.

3.2 Mathematical Formulation of Lake Circulation

The equations of fluid motion in a lake are the departure point from which all mathematical circulation models must begin. These equations include the equations of conservation of mass (or the continuity equation), and the equation of conservation of momentum in each of the three coordinate directions. For an incompressible fluid, the continuity equation is:

$$\frac{\partial u}{\partial x} + \frac{\partial v}{\partial y} + \frac{\partial w}{\partial z} = 0 \qquad (3.1)$$

where

x and y	are the horizontal direction components, as shown in Figure 3.1,
z	is the vertical direction component, measured downwards from the mean water surface elevation, and,
u, v, w	are the fluid velocity components in the x, y and z directions respectively.

The momentum equations express the acceleration of the fluid resulting from various forces. The equations in the horizontal plane are given as Equations 3.2 and 3.3. For clarity, the correspondence between the terms in the equations and the physical accelerations and forces which they represent is shown:

$$\underset{(a)}{\frac{\partial u}{\partial t}} + \underset{(b)}{\left\{u \frac{\partial u}{\partial x} + v \frac{\partial u}{\partial y} + w \frac{\partial u}{\partial z}\right\}} =$$

$$\underset{(c)}{fv} \underset{(d)}{- \frac{1}{\rho} \frac{\partial p}{\partial x}} + \underset{(e)}{A_H \left\{\frac{\partial^2 u}{\partial x^2} + \frac{\partial^2 u}{\partial y^2}\right\}} + \underset{(f)}{\frac{\partial}{\partial z} \left(A_V \frac{\partial u}{\partial z}\right)} \qquad (3.2)$$

$$\underset{(a)}{\frac{\partial v}{\partial t}} + \underset{(b)}{\left\{u \frac{\partial v}{\partial x} + v \frac{\partial v}{\partial y} + w \frac{\partial v}{\partial z}\right\}} =$$

$$\underset{(c)}{-fu} \underset{(d)}{- \frac{1}{\rho} \frac{\partial p}{\partial y}} + \underset{(e)}{A_H \left\{\frac{\partial^2 v}{\partial x^2} + \frac{\partial^2 v}{\partial y^2}\right\}} + \underset{(f)}{\frac{\partial}{\partial z} \left(A_V \frac{\partial v}{\partial z}\right)} \qquad (3.3)$$

where
- t is the time variable,
- f is the Coriolis parameter,
- p is the fluid pressure,
- ρ is the fluid density,
- A_H, A_V are the horizontal and vertical eddy viscosities respectively.

The terms of these equations have the following meanings:

a - the instantaneous or local acceleration of the fluid at a point

b - the convective acceleration, caused when fluid is transported from one point to another of different fluid velocity

c - the Coriolis force due to the earth's rotation

d - the horizontal pressure force

e - the horizontal transport of momentum due to shear stresses

f - the vertical transport of momentum due to shear stresses

The momentum equation in the vertical direction is entirely similar to those above, but includes an additional term on the right hand side to represent the force due to the gravitational acceleration, represented by g. The equation is considerably simplified by the realization that the pressure and gravitational forces dominate all others. Neglect of the lesser terms is known as the hydrostatic approximation, and leads to the equation:

$$\frac{1}{\rho}\frac{\partial p}{\partial z} = -g \qquad (3.4)$$

The boundary conditions for these equations are specified at the free surface, the lake bottom, and the lake shoreline. At the free surface, the kinematic boundary condition specifies that continuity be maintained:

$$-\frac{\partial \eta}{\partial t} - u\frac{\partial \eta}{\partial x} - v\frac{\partial \eta}{\partial y} = w \quad \text{at } z = -\eta \qquad (3.5)$$

where $-\eta$ is the free surface displacement.

An additional condition at the free surface represents the shear stress due to the wind:

$$-\rho A_V \frac{\partial u}{\partial z} = \tau_s^x \quad -\rho A_V \frac{\partial v}{\partial z} = \tau_s^y \quad \text{at } z = -\eta \qquad (3.6)$$

where τ_s^x is the x-component of the shear stress on the surface, and

τ_s^y is the y-component.

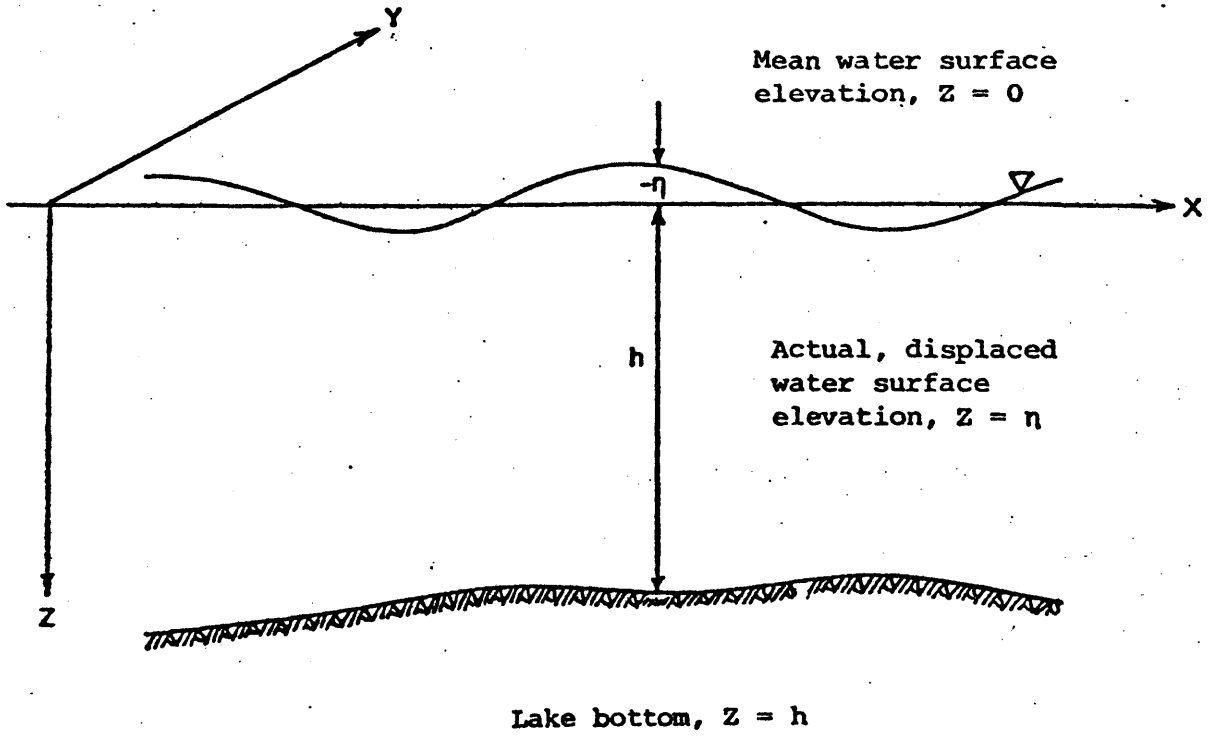

Figure 3.1
Definition sketch for mathematical formulation

At the lake bottom, a no-slip boundary condition specifies that the fluid in direct contact with the rough bottom cannot move:

$$u = v = 0 \quad \text{at } z = h \tag{3.7}$$

where h is the lake depth.

Alternatively, a shear stress condition similar to that at the surface may instead be specified:

$$-\rho A_V \frac{\partial u}{\partial z} = \tau_b^x \quad -\rho A_V \frac{\partial u}{\partial z} = \tau_b^y \quad \text{at } z = h \tag{3.8}$$

where τ_b^x is the x-component of the bottom shear stress, and

τ_b^y is the y-component.

At the lake perimeter, a no-flow no-slip boundary condition applies:

$$u = v = 0 \quad \text{at the x and y boundaries} \tag{3.9}$$

The equations and boundary conditions presented above are complex and their solution is difficult -- the non-linear convective terms and boundary conditions being particularly troublesome. As a consequence, most solution methods depend upon simplification of the equations by averaging to reduce the problem dimensions, or by neglecting the less important terms in the equations. We can gain insight into the relative importance of the various terms by transforming the equations to a non-dimensional form. This is done in Figure 3.2, where typical scales of length, depth, time and velocity have been used to normalize the dimensional variables. The scales employed are length, L; depth, H; time, 1/f; and velocity, U. As seen in Figure 3.2, this process gives rise to the Rossby number, Ekman numbers and Froude number as dimensionless parameters which indicate the relative magnitude of the terms in the equations. We will refer to these parameters in the following discussions of modeling strategies, assumptions and parameters.

Definition of Dimensionless Parameters

$$Fr = \text{Froude Number} = \frac{U}{\sqrt{gH}} \tag{3.10}$$

$$R_o = \text{Rossby Number} = \frac{U}{fL} \tag{3.11}$$

$$E_H = \text{Horizontal Ekman Number} = \frac{A_H}{fL^2} \tag{3.12}$$

$$E_V = \text{Vertical Ekman Number} = \frac{A_V}{fL^2} \tag{3.13}$$

Conservation of Mass

$$\frac{\partial u}{\partial x} + \frac{\partial v}{\partial y} + \frac{\partial w}{\partial z} = 0 \tag{3.14}$$

Conservation of Horizontal Momentum

$$\frac{\partial u}{\partial t} + Ro\left[u\frac{\partial u}{\partial x} + v\frac{\partial u}{\partial y} + w\frac{\partial u}{\partial z}\right] - v = -\frac{1}{\rho}\frac{\partial p}{\partial x} + E_H\left[\frac{\partial^2 u}{\partial x^2} + \frac{\partial^2 u}{\partial y^2}\right] + \frac{\partial}{\partial z}\left[E_V\frac{\partial u}{\partial z}\right] \tag{3.15}$$

$$\frac{\partial v}{\partial t} + R_o\left[u\frac{\partial v}{\partial x} + v\frac{\partial v}{\partial y} + w\frac{\partial v}{\partial z}\right] + u = -\frac{1}{\rho}\frac{\partial p}{\partial y} + E_H\left[\frac{\partial^2 v}{\partial x^2} + \frac{\partial^2 v}{\partial y^2}\right] + \frac{\partial}{\partial z}\left[E_V\frac{\partial v}{\partial z}\right] \tag{3.16}$$

local acceleration	convective acceleration	Coriolis force	pressure force	horizontal eddy momentum transport	vertical eddy momentum transport

Figure 3.2

Non-dimensional form of the governing equations

Conservation of Vertical Momentum (Hydrostatic Pressure)

$$\frac{\partial p}{\partial z} = -\frac{R_o}{F_r^2}\rho \tag{3.17}$$

Kinematic Boundary Condition

$$\frac{\partial \eta}{\partial t} + Ro\left[u\frac{\partial \eta}{\partial x} + v\frac{\partial \eta}{\partial y}\right] = \frac{R_o^2}{F_r^2}w \quad \text{at} \quad z = \eta\frac{F_r^2}{R_o} \quad \text{(surface)} \tag{3.18}$$

Surface and Bottom Boundary Conditions

$$\frac{\partial u}{\partial z} = \tau_s^x \qquad \frac{\partial v}{\partial z} = \tau_s^y \qquad \text{at} \quad z = \eta\frac{F_r^2}{Ro} \quad \text{(surface)} \tag{3.19}$$

$$\frac{\partial u}{\partial z} = \tau_b^x \qquad \frac{\partial v}{\partial z} = \tau_b^y \qquad \text{at} \quad z = -h \quad \text{(bottom)} \tag{3.20}$$

Figure 3.2

continued

3.3 Modeling Strategies

3.3.1 Introduction

The choice of the lake circulation model is determined by its intended use and the physical characteristics of the waterbody to be modeled. Modeling is not an inexpensive exercise, and one usually wishes to select the most appropriate and efficient model for the problem at hand. Also, a simpler model will be easier to use and less prone to error than one which is more complex, adding further impetus to the choice of an appropriate model.

This section briefly discusses the various classes of models based upon their representation of time and space. (See Figure 2.2.)

3.3.2 Temporal Representation

The temporal representations employed in lake circulation models are broadly classed as steady state or transient. The simpler steady state models produce a picture in which the lake is unchanging in time, and may be used when the lake's circulation remains roughly constant during the time scales of interest. Although they omit much detail, steady state models often supply sufficient information for the evaluation of water quality control strategies and other broad management concerns.

Transient models are those which trace the changes in the lake's circulation under time-varying conditions. Although more expensive to run that steady models, they supply considerably more information about the lake's behavior. Their greater expense demands an intelligent assessment of the need for this additional information and the level at which the information will be useful. For example, time steps for transient models can vary from on the order of minutes to days and longer and the time step must be chosen for consistency with the processes of interest and the spatial scale of the model.

A compromise between the fully transient model and the steady state is the quasi-steady model. In these models, the time variation of the process of interest is assumed sufficiently well-behaved to model the history as a series of steady states. Typically, these models operate on longer time steps (between a month and a year).

3.3.3 Spatial Representation

A much broader range is found in the spatial features of available models. Two general classifications may be considered: circulation models, which simulate two or three-dimensional flow, and simplified models with fewer dimensions. The section to follow briefly describes the possibilities within these two broad classes.

3.4 Modeling Alternatives

3.4.1 Simplified Models

Zero-Dimensional Models

The most simplified model is the zero-dimensional, in which the lake is assumed to act as if it were entirely homogeneous. This representation, referred to as the Fully-Mixed Tank (FMT) or Continuous-Flow Stirred Tank Reactor (CSTR), is not, of course, a circulation model since there is no consideration of water movement within the tank. They do appear frequently in conjunction with water quality models, however, and are simply mentioned here for completeness.

A variant on the fully-mixed tank is the multiple-box model in which different sectors of the lake are represented as connected FMT's. These models do add an increment of spatial detail to the single FMT, but still cannot be considered as circulation models, per se.

One-Dimensional Models

One-dimensional models, although not generally called circulation models, do satisfy the broad definition of this chapter. Two major types of one-dimensional models exist: vertical and longitudinal (Brown, 1978).

The vertical one-dimensional model considers the lake to be horizontally homogeneous, but with a distinct vertical density structure. A series of layers of different temperature (and thus density) represent the lake in these models, the densities changing in time according to the equations of mass conservation (continuity) and heat energy. The models consider the flux of heat at the water surface according to meteorological conditions, as well as the inflow and outflow of water at various depths in the lake. In addition, some models consider the influence of wind at the water surface as a mixing agent. Vertical circulations arise when these influences act to produce an inverse stratification (heavier water overlying light), or when water must flow from inlets at one level to outlets at another. The models are generally successful in modeling the temperature changes in deep stratified lakes. (Published models of this type are reviewed by Orlob, 1977 and by Parker, Benedict and Tsai, 1975.)

Longitudinal one-dimensional models are less plentiful than their vertical counterparts owing to their narrower applicability. These models are applicable to long, narrow lakes in which vertical variations due to stratification are negligible. The majority of lakes which lend themselves to these models are characterized by large throughflows, to the point that Brown (1978) describes them as essentially sluggish rivers. Another class of lakes for which these models may be useful are shallow lakes which are long and narrow, without necessarily large throughflows. Considerations of circulation are usually minimal in the one-dimensional models; for example, variations in the lateral velocity are captured via a dispersion coefficient rather than by explicitly modeling the non-uniform flow field. Often, flow rates are specified so that only mass conservation

is modeled, although the one-dimensional momentum equation may be considered as well.

3.4.2 Circulation Models

With two and three-dimensional models, we enter the realm of the true circulation models: those which consider the forces of the wind and bottom friction, as well as the influence of inflows and outflows, to predict the motion within the lake.

In this section, we will draw upon our own search of the literature as well as published reviews by Cheng, Powell and Dillon (1976), Lindijer (1976, 1979) and Simons (1979) to outline the major classes of models. Three classes are defined by Cheng, Powell and Dillon: single layer models, multi-layer models, and Ekman-type models. To this group we add some additional, less common, variations.

Single Layer Models

Single layer models proceed from the assumption that the lake is vertically homogeneous (unstratified) to eliminate consideration of vertical variations in currents and other parameters. The vertical variation is removed by integrating the continuity and momentum equations from the free surface to the lake bottom, reducing the three-dimensional problem to one of only two dimensions. The integration process transforms the problem variables from velocities to horizontal mass transports, defined as:

$$U = \int_h^{-\eta} u\,dz \qquad V = \int_h^{-\eta} v\,dz \tag{3.21}$$

The integration also incorporates the surface and bottom boundary conditions into the resulting equations.

Single layer models simulate mass flux and free surface motion well, but omit all detail concerning the vertical circulation structure. Their major use has been in storm surge studies in both deep and shallow lakes. Their applicability is more general in shallow lakes, however, where the assumption of vertical homogeneity holds well. A number of single layer model applications are listed in Table 3.1.

Table 3.1 Published single layer lake circulation models

Lake	Reference	Length (km)	Width (km)	Depth (m)	A_H (cm^2/s)	A_V* (cm^2/s)	Δx (km)	Δy (km)	Comments **
Erie	Platzman (1963)	400	100	64	--	40	13.9	13.9	Unsteady
Erie	Cheng and Tung (1970)	400	100	64	--	30	20	10	Finite Element
Huron	Murty and Rao (1970)	400	150	230	--	f(W)	15.2	15.2	
Michigan	Murty and Rao (1970)	500	125	80	--	f(W)	12.7	12.7	
Erie	Murty and Rao (1970)	400	100	64	--	f(W)	10.2	5.1	
Superior	Murty and Rao (1970)	600	400	406	--	f(W)	13.9	13.9	
Ontario	Simons (1971)	285	70	220	10^6	f(W)	7 & 5	7 & 5	Unsteady
Ontario	Paskausky (1971)	285	70	220	--	22.5	2.5	2.5	Unsteady, Vorticity Simulation

* f(z) indicates variation with depth, f(W) indicates variation with wind speed
** unless noted, models are steady and use a finite difference solution

Multi-Layer Models

Multi-layer models extend the single layer methodology to stratified water bodies. Basically, the process applied to the entire water column in the single layer models is applied piecewise to a number of layers through the lake. A different density may exist in each layer, and the vertical eddy viscosity may vary from layer to layer as well. The equations of continuity and momentum are vertically integrated over the depth of each layer, incorporating the free surface boundary condition into the top layer equation, and the bottom condition into the equation for the lowest layer. Inter-layer conditions must also be specified, and become part of the layer equations as well. The final result of this procedure is a series of equations which represent the motion within each layer individually. The layers are, of course, coupled via the inter-layer conditions.

Two approaches to the construction of the layers exist. In the Type I approach, the position of the layers is fixed in space and vertical transports occur between layers to maintain continuity. These transports also transfer momentum between the layers. In the Type II models, the layers are considered to be distinct, as if separated by thin membranes. No mass transport occurs between the layers; rather, the layers displace vertically to maintain continuity. The layers communicate via momentum transport due to interfacial stress.

Multi-layer models correct the deficiencies of the single layer models, and the Type I models especially predict both free surface elevation and currents well. The Type II approach is less common than the Type I, and is most appropriate to distinctly stratified lakes with a clearly developed thermocline. A selection of multi-layer models from the published literature is summarized in Table 3.2.

Ekman-type Models

The Ekman-type models simplify the equations of motion considerably more than the methods above. Based upon the assumption that the Rossby number is small, the horizontal momentum equations are linearized by dropping the convective acceleration terms. This important simplification permits the form of the vertical distribution of the horizontal velocities to be determined analytically. Once the form of the vertical structure is known, completion of the solution requires only that the variation in horizontal space be defined. This information is supplied by the solution of the vertically integrated conservation equations. The Ekman-type model solution specifies the three-dimensional variation of the horizontal currents only. The smaller vertical velocity component is not determined.

The Ekman-type solution, owing to the simplification of the equations, is the easiest method for computation. However, the assumptions made in simplifying the equations reduce the model's applicability and require that the model's suitability be evaluated for each application. The model remains useful for a wide range of lakes nevertheless, as attested by the examples shown in Table 3.3.

Table 3.2 Published multi-layer lake circulation models

Lake	Reference	Length (km)	Width (km)	Depth (m)	A_H (cm^2/s)	A_V * (cm^2/s)	Δx (km)	Δy (km)	Layers	Comments **
Ontario	Simons, 1972	285	70	220	10^6	f(W)	5	5	3	Unsteady
Constance	Hollan and Simons, 1978	60	15	250	?	50	1	1	5	Unsteady
Baikal	Paul et al, 1979	600	75	1600	10^7	10 to 1000 f(z)	7.8	15	8	Unsteady
Sea of Azov	Paul et al, 1979	360	220	13	$3x10^6$	25	9.5	6.8	8	Unsteady
Michigan	Kizlauskas and Katz, 1973	500	125	80	--	50	10.8	10.8	2	Unsteady, Type II

* f(z) indicates variation with depth, f(W) indicates variation with wind speed
** unless noted, models are steady, Type I and use a finite difference solution

Table 3.3 Published Ekman-type circulation models

Lake	Reference	Length (km)	Width (km)	Depth (m)	A_H (cm^2/s)	A_V * (cm^2/s)	Δx (km)	Δy (km)	Comments **
Okeechobee	Su, Pohl and Shih, 1976	55	49	4.5	--	10	2.5	2.5	Finite Element
Ontario	Gallagher, Liggett and Chan, 1973	285	70	220	--	200	4	4	Finite Element
Superior	Lien and Hoopes, 1978	600	400	406	--	100	25.4	25.4	
Erie	Gedney and Lick, 1972	400	100	64	5×10^5	38	3.2	3.2	
Velen	Bengtsson, 1973	7	1	9	--	15	?	?	
Mendota	Nelson, 1979	10	7	22	--	15 f(z)	0.73	0.73	Unsteady
Geneva	Bauer and Graf (described by Sundermann, 1979)	70	15	310	--	460	1	1	
Ontario	Bonham-Carter and Thomas, 1973	285	70	220	--	?	2.5	2.5	

* f(z) indicates variation with depth, f(W) indicates variation with wind speed
** unless noted, models are steady and use a finite difference solution

Longitudinal Two-Dimensional Models

A rarer type of two-dimensional model is that which computes motion in a vertical plane along the lake. These models, which are used for long, deep but relatively narrow lakes, ignore transverse variations in the flow. Invariably, lakes which satisfy these criteria are impounded streams whose hydrodynamics are dominated at the upper end by inflow current and at the lower end by temperature stratification. Such reservoirs typically exhibit a distinct two-dimensional temperature structure characterized by tilted isotherms. The two-dimensional models of this type combine the features of the two versions of one-dimensional models discussed in the previous section. The model by Edinger and Buchak (1979), for example, employs the equations of continuity, longitudinal momentum, vertical pressure and two-dimensional heat energy to simulate the transient dynamics of such reservoirs.

Fully Three-Dimensional Models

The final, and clearly the most complex, modeling alternative is the full three-dimensional model. These models attempt to determine the lake's flow field in its full complexity, often with the simultaneous consideration of the vertical density structure. The fully three-dimensional models are generally similar to the two-dimensional circulation models above except that the vertical momentum equation is retained and the horizontal equations are not vertically integrated. Models of this variety are not common, however, owing to the complexity and expense inherent in a three-dimensional grid. Thus, while examples do exist (for instance, Liggett, 1970), the general state of the art for these models is not advanced to the point of practical application.

3.5 Major Model Assumptions

The discussion above indicates many possible simplifications and assumptions which the modeler may employ. In this section, the various assumptions will be examined and criteria to evaluate their applicability will be given. Many of these criteria are drawn from Lindijer (1979).

3.5.1 Vertical Variability

When the depth of the lake is much smaller than its length, one can invoke a family of simplifications which Lindijer calls the shallow water approximation. The approximation consists, in fact, of three approximations. The first is the commonly used hydrostatic approximation, Equation 3.4. This is valid in all but the deepest lakes, and is found in virtually every circulation model.

The second shallow water approximation is the assumption that vertical velocities are so much smaller than those in the horizontal that they may be neglected in the equations for horizontal momentum (Equations 3.2 and 3.3). This approximation yields a model which is three-dimensional in the sense that the variation of horizontal velocity is determined in all three coordinate directions, but not in the sense that the three velocity components are determined.

The third shallow water approximation is that the water body is vertically homogeneous, that is, that it does not exhibit any density stratification. Field studies have shown this to be a reasonable assumption for shallow lakes, where the influence of strong winds penetrates throughout the water column and produces complete vertical mixing (Entz, 1976; and Seki, et al., 1980). Although brief periods of weak stratification can occur during the summer, even moderate winds will remix very shallow lakes. Usually, stratification persists no longer than a day or two.

A quantitative indication of the depth to which wind penetrates in the lake (and thus, the degree of vertical homogeneity) is supplied by the Ekman friction depth:

$$D = \pi \sqrt{\frac{2A_V}{f}}$$

This depth indicates roughly the depth to which the wind stress on the surface will be influential. Under criteria given by Lindijer (1979), the lake qualifies as very shallow if the ratio of the characteristic lake depth to the Ekman friction depth is less than 0.25, and as shallow if the ratio is between 0.25 and 2.0. A lake is deep if the ratio exceeds 2.0.

3.5.2 Convective Accelerations

Neglect of the non-linear convective terms leads to a considerable simplification of the momentum equations and is the key assumption of the Ekman-type models. The magnitude of the Rossby number, the ratio of

the inertial forces to the Coriolis force, determines whether or not this is a valid assumption. If the Rossby number is much less than one, the convective terms will have negligible impact upon the lake-wide circulation and may be omitted.

The phrase "lake-wide circulation" was used in the last paragraph to purposely exclude local effects. Recently, there has been a good deal of attention in the literature to the importance of local inertial effects and the ability of numerical models to capture such effects (Abbott, 1976; Abbott and Rasmussen, 1977; and Lean and Weare, 1979). Unfortunately, these investigations have addressed channel, estuarine and coastal flows where velocities, and thus convective inertia, are much greater than in wind-induced lake circulation. Nevertheless, we can conclude from these studies that where there are large abrupt changes in the bathymetry or shoreline geometry numerical models which omit the convective terms will fail to capture induced secondary circulations correctly. The severity of these local errors depends upon the coarseness of the finite difference grid, the character of the geometry, and the strength of the currents. We expect that the errors will be minor for low velocity wind-induced flow in lakes.

3.5.3 Free Surface Effects

An assumption with major impact upon lake circulation models is the rigid lid approximation. As the name implies, the assumption is that the lake behaves as if it were covered with a slippery rigid lid. This lid prevents vertical motions at the free surface, but still allows horizontal motions and pressure variations. By preventing the kinematic effects of surface motion, the rigid lid filters out high frequency inertial and gravity waves without affecting steady state solutions and with only small distortion of low frequency movements. The consequence of eliminating the high speed gravity waves is to permit an order of magnitude increase in the time step of numerical solution methods, and greater numerical accuracy and stability (Bryan, 1969).

Operationally, the rigid lid approximation is to assume $-\partial\eta/\partial t = w = 0$ in the kinematic boundary condition, Equation 3.5. Calculation of free surface displacements is still possible with this approximation by first solving the horizontal momentum equations for pressure, and then using the hydrostatic equation to determine the free surface displacement from the pressure (Cheng, Powell and Dillon, 1976).

The rigid lid approximation has very great computational advantages over the alternative free surface representation, but not without a cost in certain circumstances. Bedford and Rai (1978) give the criterion that the square of the ratio of the seiche period to the inertial period must be much less than one to use the rigid lid approximation. This is expressed mathematically for a lake of length L as:

$$\frac{L^2 f^2}{(2\pi)^2 gH} << 1$$

Others give a similar criterion without the factor of $(2\pi)^2$.

Two papers from the research group headed by Lick at Case Western Reserve explore the rigid lid approximation in some detail (Haq and Lick, 1975; and Sheng, Lick, Gedney and Molls, 1978). Their comparisons of rigid lid and free surface models were made using actual events on Lake Erie, where the ratio criterion above is not met. Their findings indicate that the rigid lid model converges to a steady state many times faster that the free surface model, but that transient currents and seiches are incorrect in the rigid lid model results. The free surface model does preserve these effects, and thus predicts greater bottom shear stresses and sediment resuspension in their linked circulation and sediment transport model.

One aspect of the approximation at the free surface is poorly presented in some papers and easily confused with the rigid lid approximation. This approximation, which we will call the small amplitude approximation, is that the free surface boundary conditions are applied at $z = 0$, rather than at the actual free surface, $z = -\eta$. (Cheng, Powell and Dillon (1976) are particularly unclear in distinguishing this approximation from the rigid lid approximation.) The small amplitude approximation is commonly used in both free surface and rigid lid models. The validity of the approximation may be evaluated with the surface boundary parameter as a guide. This parameter, which is the ratio of the square of the Froude number to the Rossby number, arises when the kinematic and wind stress boundary conditions are made dimensionless. (See Figure 3.2.) If the parameter is small, it may be assumed reasonable to employ the small amplitude approximation and apply the boundary conditions at $z = 0$ rather than at $z = -\eta$.

3.5.4 Horizontal Shear Effects

In most analytical solutions and in many of the Ekman-type models, the equations are simplified by neglect of the horizontal shear forces (term e in Equations 3.2 and 3.3). This approximation may be justified by the size of the horizontal Ekman number, the ratio of the frictional force to the Coriolis force. Where the horizontal Ekman number is small compared to one, the terms may be safely ignored.

A subtle aspect of this approximation must be considered along the shoreline, where frictional influences may be important locally. Lindijer (1979) gives an evaluation criterion for these effects based upon the bottom slope, s. The criterion states that the horizontal shear terms may be neglected for gradual slopes:

$$s << s_c = \frac{H}{L}\sqrt{\frac{E_V}{E_H}}$$

where H and L are the mean depth and length of the lake,
E_V and E_H are the vertical and horizontal Ekman numbers respectively, and
s_c is the critical bottom slope.

This condition can be interpreted as a requirement that vertical shear stresses (represented by $H\sqrt{E_V}$) remain much larger than those in the horizontal ($L\sqrt{E_H}$) despite the bottom slope.

3.6 Model Parameters

In this section we examine a number of key parameters which significantly affect the predictions of circulation models. Unfortunately, the literature presents multiple alternatives for these parameters, but no clear consensus as to which are superior.

3.6.1 Vertical Eddy Viscosity

The momentum equations presented earlier employ the assumption that the turbulent flux of momentum due to the Reynolds stresses can be represented as the product of an eddy viscosity and the first spatial derivative of the velocity. The validity of this assumption is often questioned. (See, for example, Babajimopoulos and Bedford, 1980.) However, a working practical alternative does not now exist, and it is a rare circulation model that does not make use of the eddy viscosity assumption.

Published Formulae

Perhaps because the concept is without rigorous theoretical grounds, a bewildering variety of formulations for the eddy viscosity may be found in the literature. A selection of the available formulae for the vertical eddy viscosity are shown in Figure 3.3. The obvious diversity in the proposed forms reflect significant differences in the originators' views of the turbulent transport process.

Some convergence of the literature may nevertheless be found for particular aspects of the vertical eddy viscosity formulation. There is agreement that the eddy viscosity depends upon the intensity of the turbulence and the density instability of the water column, and that it varies throughout the lake. Lick (1976) lists the following turbulence generating processes: surface wind stress, vertical shear currents due to horizontal pressure differences, internal waves, bottom friction and bathymetry, and density stability. For shallow, homogeneous lakes the surface and bottom sources of turbulence are the most influential.

The value of the eddy viscosity at the lake bottom appears to be another point of common ground within the literature. As explained by Thomas (1975), the rigid bottom inhibits vertical eddying motions and thus the viscosity closes to zero. With a few exceptions, the formulae of Figure 3.3 follow this behavior.

There is far less agreement on the proper formulation at the water surface. Many researchers view the wind stress as the driving source of turbulence and therefore feel that the vertical viscosity should be maximal at or near the surface (Lick, 1976; Lindijer, 1976; Thomas, 1975; and Bengtsson, 1973). Opposing this view is Madsen (1977), who argues that the eddy viscosity will behave similarly near any sheared boundary in the fashion described by Thomas. Accordingly, he proposes a linear increase from zero viscosity at both the surface and the bottom.

Most researchers do agree that the eddy viscosity will increase as the boundary shear increases, although this dependency is not well defined.

The uncertainty about this dependency, as well as an increase in computational difficulty, leads most modelers to assume the eddy viscosity not to vary with boundary shear or wind speed. Where a variation is modeled, the procedure is to generally assume a linear proportionality to either the wind speed or the wind friction velocity as seen in Figures 3.3d, e, f, h, k and l.

The great diversity of opinion about the vertical eddy viscosity is troublesome for the modeler who seeks a more sophisticated respresentation than to simply assume constant viscosity. Hamblin and Salmon (1975) point out the importance of this parameter in the circulation model:

> A number of experiments in which model predictions are compared with observed currents have indicated that the vertical diffusion of momentum is probably the most important internal parameter of the model....Drastic variability in the vertical profile of current can result from the specification of the magnitude and variation of the vertical eddy viscosity.

Comparison with Observations

A basis for evaluation of the eddy viscosity formulations is found in the results of laboratory and field investigations. Laboratory flume studies, such as those reviewed by Shemdin (1973), invariably reveal logarithmic velocity profiles at both the water surface and the flume bottom. The near-surface logarithmic profile has been confirmed in the field by observations of wind-drift currents in lakes (Bye, 1965; and Bhowmik and Stall, 1978). Field and laboratory data (summarized in Stolzenbach et al., 1977) also indicate that the wind factor (the ratio of the surface drift current to the wind speed) varies over the narrow range of approximately 1 to 6 percent, and that the drift current is deflected by no more than 15 degrees from the wind direction.

These observations should be replicated in the results of mathematical circulation models. The simplest of those models, the classic analytical solution by Ekman for an infinitely deep ocean and constant vertical eddy viscosity, predicts a wind factor of 3% but a surface deflection angle of 45 degrees. The development of more complex eddy viscosity formulations has largely been a reaction to his poor prediction of the deflection. Results using two of the more complex formulae are compared with those of the constant viscosity and with laboratory findings by Stolzenbach et al. (1977). They consider two cases: wind-driven flow in an infinte channel, and in a closed finite channel. They conclude that the constant eddy viscosity (Figure 3.3a) and the linear eddy viscosity (3.3f) produce unrealistic results, while the parabolic form (3.3k or l) yields a velocity profile similar to the laboratory findings. Madsen's formula (Figure 3.3h) also duplicates the log velocity profiles and predicts a deflection of roughly 10 degrees. Interestingly, the very dissimilar equation proposed by Fjeldstaad (discussed in Neumann and Pierson, 1966) was developed empirically by matching observations at a 22 meter deep location in the ocean, and thus agrees with at least one set of field data.

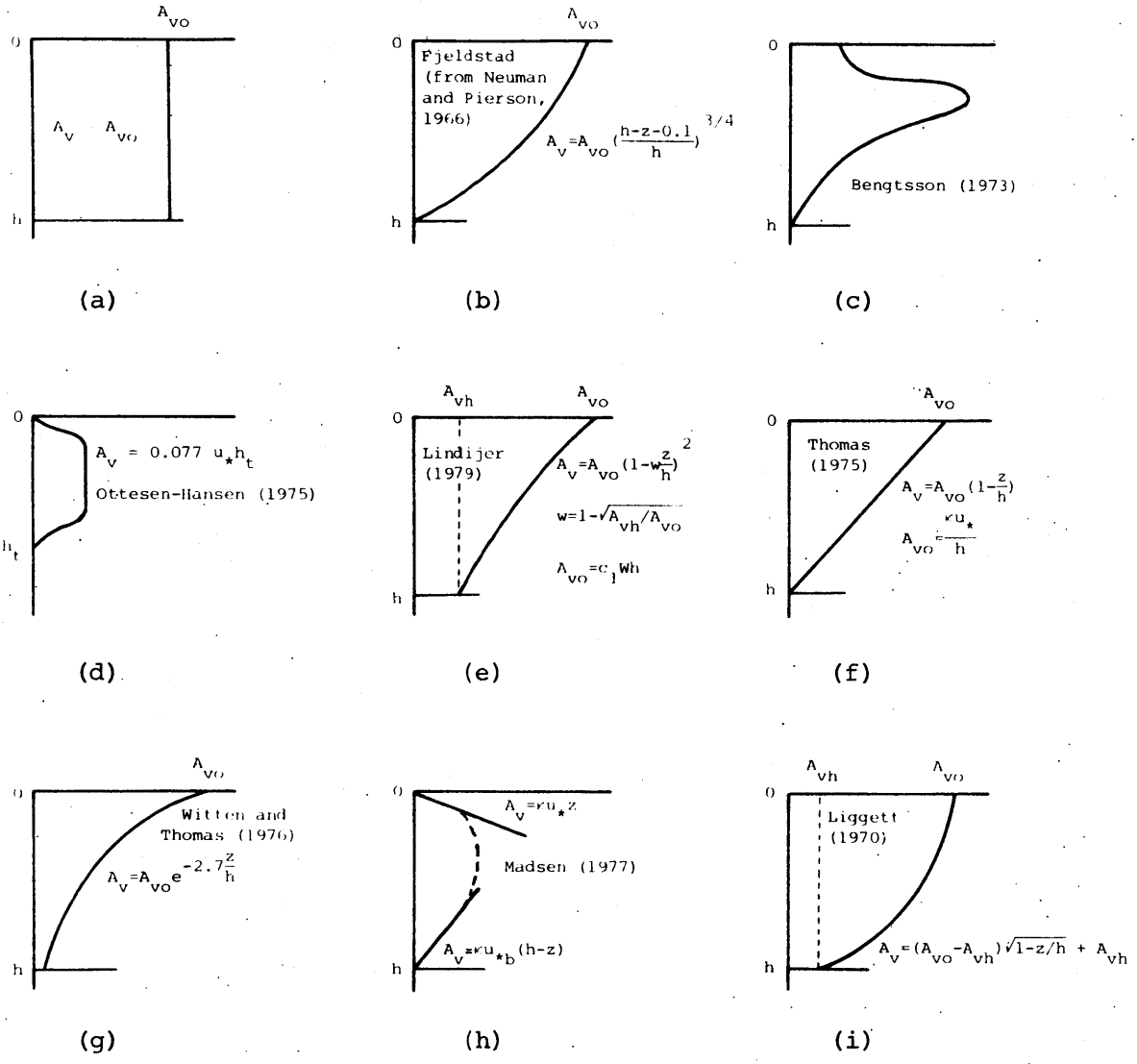

Figure 3.3

Representations of the vertical eddy viscosity

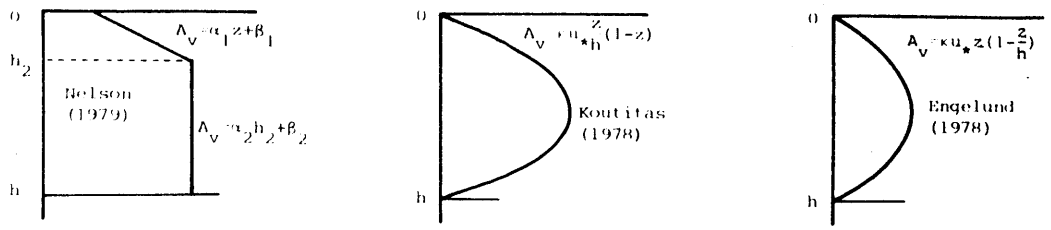

(j) (k) (l)

Variable definitions:

A_v	vertical eddy viscosity
A_{vo}	surface value of vertical eddy viscosity
A_{vh}	bottom value of vertical eddy viscosity
z	vertical direction coordinate - positive downwards
h	total water depth
h_t	depth to thermocline
u_*	wind shear friction velocity
u_{*b}	bottom shear friction velocity
κ	von Karman's constant
α_i	slope of ith linear segment
β_i	intercept of ith linear segment
c_1	constant
W	wind speed

Figure 3.3 (continued)

Representations of the vertical eddy viscosity

The comparisons by Stolzenbach et al. also illustrate that the choice of the eddy viscosity form cannot be isolated from the other parameters of the model. For example, consider the situation at the bottom boundary. If the fluid velocity is taken to be zero at the bottom, the velocity profile should be characterized by the steep velocity increase of a narrow logarithmic layer. (See Figure 3.4.) Such a velocity structure is impossible, however, if a depth-constant eddy viscosity is specified, and therefore the velocity will be underestimated. If instead, the velocity is permitted to take on some finite value at the bottom, a constant eddy viscosity may lead to a reasonable approximation of the current.

Recommendation

It is clear from our review that the vertical eddy viscosity will be a problematic parameter for the circulation model. Neither field data nor theory offer a definitive viscosity form. The viscosity function should vary with the model formulation, however the correct form may be very uncertain for the more complex models. Accordingly, our recommendation for circulation modeling is to follow the procedure employed by Shanahan et al. (1981): use theory and the literature as a guide to develop alternative viscosity functions and then test those functions in calibration runs against field data. Although this procedure leaves much to be desired, it is the most practical alternative in our opinion, given the disarray in the literature.

3.6.2 Wind Stress on the Water Surface

The specification of the surface boundary condition (Equation 3.6) requires the determination of the stress on the free surface due to the wind. This is generally given in the form:

$$\tau_s = C_z \rho_a W_z^2 \qquad (3.22)$$

where
- τ_s is the surface stress exerted in the same direction as the wind,
- C_z is the drag coefficient for a wind measured at height z above the water surface,
- W_z is the wind speed measured at a height z above the water surface (usually 10 meters), and
- ρ_a is the density of the air.

Many investigators have proposed formulae for the 10 meter drag coefficient, and these are summarized in Table 3.4 and Figure 3.5. Wu's (1969) formulae, which are approximations of more complex theoretical formulae, are probably the most frequently used, but are based on measurements in the deep ocean rather than in shallow lakes.

A recent, but not yet fully confirmed finding concerns anomalously low drag coefficients over shallow water (Hicks, Drinkrow and Grauze, 1974;

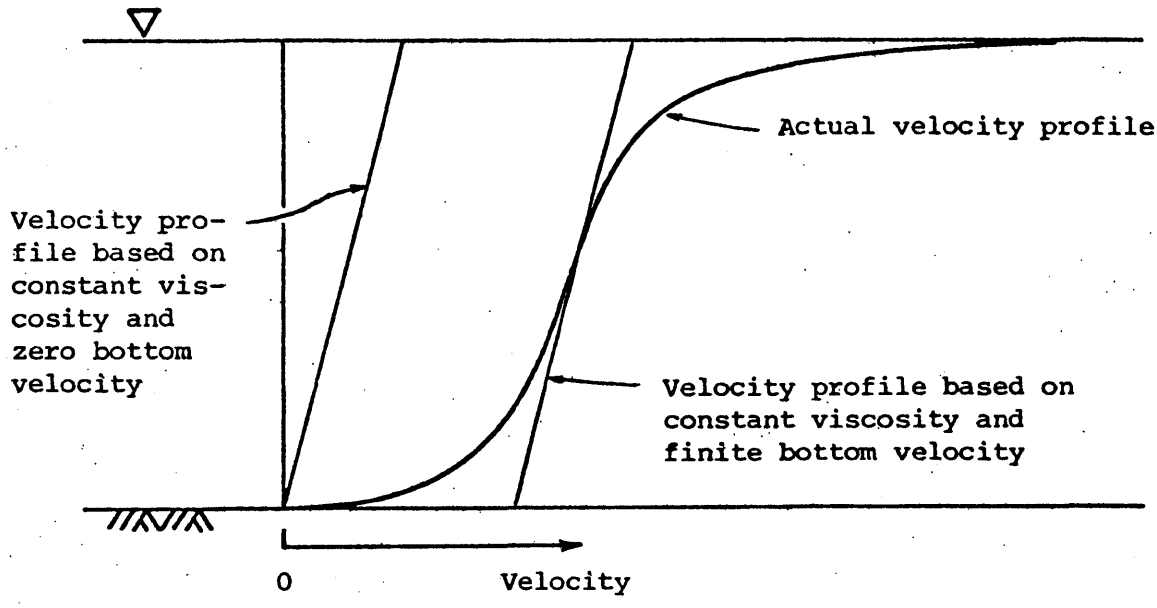

Figure 3.4

Solutions for steady flow in
an infinite one-dimensional channel
(Based on Stolzenbach et al., 1977.)

and Hsu, 1975). Hicks hypothesizes that this may be due to the absence of high frequency surface waves in shallow water, producing an aerodynamically smooth suface. He qualifies this hypothesis, however, by noting the possible influence of a biological film on the water surface, a factor which is probably also present in Hsu's study. Despite this possible interference, Hicks proposes a relation for shallow water based on an aerodynamically smooth surface:

$$C_z = \frac{\kappa}{\ell n\ (Bu_* z/\nu)} \qquad (3.23)$$

where κ is von Karman's constant, 0.41,

Table 3.4

Wind stress drag coefficients

Reference	C_{10}, Drag Coefficient	Wind Speed Range
Wu (1969)	$1.25 \times 10^{-3}\ W_{10}^{-1/5}$	$W_{10} < 1$ m/s
	$0.5 \times 10^{-3}\ W_{10}^{1/2}$	$1 < W_{10} < 15$ m/s
	2.6×10^{-3}	$W_{10} > 15$ m/s
Wilson (1960)	1.66×10^{-3}	Light winds
	2.37×10^{-3}	Strong winds
Ottesen-Hansen (1975)	0.8×10^{-3}	$W_{10} < 7$ m/s
	1.0×10^{-3}	$W_{10} > 7$ m/s
Banks (1975)	$9.0 \times 10^{-3}\ W_{10}^{-1/2}$	"Small" winds
	3.8×10^{-3}	"Medium" winds
	$0.7 \times 10^{-4}\ W_{10}$	"Large" winds
Ruggles (1970)	1.6×10^{-3}	$2 < W_{10} < 10$ m/s
Hsu (1975)	0.7×10^{-3}	$W_{10} < 5$ m/s
Van Dorn (1953)	1.11×10^{-3}	$W_{10} \leq 5.6$ m/s
	$1.11 \times 10^{-3} + 2.06 \times 10^{-3}(1 - 5.6/W_{10})^2$	$W_{10} > 5.6$ m/s

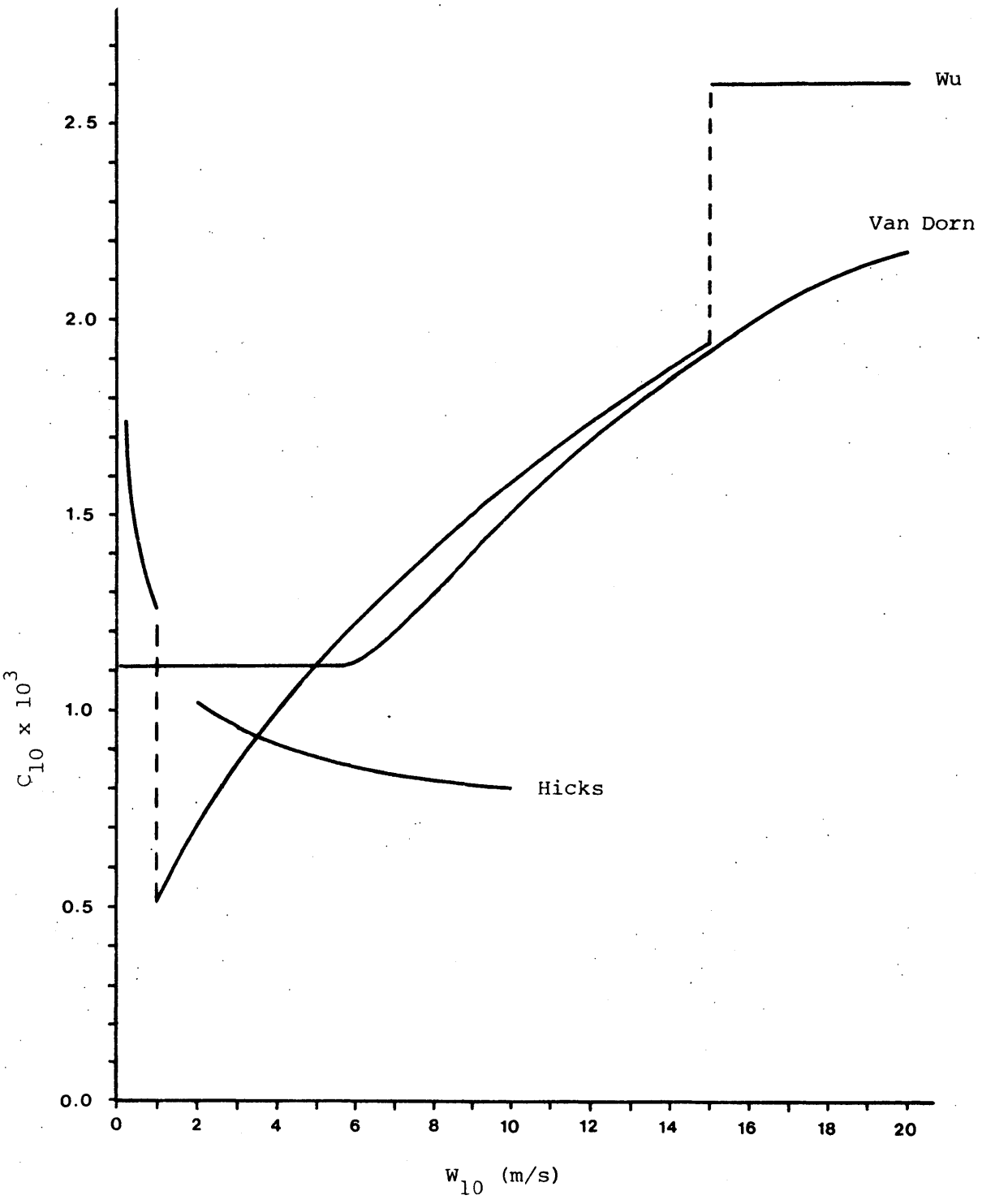

Figure 3.5

Surface drag coefficients as a function of wind speed

B is a constant, equal to 9,
ν is the kinematic viscosity of water, and
u_* is the wind friction velocity.

Hicks' formula is implicit since u_* is a function of C_z, and thus it must be solved iteratively. Hicks had insufficient data to specify an exact range of applicability, but roughly estimated the formula to be appropriate for water shallower than 3 to 7 meters.

Decreased drag in shallow water is not a universal finding, however. The very careful studies by Van Dorn (1953) in a two meter deep pond led to drag coefficients not substantially different from Wu's open-ocean results. Van Dorn makes but one peripheral reference to marine growth in the pond, so we are unable to assess the likely influence of a biological surface film. Most likely, such a film was present, though perhaps to only a limited extent. In any case, the conflicting findings of Van Dorn, Hicks et al. and Hsu do not permit a final conclusion as to the value of the wind drag coefficient on shallow water.

3.6.3 Bottom Friction

One may specify the boundary condition at the lake bottom in terms of the velocity or the shear stress. When velocity is specified, it is taken to be zero at the point of contact with the bottom. This is the no-slip condition:

$$u = v = 0 \quad \text{at } z = h \tag{3.24}$$

The shear condition is given as:

$$-\rho A_v \frac{\partial u}{\partial z} = \tau_b^x \qquad -\rho A_v \frac{\partial v}{\partial z} = \tau_b^y \tag{3.25}$$

where the shear at the bottom may be determined in a number of ways which we explore below.

The choice of the boundary condition will depend largely on the situation being modeled, the model formulation, and the values of other parameters, in particular the lake depth and the eddy viscosity. For

example, Lien and Hoopes (1978) state that the solution for mass transport in deep lakes is not influenced by the bottom condition. They define a deep lake as one having a mean depth, H, such that:

$$H > 4\sqrt{\frac{2A_v}{f}} = \frac{4D}{\pi} \qquad (3.26)$$

where D is the Ekman depth defined previously.

The choice of bottom boundary conditions carries greater influence in shallow water. For example, Murray (1975) found that a no-slip boundary led to unrealistically low current predictions when compared with field observations. His findings may result partially from his use of a constant vertical eddy viscosity as well, however. In any event, the shear boundary condition is favored by most modelers.

Cheng, Powell and Dillon (1976) describe the possible forms for the shear boundary condition in terms of the general relation,

$$\tau_b^x = BU \qquad \tau_b^y = BV \qquad (3.27)$$

where U and V are the mass transports in the x and y horizontal directions, and,
B may take on a number of forms.

They define three possible forms for B, which will be described in turn.

Linear friction laws define $B = k/h$ where k is a constant. We may broaden their definition somewhat to include as well linear relations of the form:

$$\tau_b^x = c_b u_b \qquad \tau_b^y = c_b v_b \qquad (3.28)$$

where u_b, v_b are the velocities at or near the bottom in the x and y horizontal directions, and
c_b is a constant.

Linear relations of the form of Equation 3.28 are used by Nelson (1979) and Lien and Hoopes (1978). These linear forms are sometimes called slip conditions, since they permit a slip velocity at the bottom. In the limit that k or c_b approaches infinity, the linear forms converge to a no-slip condition. The linear laws lead to a weak dependence of friction on the depth or current strength.

In quasi-linear friction laws, B takes the form,

$$B = k/h^2 \tag{3.29}$$

These forms remain linear with respect to the mass transport, keeping the computation simple, but include higher order depth dependence. They show strong influence due to depth, but not currents.

The most rigorous friction laws are based on the Chezy or Manning relations of open channel hydraulics. For these non-linear, or quadratic, friction laws, B takes the form:

$$B = \frac{k\sqrt{U^2 + V^2}}{h^2} \tag{3.30}$$

which includes strong dependency on both current and depth. Leendertse (1970) employs this form in his model, using the Chezy coefficient, C:

$$\tau_b^x = \frac{\rho g U}{C^2}\sqrt{U^2 + V^2} \qquad \tau_b^y = \frac{\rho g V}{C^2}\sqrt{U^2 + V^2} \tag{3.31}$$

The quadratic is considered the most accurate friction law, but carries a substantial computational burden due to the non-linear dependence on current. The additional computation is needed since the current must be determined by an iterative solution, rather than the direct solution possible with linear and quasi-linear friction laws.

In computer simulation of transient flow (or in an iterative computation of steady flow), the non-linear friction law may be approximated quite effectively. When the computation time step is short, or when the velocity is changing slowly, it is possible to linearize Equation 3.31 by using

the most recently computed values of U and V. Under proper conditions, this approximation will preserve the non-linear character of the bottom friction with little error and at greatly reduced computation expense.

4 LAKE BALATON: MODELING BACKGROUND

Our discussion of shallow lake dynamics in the preceding chapters has been, for the most part, in general terms. It is meaningless to continue on to the topic of model development in such terms, however. A substantive examination of modeling requires the reference point of a real application, satisfied in this research by participation in a case study of Lake Balaton, Hungary. That study, conducted by the International Institute of Applied Systems Analysis (IIASA) of Laxenburg, Austria, enjoys the cooperation of scientists from Hungary and has included participation by dozens of researchers. In this chapter, we give a brief overview of Lake Balaton's characteristics, drawing largely from the data base built at IIASA (van Straten et al., 1979; and van Straten and Somlyody, 1980). The information presented here will be used in subsequent chapters as the source of input, calibration and verification data for the Lake Balaton model.

4.1 General Characteristics of Lake Balaton

Lake Balaton, the largest lake in central Europe, is located in western Hungary. The lake is long and narrow (75 km by 8 km) with a surface area of roughly 600 square kilometers. It is an extremely shallow lake, particularly in relation to its large horizontal extent. The average depth of the lake is only 3.1 meters, and it is everywhere less than 5 meters deep except in one very small area. In this one deep section, where the Peninsula of Tihany nearly divides the lake, the width is less than 2 km and the depth reaches 11.7 meters. A map of the lake showing depth contours is included as Figure 4.1.

Lake Balaton and the surrounding countryside are a major tourist attraction for both Hungarian and foreign visitors. Pleasant weather and good water quality make the lake a particularly popular summer resort. Unfortunately, increasing population and development are apparently taking their toll on the lake, a fact demonstrated by the deterioration of the lake water quality over many years of measurements. This deterioration has been particularly rapid during the last decade, and indicates an accelerating eutrophication of the lake.

The climate of the Balaton region is temperate with an average annual air temperature of 10.7 C. The average monthly temperature drops below freezing in winter (-1.0 C in January) and ice covers the lake for roughly two months each year. A maximum mean monthly temperature of 21.4 C occurs in July. Water temperatures vary similarly, from a low monthly average temperature of 0.7 C in January to a high of 24.1 C in July. The shallowness of the lake, and its consequent strong response to summer radiation input, is responsible for the high July temperature.

Wind is an important factor in the behavior of Lake Balaton, owing to the large response of the shallow waters. Strong winds occur on several stormy days each month in a roughly uniform annual distribution. The prevailing wind direction is from the Northwest, passing across the width of the lake.

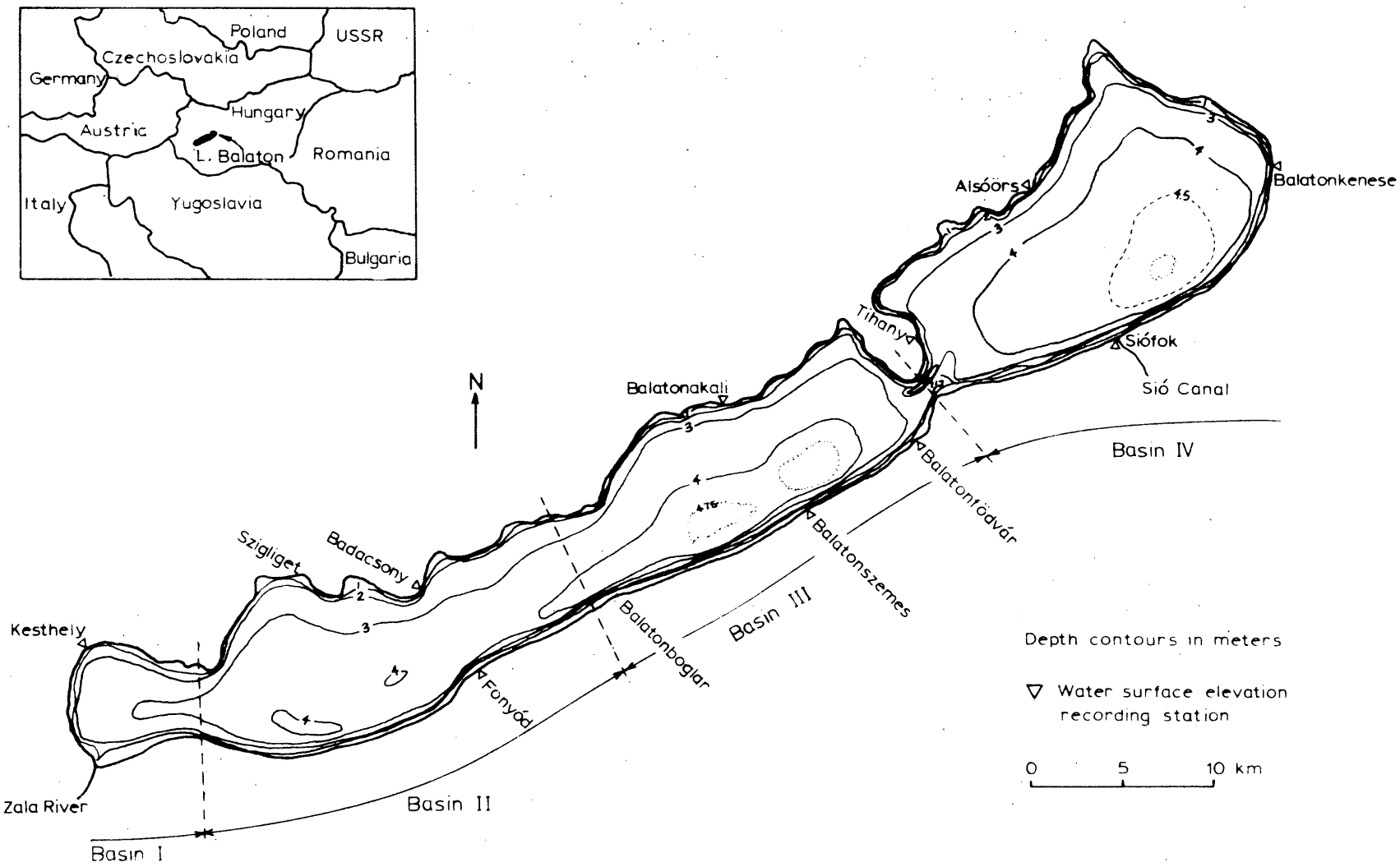

Figure 4.1

Map of Lake Balaton

4.2 Circulation in Lake Balaton

Although the existing data base is far from complete, sufficient information exists to construct an approximate description of Lake Balaton's circulation. The circulation is a composite produced by hydrologic flow through the lake, wind-induced currents, seiching, and other lesser influences. The major unknown aspects of water motion in the lake are the character of spatial variations in the current over both horizontal and vertical space, and the response of the circulation to changes in wind forces over short time periods.

4.2.1 Hydrologic Flow

We define hydrologic flow as that produced by the inflow of water to the lake from streams, runoff and rainfall, and the outflow from the lake by evaporation and stream discharge. In Balaton, such flow is dominated by the mean flow established by the stream and river inflows concentrated at the southwestern end of the lake, and the sole outlet at the Sio Canal at the lake's opposite end. The largest inflow is that from the Zala River, which drains roughly half of the watershed contributing to the lake.

The mean annual flow quantities due to the various hydrologic components are 18 m^3/s due to streamflow and runoff, 12 m^3/s from precipitation, 17 m^3/s removed by evaporation, and the discharge of 13 m^3/s at the Sio Canal (van Straten, et al., 1979). The total lake volume is 1860 million cubic meters, so that the mean hydraulic residence time is roughly four years. The longitudinal transport velocities associated with these hydrologic flows are small, on the order of 0.05 cm/sec.

Analyses of Balaton's hydrology have often been based upon a subdivision of the lake into four basins (Baranyi, 1973a; van Straten, et al., 1979). These are not basins in the usual sense -- that is, as drainage basins or watersheds. Rather, they are portions of the lake volume distinguished for the calculation of water balances, residence times and long-term exchange flows. The four basins are identified on the map of the lake in Figure 4.1 as Kezsthely (or Basin I), Szigliget (Basin II), Szemes (Basin III), and Siofok (Basin IV). The conception of the lake as four basins has influenced subsequent studies of all aspects of the lake -- for example, the basins appear in the water quality models discussed in Chapter 2.

4.2.2 Wind-Driven Flows

The influence of the wind overwhelms the slow hydrologic flow in establishing the pattern of flow in Lake Balaton. The shallowness of the lake permits a circulation response to even mild winds, producing currents one or two orders of magnitude greater than those due to the hydrologic flow.

Surrounding hills, and the geography of the lake itself, exert a major influence upon the circulation caused by the wind. The hills produce local effects by blocking and deflecting the wind, leading to a spatially non-uniform wind field. Keszthely Bay, for example, typically experi-

ences lighter winds than most of the lake (Figure 4.2). The circulation is further modified by the constraints imposed by the lake boundaries. Although comprehensive field observations of the lake circulation have not been made, a rough picture of the circulation is found in the work of Győrke (1975). Győrke used a physical hydraulic model of the western part of the lake to model circulation and sediment transport under artificial steady winds. Owing to a severe vertical scale distortion in the model (a factor of 20), the results must be considered qualitative. They do show, nevertheless, a complex system of flow gyres greatly influenced by the lake geometry and spatial variation of the wind field (Figure 4.3).

The vertical structure of wind-induced currents in the lake were the subject of recent field measurements conducted as a part of this study. The theory of wind-driven circulation predicts, for steady conditions, a profile such as that shown in Figure 4.4, where currents at the surface align with the wind, but an opposing return current is found along the bottom (Plate, 1970 or Liu and Perez, 1971). Although derived for steady winds and idealized geometry, a generally similar velocity profile could be reasonably anticipated in a lake.

In our field studies, we sought a qualitative description of the actual vertical velocity profile in Balaton, to be contrasted with the profiles given by theory and model results. We employed a simple electromagnetic current meter (Marsh-McBirney Model 201) capable of measuring speeds between 2 and 300 cm/sec in a single direction to an accuracy of ±2%. The meter is equipped with a velocity probe which is connected by 12 meters of cable to an electronics case with a visually read meter. Observations were made by lowering the probe, attached to a measured metal pipe, to various elevations in the water and rotating the pipe until the direction of maximum velocity was found. A complete description of the field studies, including tables and figures of the observed currents, is included as Appendix A of this report. In brief, the observations adhered to the theoretically predicted profile only occasionally. More typical was a highly transient velocity structure, with increasing variability as the measurement depth increased. Apparently, the currents experience the conflicting influences of the lake-wide seiche motion and the local wind-driven motion as well as the inherently transient process of turbulent momentum transport. One exception to this picture of transience and variability was in the Strait of Tihany where our observations of strong, unidirectional currents in the upper five meters corroborate Muszkalay's (1973) observations discussed in the following section.

4.2.3 Seiches

A seiche is the pendulum-like motion of the lake water surface after the cessation of a force which has displaced the surface from its equilibrium, level position. The most common forcing agent causing seiches is the shear force of a sustained wind. Such a wind will cause a set-up, the superelevation of water level on the downwind shore above the level, undisturbed position. When the wind stops blowing, the superelevated waters will flow downward, initiating the periodic seiche motion. Seiches may be especially significant in shallow lakes, since the magnitude of set-up increases as mean water depth decreases (Sibul, 1955).

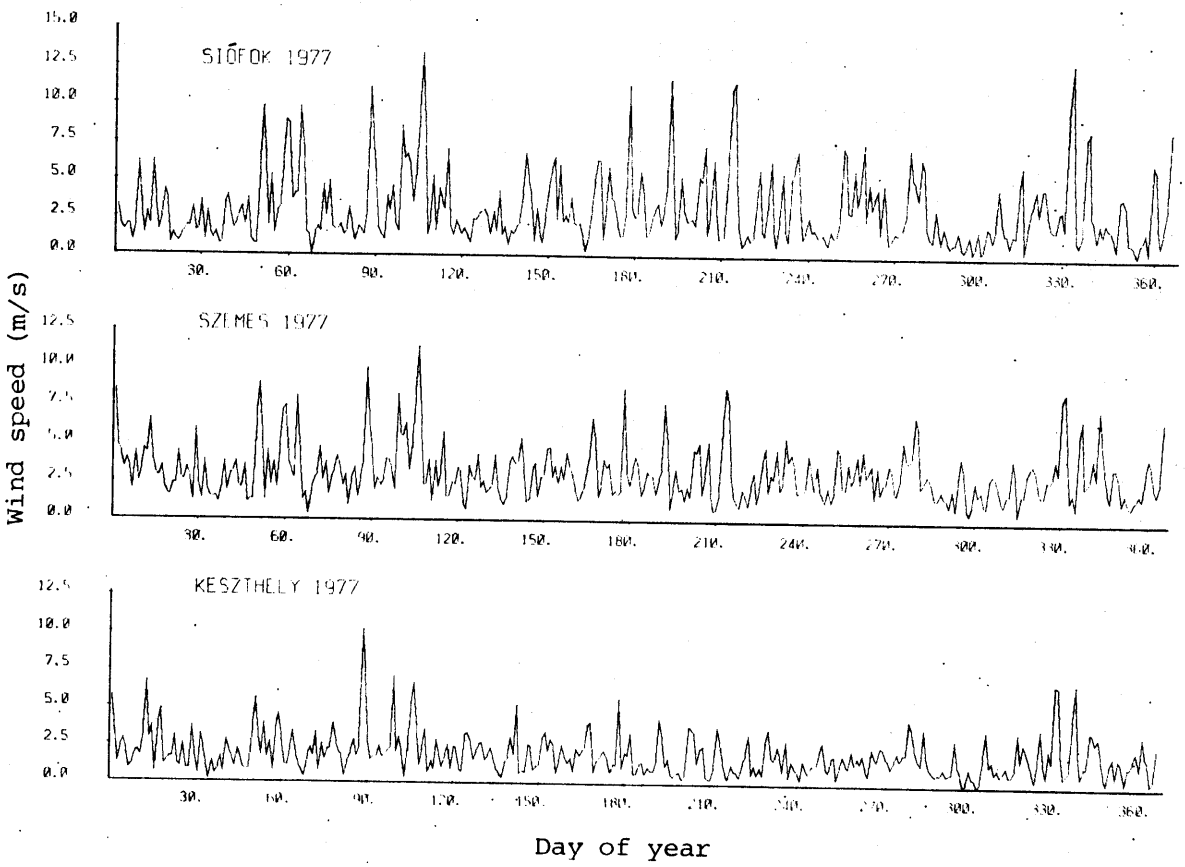

Figure 4.2

Comparison of observed daily average wind speeds
at Siófok, Balatonszemes and Keszthely, 1977

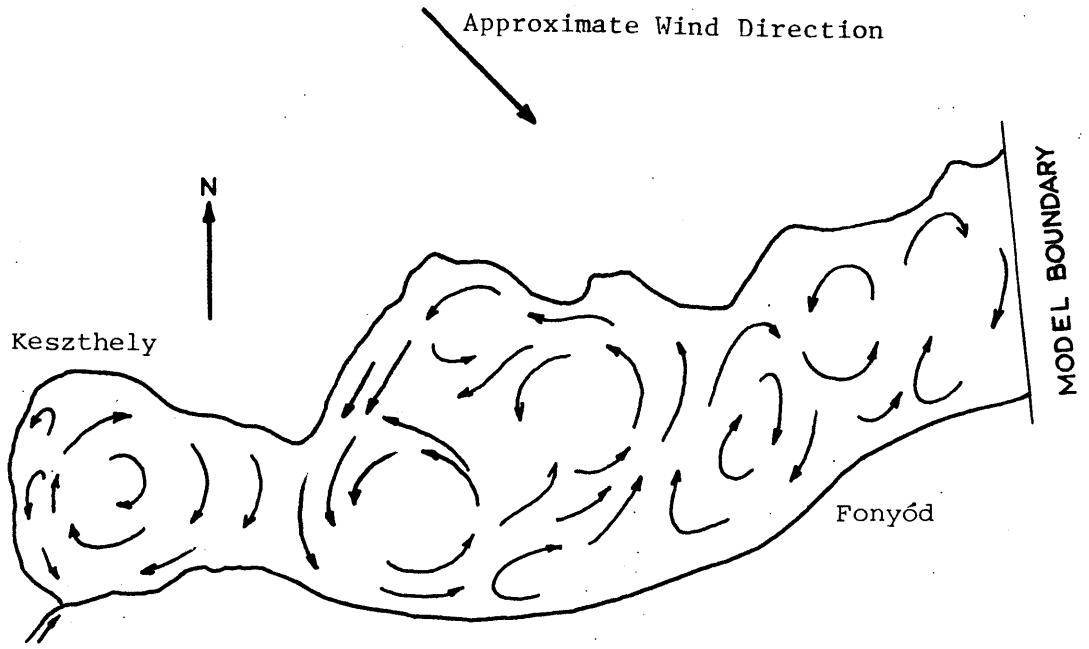

Figure 4.3

Flow pattern observed in Gyŏrke's physical model of Western Lake Balaton
(from van Straten et al., 1979)

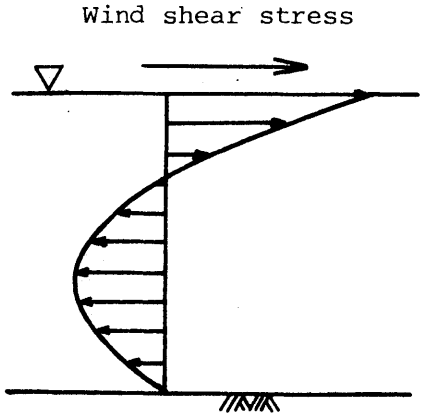

Figure 4.4

Theoretical wind-induced velocity profile
(after Liu and Perez, 1971)

The seiche is a well observed phenomenon in Lake Balaton, with different seiche periods arising according to the direction and location within the lake. Hutchinson (1975) cites work done by Cholnoky at the turn of the century which found a longitudinal seiche period of between 10 and 11.5 hours, while the transverse seiche is but 40 minutes. Other seiche periods have been distinguished for the portions of the lake to the east and west of Tihany Strait (1 hour and 2.5 hours respectively). The more recent work of Muszkalay, cited by Somlyódy (1979), found a range of seiche periods from 10 minutes to 1 day, with a mean longitudinal seiche period of 5.5 hours.

The most detailed studies of Lake Balaton's seiche are those of Muszkalay (1973). Muszkalay collected nearly a full decade of water surface elevation observations at up to ten stations around the lake. Simultaneous measurements of wind speed at three stations and of water current in the Strait of Tihany complete his data base. The measurements show the lake to be in seemingly constant motion. A strong wind, of only a few hours duration, can lead to observable seiches; a typical month-long record from Muszkalay clearly shows frequent events with both longitudinal and transverse modes evident (Figure 4.5).

With his observations as a basis, Muszkalay (1966) determined empirical formulae relating the wind strength, duration and direction to the resulting denivellation. His formula for longitudinal slope due to winds directed within 22.5 degrees of the lake's long axis is:

$$J = 0.038\, T^{\frac{1}{4}}\, (W_L - 2.8) \qquad (4.1)$$

where J is the slope of the water surface (cm/km),
T is the wind duration (hours), and,
W_L is the longitudinal wind component (m/s).

In this relation, J is determined from the difference in the extreme stages at Keszthely and Balatonkenese. It is a fictitious quantity in the sense that these stages may not, in fact, occur at precisely the same time; however, the time lag is not large. The maximum observed longitudinal denivellation (that is, the net difference from one end of the lake to the other) is roughly one meter. In the transverse, which is the more common direction for strong winds, a denivellation of 0.4 meter has been observed.

The creation of a set-up, and subsequent seiche oscillation, is accompanied by the transport of considerable quantities of water. This is particularly obvious where the lake narrows at Tihany. Muszkalay took advantage of this geometry and deployed four current meters in the Tihany Strait, placing the meters along a single vertical mooring line. Unfortunately, only intermittent records of these measurements are published, and then as the plot of a single velocity history at one meter below the water surface. Muszkalay reports that his measurements were virtual-

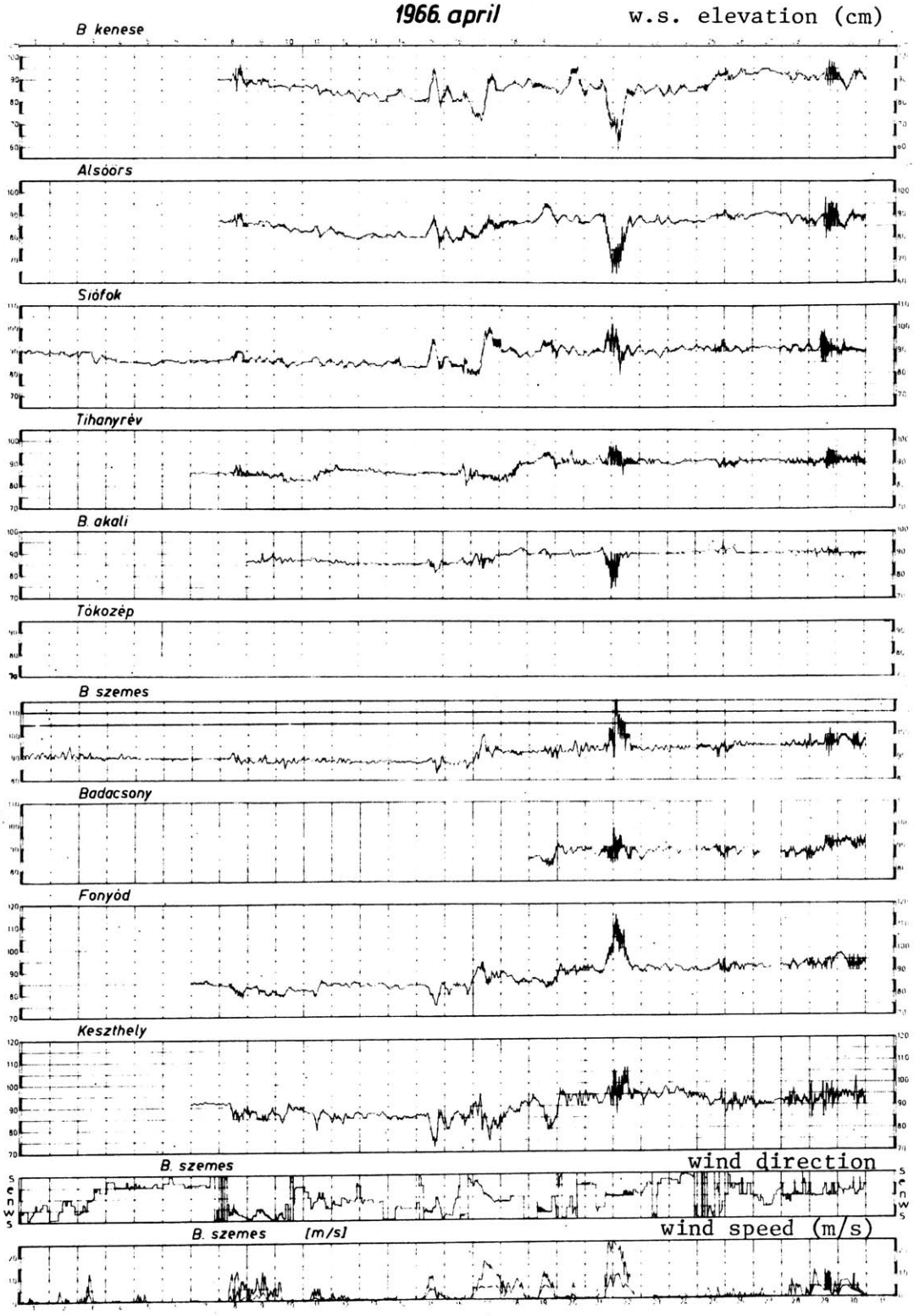

Figure 4.5

Typical water surface elevation records showing seiche motions (from Muszkalay, 1973)

ly always unidirectional throughout the water depth; thus, the 1 meter observation is probably a good indicator of velocity for the entire water column. The maximum velocity observed by Muszkalay was 1.4 meters/sec (reported in Somlyódy, 1979). Figure 4.6 shows a typical set of measurements relating wind, water surface motion, and velocity at Tihany. The event of Figure 4.6 is caused by a wind transverse to the lake, the predominant direction for storm winds and the type of event comprising most of Muszkalay's published examples.

A significant factor in the behavior of seiches is the force of friction, an influence magnified by the shallowness of Lake Balaton. The effects of friction are to lengthen the observed oscillation period to greater than that predicted by frictionless theory, and to quickly attenuate the seiche amplitude (Hutchinson, 1975). Frictionless theory predicts the period, T, to be:

$$T = 2L/\sqrt{gH}$$

where L is the lake length,
g is the acceleration of gravity, and
H is the mean lake depth.

This computes to 7.3 hours in Balaton, well below the commonly observed period of 10 to 11.5 hours. According to Hutchinson, such a marked decrease in the period is a phenomenon unique to shallow lakes, with Balaton and Lake Okeechobee in Florida the only observed examples.

The seiche motions caused by transient winds on Lake Balaton are very complex and tend to obscure the underlying basic behavior. Some of this complexity may be eliminated by invoking simple models of the lake which can be solved analytically. The simplest such model is to consider the lake as two connected oscillating basins, each with a level water surface, and presuming that all frictional energy losses are concentrated at the Strait of Tihany. With this model, we can address two fundamental aspects of the lake's seiche behavior: the free response and the forced response. Seiches are primarily free oscillation responses, the actions occuring in the absence of forces: that is, after the wind has stopped. If the equations of the two-body system are solved for the free oscillation problem we find that either of two major system responses may occur depending upon the geometrical and frictional characteristics of the lake. With the first response type, that of a heavily damped system, any initial displacement of the system from equilibrium simply decays exponentially, without any subsequent oscillatory motion. The second response is the lightly damped system, in which the system exhibits a sinusoidal oscillation, but with an exponentially decreasing magnitude.

The forced response of the lake concerns behavior under imposed wind forces of various frequencies. The two-body model yielded credible results for Kenney (1980) in an analysis of the forced response of Lake Winnipeg, Canada. Winnipeg is remarkably similar to Balaton in its geom-

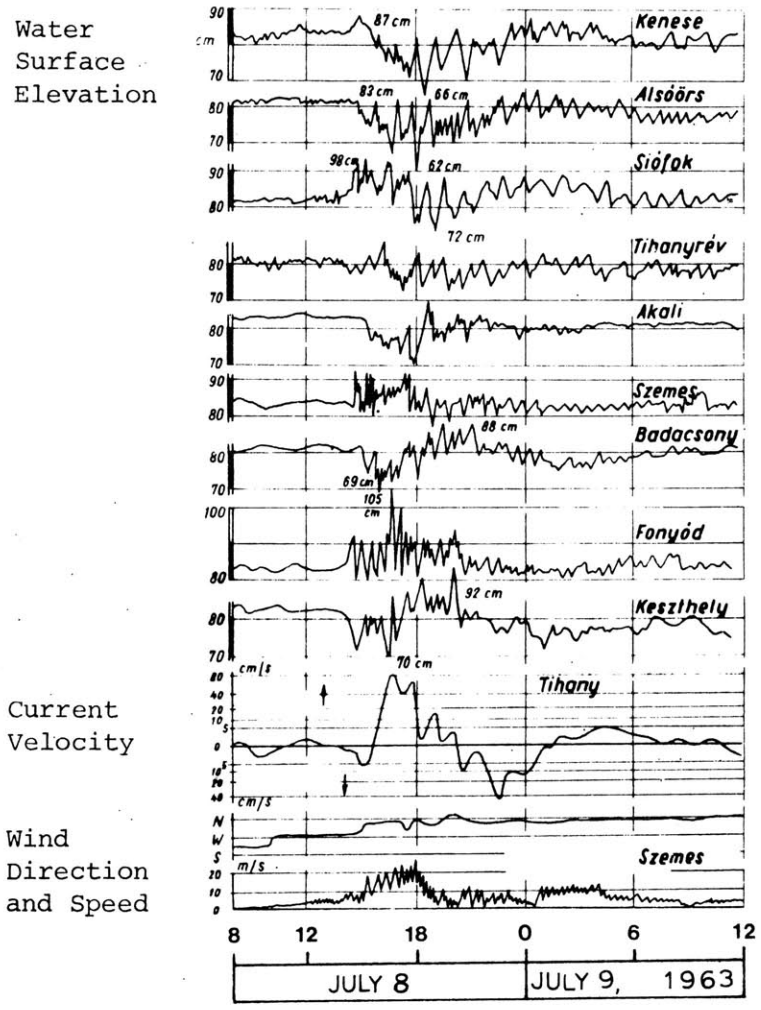

Figure 4.6

Example of Muszkalay's (1973) seiche observations

etry: it is relatively shallow (12 m), long and narrow (440 by 55 km), and consists of two distinct basins separated by narrows. As in Balaton, the narrows are the location of the greatest depth in the lake (roughly 37 m) and experience strong currents (up to 90 cm/s) due to seiche motion. Kenney employed the two-body oscillator as a conceptual model to explain the lake's frequency response behavior, which he had determined statistically by analysing time series of water surface elevation about the lake. Although his methods proved useful, and demonstrated the validity of the two-body system as a simple lake model, Kenney failed to relate the model parameters to the physical characteristics of the lake; he relied instead upon his considerable statistical information. Thus, it is not possible to extend his findings to Balaton without a similar statistical analysis.

A more physically-based study of seiching is Platzman's (1963) mathematical model of Lake Erie. Platzman solved the simplified one-dimensional equations of motion to relate the seiche response to the lake characteristics. The characteristics are represented by the Proudman number, which is related to the ratio of the viscous decay time to the seiche period, and is defined as:

$$Pr = \frac{A_v^2}{k^2 g H^2}$$

where k is the wave number equal to π/L for the uninodal seiche.

Platzman found from his simplified analysis that the seiche motion will be heavily damped if the Proudman number exceeds a critical value of 0.53. Only below this critical value will oscillatory motion be found.

Platzman also investigated the nature of the decay in seiche amplitude and found it to be constant in time for his linear system. In contrast, attenuation of the seiche in Lake Balaton depends upon the seiche magnitude. Figure 4.5, for example, shows large initial damping of the seiche of April 22, 1966, although residual motions persist through the 23rd and 24th despite very light winds. The different rates in attenuation of high and low amplitude waves is contrary to Platzman's linear theory, and suggests that non-linear frictional forces are important in Balaton.

4.3 Water Quality and Eutrophication

4.3.1 General Characteristics

Although the water quality of Lake Balaton is generally good, signs of increasing eutrophication have alarmed many. Such problems are worst in Keszthely Bay, at the southwest end of the lake, with progressive improvement along the length of the lake as one proceeds eastward. Much of this water quality deterioration is attributed to phosphorus and nitrogen nutrient loadings from agricultural runoff and domestic sewage disposal. The Zala River is an especially prominent source of input loadings, and is the major cause of Keszthely Bay's problems.

The shallowness of the lake allows the wind to prevent any long-term stratification, although intermittent weak stratification has been observed in vertical temperature profiles (Entz, 1976). Similarly, dissolved oxygen is mixed throughout the water column by the wind. The high biological oxygen demand of the input loadings has, on rare occasions, led to anaerobic conditions in Keszthely Bay during periods of low winds (van Straten, et al., 1979).

Lake Balaton is a hardwater lake, owing to the predominance of the mineral dolomite (calcium magnesium carbonate) in the drainage basin. It is characterized by high concentrations of calcium and magnesium, a high alkalinity, and a high pH. Suspended solids are always high due to resuspension of bottom material by wind action, imparting a milky color to the lake water.

Phosphorus in the lake is predominantly in the particulate form, mostly of organic origin. Orthophosphate levels are always very low -- on the order of 5 $\mu g/\ell$ and phosphorus is generally believed to be the limiting nutrient for algal growth. Phosphorus constituents exhibit significant concentration gradients along the lake, decreasing with distance from Keszthely Bay where the Zala River discharges to the lake (Figure 4.7). These gradients persist despite the mixing and circulation produced by the wind.

Biological productivity measures exhibit longitudinal gradients similar to those of phosphorus. They also indicate the deterioration of water quality; biomass, for example, has increased steadily for four years. Very high primary production has been measured in Keszthely Bay: up to a peak of 13.6 gC/m^2 day. The dominant algal species are diatoms in the spring followed by mixed phytoplankton populations in summer. Blue-green algae have started to prevail during the summertime in Keszthely Bay. According to various criteria given by Wetzel (1975), the lake's characteristics place it in a classification of eutrophic to hypereutrophic.

4.3.2 Chemistry

Interactions between phosphorus, calcium carbonate and phytoplankton appear to govern the productivity of Lake Balaton. Although the major aspects of the phosphorus-calcium carbonate system are known, the inter-

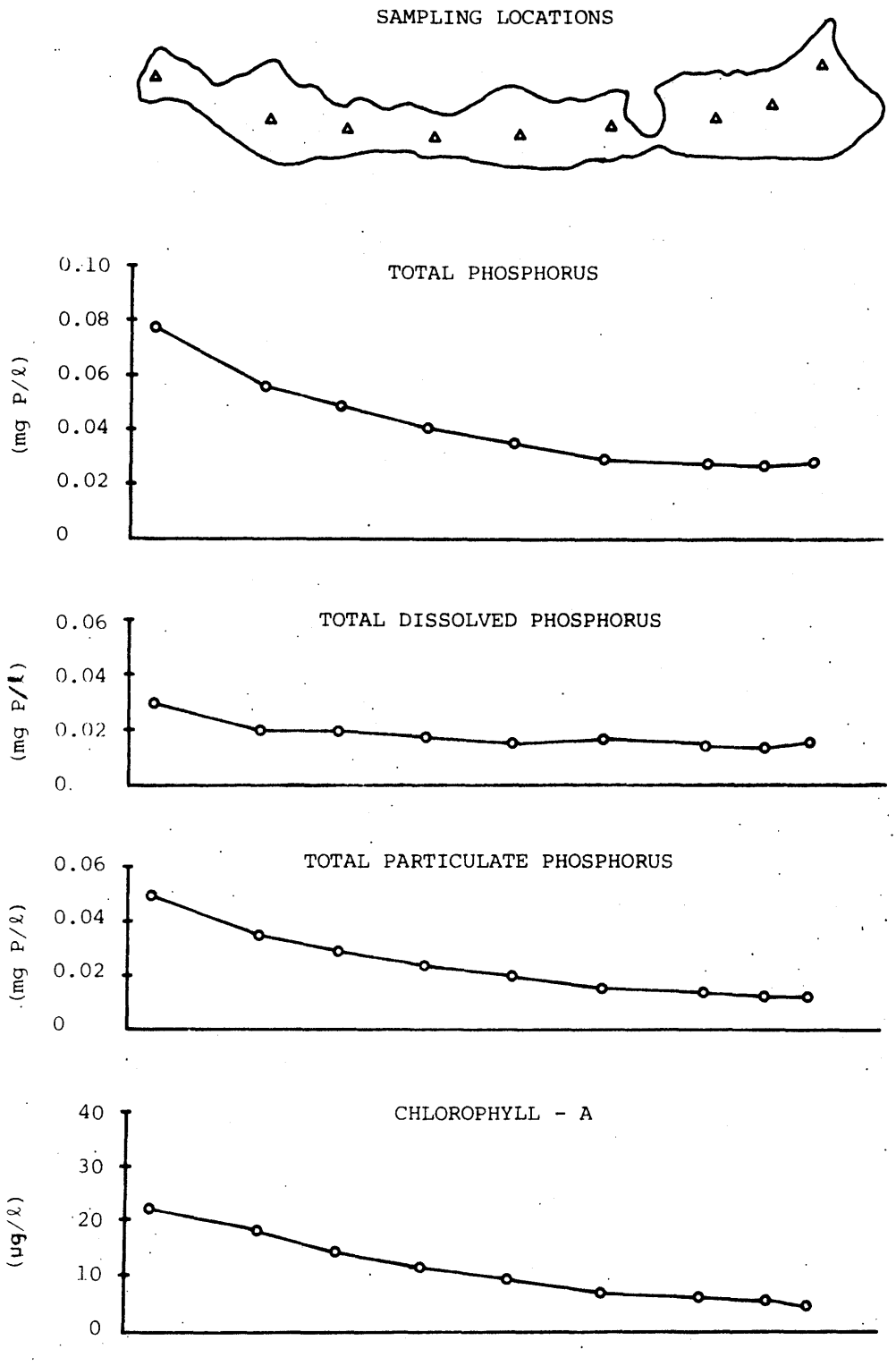

Figure 4.7

Longitudinal distribution of average phosphorus and chlorophyll-a over the period 1976-1978 (from van Straten et al., 1979)

actions of the chemistry and biology are complex and have not been fully explained.

The observed chemistry of the lake generally behaves as expected for the calcium carbonate system. The average pH of Lake Balaton water is about 8.4, consistent with water in equilibrium with calcite, $CaCO_3$, and with the atmosphere. Under the high pH and hardness in Lake Balaton, calcite precipitates readily, driven by the removal of CO_2 during algal and macrophyte photosynthesis (Müller, 1970 and 1971). As indicated in Section 2.2.1, such biogenic lime formation is accompanied by the co-precipitation of phosphorus. The importance of phosphorus co-precipitation in Lake Balaton is indicated by Jolánkai and Szöllősi-Nagy (1978) who believe that 72 percent of the phosphorus load to the lake is immediately co-precipitated and deposited in the sediments.

Under the chemical conditions of Lake Balaton, the co-precipitated phosphate is expected to form hydroxyapatite, either directly or by adsorption to precipitating calcite with later transformation. Adsorption of phosphate on hydrous oxides or clays are less important co-precipitation methods at the pH levels in Lake Balaton, but may nevertheless be significant phosphorus sinks. At the mean pH and calcium concentrations in the lake, the solubility of hydroxyapatite predicts an equilibrium orthophosphate concentration of 4 µg/ℓ, which is consistent with observations.

4.3.3 Biology

Unfortunately, the observed response of Lake Balaton's phytoplankton population is less consistent with our expectations than the observed chemistry. Under the equilibrium chemistry hypothesized above, orthophosphate concentrations will always be very low. The plentiful calcium carbonate insures this even for increased phosphorus loadings. Since orthophosphate is believed to be the only form of phosphorus the algae are able to assimilate, the increase in loading should not lead to a significant change in eutrophication. Observations in Lake Balaton have, of course, been to the contrary and, thus, other supplies of phosphate must be hypothesized and tested. In this section, we will examine what is known of the interactions between biological activity and phosphorus in Lake Balaton.

The relative importance of algal uptake on orthophosphate concentration was the topic of experimental work by Dobolyi and Herodek (1980). Their experiments determined the fate of isotope-labeled orthophosphate added to a plexiglass enclosure designed to isolate an in-situ culture of lake water. The enclosure was roughly one meter square in area, and was placed in the lake in water of about one meter depth. The box was equipped with an electric stirring paddle to maintain sediment suspension. The strength of this mixing is not clearly stated however -- it may have been insufficient to cause continued resuspension of bottom material.

Dobolyi and Herodek hypothesized three possible controls on the orthophosphate concentration: algal uptake, biogenic lime formation, and adsorption on suspended sediments. Through various procedures, they isolated the influence of the first two controls and measured their effect when labeled orthophosphate was added to the enclosure. They found that elimination of biological activity by chlorination ceased all orthophosphate uptake; hence, adsorption to suspended sediment was concluded a minor influence in the enclosure. Addition of EDTA to the box to prevent lime formation led to essentially the same orthophosphate uptake as without EDTA; thus, co-precipitation was also concluded a minor influence. Together, these results showed the major orthophosphate removal mechanism in the experiments to be uptake by phytoplankton.

Two likely sources of orthophosphate to sustain algal uptake have been identified (van Straten and Somlyódy, 1981). The first is a rapid recycling of organic phosphorus to the inorganic form. As seen above in Figure 4.7, total dissolved phosphorus constitutes a major fraction, one third to one half, of the total measured phosphorus. Orthophosphates are a very small part of this dissolved fraction; dissolved organic phosphorus and polyphosphates make up most of it. Lean's findings, discussed in Chapter 2, show bacterial remineralization of these dissolved forms may be rapid and substantial. Such remineralization is probably an important source of orthophosphate in Lake Balaton.

The second hypothesized source of phosphorus for algal growth is that released from the lake's sediments. Since Balaton is so shallow, even moderately strong winds can cause motion throughout the water column, leading to a stirring and suspension of bottom sediments. Observations have confirmed a correlation between wind events and high suspended sediments concentration (Hamvas, 1966), and with high total phosphorus levels as well (Somlyódy, 1980). The connection with orthophosphate release is less certain, however. Measurements have not shown high orthophosphate levels coincident with wind-induced total phosphorus increases. This does not rule out the release of sedimentary orthophosphate, however, since it could be consumed rapidly by algal uptake or adsorption to sediment particles. On the contrary, the liklihood of orthophosphate release is supported by measurements of the sediment made by Dobolyi (1980). He found orthophosphate concentrations on the order of 100 µg/ℓ in the interstitial water of the sediment -- a level at least twenty times higher than in the lake water. The thickness of the oxidized microzone of the sediments is only about 1 to 4 cm (Olah, cited in van Straten et al., 1979), and thus could be disturbed by strong mixing. However, further research is necessary to clarify the role of wind mixing and of diffusion in sedimentary orthophosphate release before such release can be concluded an important nutrient source.

Still another possible source of phosphate has been suggested by Hemond (personal communication). He proposes that the extensive reed belts in the shallow shoreline areas of the lake may serve as nutrient pumps, removing phosphorus from the sediments and excreting orthophosphate to the water column. (See Section 2.2.2.) Reeds cover about three percent of the lake's surface (van Straten et al., 1979) and

thus could make a potentially large orthophosphate contribution. To our knowledge, this possibility has not been investigated, although the efficiency of the reeds for phosphate removal has been studied (Tóth, 1972).

4.3.4 Nutrient Loading

Ultimately, the cause of Lake Balaton's eutrophication must be the entry of nutrients into the water column. Although these nutrients may originate from internal sources -- that is, sources within the lake itself such as bottom sediments -- external sources outside of the lake are likely more important. This is demonstrated by Somlyódy (personal communication), who shows that the increase in algal biomass in the lake coincides with a number of external factors known to increase nutrient loads: rising population and tourism, and expanding use of chemical fertilizers for example. Clearly, an understanding of Balaton's water quality requires a knowledge of the nutrient load entering the lake. In this section we will briefly examine the origin and magnitude of various loads drawing our material from a recent report by Jolánkai and Somlyódy (1981).

Nutrients enter the lake via either point sources or non-point sources. Point sources are those for which a specific point of discharge into the lake may be identified -- river or stream inflows or sewage discharges. Non-point sources include all other nutrient sources, such as that settling from the atmosphere or carried by groundwater seepage. In practice, the division between point and non-point sources is indistinct and the numerous diffuse small point sources such as urban stormwater and rainfall runoff flowing directly to the lake are included as non-point sources.

Jolánkai and Somlyódy (1981) have collected and analyzed field data from a number of sources to develop a loading classification and estimate. This is summarized in Table 4.1 as the quantities of total phosphorus, orthophosphate, and available phosphorus due to various sources. Available phosphorus is an estimate of the phosphorus which can be utilized by algae for growth -- that is, "available" to the algae. It includes orthophosphate plus unbound organic compounds from the remaining phosphorus inflow. This latter part of the load will vary between ten and thirty percent of the total phosphorus load exclusive of orthophosphate; the uncertainty of the availability percentage implies the approximate character of the available phosphorus estimate. Nevertheless, available phosphorus is a convenient indicator of the eutrophication potential of the nutrient load.

Table 4.1 includes three major loading classes which are further broken down by sub-classes. The point sources, tributary inflows plus sewage discharges, comprise the greater portion of the loading. Of the point source load, fully one-third is due to the Zala River inflow at the lake's western extreme. All other tributary loads must be taken together to arrive at a load equal to that of the Zala. The tributary loading appears in time as a series of brief high-load periods coinciding with flood events of at most a few days duration. The distribution of the load shows no regular pattern from month to month, with the monthly average load varying by no more than a factor of two. Less uniform is the spatial distribution of the tributary loads. As may be seen in Figure 4.8, the

Table 4.1

Phosphorus loading estimate for Lake Balaton
(Based on Jolánkai and Somlyódy, 1981, Table 11)

	Total P (kg/day)	Ortho P (kg/day)	Available P (kg/day)
Tributary Loads			
Zala River	225	104	128
Other streams	248	104	133
	473	208	261
Sewage Loads			
Direct sewage	105	-	105
Ponded sewage	26	-	26
	131		131
Non-Point Source Loads			
Urban stormwater	161	19	47
Direct runoff	79	11	24
Atmospheric	171	68	89
	411	98	160
Total	1015		552

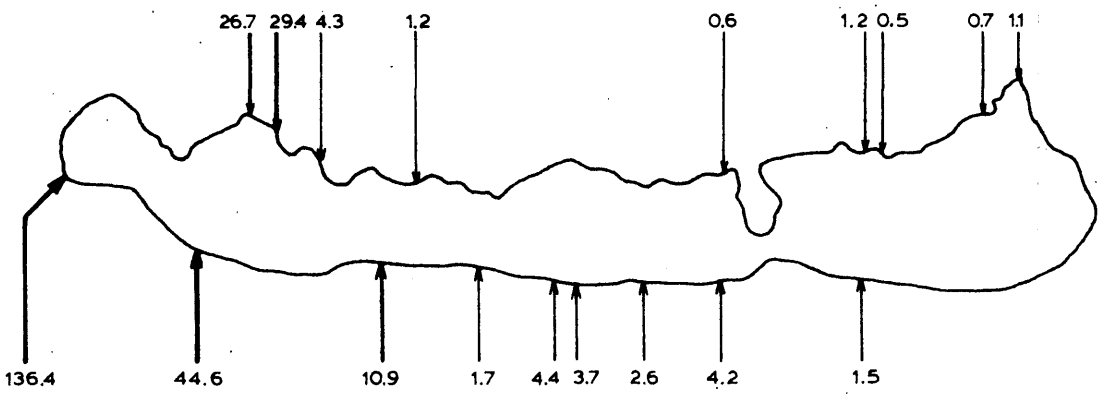

Figure 4.8

Spatial distribution of annual average available phosphorus loads (kg/day) due to tributary inflows (based on Jolánkai and Somlyódy, 1981)

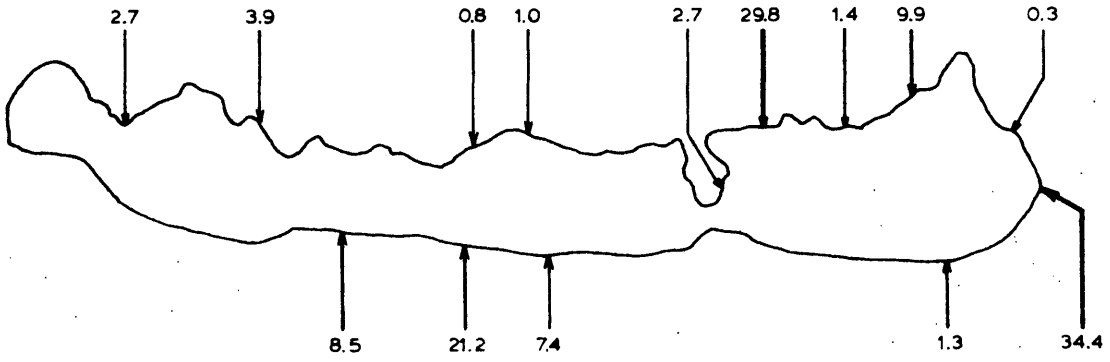

Figure 4.9

Spatial distribution of annual average available phosphorus loads (kg/day) due to sewage and sewage pond inflows (based on Jolánkai and Somlyódy, 1981)

largest tributary inflows are heavily concentrated in the western part of the lake.

Sewage effluents, which make up the final third of the point source load, fall into two categories: direct discharges and ponded discharges. The ponded discharges do not flow directly into the lake during the summer months. Rather, they are retained for those months in fish breeding ponds in a form of tertiary sewage treatment which removes roughly fifty percent of the phosphorus nutrients. These ponds are drained over about a ten-day period in early autumn, after which sewage flows directly to the lake until the ponds are reestablished the following summer. The drainage period causes a very intense nutrient input of short duration -- a significant transient point load. The remaining sewage loads are those which discharge directly to the lake without interruption. These loads exhibit a significant increase during the summer tourist season, peaking in July and August at three or four times the loading rate of the off-season. The spatial distribution of sewage loads along the lake is indicated in Figure 4.9.

Non-point sources, by their very nature, are less easily quantified than the point sources. Jolánkai and Somlyódy were able to estimate the major non-point sources other than groundwater infiltration. These estimates, which are based on scarce data and literature values, are given in Table 4.1. The very little information available suggests groundwater seepage is probably a negligible load.

The variation of the non-point source loadings in time and space is largely unquantified. Urban stormwater and direct runoff loads are directly caused by rainfall events and will vary in time accordingly. Atmospheric loads, for lack of better information, are assumed constant in time. The distribution of atmospheric and direct runoff loads is likely to be nearly uniform over the lake, while stormwater loads originate in cities and villages near enough to the lake to discharge directly to the lake rather than to a tributary stream.

5 A LINKED WATER QUALITY MODEL OF LAKE BALATON

5.1 Defining the Model

A preliminary analysis of the requirements for a water quality model can simplify its application and better its possibilities for success. In this section, therefore, we attempt to define the model characteristics in as systematic and rigorous a fashion as possible. The factors determining the model characteristics are the goals and purposes the model is to fulfill, the physical, chemical and biological processes governing the lake's behavior, and the availability of field data to confirm the model results. We evaluate these factors in Section 5.1.1 as a first step in fixing the model formulation. Then, in the remaining part of Section 5.1, we refine the model definition through more detailed examination of the individual model components.

5.1.1 Preliminary Model Definition

To define the desired water quality model we must first establish the purposes and goals of the modeling program. Ultimately, the model must be able to compare and evaluate possible water quality control alternatives for Lake Balaton. Though the root of Balaton's water quality problem is known to be the introduction of the algal nutrient phosphorus into the lake, there is less certainty over the most effective means to limit nutrient influx. Nutrients are carried into the lake by such disparate sources as the single large inflow of the Zala River and the many small stream, local runoff, and sewage inflows scattered around the lake. These inflow sources vary greatly in time -- for example, sewage inflows change with the seasonal tourist population, while the Zala River fluctuates with the annual variation of streamflow, and local runoff and streams respond to the episodic occurrence of rainfall storms. The seasonality of farming leads to still more variation in the quantity of nutrients originating from agricultural fertilizers. These various nutrient sources, which differ so much in their spatial and temporal distribution, require very different control strategies. The water quality model must distinguish the mechanisms and consequences of these controls by recognizing their spatial and temporal character.

The water quality model must also capture certain essential features of the biogeochemical system. In particular, since eutrophication is our main concern, some measure of algal biomass must be an output of the model. Moreover, we know from field data that algal concentration changes greatly along the lake and also that it can increase rapidly during one or two growth periods, or blooms, during the year. Therefore, the model would be most useful if it showed these concentration variations in time and space.

Finally, we would like the model to indicate the major causes of Balaton's problems. Although we have established this in general terms -- namely, the introduction of the nutrient phosphorus -- we cannot currently distinguish external from internal nutrient sources, nor can we identify the dominant mechanism removing orthophosphate from the water column. To satisfy these information needs, the model requires explicit formulation

of water-sediment interaction, biogenic lime precipitation, and nutrient uptake by phytoplankton.

With the water quality modeling goals identified, we can proceed to a broad definition of the model characteristics. Chapters 2 and 3 present a wide spectrum of possible water quality transport models. At the most complex end of this spectrum lies the transient three-dimensional water quality and transport model. At the simplest is the lake modeled as a fully mixed tank, operated on very long time steps and neglecting completely all internal transport. Possible model alternatives for Lake Balaton are shown in such a spectrum in Figure 5.1. Working water quality models of the lake lie near the lower end of this spectrum since they use one or four-box formulations (Csáki and Kutas, 1980; Leonov, 1980; and van Straten, 1980). The critical factor in selecting a particular model from this spectrum is the model's ability to properly couple the major processes affecting water quality: hydrodynamics and biogeochemistry.

Hydrodynamic processes in the lake interact with the biogeochemical processes by transporting and mixing the state variables. Only by coupling hydrodynamic and biogeochemical model components can the crucial description of advective and diffusive transports be provided. The success of such a coupled model depends, however, upon the consistency of the components with each other, with the processes within the lake, and with the goals set for the modeling program. A good indication of this consistency is supplied by an examination of the length and time scales important in the lake's behavior.

The magnitudes of the length and time scales of the major physical and biogeochemical processes in Lake Balaton are depicted in Figure 5.2. Though approximate, the time and length scale diagrams point out some important considerations for modeling. For example, we can see that wind-driven circulation corresponds with horizontal concentration gradients at a length scale on the order of a kilometer and a time scale of one or a few days. Vertical processes occur over somewhat shorter time scales with a length scale on the order of a few meters. Long-term eutrophication proceeds slowly at lake-wide length scales in rough correspondence with the hydrologic through-flows. These correspondences of physical and biological scales illustrate clearly those processes which we can expect to interact strongly, and those which we can assume to be essentially independent. For example, hydrologic through-flows will not affect the vertical variation of nutrient and organism concentrations, which respond instead to the wind-induced vertical mixing and the creation and destruction of temperature stratification.

We can add substance to these qualitative comparisons with a quantitative example from Lake Balaton: an evaluation of the relative importance of hydrologic through-flow and seiche currents. For estimates of the hydrologic through-flow, we draw upon van Straten et al. (1979). Through water balance calculations, they compute inter-basin flows for the four Balaton basins. Translating their results into volume transports over various time periods produces the quantities given in Table 5.1. For comparison, the volume of water transported by a typical amplitude seiche can be estimated. Assuming a difference in water surface elevation of

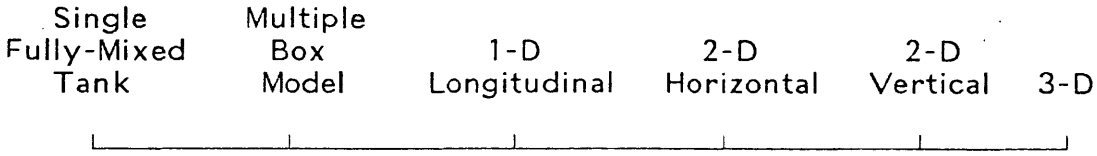

Figure 5.1

Water quality models possible for Lake Balaton

one-half meter between the ends of the lake and a linear water surface profile, the amount of water transported across the seiche nodal line is on the order of 75 million cubic meters in a time period of about 6 hours. This volume is roughly twice that transported in a month by the hydrologic flows, and two orders of magnitude greater than the monthly flows scaled down to six hours. Yet, over a year, the seiche motion produces no net flow into or out of the lake, while the hydrologic flows replace roughly 50% of the total lake volume. Our conclusion is clear: over short time scales of less than the seiche period, the seiche dominates; over long time periods on the order of the lake residence time, the hydrologic flow governs.

This analysis of length and time scales illustrates some important concepts which the modeler must consider. First, the water quality model must account not only for the particular biogeochemical processes of interest, but also the corresponding physical processes as well. And, to represent these processes and their interaction successfully, the model must operate at the correct length and time scales. This has been emphasized by Ford and Thornton (1979):

> The...conceptualization of any process, such as turbulent mixing or phytoplankton growth, constrains the ... predictions from this formulation. The conceptualization of some processes such as turbulent mixing on a daily time scale, in general, would not be appropriate to describe how that process occurs on a micro-second time scale. The conceptualization of phytoplankton production on a seasonal basis would not be expected to predict diurnal production cycles.

They further state:

> It is also important to recognize that many processes conceptualized on a micro time scale cannot simply be integrated over time to describe daily or seasonal processes.

Table 5.1

Volume transports between the Balaton basins
(from van Straten, Jolánkai and Herodek, 1979)

	Keszthely to Szigliget	Szigliget to Szemes	Szemes to Siófok
Annual	297	439	444
Summer Half-Year	133	197	200
Winter Half-Year	164	242	244
Monthly Average	25	37	37
Maximum Monthly	42	58	53
Minimum Monthly	16	25	28

All quantities are in million cubic meters.

This last point has been demonstrated in an extensive modeling study of Lake Ontario conducted by the Canadian Centre for Inland Waters (Simons and Lam, 1980). Simons and Lam coupled hydrodynamic and biogeochemical models to develop a multi-layer model of Lake Ontario's transient water quality. The lake was simulated over a number of years using a time step on the order of a day and a spatial grid of roughly 5 kilometers. Significantly, the authors conclude that the model, though able to predict seasonal and shorter term trends, is unable to model trends over a few years with high accuracy. Despite this pessimistic conclusion, the water quality model may still be able to capture the short term manifestations of eutrophication in algal blooms even if very long term trends are missed. This still permits very effective comparisons and evaluations of alternative lake water quality control schemes. Further, we believe that as experience in this type of modeling accumulates, predictive ability will improve to the point that long-term trends are successfully captured.

We qualify this length and time scale analysis by cautioning that it should be considered only as a rough, though essential, guide for model design. In this process, the modeler first decides the type of information he desires from the model: for example, long-term trends in eutrophication or day-to-day changes in algal population. This modeling goal

implies certain length and time scales, as illustrated in Figure 5.2. Once these scales are known, the lake processes likely to be influential can be identified for inclusion in the model, and rough magnitudes of the model time and space intervals can be reckoned. Thus, the scale analysis provides a systematic framework for model design, leading to general bounds on the model specifications. It should not be construed as a rigorous means to exact model definition, but rather as a convenient framework for initial model planning and design.

Superimposed upon the time and scale analysis is one last factor to be considered when selecting the water quality model: the availability of field data with which to verify the model results. Model predictions which cannot be substantiated by field observations are of little value; an unverified model cannot be used with confidence to design water quality controls. In Balaton, there are regular field measurements of water quality constituents at only nine stations along the lake ten times per year. (See van Straten et al., 1979.) And, these measurements do not evaluate concentration variations in the vertical or transverse directions. This effectively limits the model resolution to differences along the lake over time periods on the order of a few days.

We can now bring our preliminary model selection to its conclusion. The goals set for the model, and the limitations imposed by the available data, determine these bounds on the model characteristics: the model must be able to predict variations in algal abundance along the lake's long axis and over time periods as short as weeks. From our time and length scale analysis, we can see that these bounds fall below the regime dominated by hydrologic flows alone, so that the model must include the transport due to seiche and wind-driven circulation. Thus, a coupled model, which includes both a hydrodynamic component to predict circulation and a biogeochemical component to simulate phosphorus reactions, is needed. The framework for coupling the components is suggested by the rough bounds stated above; the simplest possibility is a transient, longitudinally one-dimensional water quality model. We proceed in the remainder of this section to weigh the simplifications and approximations implied by this formulation, and to examine the model components in greater detail.

5.1.2 Water Quality Transport in the Coupled Model

Development of a one-dimensional water quality transport model requires that the longitudinal velocity be obtained by integration of the velocity over the width and depth of the lake cross section. This process is also the basis to develop one-dimensional models of stream water quality, a field in which a substantial body of literature exists. For either the lake or stream, integration over the cross section causes all vertical and lateral variations in velocity to be eliminated, giving rise to the longitudinal dispersion coefficient to capture the effects of such variations on longitudinal transport. The dispersion coefficient is defined as a function of the stream velocity, as well as geometrical and other properties. The literature of stream pollution modeling cites a number of problems in this approach, including lateral velocity variations which are greater than the theoretical, dead zones in the flow, secondary circulations due to lateral and vertical velocities, and multiple flow paths

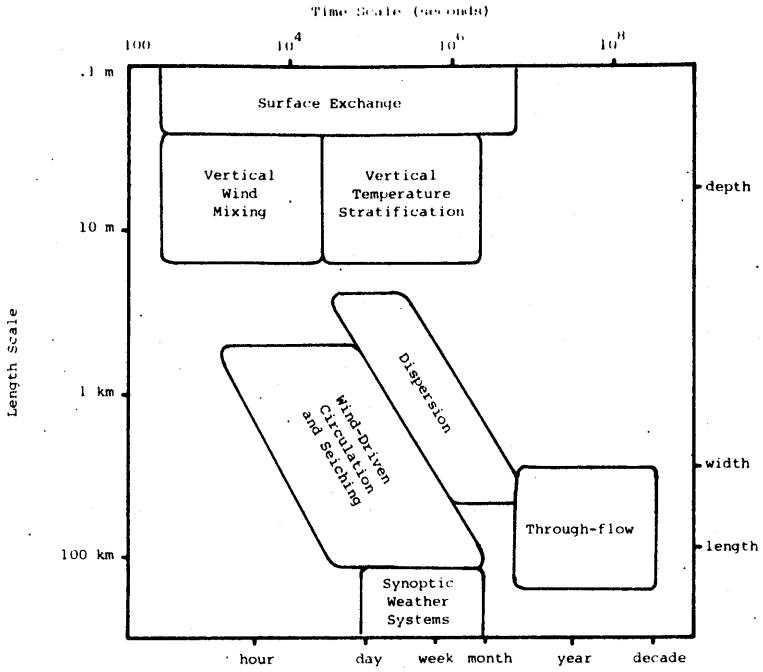

a) Physical Processes

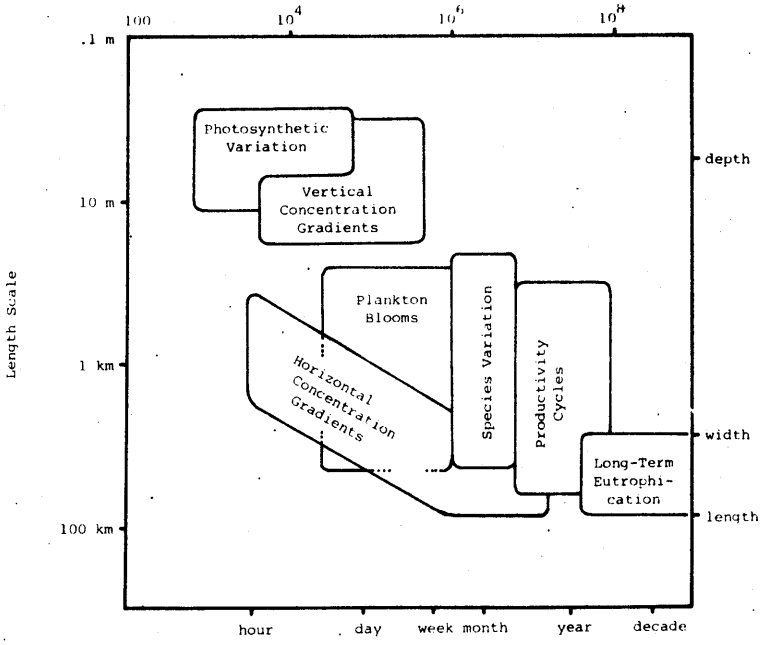

b) Biogeochemical Processes

Figure 5.2

Approximate length and time scales in Lake Balaton
(Based upon Harleman and Shanahan, 1980 and Brown, 1978)

around islands and bars. These stream characteristics all lead to large increases in the dispersion coefficient above the value predicted by theory.

Although the analogy with stream modeling is instructive, Lake Balaton has many striking differences from the stream situation. While stream flow is generally unidirectional throughout the cross section, field and hydraulic model studies have shown flow reversals in vertical and lateral space in Lake Balaton. Further, the common transverse winds lead to a significant lateral circulation in the lake. As will be shown below, these flows, which correspond to secondary circulations in streams, can be quite significant in Balaton. Thus, the cross-sectionally averaged longitudinal velocity will be far less representative for Balaton than it will be for streams. This implies a relatively larger contribution due to dispersion than would typically be found in stream modeling.

Variations of the longitudinal velocity with time are also important in Balaton due to the frequent and strong seiche motion. This type of motion is similar to that found in a tidal estuary -- suggesting an analogy between our modeling task and that of estuarine water quality. Two types of estuarine water quality models exist: the real-time model, which considers the variation of longitudinal velocity over time scales much shorter than the tidal period, and the non-tidal model, which assumes a velocity due only to the net freshwater flow into the estuary. The non-tidal model depends upon averaging over the tidal period to simplify the velocity term, whose temporal variations must then be accounted for in the longitudinal dispersion coefficient. The consequent dispersion coefficient is much greater than the corresponding coefficient for the real-time estuary model. Harleman (1971) cites severe difficulties in defining the dispersion coefficient for non-tidal models and recommends the real-time model for all serious estuary modeling efforts.

The experience in estuarine modeling offers an important lesson for our study of Lake Balaton. Clearly, averaging over sufficient time periods to eliminate seiche motion is possible, but would create considerable difficulties in the determination of the proper longitudinal dispersion coefficient. This recommends the real-time solution of the seiche motion over time steps no longer than about an hour. (In fact, use of an explicit non-rigid-lid computation scheme will impose stability constraints limiting the time step to the order of minutes.) The output from this model may then be averaged or sampled in time if it is desired to reduce the time step frequency in a linked biogeochemical model.

5.1.3 Hydrodynamic Model Component - Part I

The analysis of Lake Balaton's circulation in Chapter 4 allows us to identify the likely major hydrodynamic influences upon the water quality. The back and forth motion due to the seiche is the most obvious. This motion is primarily translational: it moves parcels of water along the lake, first in one direction and then back. Accompanying this translational, or advective, motion is dispersion, the differential movement of neighboring water parcels due to non-uniformities in the lateral and vertical velocity distributions. This mechanism will act to smear differences in the concen-

tration of water quality constituents along the lake -- it is an important hydrodynamic factor which should be determined as accurately as possible. Finally, there is the net hydrologic flow through the lake. Although this factor acts much more slowly than those above, it is nevertheless important since it acts to remove and replace water within the lake.

Hydrologic through-flow may be determined by long term water balance, however a more dynamic model is necessary to give the seiche-related transports. Thus, we are led to a hydrodynamic model component to determine the advective and dispersive transports required by the biogeochemical component. The advective transport is fairly easily supplied to a one-dimensional water quality model. The cross-sectional mean velocities can be found directly in a 1-D flow model or by averaging the results of 2-D or 3-D circulation models. Our discussion of stream and estuary modeling disclosed a possible pitfall in the use of one-dimensional models, however. Such a one-dimensional model would incorporate all the complexities due to lateral variations in the longitudinal velocity and due to transverse circulations into a single parameter, the longitudinal dispersion coefficient. Experiments with the four-box SIMBAL model have shown significant sensitivity to the magnitude of exchange flows between the boxes (van Straten, 1980). Though the exchange flows are not identical to the dispersion mechanism, they are sufficiently similar to suggest problems. In particular, the use of a time-constant dispersion coefficient as done in river and estuarine modeling may be inadequate in Balaton. In the lake, the situation is complicated by significant lateral velocities due to highly transient wind forces, reversing, unsteady seiche motion, and the influence of a finite length. It would be far better to determine a dispersive flux directly from a two or three-dimensional flow field prediction based on the wind-driven circulation.

Dispersion can be computed directly from the cross-sectional velocity distribution using methods developed by Fischer. If variations in the vertical velocity distribution are the major cause of dispersion, then the dispersion coefficient is given as (Fischer, 1966):

$$D_h = -\frac{1}{h} \int_0^h dz\, u'(z) \int_0^z \frac{dz''}{\varepsilon_z} \int_0^{z'} dz''\, u'(z'') \qquad (5.1)$$

where
- D_h is the dispersion coefficient due to vertical velocity variations,
- h is the depth,
- $u'(z)$ is the deviation of the velocity at elevation z from the vertically averaged velocity, and
- ε_z is the vertical turbulent diffusivity.

Here, D_h is determined for particular values of x and y, that is, for a particular horizontal position in the lake. A rough estimate of D_h can be determined as:

$$D_h \propto \frac{h^2 u_h^2}{\varepsilon_z} \tag{5.2}$$

where u_h is the maximum deviation of the velocity from the vertical mean velocity.

Where lateral variations in velocity are dominant, the dispersion coefficient is given by an equation developed in Appendix D. This equation is similar to that of Fischer (1967), except that it assumes lateral advection to be a more important transverse mixing mechanism than turbulent diffusion.

$$D_W = -\frac{1}{A} \int_0^W dy\, q'(y) \int_0^y dy' \frac{q'(y')}{V} \tag{5.3}$$

where
- D_W is the dispersion coefficient due to lateral velocity variations,
- A is the cross-sectional area,
- W is the width,
- V is the lateral flow per unit width, and
- q' is the deviation of the flow per unit width from the lateral mean flow per unit width, determined as a function of distance across the stream.

In this equation, D_W is a function of x, the distance along the lake. It may be taken as roughly proportional to:

$$D_W \propto \frac{W u_w^2}{v} \tag{5.4}$$

where u_w is the maximum deviation of the velocity from the lateral mean velocity, and
v is the lateral velocity.

We can evaluate the relative importance of lateral and vertical velocity variations by the ratio of Equation 5.4 to 5.2:

$$\frac{D_W}{D_h} \simeq \frac{W u_w^2 \varepsilon_z}{h^2 u_h^2 v} \tag{5.5}$$

To determine this, we will first make the reasonable approximation that $u_w \simeq u_h$ -- this is certainly accurate within an order of magnitude. The length scales are known from the lake geometry: W = 8000 m, and h = 3 m. The vertical diffusivity ε_z can be estimated by measurements given in the literature to be about 30 cm^2/sec, while the lateral velocity v can be taken as roughly 5 cm/sec from measurements described in Appendix A. With these values, we can give an order of magnitude estimate for the dispersion coefficient ratio, $D_W/D_h \simeq 50$.

Our analysis is not yet complete, however, since we have not accounted for one assumption implicit in the formulae given above. That assumption is that there has been sufficient time after the dispersant has been introduced into the flow for that material to have mixed throughout the cross section. Holley, Harleman and Fischer (1970) show that this is often not the case in the oscillating flow of estuaries since the oscillation period may be less than the time for mixing. The time for mixing, T_c, is given by Holley et al. as:

$$T_c = \frac{\lambda^2}{\varepsilon} \tag{5.6}$$

where λ is the distance over which mixing must occur, equal to the distance from the boundary to the point of maximum velocity in the cross section, and

ε is the diffusivity in the direction corresponding to λ.

The vertical mixing time is small compared to the seiche period in Balaton and the assumption of sufficient mixing time holds for D_h. For horizontal mixing due to lateral velocity, the mixing time is:

$$T_c = \frac{\lambda}{v} \approx \frac{W}{2v}$$

T_c is thus on the order of twenty hours, or a few times the seiche period.

Holley et al. (1970) present a theory relating the effect of insufficient mixing time on the dispersion coefficient. Although the theory is not strictly applicable to lake environments, we may use it as an approximation. For the ratio of seiche period to mixing time determined above ($T/T_c \approx 0.4$), the realized dispersion will be roughly half that predicted without considering the mixing time. Thus, dispersion due to variations in the lateral velocity distribution will still dominate those due to vertical velocity non-uniformities by roughly an order of magnitude.

This analysis of dispersion allows us to select an adequate hydrodynamic model component as a horizontal two-dimensional circulation model -- the single-layer model identified in Section 3.4.2. The single layer model determines the distribution of flow both along and across the lake. The latter information supplies the resolution in lateral space necessary to determine dispersion. Summation of the lateral fluxes across the lake gives the advective flux.

5.1.4 Hydrodynamic Model Component - Part II

The single layer circulation model, as explained in Chapter 3, offers both advantages and disadvantages. By far its greatest advantage is its simplicity and consequent low simulation expense. This is made possible, however, by a number of assumptions and approximations which may limit the use of the model. Therefore, before we can employ such a model with confidence, we must first examine its assumptions in light of the criteria given in Chapter 3 and the physical characteristics of the application lake.

In Section 3.5 we presented the assumptions possible in circulation model formulation; these include the shallow water assumptions, neglect of convective acceleration, the rigid-lid and small amplitude approximations,

and neglect of horizontal frictional forces. These approximations will be examined in turn below using as a basis the physical parameters gathered from various sources in Table 5.2. In this table, the value of the horizontal eddy viscosity has been assumed based on similar data published for other lakes. Although the value used is reasonable for Lake Balaton, it is not, in fact, determined by actual measurements. Also included in Table 5.2 are the various dimensionless numbers (force ratios) computed from the physical parameters.

The shallow water assumptions are permitted if the lake depth is sufficiently small. In Balaton, the ratio of depth to length is on the order of 10^{-4}. As well, the Ekman friction depth, which indicates roughly the depth to which wind surface stress will be influential, is at least 14 meters. This is sufficiently greater than the average lake depth that the lake may be classified as "very shallow" under criteria given by Lindijer (1979). Finally, field measurements reveal that the lake's vertical stratification is weak and intermittent (Entz, 1976). These data safely assure the propriety of using the shallow water assumptions.

Neglect of convective acceleration is permissible if the Rossby number, the ratio of inertial to Coriolis forces, is small. As seen in Table 5.2, this ratio lies within the range of 0.02 to 0.2, sufficiently small to permit neglect of the convective terms. Even smaller is the horizontal Ekman number, easily allowing the neglect of viscous effects in the horizontal plane.

The condition to impose a rigid lid condition is that the square of the seiche period be much less than the square of the inertial period. This criterion is easily satisfied in Lake Balaton for transverse seiches, but only marginally for longitudinal. Since the rigid lid approximation may greatly distort predicted transient motions, it would be unwise to employ it given its small safety margin for Lake Balaton.

According to the free surface boundary parameter, it is safe to employ the small amplitude approximation and apply boundary conditions at the undisplaced free surface location. However, the parameter in Table 5.2 is based upon the lake's average depth and is clearly inappropriate in the shoreline regions where the displacement may exceed the depth. Thus, it may be wise to base computations on the actual free surface, rather than the undisplaced level.

Unfortunately, the data of Table 5.2 do not give a complete picture of the lake's behavior since important local effects are ignored. Along the shoreline, and at Tihany Peninsula, local influences can be expected to produce significant divergence from the general behavior outlined above. At Tihany, for example, convective accelerations may be important and possibly frictional influences as well (large Rossby and horizontal Ekman numbers, respectively). In this local region, therefore, a linearized model may not be able to reproduce the lake circulation with great accuracy. As long as this error is confined to a small region, however, such a model remains useful for the lake-wide circulation needed as input to a water quality model.

Table 5.2

Physical parameters for Lake Balaton

Length	$L = 75$ km
Width	$W = 8$ km
Depth	$H = 3.2$ m
Velocity (due to seiche)	$U = 0.20$ m/s
Coriolis parameter	$f = 10^{-4}$ rad/s
Horizontal eddy viscosity (assumed value)	$A_H = 10^4$ cm^2/s
Vertical eddy viscosity	$A_V = 15$ cm^2/s
Froude number	$Fr = U/\sqrt{gH} = 0.025$
Rossby number	$Ro = U/fL = 0.02$, or $Ro = U/fW = 0.2$
Surface boundary parameter	$Fr^2/Ro = 0.035$ or 0.0035
Horizontal Ekman number	$E_H = A_H/fL^2 = 1.8 \times 10^{-6}$, or $E_H = A_H/fW^2 = 1.6 \times 10^{-4}$
Vertical Ekman number	$E_V = A_V/fH^2 = 1.5$
Ekman friction depth	$D = \pi\sqrt{2A_V/f} = 17$ m
Critical bottom slope	$s_c = H\sqrt{E_V}/L\sqrt{E_H} = 0.04$
Longitudinal seiche period	
(computed)	$T_l = 2L/\sqrt{gH} = 7.5$ hr
(observed)	$T_l = 10$ to 11.5 hr
Transverse seiche period	
(computed)	$T_t = 2W/\sqrt{gH} = 48$ min
(observed)	$T_t = 40$ min
Inertial period	$T = 2\pi/f = 18$ hr
Proudman number	$Pr = A_v^2/(\pi/L)^2 gH = 0.4$

Local effects must also be considered in the form of frictional influences along the shoreline. (See Section 3.5.4.) It is reasonable to neglect horizontal frictional forces in the shoreline regions if the bottom slope, s, is less steep than the critical slope, s_c. From Table 5.2, the critical slope is at most 0.04, corresponding to a very steep slope. Thus, this criterion is satisfied in all but a few locations, most obviously the deep channel at Tihany.

To summarize the findings of this and the last section, we have determined that a two-dimensional horizontal circulation model would be a proper hydrodynamic component for our water quality model. This component can supply the dynamic advective transport due to seiche motion, as well as resolve the associated dispersive transport. An analysis of Lake Balaton's physical properties found that the circulation model could safely employ an assumption of shallow water and could be linearized by neglect of convective acceleration. However, it was found that the motion of the free surface required cautious treatment, preventing use of a rigid lid assumption and small amplitude approximation.

5.1.5 Biogeochemical Model Component

Our approach in specifying a biogeochemical model component differs from our approach to the hydrodynamic model. Unlike the hydrodynamic model, of which a working transient version for Lake Balaton did not exist, the three Balaton biogeochemical models described in Chapter 2 preceded our work. Considerable knowledge and experience on Lake Balaton was a key contribution to the development of the earliest of the models, BEM, and carried through to the subsequent BALSECT and SIMBAL models. All of these models include the phosphorus interactions which we deemed essential in Section 5.1.1. Thus, our task was simplified for the biogeochemical model, requiring only that a model be incorporated with our transport model and hydrodynamic component. In this section, we very briefly review the selection of the biogeochemical formulation incorporated into our model.

The choice of the phosphorus cycle formulation depends as much on a philosophy of modeling as anything else. A basic problem is the level of detail desired -- that is, the number of phosphorus compartments. Models with few compartments take, in effect, a lumped parameter approach, in which the more numerous compartments of complex models are aggregated. Though a more complex subdivision may be pleasing from a theoretical viewpoint, the lumped component approach is probably more economical and useful for practical engineering studies. The user of the simplified model must be satisfied with a more empirical, less theoretically grounded model, however.

A further factor in deciding model complexity is the availability of field data for model calibration. As indicated in Section 2.4, calibration data should increase roughly as the square of the number of state variables -- thus, data needs grow very rapidly as complexity increases.

With these factors in mind, we chose van Straten's formulation of the phosphorus cycle for use in our model. His model, SIMBAL, is the simplest of the Balaton models, yet it shares the theoretical basis of the BEM model and thus much of the understanding of Balaton's water quality processes. The model simplicity is an important attraction, since we will be employing much greater spatial detail in our model of the lake, and thus making many more repetitions of the solution procedure. The savings in computer time by using a simpler model can therefore be substantial.

Further, SIMBAL is perhaps the most rigorously calibrated of the Balaton models. Its simpler structure requires fewer data for calibration, but also, van Straten (1980) has used an objective criterion to judge the calibration. A robust calibration is important if the model is to be extended to greater spatial detail without serious problems.

In summary, SIMBAL was selected as our biogeochemical model component since it was designed to address Balaton's problems specifically and has proven reasonably successful in reproducing historical data; since it is the simplest of the available models; and, since it has been calibrated in a rigorous manner.

5.2 Formulation of Water Quality Transport

The preceding discussion has emphasized the role of the hydrodynamic and biogeochemical components as the major parts of the water quality model. However, the model does not exist as isolated, unconnected parts; a vehicle is required to join the components as a coupled water quality model. This vehicle is the water quality transport model: the conceptualization of the lake as a group of individual volumes or locations where water quality constituents react and between which the constituents move. The transport model is virtually independent of what the water quality constituents are and how they react -- this is the business of the biogeochemical component. It is further independent of the means used to determine the mass transport fluxes which move the water quality constituents -- this task belongs to the hydrodynamic model component. The water quality transport model merely accepts the computations of the model components as inputs for its solution of the distribution of constituent concentrations within the lake. In this section, we describe the formulation of the water quality transport equations and their numerical solution.

5.2.1 Transport Equation

In formulating the water quality model, two approaches were followed simultaneously. The first, which we will call the finite difference model, approximates the continuous functions and derivatives of the governing differential equation. As such, it views the lake as a continuum. In contrast, the second approach is a lumped parameter multiple-box model. It is this second approach which has been used in the existing Lake Balaton models as well as most other lake water quality models.

The finite difference model is a direct approximation of the partial differential equation of mass transport. The equation represents the changes with time in the concentration of phosphorus at a point along the lake due to advection, dispersion and biological or chemical reaction. Phosphorus includes more than a single species and must thus be shown in the equations as a vector. The equation, in vector form, is:

$$\frac{\partial \underline{c}}{\partial t} = -\frac{1}{A}\frac{\partial (Q\underline{c})}{\partial x} + \frac{1}{A}\frac{\partial \underline{F}}{\partial x} + \underline{N} + \underline{L}' \qquad (5.7)$$

where
- $\underline{c}$ is a vector of phosphorus component concentrations,
- t is time,
- Q is the cross-sectional mean flow,
- A is the cross-sectional area,
- x is the distance along the lake,
- $\underline{F}$ is a dispersive flux vector,
- $\underline{N}$ is a biogeochemical reaction vector, and
- $\underline{L}'$ is a vector of loading per unit volume.

Two transport mechanisms are included in the equation: advective mass flux, equal to $Q\underline{c}$, and dispersive mass flux, represented by $\underline{F}$ in our notation. Usually, dispersion is computed using the dispersion coefficient D, so that the dispersive flux is given as:

$$\underline{F} = DA\frac{\partial \underline{c}}{\partial x} \qquad (5.8)$$

For now, however, we will retain the more general notation that $\underline{F}$ is the dispersive flux vector.

Also included in the equation is a generalized expression for all reactions and transformations affecting the phosphorus component concentrations. This is the reaction vector $\underline{N}$, which is a function of the concentration vector, as well as environmental factors which vary with time. As will be seen in Section 5.4, $\underline{N}$ represents a complex set of interrelationships taken from the SIMBAL model of Lake Balaton.

Finally, the equation includes the influx of nutrients due to external loads. This is represented by the loading vector $\underline{L}'$, which varies with both time and space. The loading vector includes nutrient flows from the various external sources identified in Section 4.3.4. Internal sources due to release from the sediments, however, are included as a part of the reaction vector rather than the loading vector.

A mathematically less formal approximation than Equation 5.7 is also possible. This method, similar to the finite section approach of Thomann (1972), conceives the lake as a series of fully-mixed tanks or boxes.

Treating each tank as a control volume and applying the principle of mass conservation is a conceptually direct route to a numerical formulation. Applied to the ith tank in a series, the approach leads to the following finite section equation which is analogous to Equation 5.7:

$$V_i \frac{d\underline{c}_i}{dt} = Q_i \underline{c}_{i-1} - Q_{i+1} \underline{c}_i + X_{i+1} (\underline{c}_{i+1} - \underline{c}_i)$$

$$- X_i (\underline{c}_i - \underline{c}_{i-1}) + V_i \underline{N}_i + V_i \underline{L}_i \qquad (5.9)$$

where $\underline{c}_i$ is the concentration in section i,

V_i is the volume of section i,

Q_i is the flow from section i-1 to section i,

X_i is the equal and opposite dispersive exchange flow between sections i-1 and i,

$\underline{N}_i$ is the rate of increase in concentrate mass due to reaction, and

$\underline{L}_i$ is the mass influx to the section.

In this equation, flow is presumed to go from section i-1, to section i, to section i+1; were the flow reversed, the signs on the flow terms would be changed accordingly. Equation 5.9 is the form used in the current models of Lake Balaton. It will also be used in this study for comparison with the finite difference method.

5.2.2 Numerical Solution

For practical problems, Equations 5.7 or 5.9 must be solved numerically on the digital computer. Equation 5.9 is already in a discrete form amenable to computer solution. However, Equation 5.7 must be replaced by an analogous but approximate difference equation (Leendertse, 1971). In the difference equations, the terms of Equation 5.7 are replaced by approximations in which finite differences in x and t take the place of partial derivatives. For example, in space the lake is subdivided into a number of small spatial increments of length Δx to form a finite difference grid. The equations are solved to give the concentration at a finite number of grid points as an approximation to the continuous function which satisfies Equation 5.7.

Before showing the numerical approximation of Equations 5.7 and 5.9, it is convenient to first discuss the procedure for solving the equations through time. This procedure was developed as an extension of the Fractional Step Method proposed by Verboom (1976). Verboom demonstrated

that it is possible to solve the advective-dispersive equation as a series of sub-problems while preserving the accuracy and other properties of the whole problem. Rather than solve the entire equation at each time step, Verboom solved portions of the equation in fractional steps: solving first for the advective term and then for the dispersive term. The procedure is advantageous since it is usually easier to solve a series of simple problems than to solve one large problem, and because individual solution schemes appropriate to each part of the equation may be developed.

In our extension of the fractional step method, described more fully in Appendix B, we have subdivided Equation 5.7 or 5.9 into three portions: advection, dispersion, and reaction and loading. These processes may show very different behavior in time -- some varying rapidly while others change only slowly. Therefore, we have added to the fractional step method a mixed time step procedure. Under this procedure, different solution step time increments may be used for the different fractional steps according to their individual stability and accuracy requirements. For example, suppose the reaction and loading processes are less constraining than the advective, and a much larger time increment may be used for the reaction computation. Since the reaction calculation is complex, substantial savings in computer time occur when the time increment is increased. Without mixed time steps, all parts of the computation must be done at the time increment of the most limiting process -- that is, at the shortest time step.

The numerical equations are shown in Figure 5.3. The approximation for each of the three fractional steps is shown separately, and a different time increment Δt is presumed for each step. As explained in Appendix B, the intermediate solutions c* and c** have no physical significance; the solution is not meaningful until it has been completed through the full cycle of steps.

In constructing Equations 5.10 and 5.11 (the advective and dispersive step equations of Figure 5.3) an effort was made to generalize the equations as much as possible. This has the unfortunate side effect of making the equations appear as confusing as possible, and some explanation of their form is due. Firstly, the equations employ what is sometimes termed theta-weighting to control the degree of implicitness in the equations (Hornbeck, 1975). Consider the following simple example of this technique:

$$c_i^{t+\Delta t} = c_i^{t} + \Delta t \left\{ \theta \left[fc_i^{t} + gc_{i-1}^{t} \right] + (1 - \theta) \left[fc_i^{t+\Delta t} + gc_{i-1}^{t+\Delta t} \right] \right\}$$

Advective step

$$\underline{c}_i^* = \underline{c}_i^t - \frac{\Delta t_a}{\Psi_i}\{Q_{i+1}^t[\gamma_{i+1}(\theta_a\,\underline{c}_i^t + (1-\theta_a)\underline{c}_i^*) + (1-\gamma_{i+1})(\theta_a\,\underline{c}_{i+1}^t + (1-\theta_a)\underline{c}_{i+1}^*)]$$

$$- Q_i^t[\gamma_i(\theta_a\,\underline{c}_{i-1}^t + (1-\theta_a)\underline{c}_{i-1}^*) + (1-\gamma_i)(\theta_a\,\underline{c}_i^t + (1-\theta_a)\underline{c}_i^*)] - Q_{out,i}^t[\theta_a\,\underline{c}_i^t + (1-\theta_a)\underline{c}_i^*]\} \tag{5.10}$$

Dispersive step

$$\underline{c}_i^{**} = \underline{c}_i^* + \frac{\Delta t_d}{\Psi_i}\{X_{i+1}^t[\theta_d(\underline{c}_{i+1}^* - \underline{c}_i^*) + (1-\theta_d)(\underline{c}_{i+1}^{**} - \underline{c}_i^{**})]$$

$$- X_i^t[\theta_d(\underline{c}_i^* - \underline{c}_{i-1}^*) + (1-\theta_d)(\underline{c}_i^{**} - \underline{c}_{i-1}^{**})]\} \tag{5.11}$$

Reaction step

$$\underline{c}_i^{t+\Delta t} = \underline{c}_i^{**} + \Delta t_r\,\underline{N}_i^t(\underline{c}_i^{t+\Delta t}, \underline{c}_i^{**}) + \frac{\Delta t_r}{\Psi_i}\underline{L}_i^t \tag{5.12}$$

Notation:

$\underline{c}_i^t$	concentration vector for grid or section i at time t
Δt	time step increment (differs for advective, dispersive and reactive steps)
Ψ_i	generalized volume: $\Psi_i = V_i$ for finite section i; $\Psi_i = \frac{1}{2}(A_i + A_{i+1})\Delta x_i$ for finite difference grid i
V_i	volume of finite section i
A_i	cross sectional area at upstream face of grid i
Δx_i	length of grid or section i
Q_i^t	flow from grid or section i-1 to grid or section i at time t
X_i^t	dispersive exchange flow between grids i and i-1 at time t
θ	implicit-explicit weighting parameter
γ_i	spatial centering parameter for upstream face of grid or section i
$\underline{N}_i^t$	reaction rate vector at grid or section i at time t
$Q_{out,i}^t$	outflow from grid or section i at time t
$\underline{L}_i^t$	mass influx (or loading) vector at grid or section i at time t

Figure 5.3

Steps in numerical solution of mass transport equation

If $\theta = 1$, the equation is explicit; $c_i^{t+\Delta t}$ may be solved entirely from the known values c_i^t and c_{i-1}^t. Explicit solutions are usually limited to short time steps in order to be well behaved numerically (stable). If θ is less than one, $c_i^{t+\Delta t}$ is an implicit function of itself, as well as of the unknown $c_{i-1}^{t+\Delta t}$. Due to this latter dependency, it is impossible to solve for $c_i^{t+\Delta t}$ without simultaneously solving for $c_j^{t+\Delta t}$ at all other locations j. Although this requires an expensive matrix solution, the solution is stable for large values of Δt. Substitution of a few, large implicit time steps is often less costly than many, short explicit steps. In general, accuracy increases as θ approaches 1 while stability increases as θ goes to zero. A value of $\theta = 0.55$ is an effective compromise, used in these studies.

Additional solution parameters are included in Equations 5.10 and 5.11 to permit either the finite difference or multiple-box approach to be used. The parameter γ controls the spatial weighting of the flow between a grid and its upstream and downstream neighbors. For the multiple-box approach, conservation of mass requires the following:

$$\gamma_i = 1 \quad \text{if } Q_i \geq 0$$

$$\gamma_i = 0 \quad \text{if } Q_i < 0$$

In contrast, these values are rarely appropriate for the finite difference approach, in which continuous derivatives of Q with x are represented. In this study, γ will be taken as one-half for the finite difference model; as shown by Leendertse (1971), this is equivalent to centered finite differences. Using values of γ other than one-half leads to upstream differencing, a technique which improves numerical stability at a cost in accuracy (due to numerical or artificial dispersion).

Also differing between the multiple-box and finite difference approaches is the value of the generalized volume parameter $\forall$. For a single box in the multiple-box model, the value may be unambiguously taken as the box volume. In a finite difference equation, the volume parameter is part of the approximation to the continuous functions and derivative of the advective term. A number of approximations are possible -- one is the average cross-sectional area times the grid length:

$$V_i = \frac{1}{2} (A_i + A_{i+1}) \Delta x_i$$

For most geometries, and particularly those without off-channel storage, this approximately equals the grid volume.

The dispersive step, Equation 5.11, also uses a generalized notation employing the exchange flow, X. This term derives from a conceptual model of dispersion as an equal but opposite exchange of mass between neighboring parcels of water -- a model which must be squared with our previous explanations that dispersion arises from spatial averaging. In its most basic form, the dispersive flux is expressed in terms of deviations from the spatial average:

$$F = \int_A u''c''dA \qquad (5.13)$$

where A is the cross-sectional area,
u" is the local deviation of the velocity at a point in the section from the mean velocity in the section, and
c" is the similar deviation of the concentration.

Usually, dispersion is specified in the diffusion form, Equation 5.8, so that the dispersion term appears in the mass conservation equation 5.7 as:

$$\frac{1}{A} \frac{\partial}{\partial x} \left(DA \frac{\partial c}{\partial x}\right)$$

This may be represented in finite difference form, using the notation of Figure 5.3, as:

$$\frac{1}{\frac{1}{2} (A_i + A_{i+1}) \Delta x} \left[D_{i+1} A_{i+1} \left(\frac{c_{i+1} - c_i}{\frac{1}{2} (\Delta x_{i+1} + \Delta x_i)} \right) - D_i A_i \left(\frac{c_i - c_{i-1}}{\frac{1}{2} (\Delta x_i + \Delta x_{i-1})} \right) \right]$$

where D_i is the dispersion coefficient between grids i and i-1.

Upon rearrangement, this expression is:

$$\frac{1}{V_i}\left[\frac{D_{i+1}\,A_{i+1}}{\frac{1}{2}\,(\Delta x_{i+1}+\Delta x_i)}\,(c_{i+1}-c_i)-\frac{D_iA_i}{\frac{1}{2}\,(\Delta x_i+\Delta x_{i-1})}\,(c_i-c_{i-1})\right]$$

Comparison of this equation with the mass balance model in Equation 5.9, reveals a perfect equivalence to the exchange flow, X_i -- the dispersion coefficient of the finite difference model and the exchange flow of the multiple-box model are related by:

$$X_i = \frac{D_iA_i}{\frac{1}{2}\,(\Delta x_{i-1}+\Delta x_i)} \qquad (5.14)$$

In the multiple-box approach, the exchange flow may be specified directly rather than using a dispersion coefficient. For example, van Straten (1980) defines a return velocity as a parameter in the SIMBAL model to capture a dispersion effect. With this parameter, the exchange flow is:

$$X_i = v_{ret}A_i$$

where v_{ret} is the return velocity parameter.

The relation between the dispersion coefficient and the exchange flow is convenient for formulation of a single computer model capable of employing either of our two model approaches. As we have seen in Chapter 2 however, there is at best a very indirect physical relation between exchange flows and dispersion coefficients.

5.3 Formulation of the Hydrodynamic Component

5.3.1 Description of the Model

General specifications for the hydrodynamic component of the water quality model have been presented in Section 5.1. A model conforming to these specifications was developed, using as a guide a three-dimensional model previously applied to Lake Balaton (Shanahan, Harleman and Somlyódy, 1981). (A concluding discussion on the 3-D model is included as Appendix C.) The newly developed model is a fully transient, two-dimensional model based upon the linearized equations of motion. The model solves for mass transport in the two coordinate directions and displacement of the water surface as functions of time and horizontal space. The model permits a time-varying wind field to be specified for determination of the transient forces upon the water surface, and accounts for the non-linear force of friction at the lake bottom as well. An explicit finite difference technique is employed to solve the equations.

Model Equations

The equations of motion upon which the 2-D model is based employ the shallow water approximation and omit both the convective acceleration terms and the horizontal shear terms. The simplified conservation of momentum equations, after integration over the lake depth are thus:

$$\frac{\partial U}{\partial t} = -g(h+\eta)\frac{\partial \eta}{\partial x} + fV - \frac{\tau_b^x}{\rho} + \frac{\tau_s^x}{\rho} \qquad (5.15a)$$

$$\frac{\partial V}{\partial t} = -g(h+\eta)\frac{\partial \eta}{\partial y} - fU - \frac{\tau_b^y}{\rho} + \frac{\tau_s^y}{\rho} \qquad (5.15b)$$

where the notation is the same as in Chapter 3. The vertically integrated mass conservation equation is employed:

$$\frac{\partial U}{\partial x} + \frac{\partial V}{\partial y} = \frac{\partial \eta}{\partial t} \qquad (5.16)$$

In these equations, the mass transports U and V are the variables representing water motion as the discharge per unit of horizontal length:

$$U = \int_h^{-\eta} u\,dz \qquad V = \int_h^{-\eta} v\,dz \tag{5.17}$$

U and V have the units of area per unit time.

The water of the lake is subject to shear forces at the water surface and lake bottom. These appear as the surface and bottom shear stresses, τ_s and τ_b, in Equations 5.15. The wind-induced surface stresses are calculated from Equation 3.22:

$$\tau_s^x = C_2\,\rho_a\,|W|\,W_x \qquad \tau_s^y = C_2\,\rho_a\,|W|\,W_y \tag{5.18}$$

where the notation is the same as used in Chapter 3 with the exception that we have broken the wind vector, W, into its x and y components, W_x and W_y. The two-meter wind drag coefficient, C_2, is either fixed as a constant or calculated from one of the formulae in Table 3.4.

At the lake bottom, the shear stress is taken as a non-linear function of the depth-average velocity:

$$\tau_b^x = \frac{\rho g}{C^2}\,\bar{u}\,\sqrt{\bar{u}^2 + \bar{v}^2} \qquad \tau_b^y = \frac{\rho g}{C^2}\,\bar{v}\,\sqrt{\bar{u}^2 + \bar{v}^2} \tag{5.19}$$

The depth-average velocities are defined as:

$$\bar{u} = \frac{U}{h+\eta} \qquad \bar{v} = \frac{V}{h+\eta}$$

The other terms are the Chezy coefficient, C, and the water density, ρ, as defined in Chapter 3.

Finite Difference Solution

Simulation of transient wind-driven circulation events requires solution of Equations 5.15 and 5.16 in time and horizontal space. This is accomplished in the 2-D model using an explicit finite difference scheme, alternately solving the momentum equations and the continuity equation.

Application of the finite difference scheme requires the division of the lake into a grid of discrete rectangular areas. A square grid, or more precisely, two square grids are used in the model. The two grids arise from the use of a staggered grid scheme on which velocity components are determined on the grid mid-sides, while water surface displacements are found at the grid center points. (See Figure 5.4.)

An explicit solution technique is employed, first solving the momentum equations for the current velocities at full time steps, then using those velocities in the continuity equation to solve for the water surface elevation at half time steps. From the surface elevations, surface slopes can be determined for substitution into the momentum equation, which is solved at the next time step. This cycle is repeated until the simulation period is completed.

In solving the equations, the solution proceeds along the rows of the finite difference grid from left to right, solving for all columns in a row before moving up to the next row. This sequence is followed until all rows have been completed, and is repeated for first the momentum and then the continuity equation each time step. The particular sequence employed implies that the solution at a grid depends upon a mixture of variable values determined at the current and preceding time step. This is permitted by a short computation time step, as discussed briefly below.

The explicit solution scheme employed for the hydrodynamic model is conditionally stable, requiring certain conditions be met in order to achieve a solution. The stability conditions are defined by the well-known Courant condition, which limits the solution time step to the time required for a surface gravity wave to traverse a grid square:

$$\Delta t < \frac{\Delta x}{\sqrt{g(h+\eta)}} \qquad (5.20)$$

where Δt is the solution time step increment, and
Δx is the finite difference grid spatial increment.

This limit arises since the model employs a free surface formulation, rather than the rigid lid approximation.

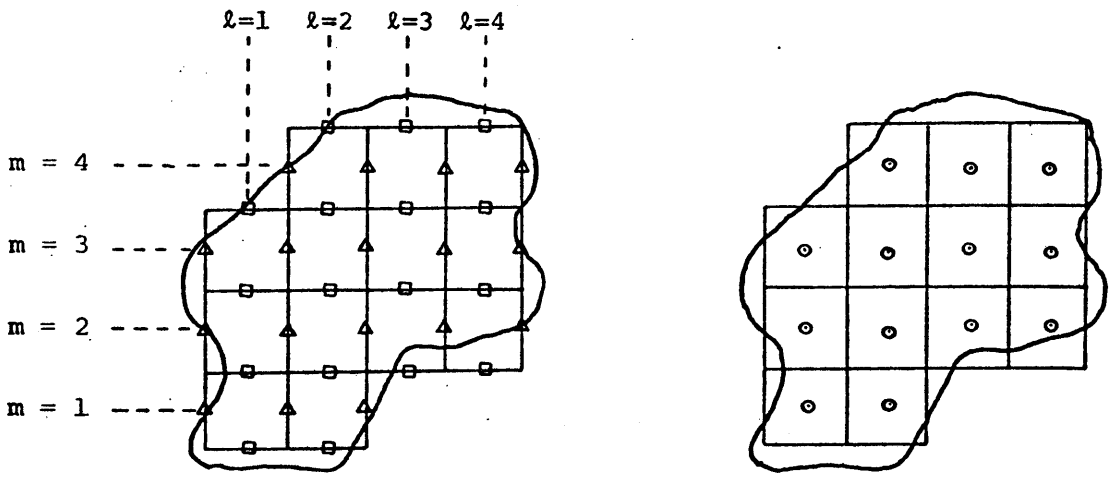

Figure 5.4

Finite difference solution procedure

Although the limit imposed on the time step by stability conditions is stringent, it is not without its advantages. Since the resulting time step is quite short, we can make a number of simplifications in the solution, confident in our knowledge that changes in mass transport will be small over a single time step. For example, stepping the solution over space in the row by row fashion described earlier is permitted by the small time step. Also, the non-linear friction term can be linearized for computation by using velocities found at the previous time step. This is linear in the computational sense since an iterative solution for U and V is not required. However, the small change in velocity over a time step insures an essentially non-linear dependence of bottom friction on velocity.

5.3.2 Application to Lake Balaton

Application of the 2-D model to Lake Balaton proceeded in two phases. Lacking a concensus from the literature on the value and form for the important parameters, the first phase consisted of a series of model sensitivity studies. Through trial and error, reasonable values for the parameters were sought, simultaneously determining the sensitivity of the results to the various parameters. After this step was completed, and a reasonable set of input parameters was available, the second phase was possible: verification of the model results against actual historical events. The procedure closely parallels that employed in the previous 3-D model application (Shanahan et al., 1981).

Model Input Data

Execution of the circulation program requires the specification of such inputs as the model parameters, the lake geometry, a wind history, and various execution and output controls. Of the program inputs, the surface and bottom friction coefficients constitute the major unknowns, to be determined by calibration. These parameters, as well as the wind histories employed, will be described in the sections to follow.

The geometry of the lake must be represented in the model via the finite difference grid. The modeler is free to choose the finite difference grid size, Δx, so long as he then chooses a compatible Δt using Equation 5.20. Usually, the choice of Δx is a trade-off between a small grid size to accurately capture the lake's bathymetry and a large size to reduce computation expenses. For Lake Balaton, we constructed and tested two grids. The first, denoted as the coarse grid, uses a grid size of 1900 meters and is shown in Figure 5.5. This grid size is the largest able to reasonably approximate the geometry of Tihany Strait. An alternative grid, the fine grid, employs a grid spacing of 950 meters, one half that of the coarse grid. The fine grid is shown in Figure 5.6. The effect of the grid size was tested in sensitivity runs described below.

Model Calibration

Calibration of the model was accomplished using a simple hypothetical event as a standard simulation. This simulation was designed to exercise the model under uncomplicated conditions which would reveal the basic behavior of the model. The standard calibration simulation was a simplified seiche event which supposes the following situation. A steady wind of speed W_L blows along the long axis of the lake, directed from the western end (Keszthely) to the eastern end (Balatonkenese). The lake is initially still and level, but responds to the wind with a set-up at Balatonkenese and set-down at Keszthely. The wind blows steadily during the first part of the simulation; then decreases linearly in two hours time to a value of zero at time T. The notation W_L and T is employed here to be consistent with Equation 4.1.

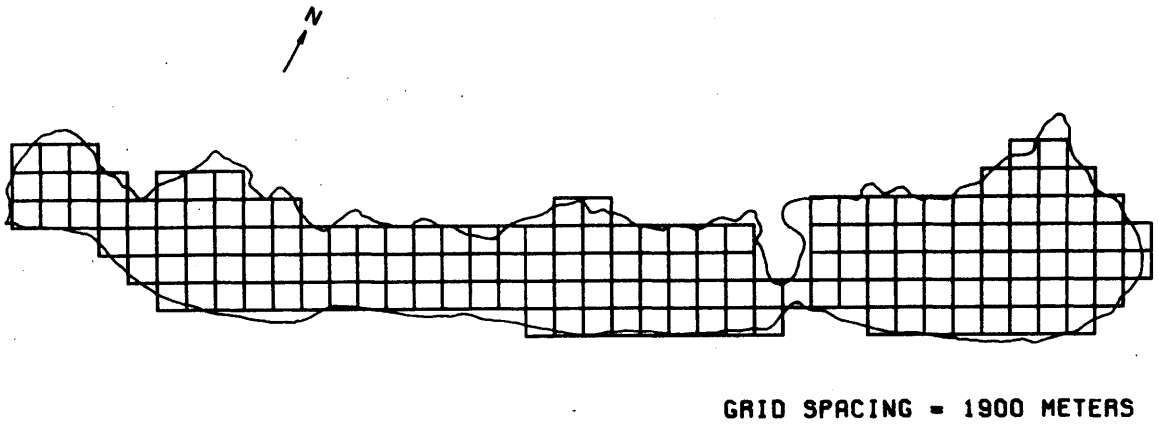

Figure 5.5
Coarse finite difference grid for Lake Balaton

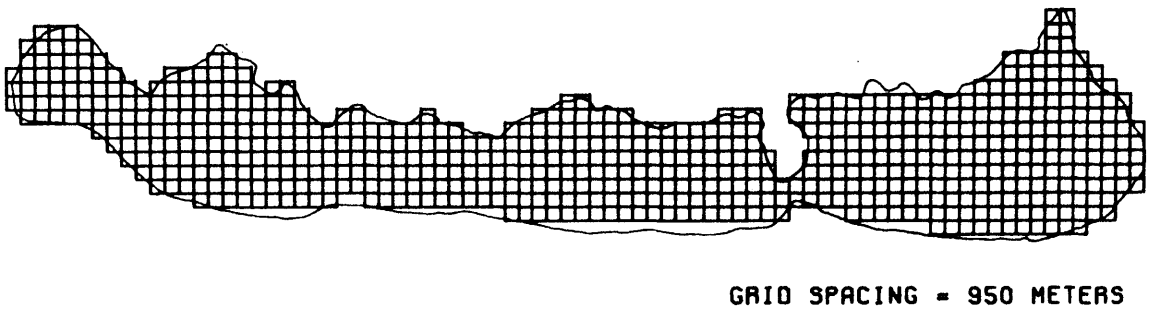

Figure 5.6
Fine finite difference grid for Lake Balaton

Model performance was evaluated using predicted water surface elevation at Keszthely and Balatonkenese as an indicator of seiche behavior. These model results were examined for conformity with the following criteria:

1. Oscillatory behavior - Field data show that the longitudinal seiche, though heavily damped, nevertheless persists for at least three perceptible cycles.

2. Seiche period - Frictional forces are known to lengthen the longitudinal seiche period beyond the 7.5 hours predicted by inviscid theory.

3. Wind set-up - Muszkalay (1966) gives empirical formulae to determine the set-up in Lake Balaton as a function of wind speed and duration; we have shown his relation for longitudinally directed winds in the previous chapter as Equation 4.1. Muszkalay's relation is based upon field data which necessarily show significant scatter about the empirical formulae.

These criteria, though approximate and incomplete, served as a consistent and reasonable test of the model's ability to reproduce the system behavior and enabled the selection of a set of parameters judged to credibly represent the system.

The calibration runs varied two parameters: the Chezy bottom friction coefficient and the wind drag coefficient. Typical simulation results are shown in Figure 5.7 to illustrate the sensitivity of the seiche amplitude to these parameters. Comparisons with Muszkalay's relation are shown in Figure 5.8. The parameter set found to do best was a fixed wind drag coefficient, $C_D = 0.0013$, and a Chezy coefficient of $C = 60$. Although far from a perfect match to Muszkalay's results, the agreement was acceptable given the approximation inherent in his empirical results. The findings were corroborated in similar work by Somlyódy (personal communication) to calibrate a one-dimensional longitudinal model of Lake Balaton.

Sensitivity Testing

In addition to the parameter sensitivity tests completed with the calibration runs, two further factors were considered: the effect of the finite difference grid size and of variation in the wind speed over space. Both the transient seiche simulations described above and steady state circulation predictions were compared in these tests. The steady state situation is, however, a highly artificial one -- wind on Lake Balaton varies

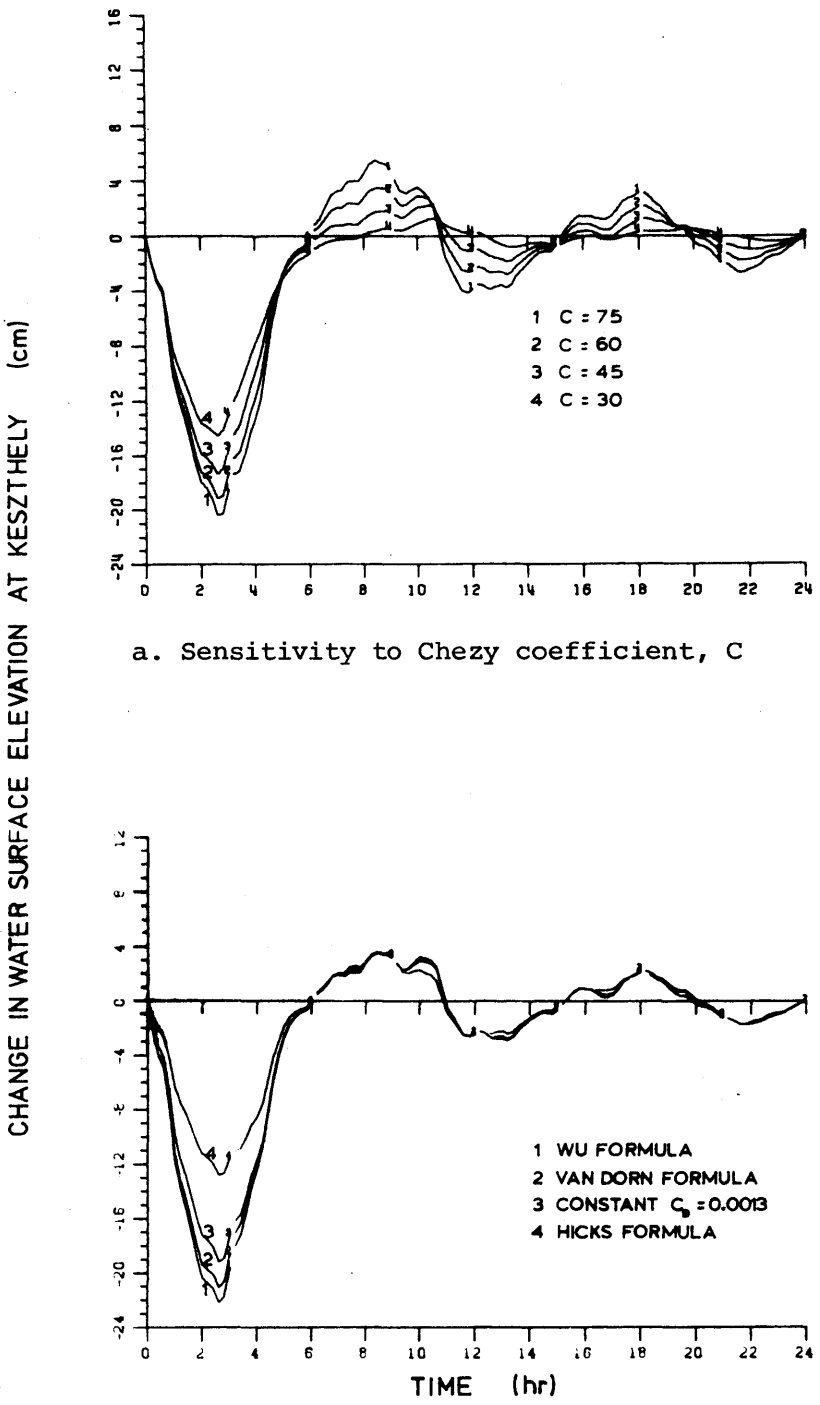

a. Sensitivity to Chezy coefficient, C

b. Sensitivity to wind shear drag coefficient, C_D

Figure 5.7

Sensitivity of predicted seiche to Chezy coefficient and wind shear drag coefficient

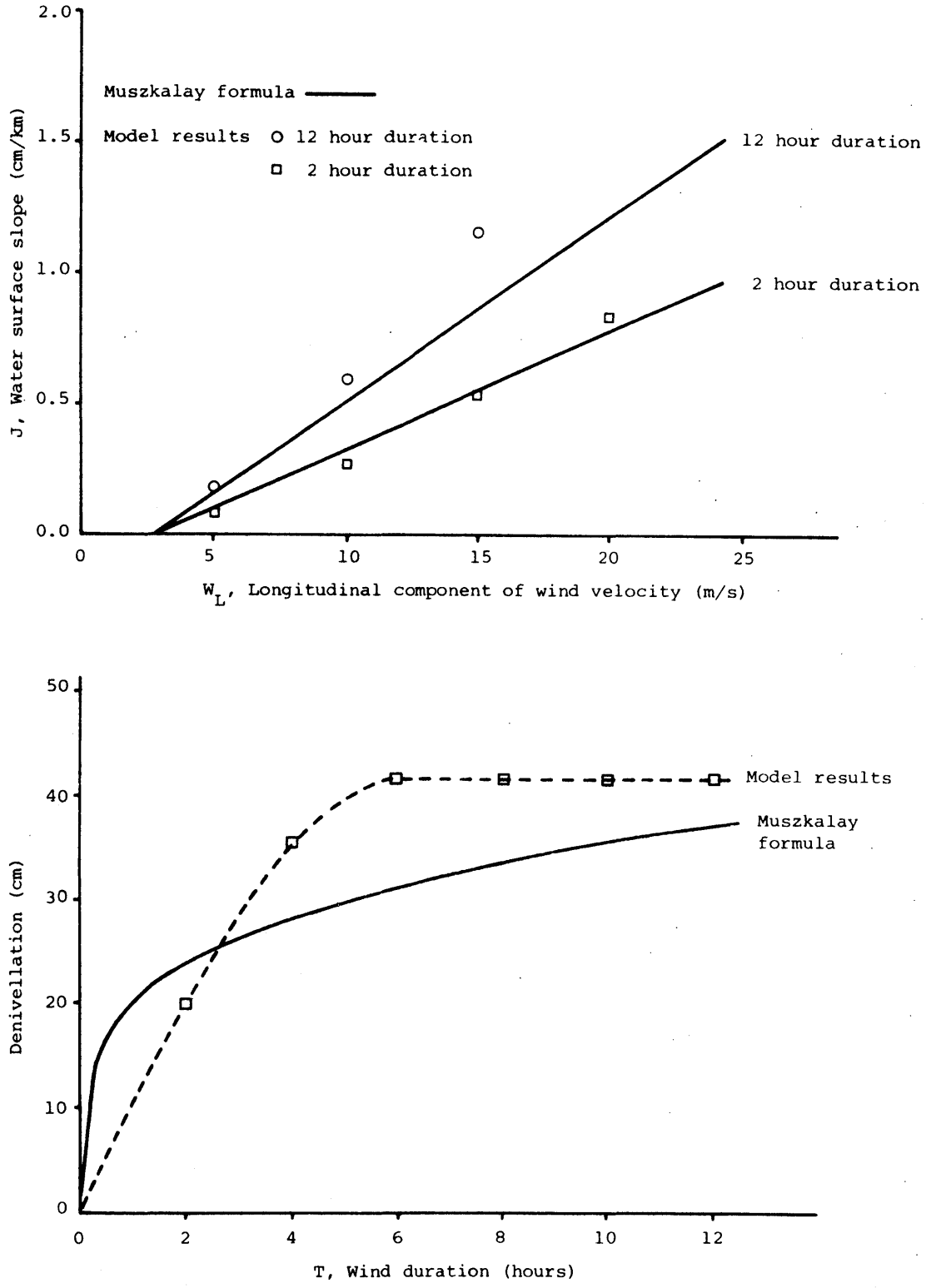

Figure 5.8
Comparison of model results (with C = 60, C_2 = 0.0013) with Muszkalay's (1966) empirical formula

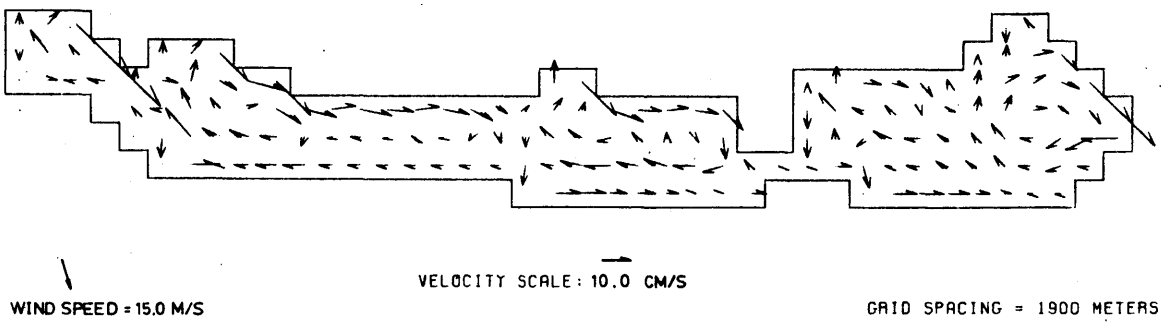

a. Coarse grid

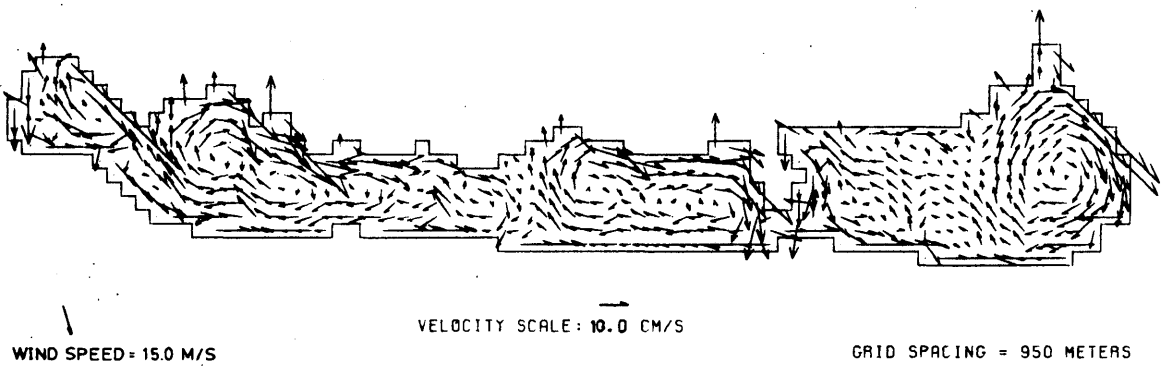

b. Fine grid

Figure 5.9

Effect of grid size on steady-state horizontal circulation

more rapidly than the time for the longitudinal seiche to damp out, so that steady conditions are rarely, if ever, approached.

Neither the transient nor steady-state simulations differed remarkably when produced using the coarse grid versus the half-size fine grid. Minor differences occurred, but not enough to cause concern. This also proved the case in further tests, described in Section 7.2. The results of the steady state simulations are otherwise of interest as an indicator of the degree of horizontal circulation in the lake. Plots of the steady state circulation, included as Figure 5.9, show a relatively complex horizontal flow pattern which includes numerous gyres.

Other sensitivity tests evaluated the influence of spatial variation in wind speed. As might be anticipated, model results proved very dependent upon these variations in the force driving the system. Two factors were found particularly critical. The wind direction, when it is in the north to northwest range, is nearly perfectly transverse to the lake's long axis and can lead to very different longitudinal currents and seiches with only small changes in direction. Unfortunately, this is the typical direction of travel for storm systems and thus the stronger wind events. Horizontal non-uniformities in the wind speed, known to exist in the prototype system, proved to be a relatively minor factor in the model response provided that the average wind strength (speed) over the lake is roughly correct. For example, winds are typically much lighter at Keszthely than over the rest of the lake. Therefore, if the wind record from Keszthely is used in a simulation, the wind speed must be scaled up to a value which better reflects the higher lakewide average wind. The procedure followed is described by Shanahan et al., 1981.

Model Verification

To verify the 2-D circulation model we repeated the historical event simulations described by Shanahan et al. (1981). Three events were simulated and they are briefly described in turn below.

The event of July 4 and 5, 1961 was produced by winds with a significant component along the lake's long axis. The consequent strong longitudinal seiche was well-captured in the simulation, as shown by the comparison of stage at the two extreme ends of the lake in Figure 5.10.

The event of July 8 and 9, 1963 produced a longitudinal seiche with comparable displacement to the July 1961, but with much stronger simultaneous transverse seiching. Model results are compared with observations in Figure 5.11. Prediction of the stage at Keszthely is poor, while that at Balatonkenese is generally good. Missing from the model predictions are most of the high frequency oscillations seen in the observation record as a result of transverse seiching. This is likely due to the smooth wind record (hourly averages) relative to the forty minute transverse seiche period. Also contrasted in Figure 5.11 is the observed and predicted discharge through Tihany Strait. The observation record is based on a single velocity recorder but is probably accurate within about twenty-five percent according to Muszkalay and Somlyódy (personal communication, 1981). In our earlier analysis of this event (Shanahan et al.,

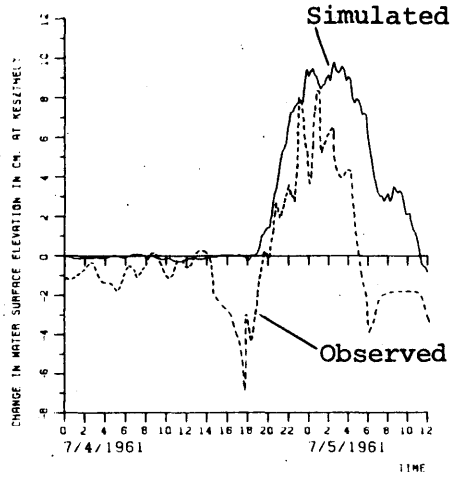

a. Water surface elevation at Keszthely

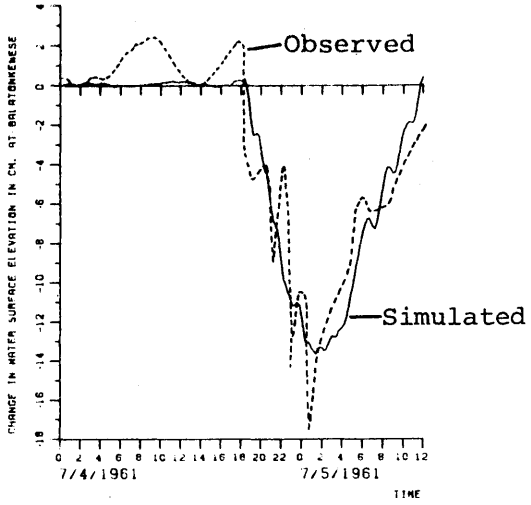

b. Water surface elevation at Balatonkenese

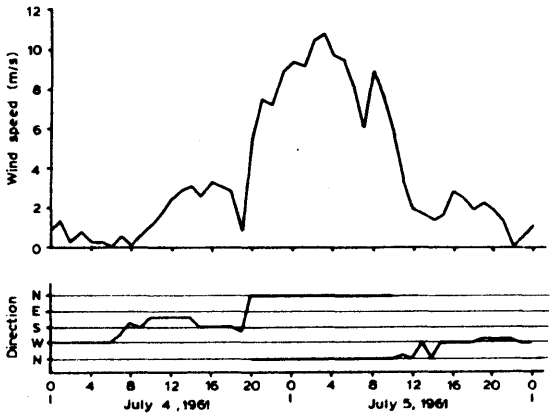

c. Wind speed and direction recorded at Keszthely

Figure 5.10

Comparison of simulation results and observations for event of July 4 and 5, 1961

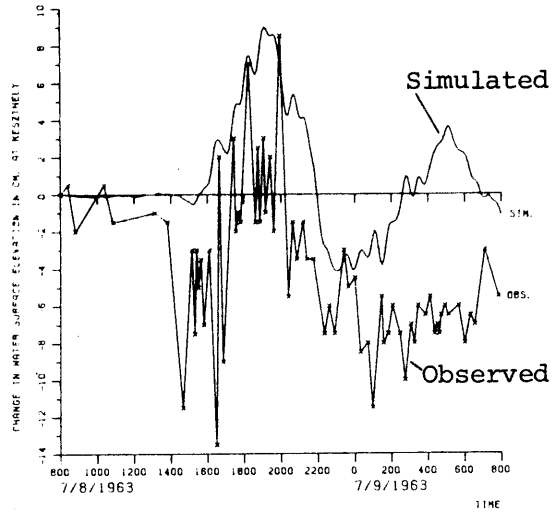

a. Water surface elevation at Keszthely

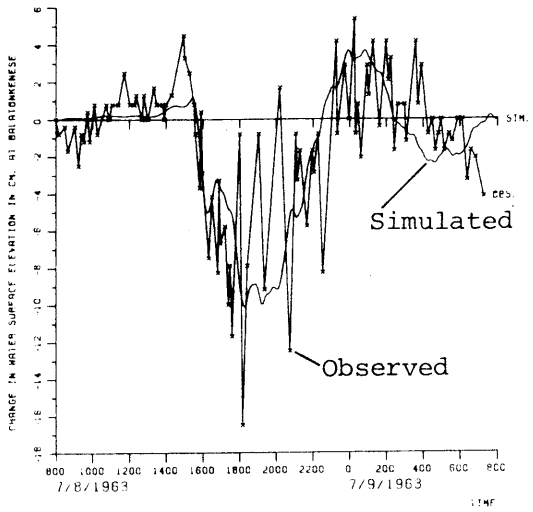

b. Water surface elevation at Balatonkenese

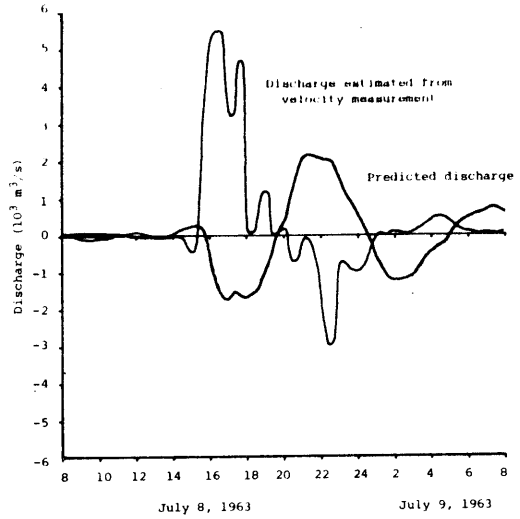

c. Current in Tihany Strait

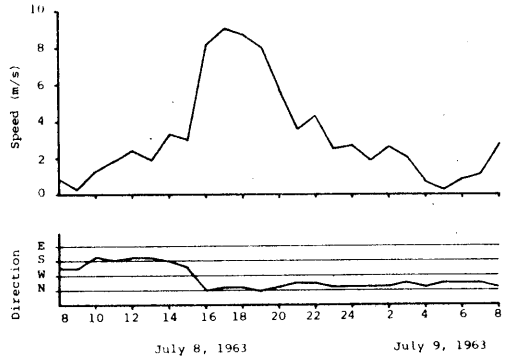

d. Wind speed and direction recorded at Keszthely

Figure 5.11

Comparison of simulation results and observations for event of July 8 and 9, 1963

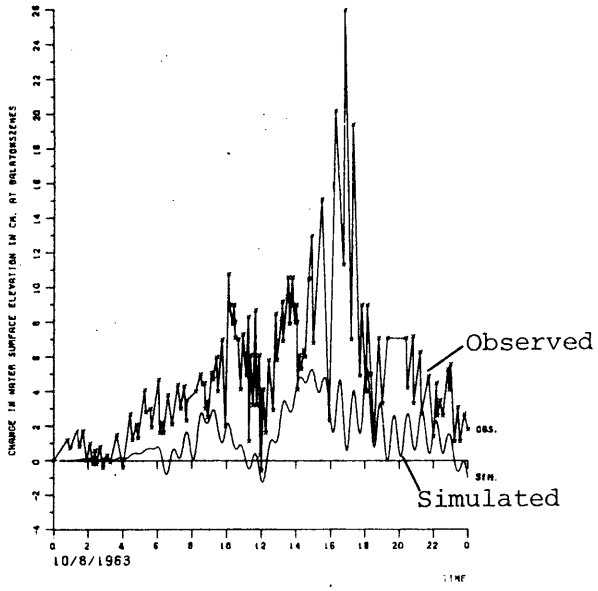

a. Water surface elevation at Balatonszemes

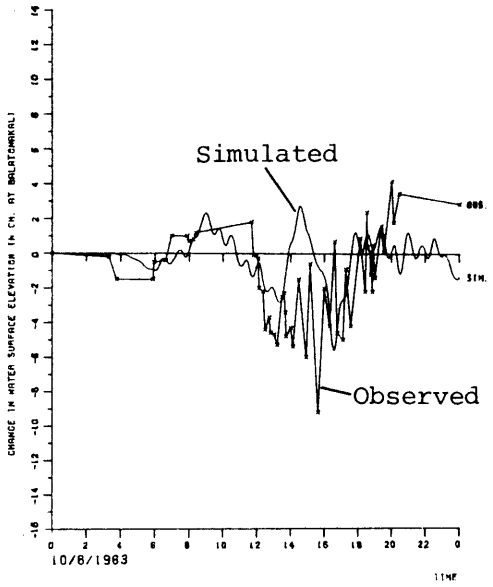

b. Water surface elevation at Balatonakali

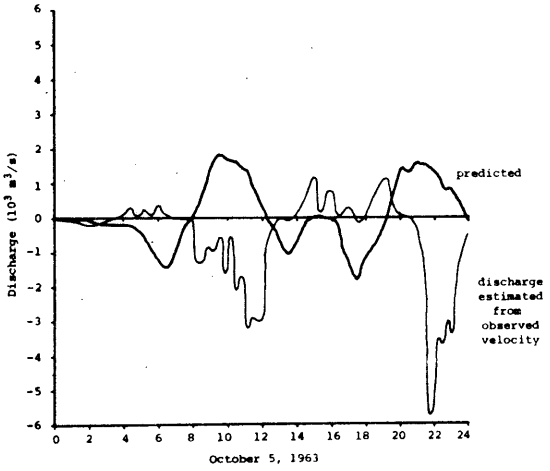

c. Current in Tihany Strait

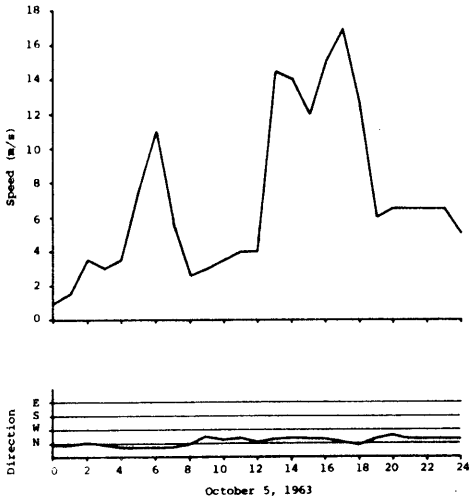

d. Wind speed and direction recorded at Balatonszemes

Figure 5.12

Comparison of simulation results and observations for event of October 5, 1963

1981) we suggested a possible error in the direction shown for the observation data, since the flow is in opposition to the simultaneous changes in water level at the lake ends. A review of the original recordings by Muszkalay and Somlyódy showed there is no error, however, so that the match between prediction and observation is quite poor. Nevertheless, the field data show sustained flows in Tihany Strait opposite that necessary to cause the water surface changes observed -- see Figure 4.6. There thus remain serious questions about either the field data or the lake's behavior.

The final event considered is that of October 5, 1963. Unlike the two previous events, which began with longitudinal winds, the storm of October 1963 brought only transverse winds. In fact, during the entire event the wind is nearly perfectly perpendicular to the lake. Under this situation, small changes in the wind direction lead to great changes in the magnitude of the longitudinal wind component including frequent reversals in longitudinal direction. Under such conditions, local modifications of the wind field and errors in the wind data critically influence the model results making accurate predictions virtually impossible. This is confirmed by the comparisons of predicted and observed transverse seiche and Tihany Strait discharge in Figure 5.12.

The preceding comparisons of model results with observations of actual historical events show a general ability to capture the character of transport in Lake Balaton -- particularly longitudinal transport -- but an inability to duplicate the fine structure of the seiche behavior and the flow through Tihany Strait. The model's ability to reproduce the character of large scale transport is sufficient for water quality predictions, particularly over time periods of about a week or more. The model's failures can be ascribed to uncertainties in the data available to drive and test the model. For example, wind data to drive the model is available from at most three stations on the lake, two of which are on the southern shore. However, the northern shore of the lake is quite hilly, and the northerly winds which typify most storm events are significantly deflected and modified in their passage over the hills. These local non-uniformities in the wind field are important -- for example, they possibly explain the observation of flow in Tihany Strait against the recorded wind. Unfortunately, local variability in the wind field cannot be detected by the sparse measurement network, and is thus unavailable as model input data.

5.3.3 Hydrologic Flow Computation

The hydrodynamic model considers only the influence of the wind in establishing transport in the lake; inflows and outflows are not included in the model. Thus, there can be no lakewide change in water surface elevation nor any replacement of lake water due to inflow and outflow. In fact, however, the lake elevation is controlled by releases at the Sió Canal: it is drawn down in winter and generally refills through the rainy period during the first four months of the year (van Straten et al., 1979). Typically, the average water surface elevation varies over a range of 30 centimeters during the year; however, larger ranges, up to even 1 meter, are possible. Besides changing the lake water surface elevation, inflows and outflows establish the hydrologic through-flow of the lake

which can significantly influence water quality. For example, the annual spill from Lake Balaton at the Sió Canal releases roughly one-fifth of the lake's volume each year: a net transport important to water water quality. Clearly, the hydrologic through-flow and changes in surface elevation imply transport fluxes which should be included in the water quality computations.

A few assumptions were made in computing the hydrologic flow. First, it was assumed that the hydrologic flow changed sufficiently slowly that monthly values of the flows were adequate. This assumption was necessitated by the data available to us for the Sió Canal release and for precipitation and evaporation. A second assumption was that the hydrologic through-flow could be superimposed upon the transport determined by the hydrodynamic circulation model, the combination thus forming the total transport. This is consistent with the linearity of the hydrodynamic model, however it neglects any contribution that the hydrologic through-flow may make to the dispersive transport. The low velocities of the through-flow insure that these contributions to dispersion will be small.

The principle in computing the hydrologic through-flow is a simple water balance. The net change in the lake water surface elevation during a month is computed by summing the Zala River, tributary and precipitation inflow, and subtracting the outflow due to discharge at the Sió Canal and evaporation. These inflows and outflows are available from the Lake Balaton data base; contributions due to water withdrawal, sewage inflows and local runoff are neglected. Once the net change in surface elevation is known, the flow between the grids or basins to be used in the water quality transport model may be found. These are calculated so that the water surface change for each grid will be the same, maintaining an equal mean level throughout the lake. The method is the same as that used by Baranyi (1973a): the outflow from one basin or grid to the next downstream is the total inflow to the upstream basin, less the total outflow and less the change in storage, with inflow, outflow and storage all expressed as water surface elevation changes (that is, normalized by the surface area of the upstream basin). The water balance equation for the ith grid over a time period is:

$$\Delta h = P + I_i + \frac{A_i}{A_{i-1}} Q_{i-1} - E - Q_i - O_i \qquad (5.21)$$

where
- Δh is the lake-wide elevation change,
- P is the precipitation,
- E is the evaporation,
- I_i is the inflow to grid i,
- O_i is the outflow from grid i,
- Q_i is the flow from grid i to grid i+1, and
- A_i is the surface area of grid i.

All terms in Equation 5.21 are expressed in units of length -- for example, precipitation in millimeters. Flow quantities, such as the inflow, are determined by summing the total inflow over a period to get an inflow volume, and then dividing by the surface area of the grid to convert to length units. The equation is solved for Q_i, proceeding stepwise through the grids from i=1. The lake-wide elevation change is computed before the individual grid water balances are done:

$$\Delta h = P + \frac{1}{A_t} \sum_i A_i I_i - E - \frac{1}{A_t} \sum_i A_i Q_i \qquad (5.22)$$

where A_t is the total lake surface area.

5.4 Formulation of the Biogeochemical Component

5.4.1 Description of the Model

The selection of SIMBAL as the biogeochemical model component of our water quality model is discussed in Section 5.1 and its general characteristics are presented in Section 2.4. The discussion here will be a detailed look at the mathematical relations employed in the model and their solution. The information presented is taken from van Straten (1980), van Straten and Somlyódy (1980) and the source listing of the SIMBAL computer program. We have adopted a modified notation in presenting the model, using the more systematic notation of Najarian and Harleman (1975) as a guide.

Phosphorus Transformation Equations

The element cycles employed in SIMBAL are shown in Figure 5.13, which depicts the phosphorus compartments, the reactions linking the compartments, and relations controlling the reactions. The phosphorus compartments are:

P_1 - summer phytoplankton phosphorus

P_2 - winter phytoplankton phosphorus

P_3 - detritus phosphorus

P_4 - dissolved inorganic phosphorus

The chemical forms included within each compartment are described in Section 2.4.

The controlling relations for the two phytoplankton compartments are similar:

$$\frac{dP_1}{dt} = R_{41} \frac{P_4 P_1}{K_4 + P_4} - R_{13} P_1 \qquad (5.23)$$

$$\frac{dP_2}{dt} = R_{42} \frac{P_4 P_1}{K_4 + P_4} - R_{23} P_2 \qquad (5.24)$$

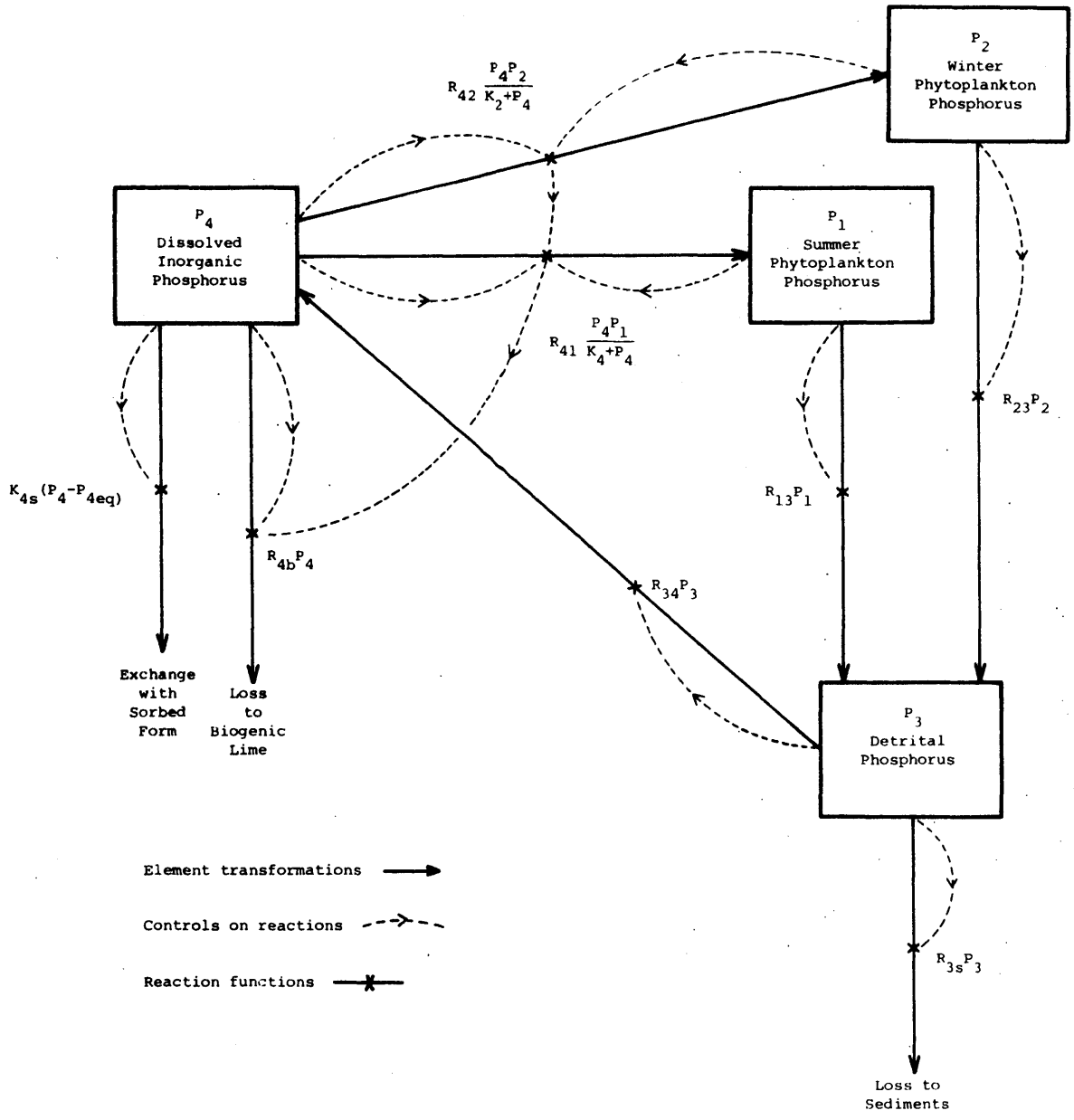

Figure 5.13

Phosphorus cycle structure in the SIMBAL model

Here, R_{41} and R_{42}, which are the growth rates of the algae, are the control rates for transformation from P_4 to P_1 and to P_2. Similarly, R_{13} and R_{23}, the algae mortality rates, control transformation from P_1 and P_2 to P_3. K_4 is the half-saturation constant for the uptake of P_4. The reaction rates R_{41}, R_{42}, R_{13}, and R_{23} include dependencies on the water temperature and incoming light. These are shown in Figures 5.14 and 5.15.

Detrital phosphorus behavior is modeled by the equation:

$$\frac{dP_3}{dt} = R_{13} P_1 + R_{23} P_2 - R_{34} P_3 - R_{3s} P_3 \qquad (5.25)$$

According to this equation, detritus increases with the influx of dead phytoplankton but is reduced by two processes. First is the transformation of detritus to dissolved inorganic phosphorus -- controlled by the mineralization rate, R_{34}. In addition, a fraction of the detritus settles from the water column and is lost to the sediments, at a rate modulated by the settling loss rate, R_{3s}. These terms are defined in greater detail in Figure 5.16.

The final compartment, dissolved inorganic phosphorus, enters into reactions with the other three compartments and in three reactions with the sediments. Its equation is:

$$\frac{dP_4}{dt} = -R_{41} \frac{P_4 P_1}{K_4 + P_4} - R_{42} \frac{P_4 P_2}{K_4 + P_4} + R_{34} P_3$$

$$- R_{4b} P_4 + L_{s4} - R_{4s} (P_4 - P_{4\,eq}) \qquad (5.26)$$

The first two terms of the right-hand side are the uptake of dissolved inorganic phosphorus by the algae; the third term is the mineralization of detritus. Biogenic lime precipitation is controlled by R_{4b} at a rate proportional to the growth of phytoplankton. Interaction with sediments is

$$\frac{dP_1}{dt} = R_{41} \frac{P_4 P_1}{K_4 + P_4} - R_{13} P_1$$

R_{41} = growth rate = $R_{41,max}\, g(I)\, f_1(T)$

$R_{41,max}$ = maximum growth rate

$g(I)$ = Steele light limitation function

$$= \frac{e}{k_e h} \left[\exp\left(-\frac{I}{I_s} \exp(-k_e h)\right) - \exp\left(-\frac{I}{I_s}\right)\right]$$

k_e = extinction coefficient = $k_o + k_s(P_1 + P_2)$

k_o = natural extinction coefficient

k_s = self-shading extinction factor

I = incident radiation

I_s = optimal radiation = $I_{sm} + I_{se}T$

I_{sm}, I_{se} = coefficients

T = water temperature

$f_1(T)$ = temperature dependency for P_1

$$= \left(\frac{T_{c1} - T}{T_{c1} - T_{*1}}\right) \exp\left(1 - \frac{T_{c1} - T}{T_{c1} - T_{*1}}\right) \quad \text{for } T < T_{c1}$$

$$= 0 \quad \text{for } T \geq T_{c1}$$

T_{c1} = critical temperature

T_{*1} = optimal temperature

K_4 = half-saturation constant

Figure 5.14

Transformation relations for summer algae, P_1

R_{13} = mortality rate = $R_{13,20}\ \theta_{13}^{(T-20)}$

$R_{13,20}$ = mortality rate at 20 C

θ_{13} = temperature factor

Figure 5.14

continued

$$\frac{dP_2}{dt} = R_{42} \frac{P_4 P_2}{P_4 + K_4} - R_{23} P_2$$

R_{42} = growth rate = $R_{42,max}\, g(I)\, f_2(T)$

$R_{42,max}$ = maximum growth rate

$g(I)$ = Steele light limitation function (see Figure 5.14)

$f_2(T)$ = temperature dependency for P_2

$$= \left| \frac{T_{c2} - T}{T_{c2} - T_{*2}} \right| \exp \left(1 - \left| \frac{T_{c2} - T}{T_{c2} - T_{*2}} \right| \right)$$

T_{c2} = critical temperature

T_{*2} = optimal temperature

T = water temperature

R_{23} = mortality rate = R_{13} (see Figure 5.14)

Figure 5.15

Transformation relations for winter algae, P_2

$$\frac{dP_3}{dt} = R_{13} P_1 + R_{23} P_2 - R_{34} P_3 - R_{3s} P_3$$

R_{13} = mortality rate for summer algae (see Figure 5.14)

R_{23} = mortality rate for winter algae (see Figure 5.15)

R_{34} = mineralization rate = $R_{34,20}\ \theta_{34}^{(T-20)}$

$R_{34,20}$ = mineralization rate at 20 C

θ_{34} = temperature factor

R_{3s} = settling loss rate = $\frac{V_{s3}\ (1 - \gamma_3)}{h}$

V_{s3} = detritus settling velocity

γ_3 = dissolved fraction of detritus

h = water depth

Figure 5.16

Transformation relations for detritus, P_3

$$\frac{dP_4}{dt} = -R_{41}\frac{P_4P_1}{P_4+K_4} - R_{42}\frac{P_4P_2}{P_4+K_4} + R_{34}P_3 - R_{4b}P_4 + L_{s4} - R_{4s}(P_4 - P_{4eq})$$

R_{41} = growth rate of summer algae (see Figure 5.14)

R_{42} = growth rate of winter algae (see Figure 5.15)

K_4 = half-saturation constant

R_{34} = mineralization rate (see Figure 5.16)

R_{4b} = biogenic lime precipitation rate

$$= R'_{4b}\left(R_{41}\frac{P_4P_1}{P_4+K_4} + R_{42}\frac{P_4P_2}{P_4+K_4}\right)$$

R'_{4b} = biogenic lime formation rate related to algal growth rate

L_{s4} = sediment internal load $= \dfrac{L_{s4,20}\,\theta_{s4}^{(T-20)}}{h}$

$L_{s4,20}$ = release rate at 20 C

θ_{s4} = temperature factor

h = water depth

R_{4s} = first order absorption/desorption rate

$P_{4,eq}$ = equilibrium dissolved inorganic phosphorus concentration

Figure 5.17

Transformation relations for dissolved inorganic phosphorus, P_4

via a temperature dependent release, L_{s4}, and by adsorption/desorption to the sediments. This last interaction is modeled assuming an equilibrium level of dissolved inorganic phosphorus. Dissolved inorganic phosphorus is adsorbed to sedimentary matter and lost if its concentration in the water rises above this level, it is released back to the water when concentrations fall below the equilibrium level. For further information on this portion of the model, refer to van Straten (1980). A full specification of the dissolved inorganic phosphorus transformation equations is given in Figure 5.17.

Solution of the Equations

Within any one grid, Equations 5.21 through 5.24 constitute a set of coupled ordinary differential equations to be solved for four unknown phosphorus component concentrations as functions of time. We solved these equations numerically using a fourth order Runge-Kutta method integrating over three hours in a time step. A lake-wide mass balance checked the computation accuracy (as ability to conserve mass) over a simulation duration.

5.4.2 Application to Lake Balaton

As with the hydrodynamic component, the biogeochemical model required calibration to determine model parameters for Lake Balaton. The calibration of SIMBAL was performed by van Straten (1980) using the Monte Carlo simulation procedure described previously. In the work reported here, we accepted van Straten's calibration without modification, using the mean parameter values determined in his calibration. It is worthwhile, however, to review his calibration procedure to point out its assumptions and possible weaknesses.

van Straten's calibration employed his four-box model of Lake Balaton with data for the year 1977. Field data for the same year allowed him to specify boundaries on the model results to delimit acceptable agreement with the lake's observed behavior. This evaluation was possible only for field data directly comparable to the model compartments, however. Significantly, algal abundance, measured in the field as chlorophyll-a concentration, was not comparable.

The calibration procedure selected a portion of the least certain model parameters as calibration parameters. Values for these parameters were sampled at random from within prescribed ranges and a simulation of the year 1977 was performed. The results from the simulation were then checked against the acceptable ranges determined from field data to determine if the parameter set was valid -- that is, yielding acceptable results. This sequence of random parameter sampling, simulation and evaluation was repeated hundreds of times to find sets of acceptable parameters. The average of these sets are what we employ as the calibrated parameters. The parameters, both determined by calibration and fixed with literature values, are given in Table 5.3.

Table 5.3

SIMBAL model parameter values

Parameters found by calibration

K_4	Half-saturation constant	10.2	µg/l
θ_{13}	Mortality rate temperature factor	1.14	
$R_{34,20}$	Mineralization rate	0.035	day^{-1}
V_{S3}	Detritus settling velocity	0.036	m/day
$L_{S4,20}$	Sediment release rate	0.38	$mg/m^2/day$
R_{4S}	Sorption rate	0.16	day^{-1}
$P_{4,eq}$	Equilibrium concentration	5.8	µg/l
V_{ret}	Exchange flow velocity	0.0016	m/s

Fixed parameters

K_o	Natural extinction coefficient	2.5	m^{-1}
K_S	Self-Shading extinction factor	0.015	m^2/mg
I_{sm}	Optimal light intensity factor	96.0	cal/m^2
I_{se}	Optimal light intensity factor	9.6	$cal/C\ m^2$
T_{C1}	Critical temperature - summer algae	30	C
T_{*1}	Optimal temperature - summer algae	26	C
T_{C2}	Critical temperature - winter algae	10	C
T_{*2}	Optimal temperature - winter algae	8	C
$R_{41,max}$	Maximum growth rate - summer algae	6	day^{-1}
$R_{42,max}$	Maximum growth rate - winter algae	2	day^{-1}
$R_{13,20}$	Mortality rate	0.13	day^{-1}
θ_{34}	Mineralization rate temperature factor	1.18	
γ_3	Dissolved detritus fraction	0.4	
R_{4b}	Biogenic lime precipitation	0	l/µg
θ_{S4}	Sediment release temperature factor	1.18	

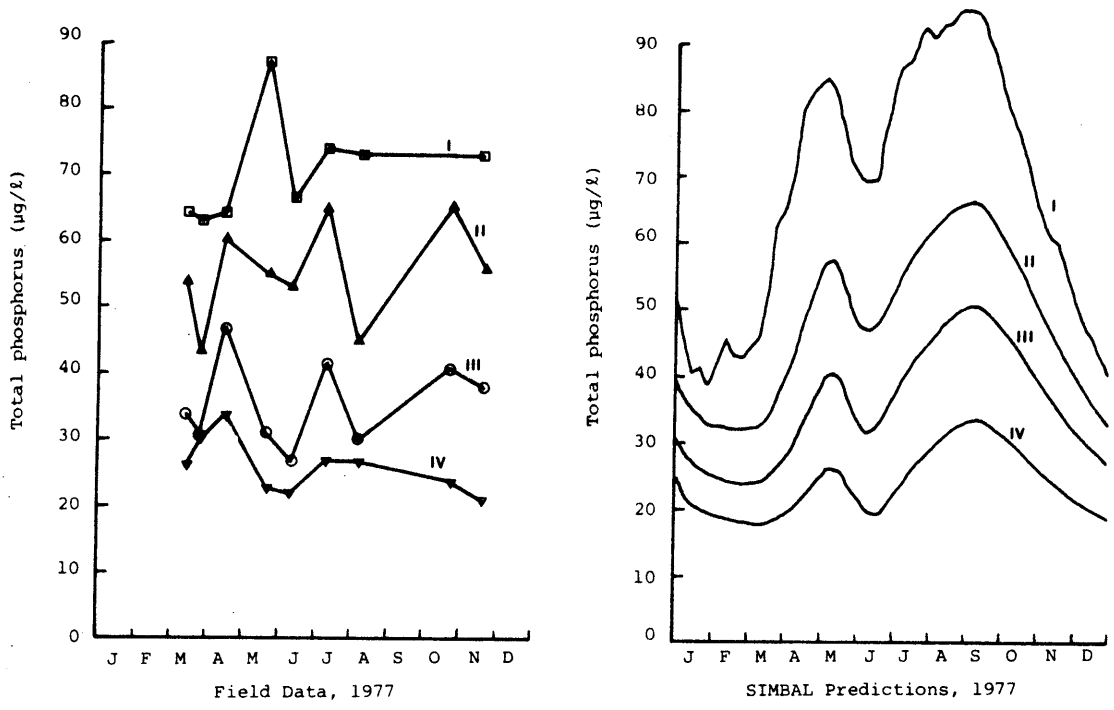

a) Total Phosphorus

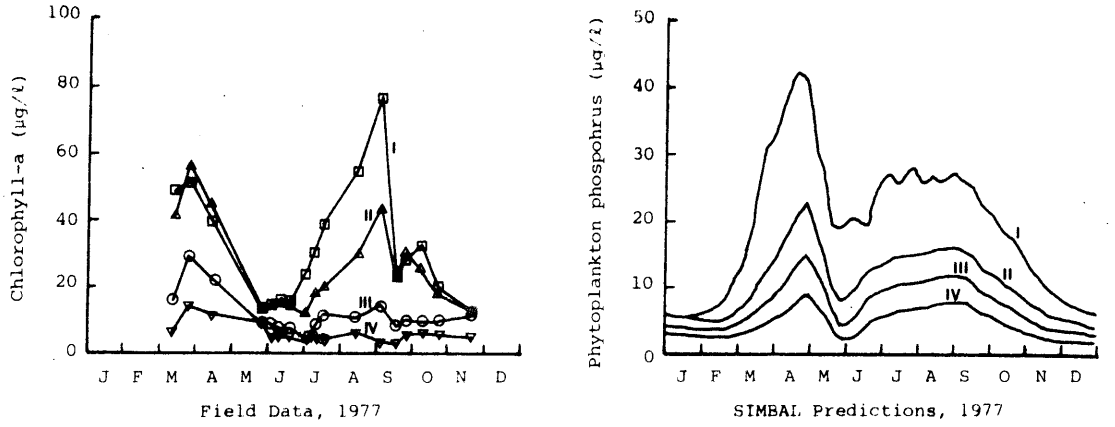

b) Chlorophyll-a and algal phosphorus

Figure 5.18

Comparisons of SIMBAL predictions with field data
(from van Straten, 1980)

As stated, evaluation of the model results against field data was possible for only a part of the model output. A portion of van Straten's (1980) comparisons are reproduced as Figure 5.18. Compared were total phosphorus, observed orthophosphate (against predicted dissolved inorganic phosphorus), and observed total dissolved phosphorus (against dissolved inorganic plus forty percent of the detrital phosphorus). The comparison for total phosphorus is included as Figure 5.18a. Although there is order of magnitude agreement between predicted and observed values, the time trace of the predictions differs significantly from the observations. The predicted summer peak in particular is much too high. Predicted algal phosphorus could not be directly compared with field data, although observed chlorophyll-a was taken as an indicator of the change in algae during the year. (An approximate conversion that the chlorophyll-a concentration equals twice the algal phosphorus concentration is implicit in van Straten's comparisons in Figure 5.18b.) Although certain trends are seen in both the field data and model results, there are some significant discrepancies. For example, spring and summer algal blooms are correctly predicted -- however, the summer bloom is far too low in the Keszthely Bay predictions. Unfortunately, this is probably the single most important model output from the standpoint of water quality management in Lake Balaton.

Despite misgivings about the predictions, our opinion is that the model is probably as well calibrated as can be expected. Improvement of the model predictions requires, we believe, improvements in the model formulation -- an effort which awaits more field data and basic research, particularly on the behavior of the sediments as phosphorus sources or sinks. In the meantime, we have employed the SIMBAL model as calibrated by van Straten as our biogeochemical model component.

5.5 Coupled Hydrodynamics and Water Quality

5.5.1 Introduction

In Section 5.3.1 we identify three major components of water motion in Lake Balaton: hydrologic through-flow, back-and-forth advection due to seiching, and dispersion due to lateral velocity variations. Hydrologic through-flow varies slowly and is determined by the monthly water balance computation described in Section 5.3.3. The seiche-driven advection is far more dynamic, and is computed by the 2-D circulation model as the net discharge across a lateral section of the lake. This advection is highly transient due to the oscillatory nature of the seiche, reversing direction each half-seiche period. The seiche-driven advection leads to much greater flow velocities than the hydrologic through-flow, and can thus cause much greater dispersion. In fact, we will make the assumption that dispersion due to the hydrologic flows is negligible.

In the remainder of this section we will discuss the character of the dynamic wind and seiche-driven flows and how these flows may be linked to the water quality model.

5.5.2 Advection

An important characteristic of the seiche-driven advection is the fact that it causes no net motion along the lake. Over long periods of time, the time-average velocity due to this motion is zero: the seiche will cause parcels of water to move back and forth, but in the absence of a net through-flow the parcels will return to their original position after the seiche has completely dissipated. Accordingly, if a pulse of some concentrate is introduced into a parcel of water, it will behave similarly. The concentration profile will retain its initial distribution (in the absence of mixing due to diffusion or dispersion) and this distribution will oscillate back and forth.

We can estimate the distance the seiche travels back and forth rather simply. The distance between the two extremes of its travel is the seiche excursion, determined as the integral of the advective velocity over one-half seiche period. In Balaton, the seiche excursion, ℓ, for a typical amplitude seiche is on the order of a few hundred meters. (See Section 6.2.)

The small excursion creates problems in numerical modeling. Clearly, oscillations of a few hundred meters are small perturbations relative to the total 75 kilometer length of the lake. To properly capture the influence of such small excitations upon the observed water quality, the water quality model requires a spatial increment, Δx, which is many times smaller still. Consider the effects of Δx much greater than the seiche excursion. In the absence of dispersion, reaction and loading, the water quality model should cause no change in an initial concentration distribution other than to advect it up and back the distance of the seiche excursion. In fact, however, the distribution will be smeared by the model if Δx is not sufficiently smaller than the seiche excursion. We can see this conceptually through a simplified picture based on fully-mixed tanks (Figure 5.19).

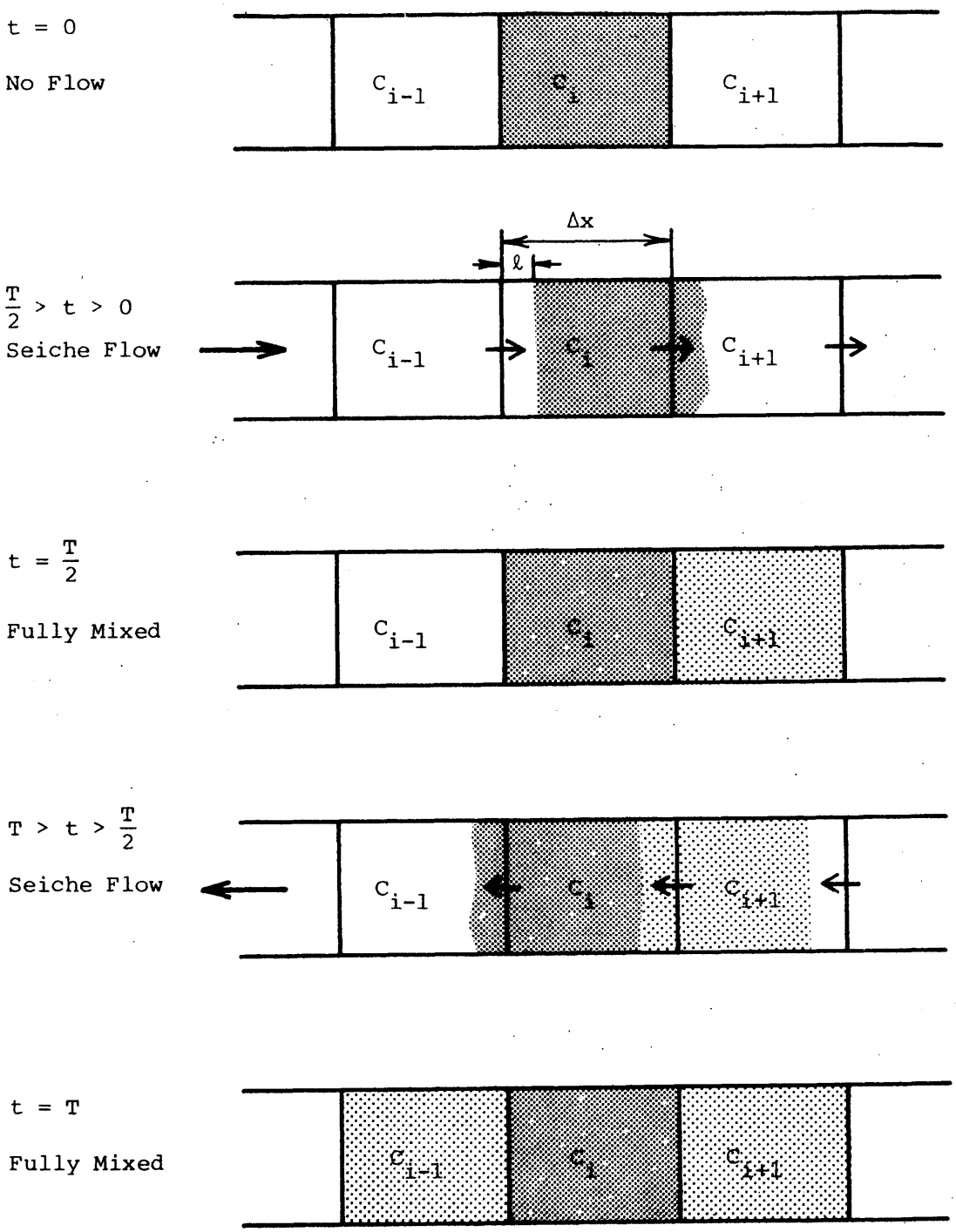

Figure 5.19

Numerical dispersion in oscillating flow

Over the first half of the seiche cycle, flow will be from cell i-1 to cell i, and cell i to cell i+1. Assume at the end of the seiche cycle the cells mix fully, and the flow is then back from cell i+1 to i and cell i to i-1. The change in concentration in cell i will be:

$$c_i^T - c_i^o = (\alpha - \alpha^2)(c_{i+1}^o - 2\,c_i^o + c_{i-1}^o)$$

where c_i^T is the concentration in cell i at the end of the seiche period,

c_i^o is the concentration at the start,

α is the ratio of volume outflow to the tank volumes = TQ/2V,

Q is the average flow over the seiche half-period,

T is the seiche period, and

V is the tank volume, assumed equal for all tanks.

The form of this equation is suggestive. If we divide by T and take the limit that T and the cell length become difference quantities, Δt and Δx, the equation becomes the finite difference approximation to:

$$\frac{\partial c}{\partial t} = \left(\frac{\Delta x U_T}{2} - \frac{\Delta t U_T^2}{2}\right)\frac{\partial^2 c}{\partial x^2}$$

Under pure advection, the concentrate should have returned to its original location unchanged so that $\partial c/\partial t = 0$. The non-zero term above is the numerical dispersion due to the average velocity, U_T, determined over one-half seiche period. It is given as $2U_{max}/\pi$, where U_{max} is the maximum seiche velocity. The numerical dispersion found above is identically that given by Equation 2.17 with $\gamma_i = \gamma_{i+1} = 1$, suggesting that there is no numerical dispersion peculiar to oscillatory flow other than that due to advection errors. Nevertheless, the cumulative effect of this error over many months of simulation is substantial.

Elimination of numerical dispersion is a thorny problem. The error cannot be curtailed by a simple change in the numerical formulation of the advective term since the value of Δx will remain large relative to the seiche excursion. (The seiche excursion can be taken as the wave length of the system disturbance as employed in the Fourier or von Neumann method to study stability and accuracy -- see Verboom and Vreugdenhil, 1975). Although the formulation used in Equation 5.10 to solve the advective term is known to be dispersive, substitution of a low dispersion

formulation by Holly (1975) yielded no improvement. For another low dispersion method, the Stone and Brian (1963) formula, it is possible to estimate the desired value of Δx using relations developed by Dailey and Harleman (1972). The value found, which is independent of the model time step, is 67 meters, or 1125 grids to cover the length of the lake! This sort of detail is obviously impractical. To our knowledge, there are no treatments of the advective term which will operate accurately in the range of Δx we require for practicality.

There does remain one easily implemented alternative, however. The desire is to find a method which will allow the seiche advection to, in essence, do nothing. That is, over the time periods of interest in the lake, there should be no net effect due to seiche advection. The dispersive effects of seiche motion will, of course, be felt, but advective effects will not. The obvious solution, therefore, is to isolate the dispersive effect and entirely neglect the oscillatory advection. The procedure we will follow is thus to consider the influences of advection due to hydrologic through-flow and of dispersion due to seiche motion, and to neglect the minor perturbation of seiche-driven advection.

It is important to consider the approximations entailed by this procedure. Neglect of the advection will lead to the minor loss of some mixing effects at the ends of the lake and where geometry changes abruptly, as at either side of Tihany Strait. This approximation will be minor since dispersion is generally large at these locations. A more important factor may be the neglect of the dispersing action which occurs in oscillatory flow as lake water advects back and forth next to a shoreline nutrient discharge. The influence from such a load will be spread over the distance of the seiche excursion causing an effect somewhat like dispersion. This will be lost in the non-oscillating model -- however, the approximate effect can be captured if Δx is on the order of the typical seiche oscillation. This will fail to capture the effects of the occasional event with large excursion, but such events are rare and the error will be minor. For the typical event, the load is mixed within the grid square and thus over roughly the same distance as the seiche excursion.

5.5.3 Dispersion

With the realization that the seiche excursion is too short for seiche-driven advection to be influential, dispersion becomes the critical link between the hydrodynamic component and the water quality transport model. In this section, we explore a method to determine dispersion from the hydrodynamic model predictions.

The concept of the dispersion coefficient is introduced in Chapter 2. Dispersion arises when a multi-dimensional transport process is modeled in an approximation of fewer dimensions -- in this case, one dimension. Non-uniformities in the velocity and concentration distributions transverse to the major axis lead to an apparent smearing, or dispersion, of the 1-D concentration profile. The origin of this effect may be determined mathematically by averaging the full three-dimensional equation of mass transport over the lateral and vertical dimensions -- this derivation is done in Appendix D. Proceeding from such a derivation, Fischer

(1967) presents an equation to determine the dispersion coefficient from the observed velocity distribution. Presuming lateral velocity and concentration non-uniformities dominate those in the vertical, the dispersion coefficient is:

$$D = -\frac{1}{A} \int_0^W dy\, q'(y) \int_0^y \frac{dy'}{\varepsilon_y h} \int_0^{y'} dy''\, q'(y'') \qquad (5.27)$$

where
- A is the cross section area,
- y is the lateral space coordinate,
- h is the depth (a function of y),
- q' is the deviation flow per unit width,
- W is the width, and
- ε_y is the lateral turbulent eddy diffusivity,

This equation may be approximated as (Fischer, 1969):

$$D = \frac{\overline{I(u')^2}\, W^2}{\overline{\varepsilon_y}} \qquad (5.28)$$

where
- u' is the local deviation of the depth averaged velocity from the cross-sectional mean (= q'/h), and
- I is a constant equal to about 0.1.

The overbars in the equation indicate averages over the cross section. Fischer constructs Equation 5.28 by non-dimensionalizing the terms within the integrals in Equation 5.27, to leave the value of the integral I dependent only upon non-dimensional cross-sectional distributions of u', h and ε_y. Proceeding with reasonable assumptions for these distributions, he determines I.

Effect of Oscillating Flow

The predicted dispersion coefficient in Equation 5.27 or 5.28 is predicated upon an assumption of a steady velocity profile. In oscillating flow, this assumption will, of course, be violated. Holley, Harleman and Fischer (1970) show that the effective dispersion in oscillatory flow is often less than that predicted by Equation 5.27 or 5.28. In steady flow, dispersion is controlled in part by the time required for mixing transverse to the flow. Consider the interaction of the flow period and the lateral mixing time in a simple example. Suppose that a curtain of tracer dye is

somehow placed through the water column lateral to the flow axis. As the seiche flowed in one direction, it would sweep the dye along, carrying different parts at different velocities. If lateral mixing were very, very slow, there would be no communication between these displaced dye parcels -- upon return of the seiche, the dye would be carried back to its original location with no change. If lateral mixing were faster, however, the differentially convected dye parcels would mix across the lake, moving to sectors of the flow field with different velocity. Upon return of the seiche, these laterally mixed parcels would be convected back at different velocities than the velocities which originally carried them away. They would thus return to different longitudinal positions than they held originally. The net effect would be a smearing, or dispersion, of the original line of dye along the axis of the flow. The magnitude of the dispersion depends upon the lateral mixing: the greater the distance of lateral communication by the displaced dye parcels, the greater will be the dispersion. In oscillating flow, the rate of lateral mixing is not important in an absolute sense, but as a rate relative to the oscillation frequency. Holley et al. capture this relation through the ratio of the oscillation period to a representative cross-sectional mixing time, and develop formulae to compute the reduction in dispersion as a function of the time scale ratio.

The preceding paragraphs indicate the important part played by transverse mixing in the computation of dispersion. Such mixing enters into Equations 5.27 and 5.28 through the lateral diffusivity, ε_y. Further, transverse mixing is particularly crucial in the special computations necessary to account for oscillating flow conditions.

The character of lateral mixing is a key assumption required to derive Equation 5.27 or 5.28 from the three-dimensional equations of mass conservation, repeated here as Equation 5.29:

$$\frac{\partial c}{\partial t} + u \frac{\partial c}{\partial x} + v \frac{\partial c}{\partial y} + w \frac{\partial c}{\partial z} =$$

$$\frac{\partial}{\partial x}\left(\varepsilon_x \frac{\partial c}{x}\right) + \frac{\partial}{\partial y}\left(\varepsilon_y \frac{\partial c}{\partial y}\right) + \frac{\partial}{\partial z}\left(\varepsilon_z \frac{\partial c}{\partial z}\right) \qquad (5.29)$$

For open-channel flows, one can assume as Fischer that the lateral advective term,

$$v \frac{\partial c}{\partial y}$$

is negligible compared to lateral diffusion,

$$\frac{\partial}{\partial y}\left(\varepsilon_y \frac{\partial c}{\partial y}\right) .$$

This is tantamount to assuming negligible secondary currents. A scaling analysis based on typical magnitudes for Lake Balaton shows that the opposite is the case there: lateral advection dominates diffusion. This change has far-reaching impact on the resulting analysis. Consider, for example, the cross-sectional mixing time based on diffusive transport:

$$T_c = \frac{\left(\frac{W}{2}\right)^2}{\varepsilon_y}$$

Assuming, as in Section 5.1.3, that $\varepsilon_y = 10^4$ cm^2/sec, this predicts a mixing time of almost 200 days in Lake Balaton. This is clearly a high estimate, given the likely strength of wind-driven circulation. If we instead estimate a time scale for lateral advection, using 5 cm/s as the typical velocity observed in our field studies (Appendix A) we find:

$$T_c = \frac{\frac{W}{2}}{V} \simeq 1 \text{ day}$$

Even with a more conservative velocity of 1 mm/sec, T_c is still only 50 days. This is much shorter than the diffusion-based mixing time and will lead to a much greater value of the dispersion coefficient than if the diffusion-based theory of Fischer were employed.

For complete consistency in the determination of the dispersion coefficient, we must rederive Equations 5.27 and 5.28 proceeding from our revised assumptions. The complete derivation is given in Appendix D. The result, after following similar steps as Fischer (1966) is:

$$D = \frac{1}{A} \int_0^W dy\, q' \int_0^y dy' \frac{q'}{V} \qquad (5.30)$$

where q' is the deviation flow per unit width as defined for Equation 5.1, and
V is the lateral flow per unit width.

Equation 5.30 is approximated in the same fashion as Equation 5.27:

$$D = \frac{IW\ \overline{(u')^2}}{\bar{v}} \qquad (5.31)$$

where $\bar{v}$ is the mean lateral velocity in the cross section.

Using reasonable assumptions for the distribution of $\bar{v}$ and q' in the cross section, I is found once again to be about 0.1.

The dispersion coefficient given by Equation 5.30 or 5.31 does not account for the reduction due to oscillating flow. Following Fischer's (1969) arguments still further, the reduction factor, f(T'), is found to depend upon the dimensionless ratio of the oscillation (seiche) period to the lateral mixing time:

$$T' = \frac{T_1}{T_c} = \frac{T_1}{\frac{W}{2\bar{v}}}$$

where T_1 is the uni-nodal seiche period.

Holley, Harleman and Fischer (1970) give a formula and plot of f(T'). For $T' < 0.1$ they give the following relation:

$$f(T') = 10(T')^2$$

According to Holley et al., f(T') is a reduction factor used to find the average dispersion over an oscillation period from the equivalent steady flow dispersion:

$$\frac{D_{osc}}{D_{steady}} = f(T')$$

where D_{osc} is the average dispersion coefficient over an oscillation period, and

D_{steady} is the integral over the oscillation period of the instantaneous steady dispersion coefficient.

The instantaneous steady dispersion coefficient is the coefficient which would be computed from the velocity distribution at any instant, treating the distribution as though it were steady.

To apply the methods of the previous paragraph to lake circulation is clearly speculative. The reduction factor was not determined for lake conditions, although it was derived for prismatic and natural open-channel conditions as well as for pipe flow, finding variation within an order of magnitude. (Holley, Harleman and Fischer, 1970, and Chatwin, 1975). The robustness of the theory over this range of conditions, as well as the lack of any alternative method, has prompted us to employ it in this application. Nevertheless, use of Holley's method should be clearly understood to be an extension beyond the purposes for which they were originally intended. Until more research has been done on dispersion in oscillatory flow we can only assume it appropriate to employ the theory as we have done.

Summary

To summarize our procedure, the dispersion coefficient will be computed at selected time intervals during the seiche period employing a new formula (Equation 5.31). This formula was developed following similar derivations by Fischer, but proceeding from the assumption that secondary currents dominate lateral mixing. The values of the dispersion coefficient will be averaged through the seiche cycle, and then reduced by a reduction factor given by Holley et al. (1970). The argument of this function, the dimensionless ratio of the seiche period to the lateral mixing time, T', will be based upon the average of the absolute value of lateral velocity over the seiche period. These procedures are consistent with those of Holley et al., although it should be understood that the application of the method to lakes is an extension beyond Holley et al.'s original intentions.

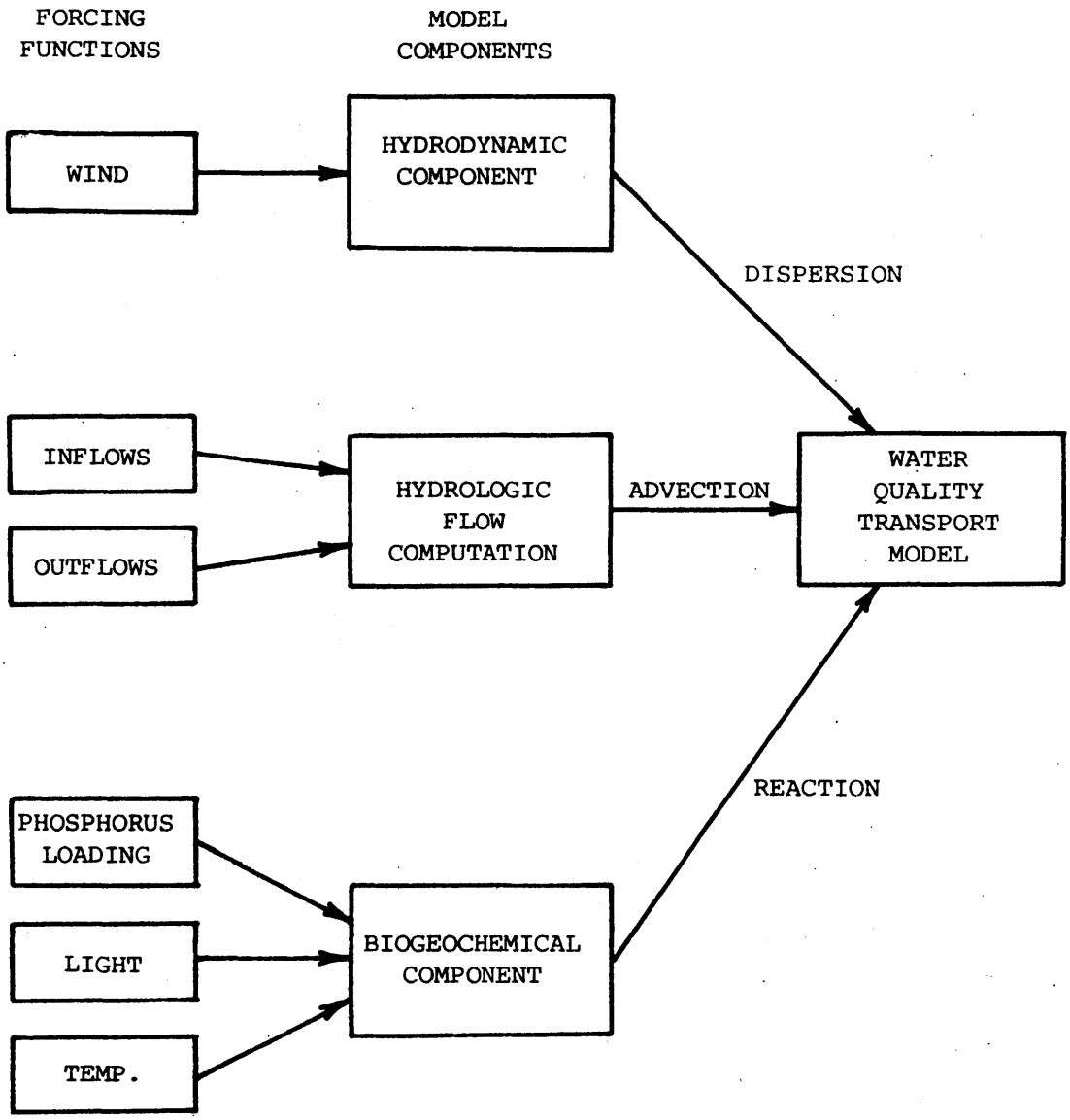

Figure 5.20

Structure of the linked water quality model

5.6 Summary of the Model Construction

The linked water quality model consists of three main parts. The basic framework of the model is established by the water quality transport model. This model determines the changes in constituent concentrations due to the hydrodynamic influences of advection and dispersion and due to biogeochemical reactions. Our model incorporates two alternative transport model approaches: the finite difference model, founded on a concept of the lake as a continuum, and the multiple-box model, which divides the lake into discrete volumes with lumped parameters for each.

The two other main parts of the model are the hydrodynamic and biogeochemical components. The biogeochemical component is a model of the biological phosphorus cycle. It determines the reactions between dissolved inorganic phosphorus, detrital phosphorus and two algal populations subject to transient meteorologic and phosphorus loading conditions. The rates of these reactions are transmitted to the water quality transport model to construct the reaction terms of the transport equation.

The hydrodynamic component is a transient, single-layer circulation model which determines the two-dimensional horizontal transport in the lake. This component employs the time-varying record of observed wind over the lake in a continuous simulation of depth-averaged water motion and water surface displacement.

The hydrodynamic component is linked to the water quality transport model via the dispersion coefficient. Only dispersion is employed in the linkage since longitudinal advection participates only as seiche motion of short excursion which has minor influence on the net mass transport. Dispersion is computed as the average value over the seiche period using formulae which account for the reducing effect of oscillatory flow. The dispersion coefficient is computed from the instantanteous flow field at frequent intervals within the seiche period assuming lateral advection to be the dominant source of lateral mixing. The average of the summed instantaneous coefficients is then reduced by the procedure of Holley et al. (1970). This average reduced dispersion coefficient, determined over the seiche period, is supplied as a function of time to the water quality transport model.

In addition to the circulation model, there is the water balance calculation to determine the hydrologic through-flow. Using simple budgeting of inflow and outflow, this program computes monthly average flows along the lake which are linked to the water quality transport model through the advective term.

Figure 5.20 summarizes the model components and their linkage in a schematic diagram.

6 LINKED MODEL SIMULATION OF LAKE BALATON

6.1 Introduction

Evaluation of the modeling strategies and study of water quality dynamics in Lake Balaton was accomplished through simulations of the year 1977. This particular year was dictated by the availability of data necessary as input to the model components. In addition, water quality field data was available and permitted the model results to be evaluated while the work of other researchers on the same year allowed comparisons. All of the data employed were generously supplied by IIASA from their Lake Balaton Data Base.

The simulations were approached with the philosophy that they were to be experiments to evaluate the influence of hydrodynamics upon the water quality predictions and to compare the one-dimensional finite difference and box model formulations. Insufficient data and resources precluded the possibility of detailed calibration (and perhaps reformulation) of the biogeochemical model in an attempt to duplicate field data with the model results. Further, the data base to provide true verification simply does not exist. Uncertainties in wind data and model verification further trouble the hydrodynamic component. The approach taken was thus to produce a plausible model of the lake's behavior and exercise it under different hydrodynamic assumptions. This freed our time to concentrate on the important questions which concern the formulation of lake water quality models and the development of procedures to link hydrodynamic and water quality models.

6.2 Hydrodynamic Simulation

The wind-driven circulation model served as the hydrodynamic component of the water quality model, determining the dispersion coefficient as a function of time and space. In this section, we describe the procedures followed in accomplishing this task for the simulation of Lake Balaton's water quality for 1977. In addition, the circulation model stands as a simulation model of its own, and we report selected results from the model to indicate the character of motion in the lake.

6.2.1 Modeling Procedures

The necessary input data to execute the circulation model are outlined in Section 5.3.2. To simulate 1977, we employed the coarse model grid with the parameters found by calibration -- a Chezy coefficient of C = 60 and a fixed wind drag coefficient, C_2 = 0.0013. For wind data, a continuous record of three-hourly averaged wind speed and direction measured at Keszthely was used. The wind speed was adjusted to account for the generally lower wind speed observed at Keszthely in the manner described by Shanahan et al. (1981).

The hydrodynamic model was run once to prepare a transfer data file for repeated use in the water quality simulations. For the sake of economy, we took advantage of the nearly uniform pattern of wind with time and simulated the circulation for only July and August as a typical period. Longer periods were simulated in the water quality model, and for those, the July-August hydrodynamic history was repeated continuously to create an artificial record spanning the entire simulation period. Execution costs are substantial for the circulation model program: roughly 350 CPU seconds of computer time were required to simulate one month on MIT's IBM 370/168 computer.

6.2.2 Simulation Results

Typical results from the circulation simulations for 1977 are plotted in Figure 6.1. In Figure 6.1 we show the longitudinal water motion found for the months of July and August at a mid-lake section near Balatonboglar, a location corresponding roughly to the Basin II - Basin III boundary in the four-box model. Figure 6.1 shows both the advective flow and what we will term the dispersive flow. The dispersive flow is shown as an indicator of the non-uniformity of the velocity distribution. It is computed as follows. First, the average velocity in the cross section is determined. Then, in each grid across the section, the difference between the grid velocity and the section average is found. This difference is multiplied by the grid width and depth to convert to a flow rate. All such flows found to be positive are summed to give the dispersive flow. The similar quantity found by summing negative flows is equal, but opposite in sign. We have called this flow "dispersive" since, as a meas-

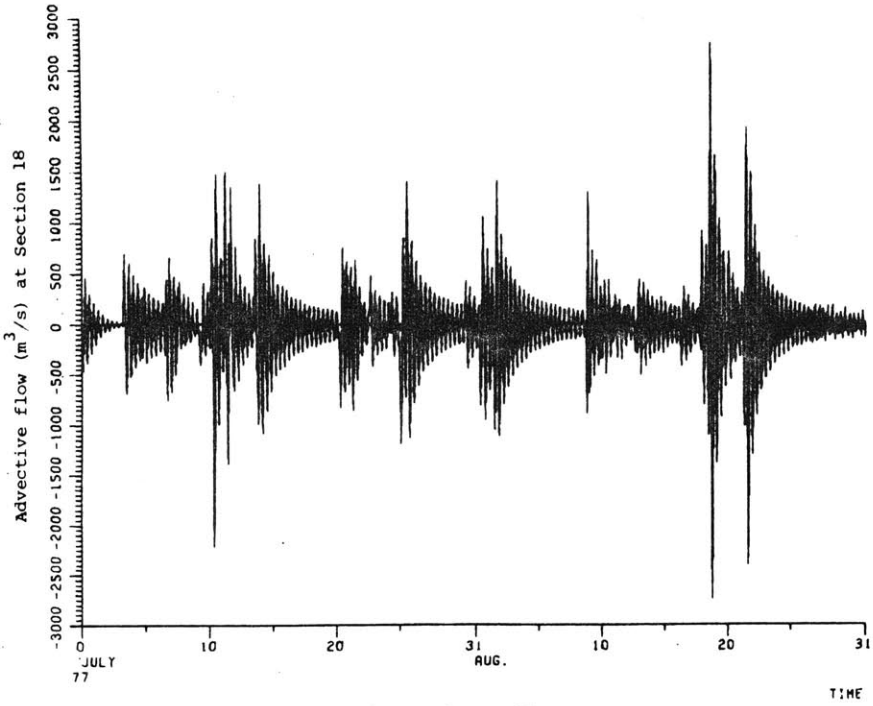

a. Advective flow

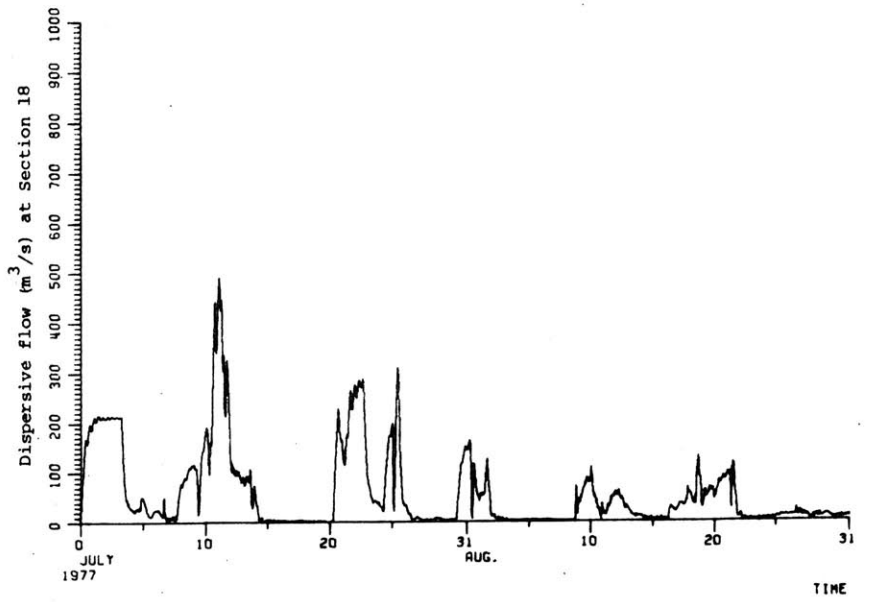

b. Dispersive flow

Figure 6.1

Advective and dispersive flow at mid-lake
(circulation model results at Section 18)

ure of the velocity profile non-uniformity, it is indicative of the magnitude of dispersion. However, as shown in Chapter 2, such flows cannot be directly related to dispersion or model exchange flow.

Both the advective and dispersive flow components are highly transient, responding to episodic wind events. The advective motion's oscillatory character is striking, but it should be clear that there is no net translation of water over long time periods due to this component. This can be seen in Figure 6.2, which shows the cumulative seiche excursion determined from the predicted advective flow as a function of time. The results are for a location midway through Basin III, roughly the nodal point of the uni-nodal seiche. The nodal point is the location along the lake at which the discharge due to the seiche is greatest. The small excursions seen in Figure 6.2 confirm our decision in Section 5.5.2 to neglect seiche advection.

The dispersion coefficient was computed from the velocity profile following the procedure described in Section 5.5. In employing this procedure, instantaneous dispersion coefficients were computed at intervals of one-half hour and then averaged over the model seiche period (8.5 hours) consistent with Holley et al.'s procedure. The average transverse speed over the same period was then used to compute the reduction factor for oscillatory flow. The computed dispersion coefficient is shown in Figure 6.3 at Sections 6 and 18. The general trends observed in the dispersive flow (Figure 6.1b) are preserved in the dispersion coefficient (Figure 6.3). During most of the time, dispersion is low -- strong mixing occurs on an occasional but fairly regular basis due to wind events. The spatial distribution of the average dispersion coefficient over the two-month simulation period is shown in Figure 6.4. A constant value of $D = 1.0\ m^2/s$ is also shown as a reference point. Dispersion is highest as the locations of greatest change in geometry due to the larger secondary currents at those sections. Also, a somewhat higher dispersion is maintained in Keszthely Bay and the Siófok basin (Basin IV) where, as we will show below, there is a greater tendency to gyre motion.

6.2.3 Analysis of an Event Simulation

Besides serving as the water quality model's hydrodynamic component, the circulation model is a tool which we can use to study the motion within the lake. Of particular interest for the Lake Balaton study are those motions which will significantly affect the water quality within the lake. In this section we will examine selected results from our simulation of the July 8 and 9, 1963 event to illustrate the spatial and temporal character of motion within the lake.

The motion within the lake during one-quarter of a seiche cycle is shown in Figure 6.5. This sequence of vector plots shows the predicted depth-averaged current at one hour intervals from the time of maximum flow towards Keszthely to the time immediately after the seiche current reverses direction. In the central portion of the lake, strong unidirectional currents dominate the motion, while flow gyres are more evident in the eastern Siófok basin and in the western Keszthely and Szigliget Bays. The character of the bulk motion in time is indicated in

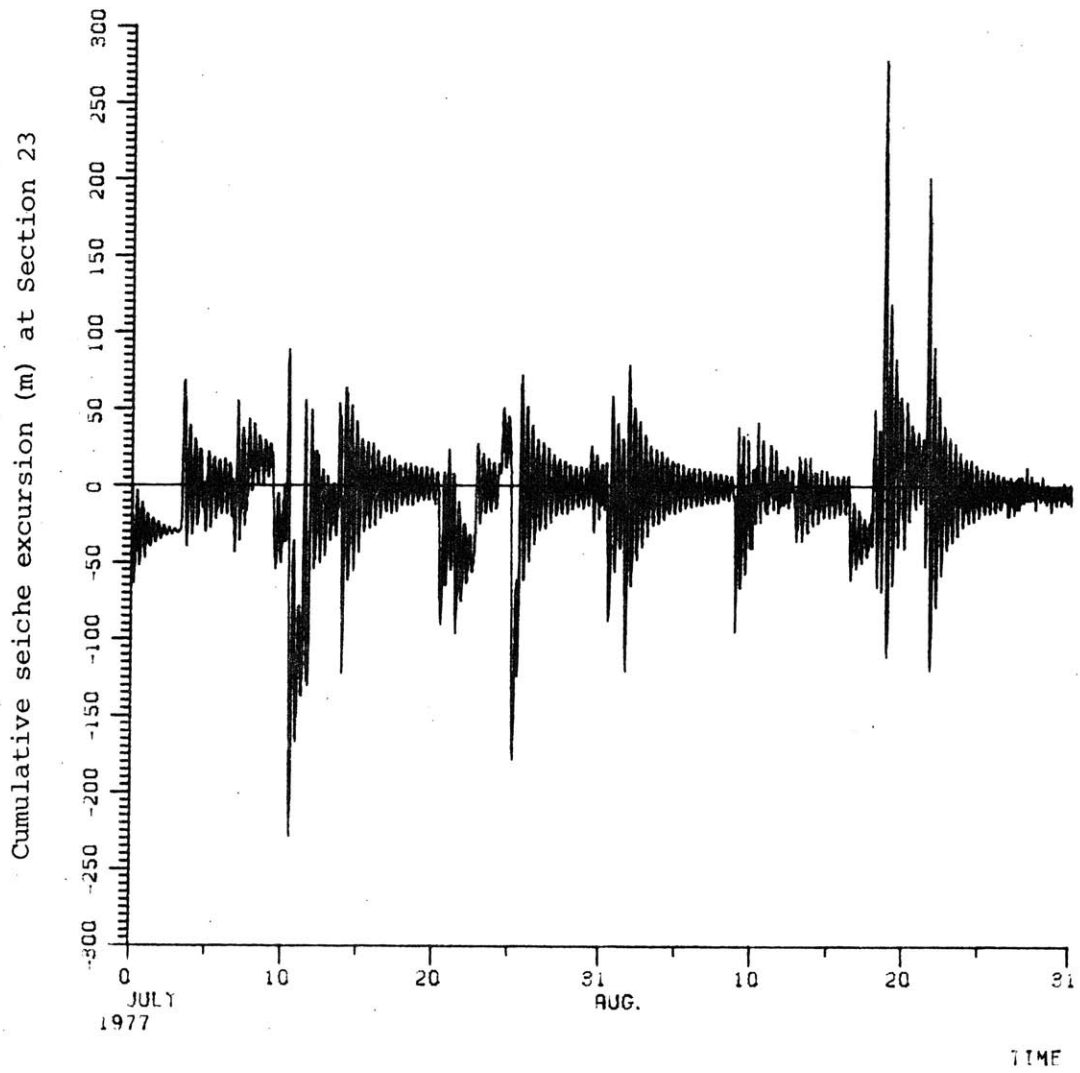

Figure 6.2

Longitudinal translation due to seiche advection

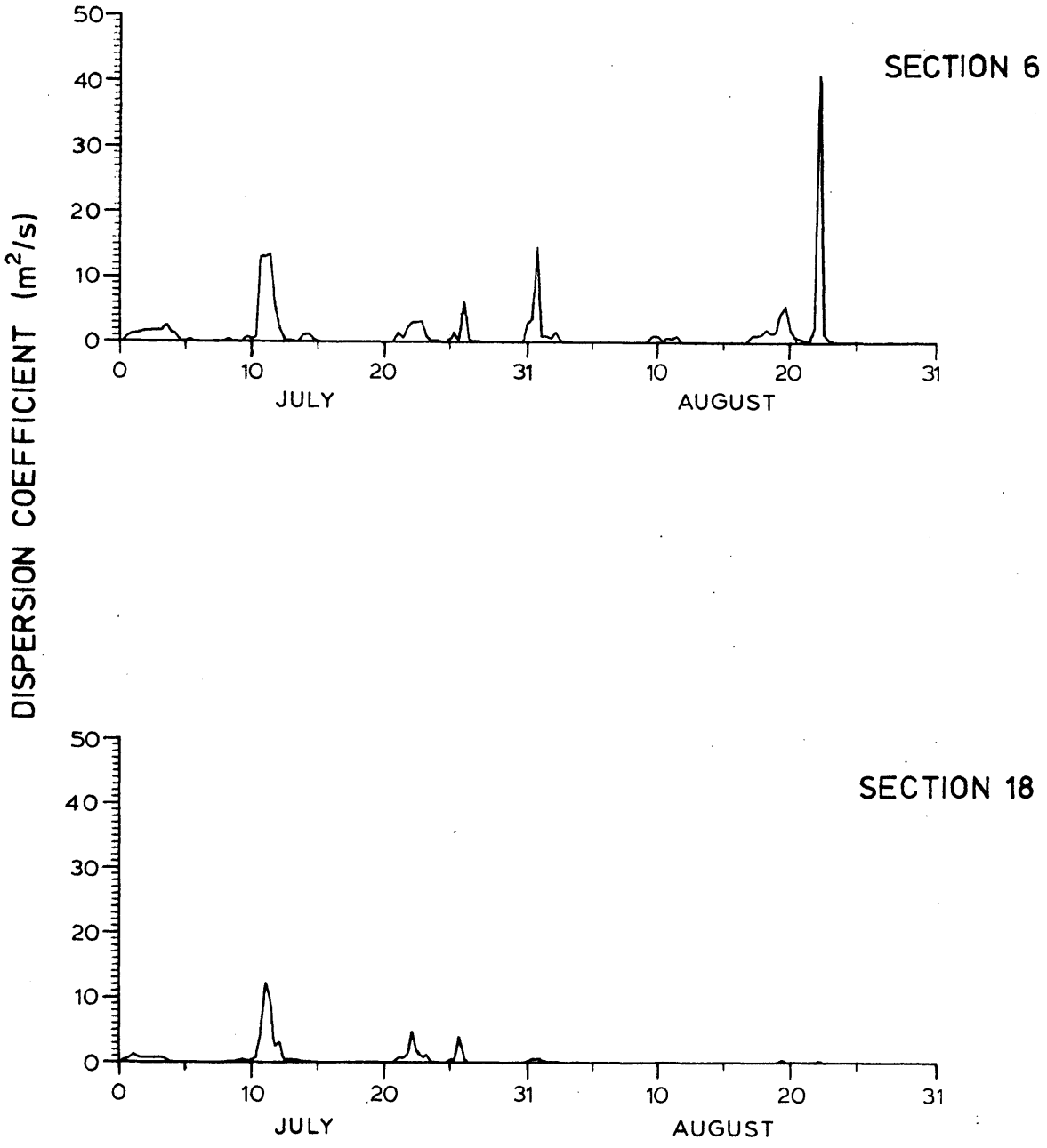

Figure 6.3

Computed dispersion coefficient at two lake locations during July and August 1977

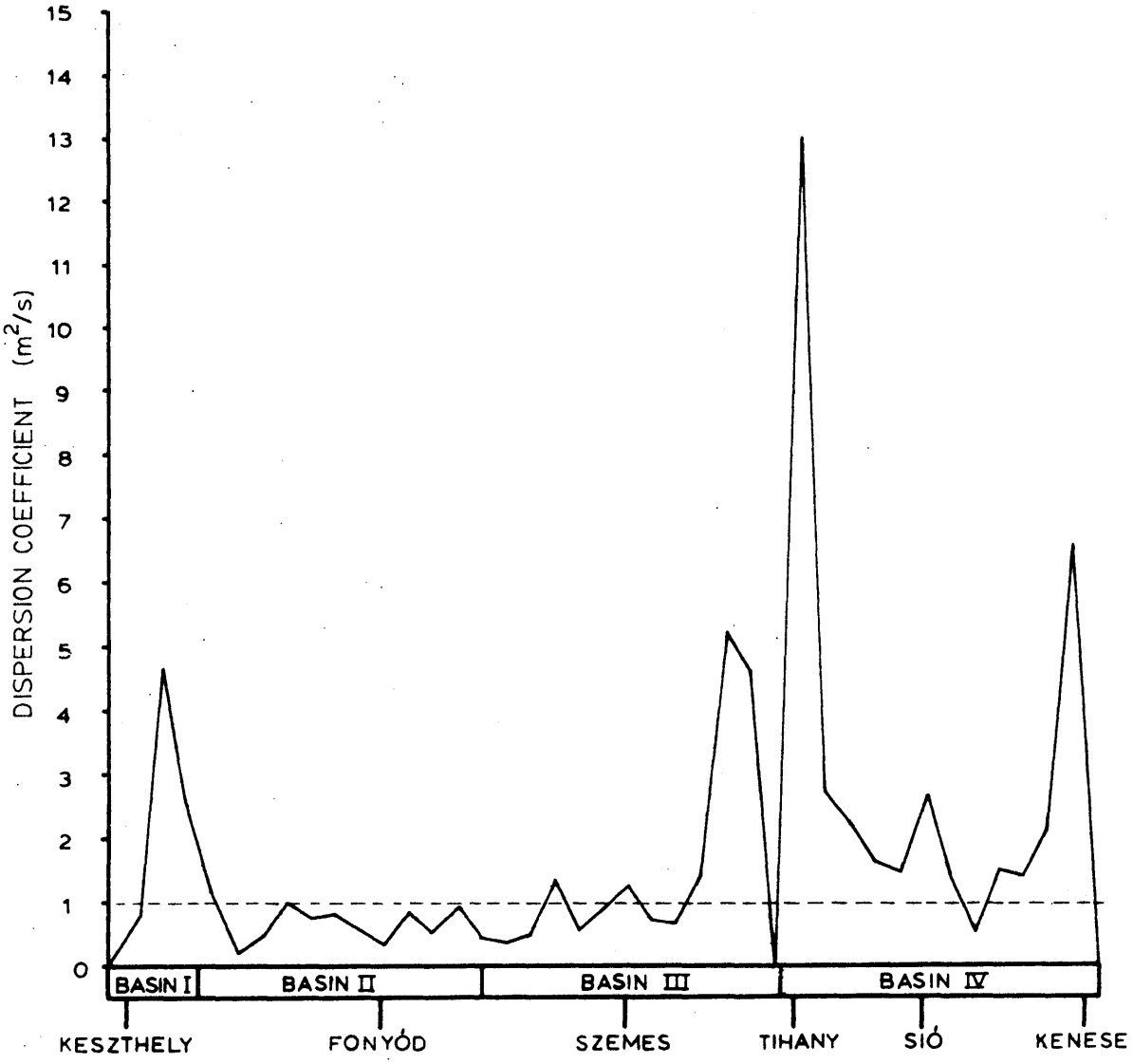

Figure 6.4

Spatial distribution of computed dispersion coefficient averaged over July and August 1977

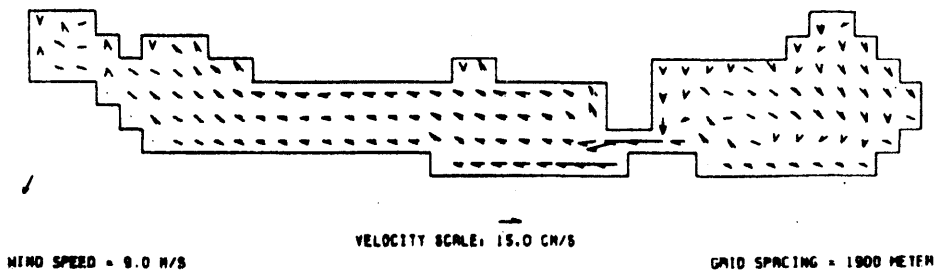

July 8, 1900 hours

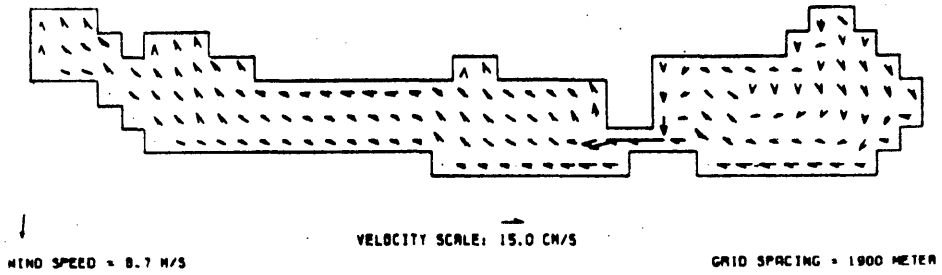

July 8, 2000 hours

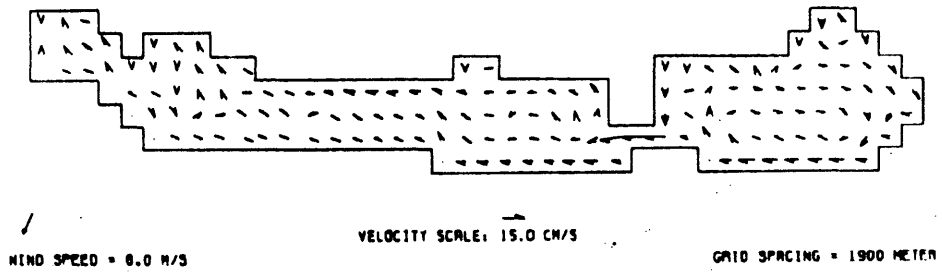

July 8, 2100 hours

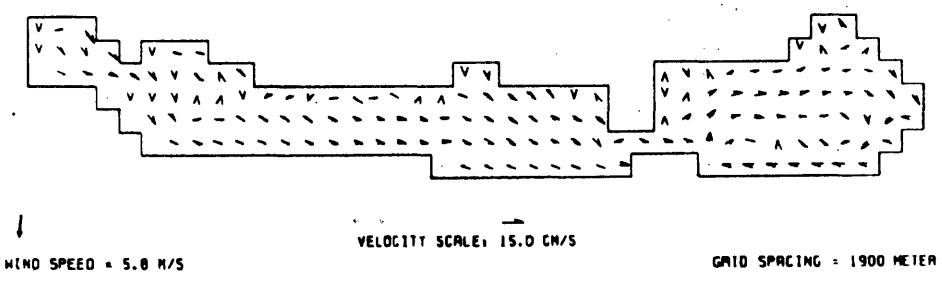

July 8, 2200 hours

Figure 6.5

Wind-driven circulation from simulation of July 8-9, 1963 event

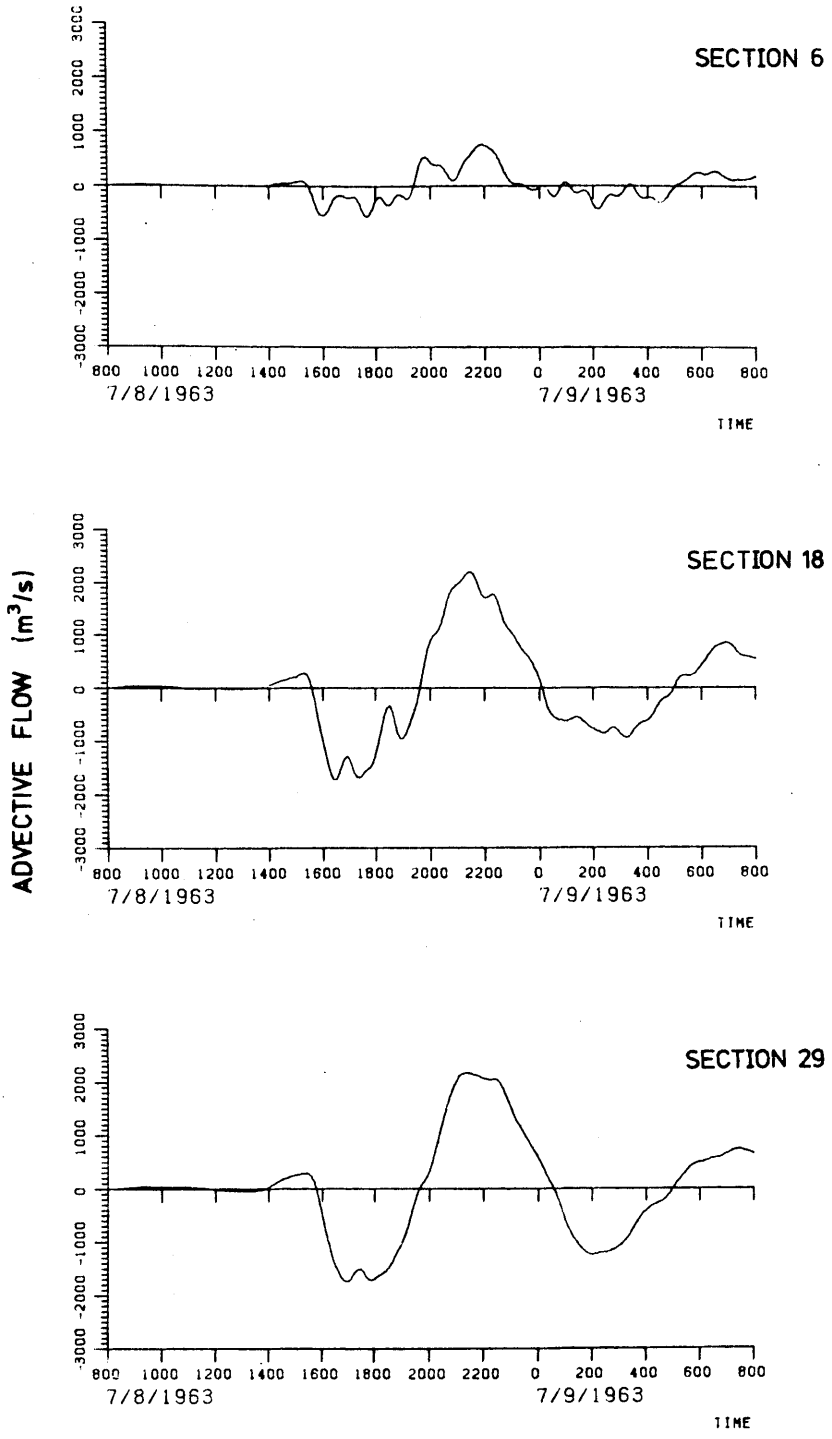

Figure 6.6

Advective flow from simulation of July 8-9, 1963 event

Figure 6.6 in time plots of the discharge at three sections along the lake. The sections selected correspond to the boundaries between the four lake basins, defined in Section 4.2. The flows are shown to be large, exceeding the hydrologic through-flow by two orders of magnitude. However, they are of the same magnitude as the flows shown in Figure 6.1, thus the seiche excursion will be comparable to that found in Figure 6.2.

The transports shown in Figure 6.6, being net transports, ignore all variation in the current across the lake section. Such variations are, of course, responsible for dispersion and are thus very important to the water quality predictions. The magnitude of such current variations are shown in Figure 6.7 and 6.8 for two locations along the lake. Shown are the lateral profiles of the depth-average velocity at intervals of one-half hour. The locations of these profiles are Section 18, typical of the middle of the lake where unidirectional flows dominate, and at Section 36, midway in the Siófok Basin, where gyre motion is more in evidence. The velocity profiles at this latter section are considerably less uniform than those at the mid-lake location. At either section, flow variations in time are greater than those in the lateral direction.

We also experimented with different grid sizes in simulating the July 1963 event to examine the influence of the grid size on the model results. Section 5.3 previously discussed the grid size and showed the alternative coarse and fine grids in Figures 5.5 and 5.6. Figure 6.9 contrasts predictions of water surface elevation, advective flow and dispersive flow made using the coarse and fine grids. Water surface elevation and advective flow differ inconsequentially, and the difference in the dispersive flow is very small. Hence, the decision to employ the coarse grid in the 1977 simulations is justified.

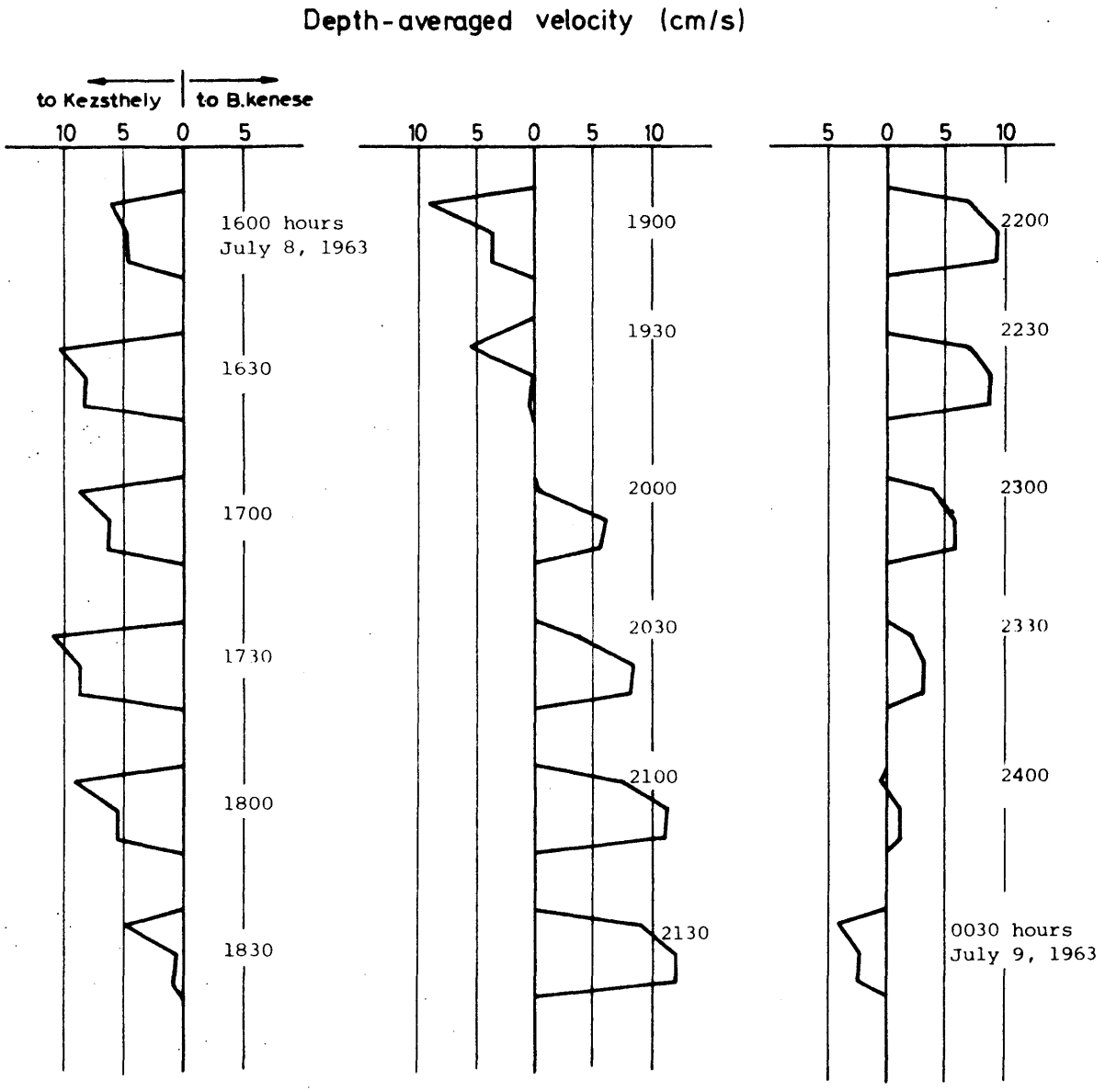

Figure 6.7

Lateral velocity profiles at Section 18
from simulation of July 8-9, 1963 event

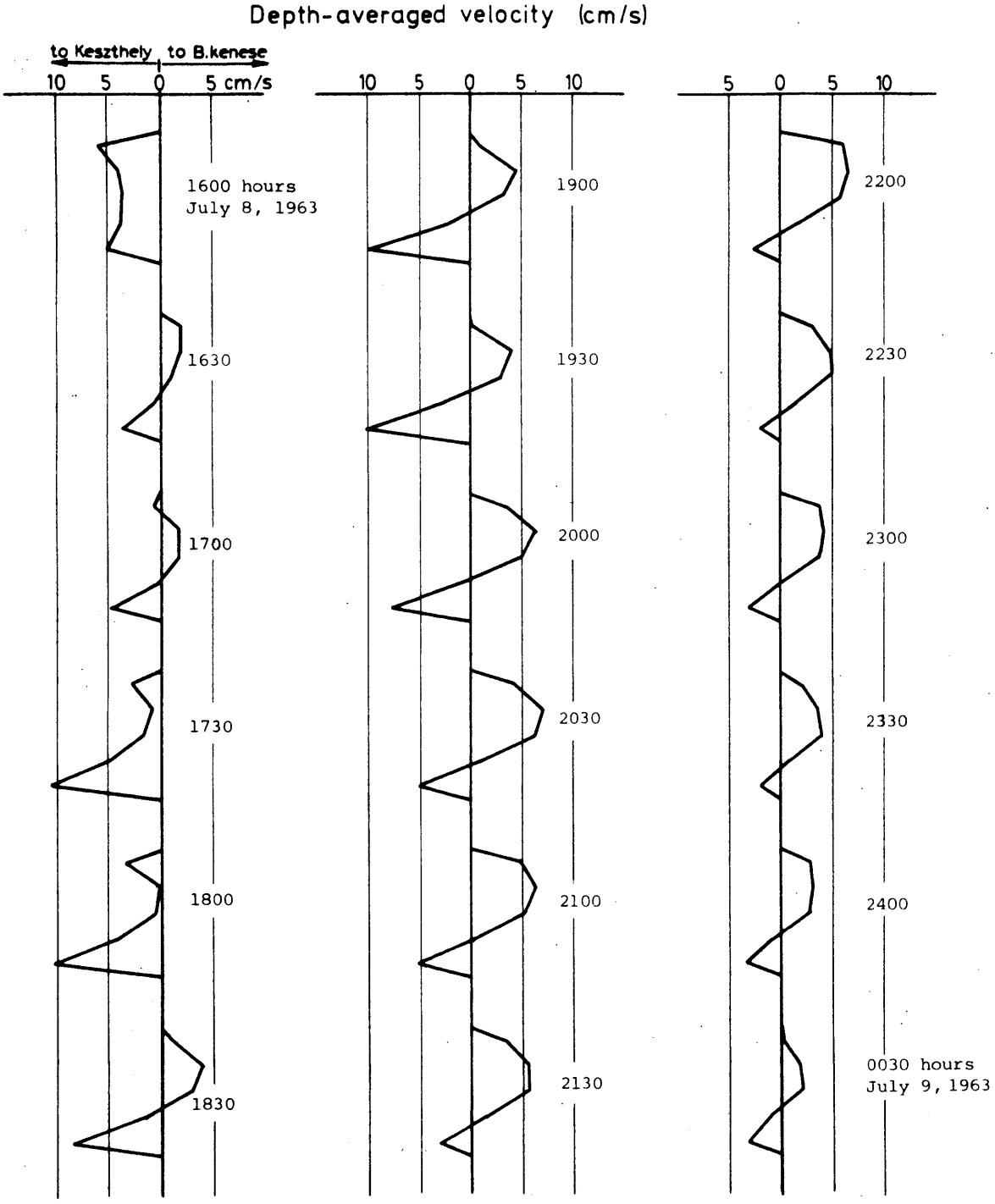

Figure 6.8

Lateral velocity profiles at Section 36
from simulation of July 8-9, 1963 event

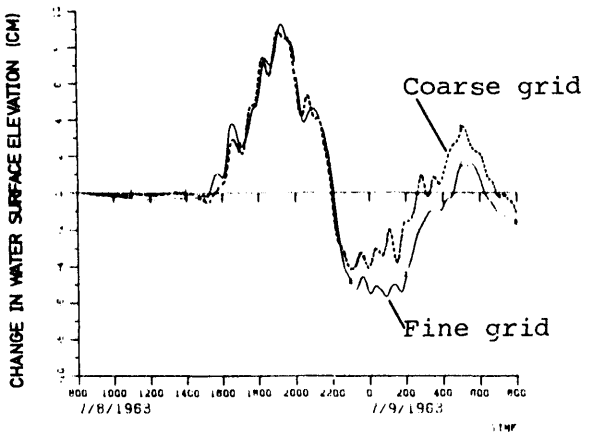

a. Water surface elevation at Keszthely

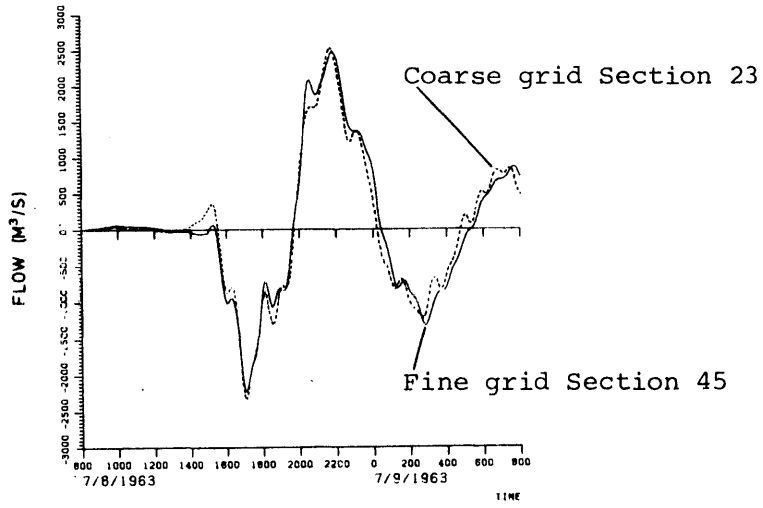

b. Advective flow at coarse grid Section 23

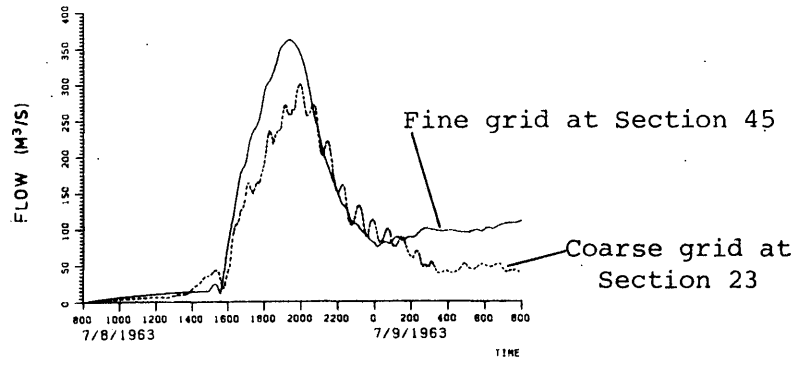

c. Dispersive flow at coarse grid Section 23

Figure 6.9

Comparison of coarse and fine grid simulation results for July 8-9, 1963 event

6.3 Water Quality Simulation

6.3.1 Data for the 1977 Simulations

Data needs for the water quality model include the lakes's bathymetry, the spatial and temporal distribution of phosphorus loads, the biogeochemical model parameters, and meteorological forcing functions. In addition, the hydrodynamic inputs from the water balance and wind circulation models are also necessary. Finally, field data to permit comparisons with observed behavior are helpful. We discuss a portion of this data elsewhere: the biogeochemical model parameters are determined by van Straten (1980) by calibration and are given in Section 5.4, and the outputs from the wind circulation model are discussed in the section above. We will briefly outline the preparation of the remaining data in this section.

Physical Data

A forty-element one-dimensional finite difference grid for the water quality model was constructed to correspond with the longitudinal grid boundaries of the hydrodynamic coarse grid, Figure 5.5. Cross-sectional areas were required for the faces which separate neighboring grids. These were determined by trapezoidal integration over the depth contours in the bathymetric map of the lake. The surface areas of the grids were found from the map by planimetry, and the grid volumes were determined from the grid length and the average of the bounding cross section areas. The data employed are given in Appendix E. The four-box model characteristics were chosen to agree with those used by van Straten (1980); they are also included in Appendix E.

Monthly average hydrologic flows were computed by water balance based on the measured inflow of the Zala River and outflow to the Sió Canal, evaporation and precipitation, and tributary inflows. Tributary data were available only as lake-wide sums and were disaggregated by tributary based on average flows given by Jolánkai and Somlyódy (1981). They were further distributed by month, correlating with the Zala River inflow distribution. The results of the water balance calculations are given in Appendix E for both the finite difference grid and four-box models.

Phosphorus Loading Data

The input phosphorus load was prepared with information from Jolánkai and Somlyódy (1981) and with additional instructions and data given by Somlyódy (personal communication). Five sources were considered: the Zala River inflow (daily values), other tributary streams, sewage inflow, sewage pond inflows (all monthly values), and atmospheric deposition (constant in time). Neglected were urban runoff and direct non-point sources. For consistency with the model compartments, it was necesary to subdivide the load into detrital phosphorus and dissolved inorganic phosphorus. Following the references cited above, we assumed dissolved inorganic phosphorus to consist of the measured orthophosphate plus any polyphosphate compounds. The portion of the remaining load allocated to detrital phosphorus includes any unbound organic phosphorus "available"

for algal growth, as explained in Section 4.3.4. For sewage inflows, the total measured phosphorus was assumed to consist entirely of dissolved inorganic phosphorus. However, the tributary inflows (including the Zala River) required the load to be subdivided. To do this, the measured orthophosphate fraction of the load was allocated to dissolved inorganic phosphorus, while twenty percent of the remaining portion of the measured total phosphorus was assumed biologically active and taken as detrital phosphorus. The time variation of the summed input loads is shown in Figure 6.10. Atmospheric deposition, not included in Figure 6.10, is specified as a constant rate per unit surface area which sums to a total phosphorus load of 85 kg/day distributed uniformly over the lake.

Water Quality Field Data

Measurements of phosphorus and chlorophyll-a, obtained from the IIASA data base, were employed to check model performance and to determine initial conditions. Since calibration was not attempted in these studies, the field data were not used for detailed comparison with model results. They did prove useful, nevertheless, as indicators of the type of behavior the model should be producing and for order of magnitude checks on the predictions. Data for total phosphorus and orthophosphate are shown in Figure 6.11 as a series of profiles. The total phosphorus, excluding particulate (sedimentary) inorganics from the field observations, is comparable to the model total phosphorus results. The orthophosphate, which is near the limits of accurate measurement, corresponds to dissolved inorganic phosphorus in the model. Figure 6.12 shows the profiles of measured chlorophyll-a concentration along the lake. These data cannot be directly compared with model results; however the total algal phosphorus concentration predicted by the model should mirror the spatial and temporal trends observed in chlorophyll-a in the field. The data of Figure 6.11 and 6.12 show the trends seen in the long-term averages (Figure 4.7) to be fairly constant over the year. On the other hand, the data for March 28 and 29 in Figure 6.11 dramatically illustrate the possibilities for individual data to be erroneous or unrepresentative. A storm with winds of 12 m/s (measured at Keszthely) separates the measurements on March 28 and 29.

6.3.2 Simulation Procedures

The simulations were started on February 25, 1977 with initial concentration profiles based on field data (Figure 6.13). Simulations were run through the summer and on to October 31 (and in some runs to December 31).

The cost of simulation depends upon the number of grids. The CPU time for program execution on the MIT IBM 370/168 is roughly one-half CPU second per grid per month. This cost does not include the circulation model execution time which is reported earlier.

Some general checks on model performance were built into the computer program to detect possible errors. Predictions of negative concentrations in the biogeochemical component were monitored but never detected. A lake-wide mass balance over the simulation determined if program errors or accumulated round-off led to loss or gain in phosphorus mass: the error was always below one percent.

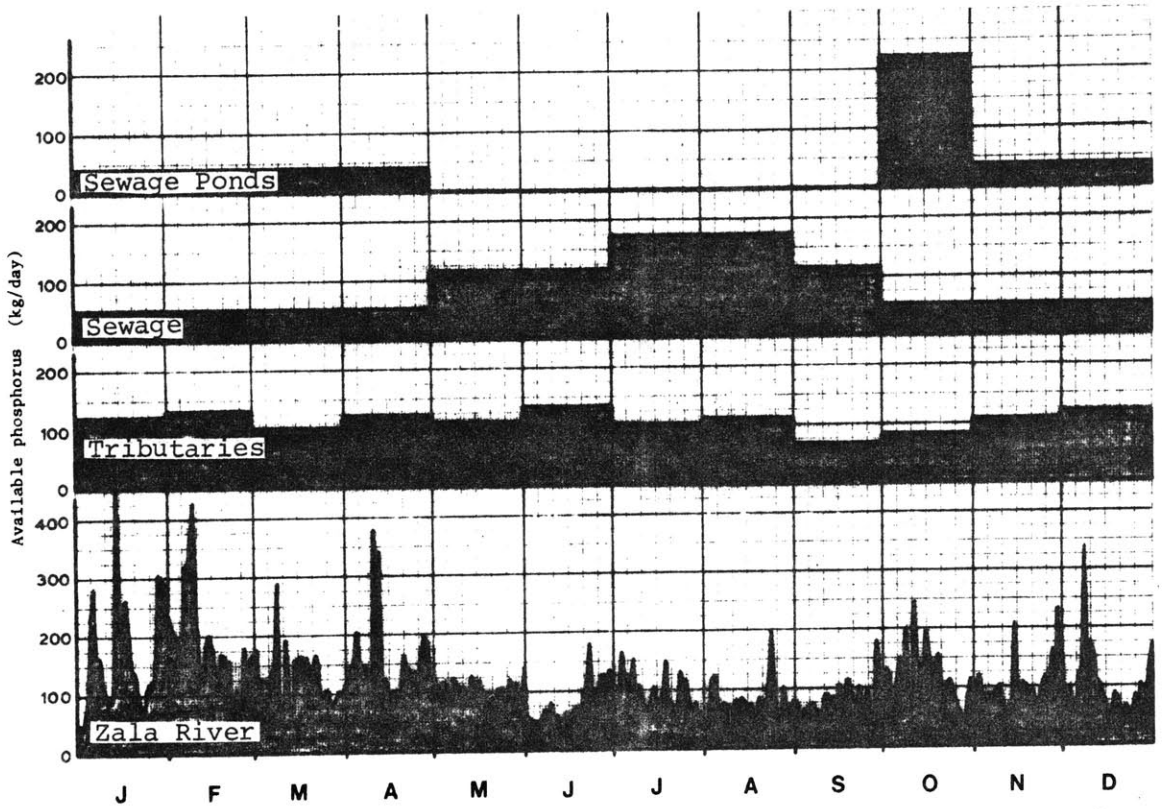

Figure 6.10

Temporal variation of available phosphorus load
for 1977 by source

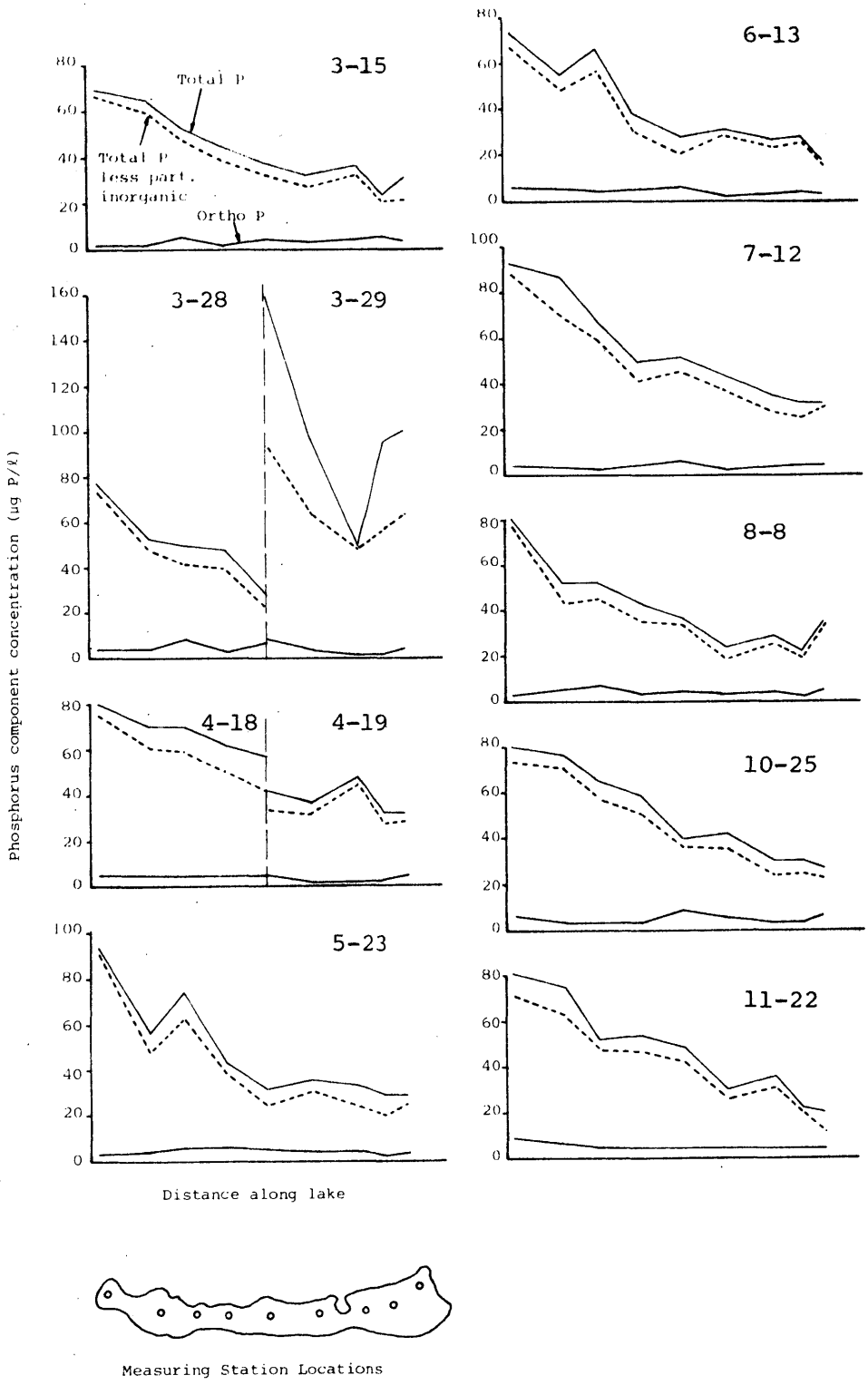

Figure 6.11

Measured phosphorus component concentrations for 1977

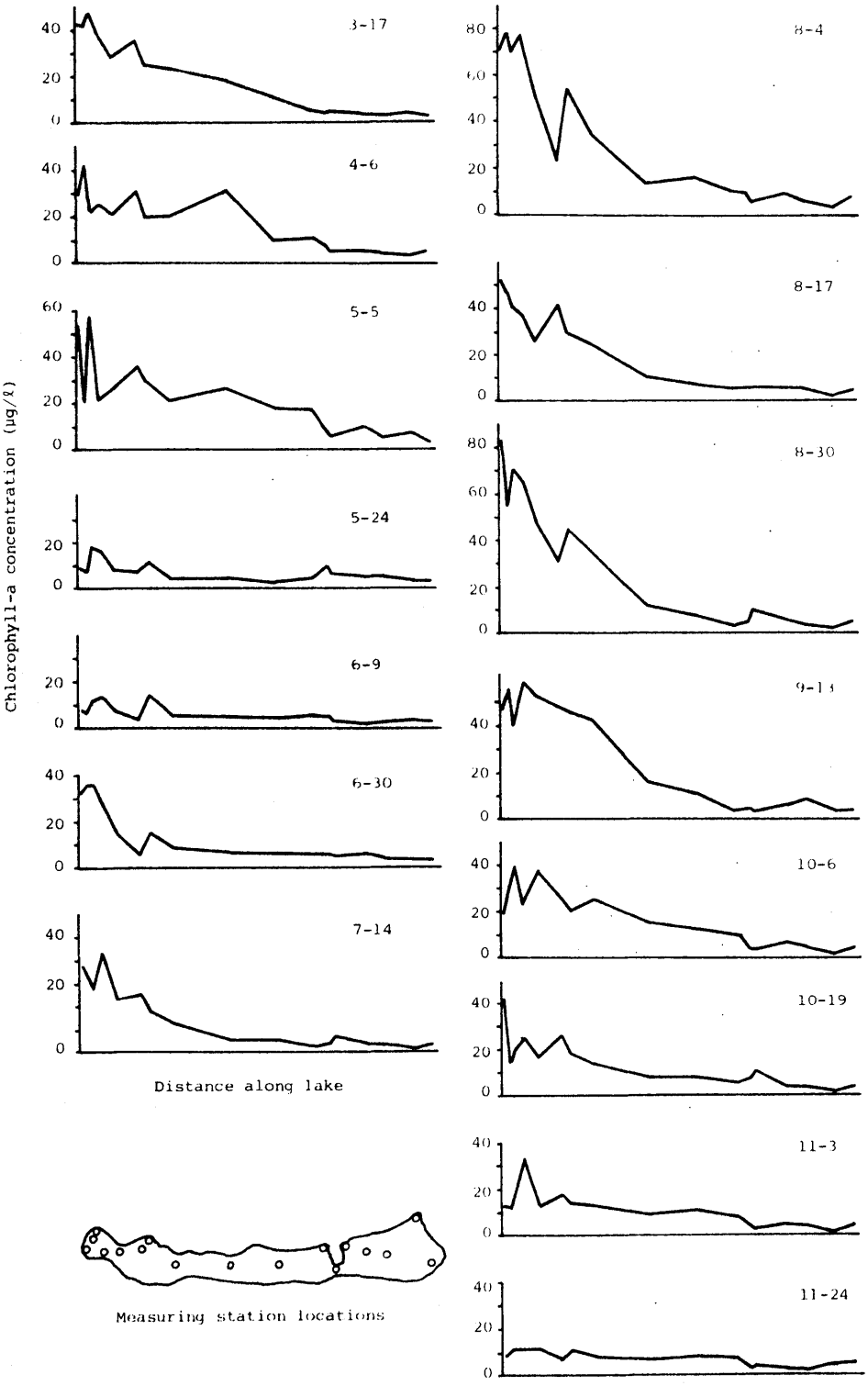

Figure 6.12

Measured chlorophyll-a concentrations for 1977

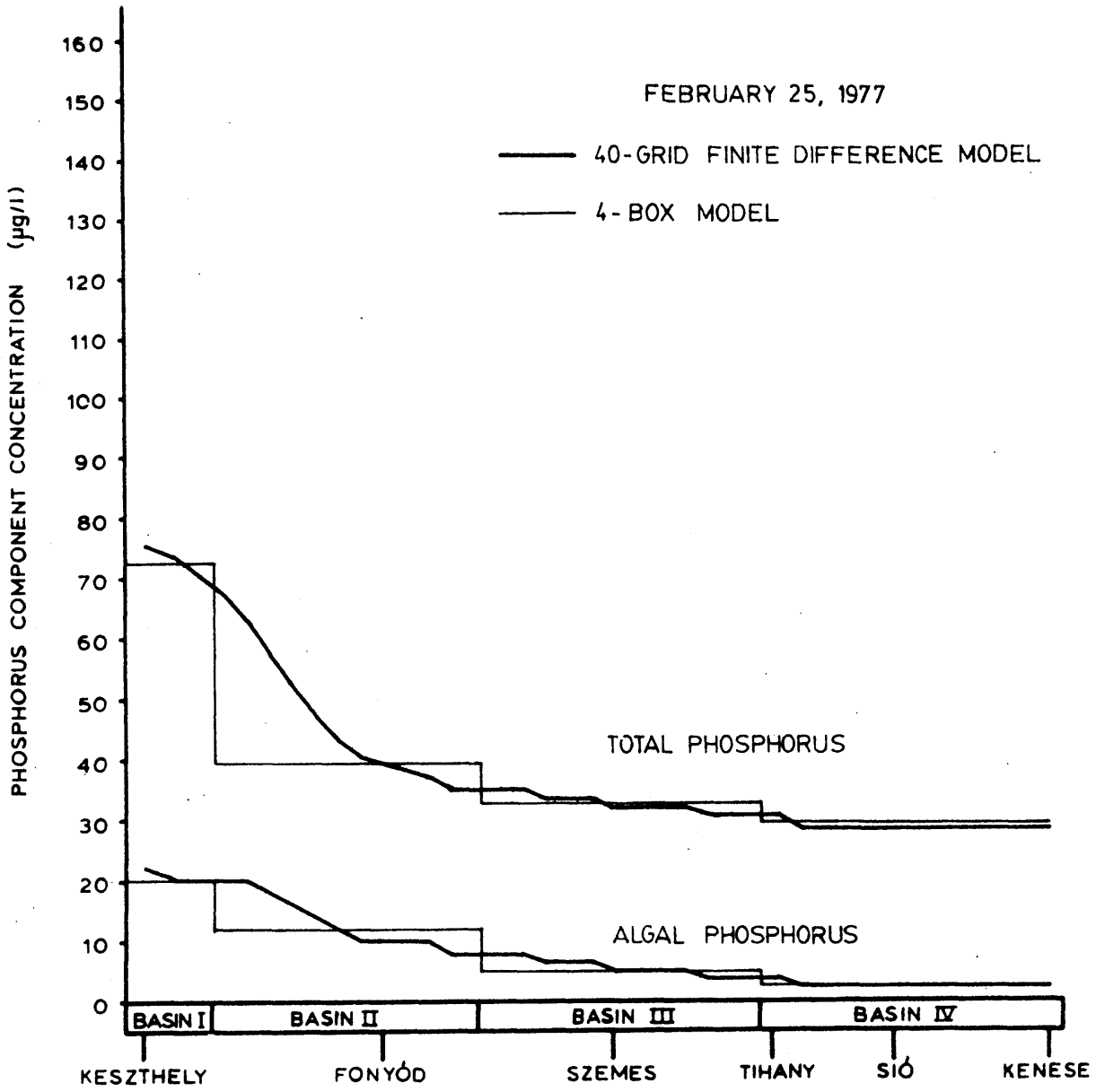

Figure 6.13

Initial conditions for Lake Balaton water quality simulations

6.4 Water Quality Simulation Results

The simulations performed were designed to compare the multiple-box and one-dimensional finite difference model approaches, to evaluate the importance of hydrodynamic influences on the model results, and to study the relative effects of different factors upon the model predictions. Since there is an enormous quantity of output produced by simulating four phosphorus components over many months in as many as forty grids, we must be selective in the material we show. Spatial concentration profiles of total and algal phosphorus are shown for August 4, a period of low flow when phytoplankton are near their peak summer concentration. The profile results illustrate the influence of dispersion and other hydrodynamic influences clearly, as well as show the differences in spatial detail between the forty-grid continuum model and the four-box model. In addition, time plots of phosphorus constituents and total phosphorus are shown for Keszthely Bay for selected simulations.

6.4.1 Results with the Forty-Grid Model

Hydrodynamic Influences

The influence of the hydrodynamic component upon the water quality predictions was evaluated in a series of runs in which the representation of the dispersion was varied. As our base case simulation for this and all subsequent comparisons, we will employ the simulation in which the dispersion coefficient is computed from the lateral velocity distribution in the method described in Section 5.5. The predicted August 4 profiles from this simulation are shown in Figure 6.14.

Also shown in Figure 6.14 are the simulation results from a run in which the only hydrodynamic information used is the monthly average hydrologic flow. This is equivalent to the plug flow reactor described in Chapter 2. These results show a very jagged profile in which each local peak corresponds to a tributary or sewage nutrient inflow. Without the influence of dispersive mixing, the inflowing phosphorus simply collects near the source. The effect is particularly striking at the lake's eastern end which is out of the main flow path between the Zala River and the Sió Canal. The large sewage discharge from the city of Balatonkenese accumulates in the end grid of the model to reach extreme levels.

The results of the run with only hydrologic flow are obviously unrealistic -- mixing will be an important influence on water quality and must be captured in the model. The contrast between the base case run with dispersion and the no dispersion run in Figure 6.14 clearly shows this influence. Although local concentration peaks occur -- most prominently near the Zala River source at Keszthely -- there is a distinct tendency for dispersion to smooth the profiles.

For comparison with the base case simulation, in which dispersion varies in both time and space, two simulations with fixed dispersion coefficients were run. The August 4 profiles, for fixed dispersion coefficients of 1 m^2/sec and 10 m^2/sec, are shown in Figure 6.15. The run with D = 1 m^2/sec shows fair agreement with the base case run employing

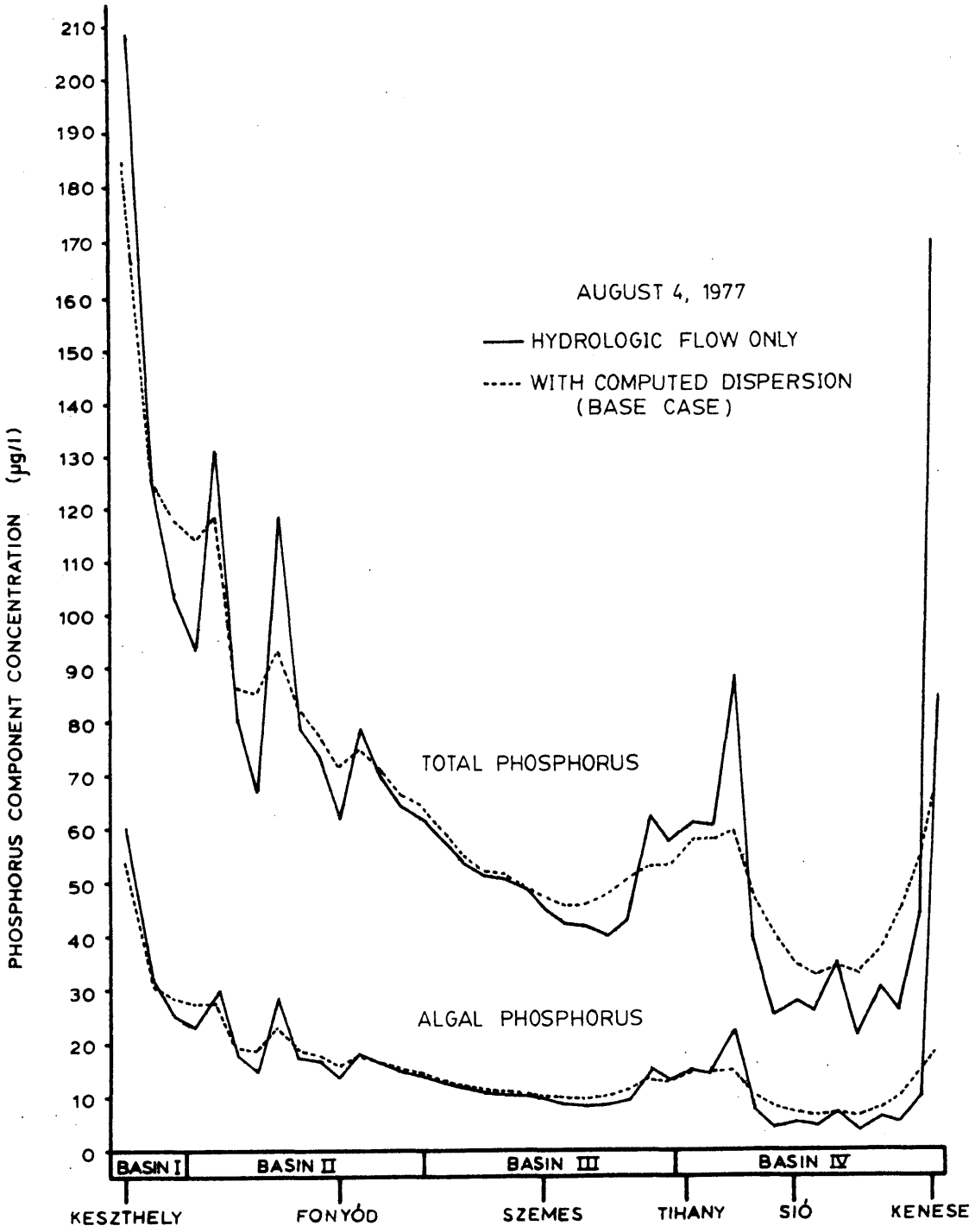

Figure 6.14

Predicted water quality profile for August 4, 1977
with and without effects of dispersion

the computed dispersion coefficient: the D = 1 run is perhaps too high at the lake's western end, too low in the eastern part, but overall the agreement is good. The simulation with D increased by an order of magnitude shows the importance of the dispersion coefficient to the model results. The higher dispersion smooths the predicted profile substantially, removing all local concentration peaks. The portion of the lake east of Tihany (Basin IV) is much more thoroughly mixed, virtually eliminating the concentration gradients seen in the base case simulation.

Figure 6.16 addresses the temporal character of the model predictions by comparing concentration histories for Keszthely Bay from various simulations. Significantly different predictions result according to the hydrodynamic component employed. The simulation employing only hydrologic flow (Figure 6.16a) gives results strongly dependent upon the monthly variation in mean flow. During the high flow spring months, the Zala River inflow is advected more strongly downstream into the lake, leading to a higher spring concentration peak than in the other simulations. A lower peak occurs during the low flow summer months. The constant dispersion (D = 1 m^2/s) simulation in Figure 6.16c is similar to the varying dispersion coefficient run (6.16b) except that the curves have been smoothed by the elimination of the temporal dispersion variation. The increased dispersion run with D = 10 m^2/s (Figure 6.16d) shows much lower concentrations than the other runs -- a consequence of dilution caused by mixing with lower concentration waters to the east. Too large a dispersion coefficient can thus lead to underprediction of the water quality problems in Keszthely Bay.

Influence of Reaction and Loading

The predicted water quality is a consequence of the competing influences of hydrodynamic advection and mixing, biogeochemical reaction, and the distribution of loading in space and time. We can see some of the effect of loading and reaction in model simulations from which they have been eliminated. For example, in Figure 6.17 we contrast concentration predictions on August 4 using the varying dispersion coefficient model with and without the biogeochemical component. The simulation without biogeochemical reaction treats the phosphorus components as conservative tracers subject to the same initial conditions and the same loadings as the reactive phosphorus components. Although the absence of reaction leads to large differences in algal and total phosphorus concentration at Keszthely, the differences throughout the lake are not as large as we would have anticipated. In fact, the discrepancies are generally of a similar magnitude to those due to the different dispersion hypotheses shown in Figure 6.15. A surprising conclusion one may draw from the results of Figure 6.17 is that there is a relatively narrow band of variation possible in model results due to modification of the biogeochemical component. Hence, calibration of the model by modifying reaction rate constants cannot be used as the sole control on model performance: the influence of the hydrodynamic component cannot be neglected, as it has in many biogeochemical models, if a correct calibration is to be achieved.

Of considerably greater impact is the elimination of all nutrient loads, as shown in Figure 6.18. Again, the base case run with a varying

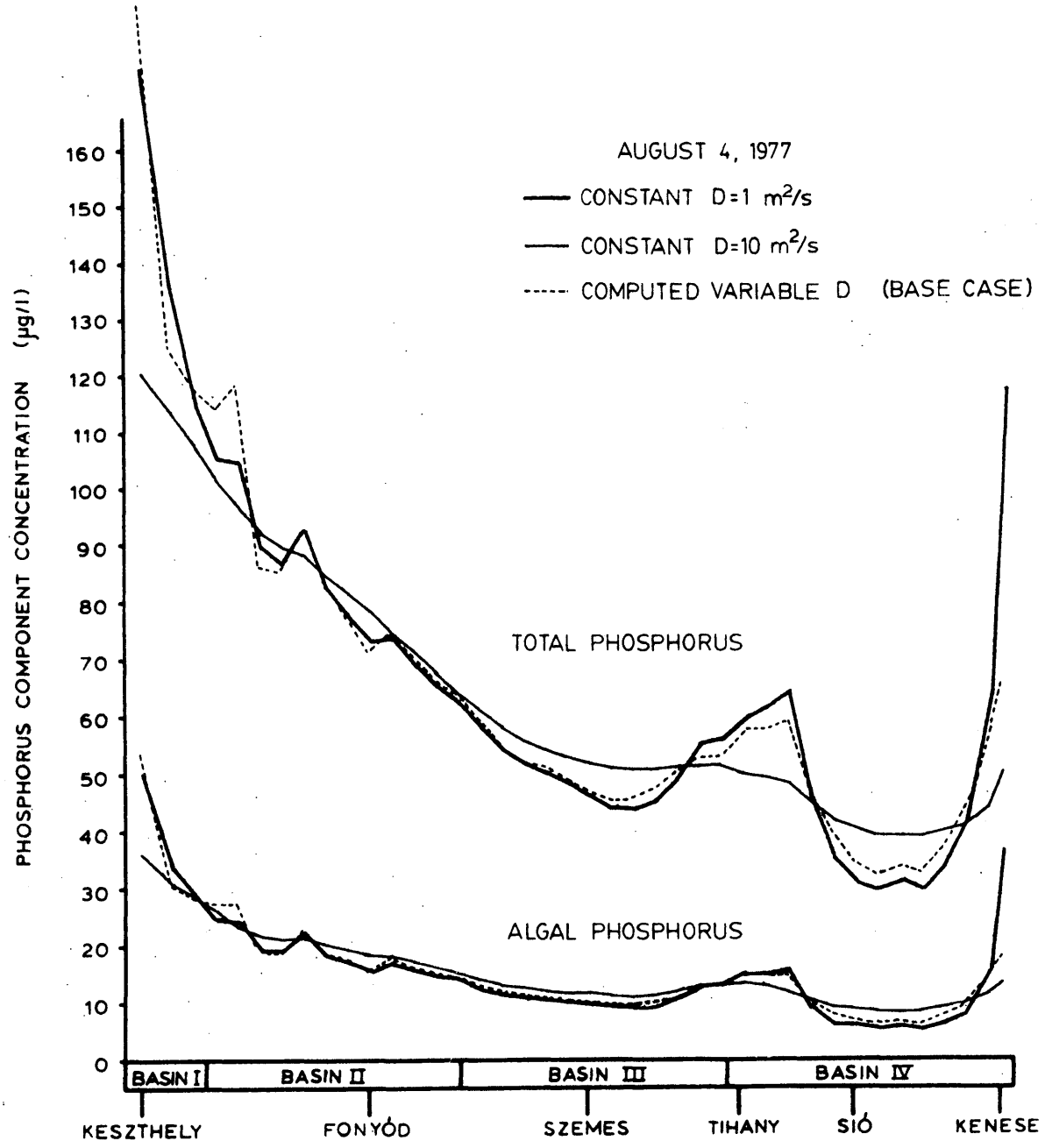

Figure 6.15

Predicted water quality profile for August 4, 1977
with fixed and varying dispersion coefficients

Key: 1 Total algal phosphorus
2 Detrital phosphorus
3 Dissolved inorganic phosphorus
4 Total phosphorus

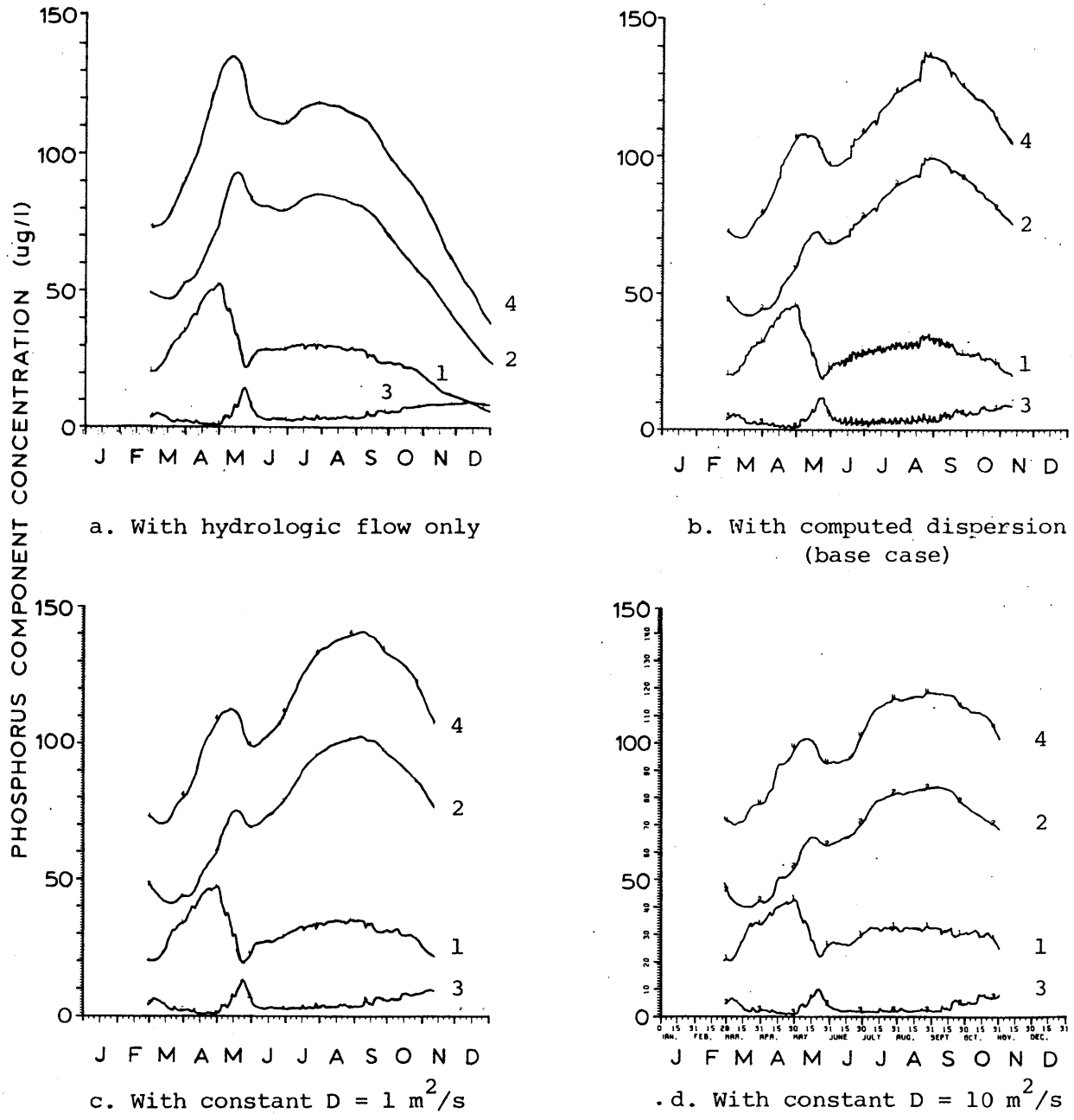

Figure 6.16

Predicted phosphorus concentrations versus time for Keszthely Bay

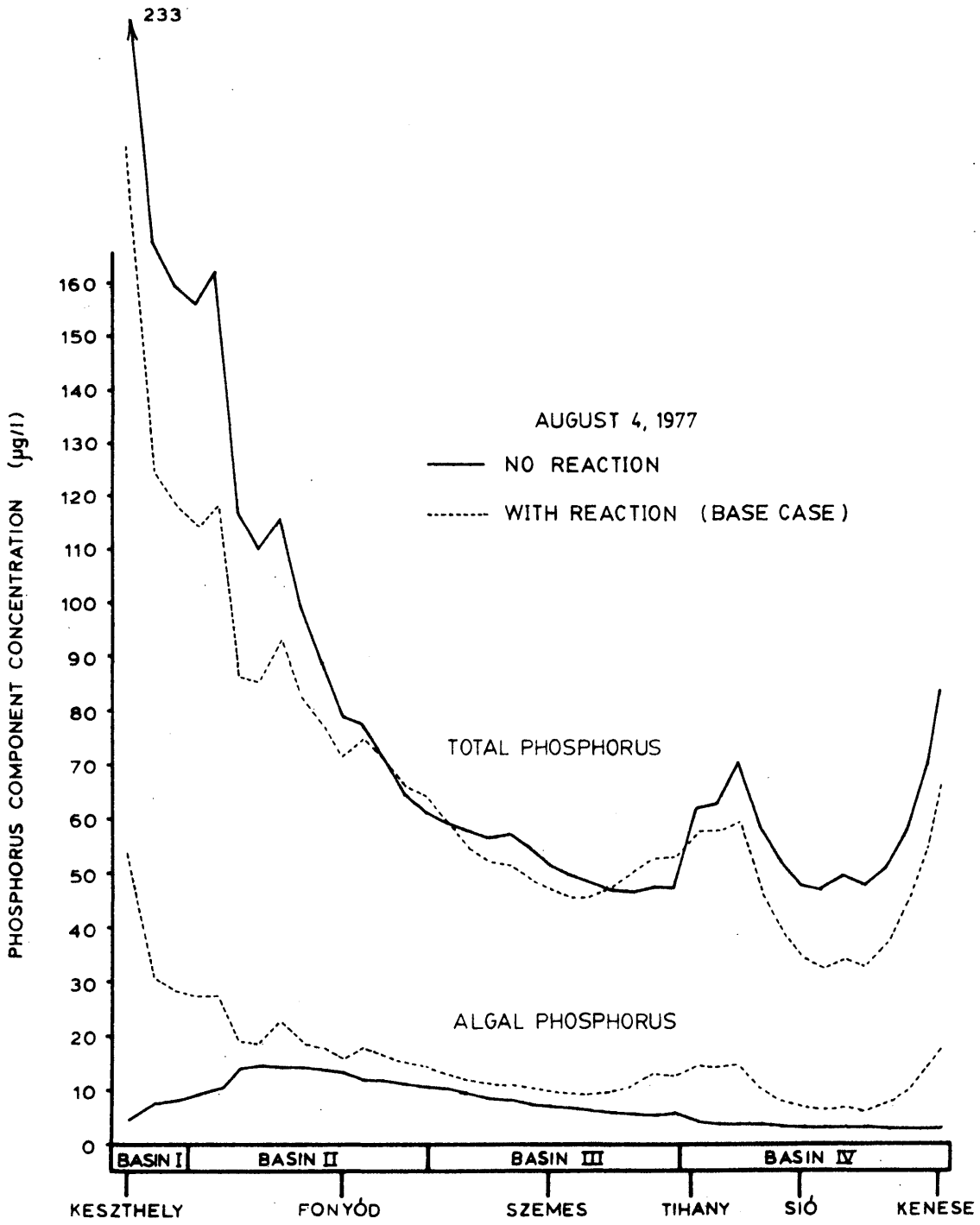

Figure 6.17

Predicted water quality profile for August 4, 1977
with and without biogeochemical reaction

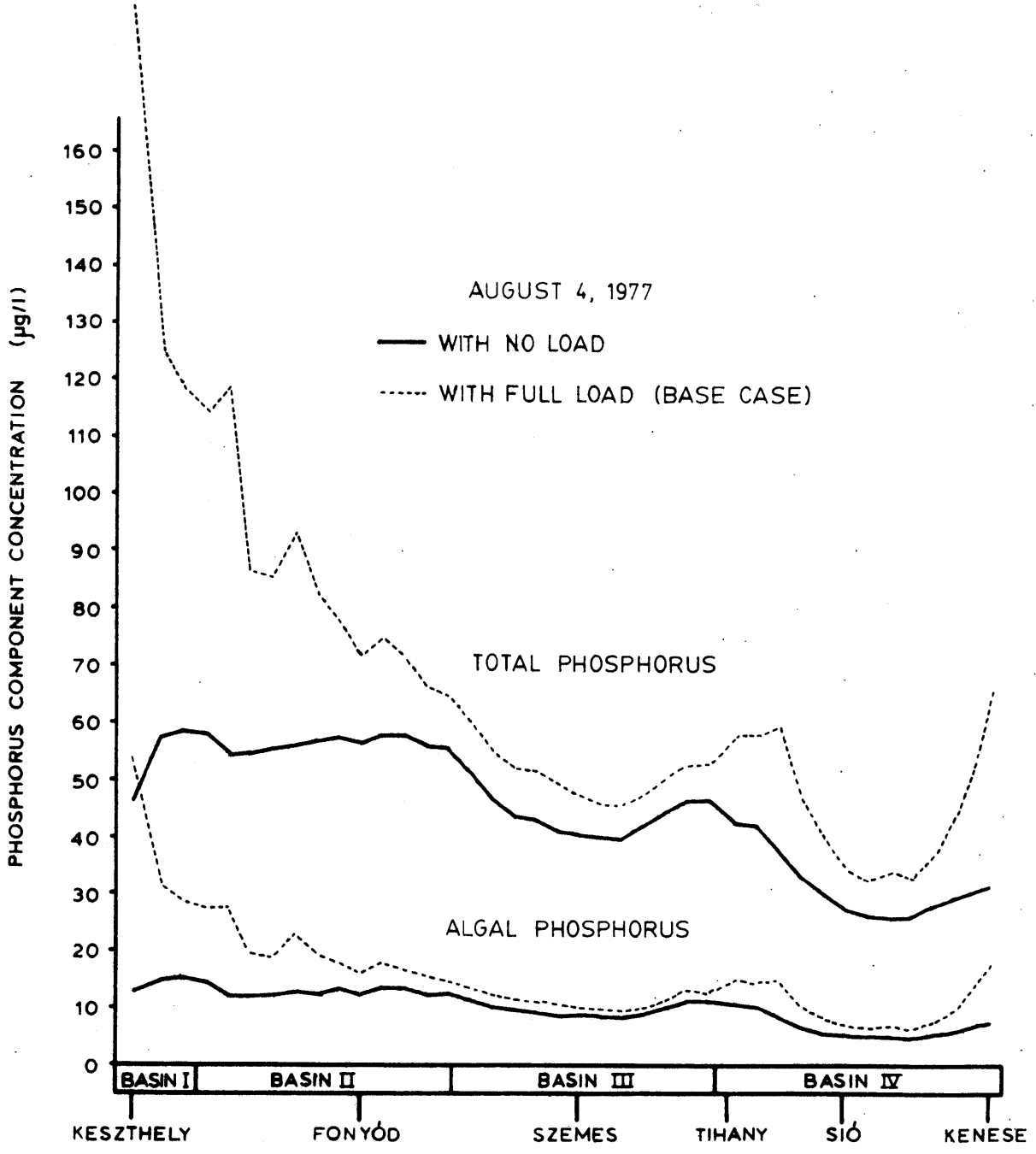

Figure 6.18

Predicted water quality profile for August 4, 1977
with and without phosphorus loading

dispersion coefficient is included for comparison. The run without loading employs the varying dispersion coefficient as well, so the simulations are identical except for the inclusion of nutrient loads. The cessation of loading can be seen to have had a great impact on the lake's water quality in just the few months between the February 25 starting date and the August 4 predictions in Figure 6.18. Almost all of the dominant west-east concentration gradient has disappeared and there remains only a residual indication of the initial conditions. The results without the nutrient loads make clear that the observed longitudinal gradients in phosphorus concentration (Figure 4.7) are sustained almost entirely by the spatial distribution of the loading. Hydrodynamic influences may affect the profile significantly at local points, but on a lake-wide basis they are dominated by the loading distribution.

Finally, in Figure 6.19, we consider the situation in which the Zala River nutrient load has been cut in half. Reduction of the Zala River load is a prime water quality management strategy for the lake (van Straten et al., 1979), so this simulation is similar to those which might employ the model in a predictive mode. Comparison with the base case simulation in Figure 6.19 shows that, other than in Keszthely Bay, the elimination of one-half the Zala load causes little change in the predicted profile. Changes beyond Keszthely Bay are insignificant since neither advection nor mixing is sufficiently strong to make the loading changes felt beyond the immediate area of the discharge point within the five and one-half months simulated. Comparison of the half-load simulation with the full load runs based on the different dispersion hypotheses is also instructive. The half-load run with the computed dispersion coefficient predicts a concentration in Keszthely Bay very similar to that predicted with a full load using the increased dispersion coefficient, D = 10 (Figure 6.15). An implication of this result is that mixing can be as effective as loading reduction in ameliorating Keszthely Bay's problems. A more troubling implication is that improper mixing in a water quality model can completely mask the predicted effects of water quality controls.

Conclusions

The water quality model simulation results support the following conclusions:

- The use of the dispersion coefficient computed from the lateral velocity profile leads to predicted behavior much alike that observed in Lake Balaton.

- A constant dispersion coefficient of D = 1 m^2/sec is a fair approximation to the dynamically varying dispersion coefficient.

- The hydrodynamic component holds comparable influence upon the model results as the biogeochemical component, and hence both components will influence the calibration of water quality models.

- The primary determinant of the lake-wide phosphorus distribution is the spatial distribution of the nutrient sources. The local character

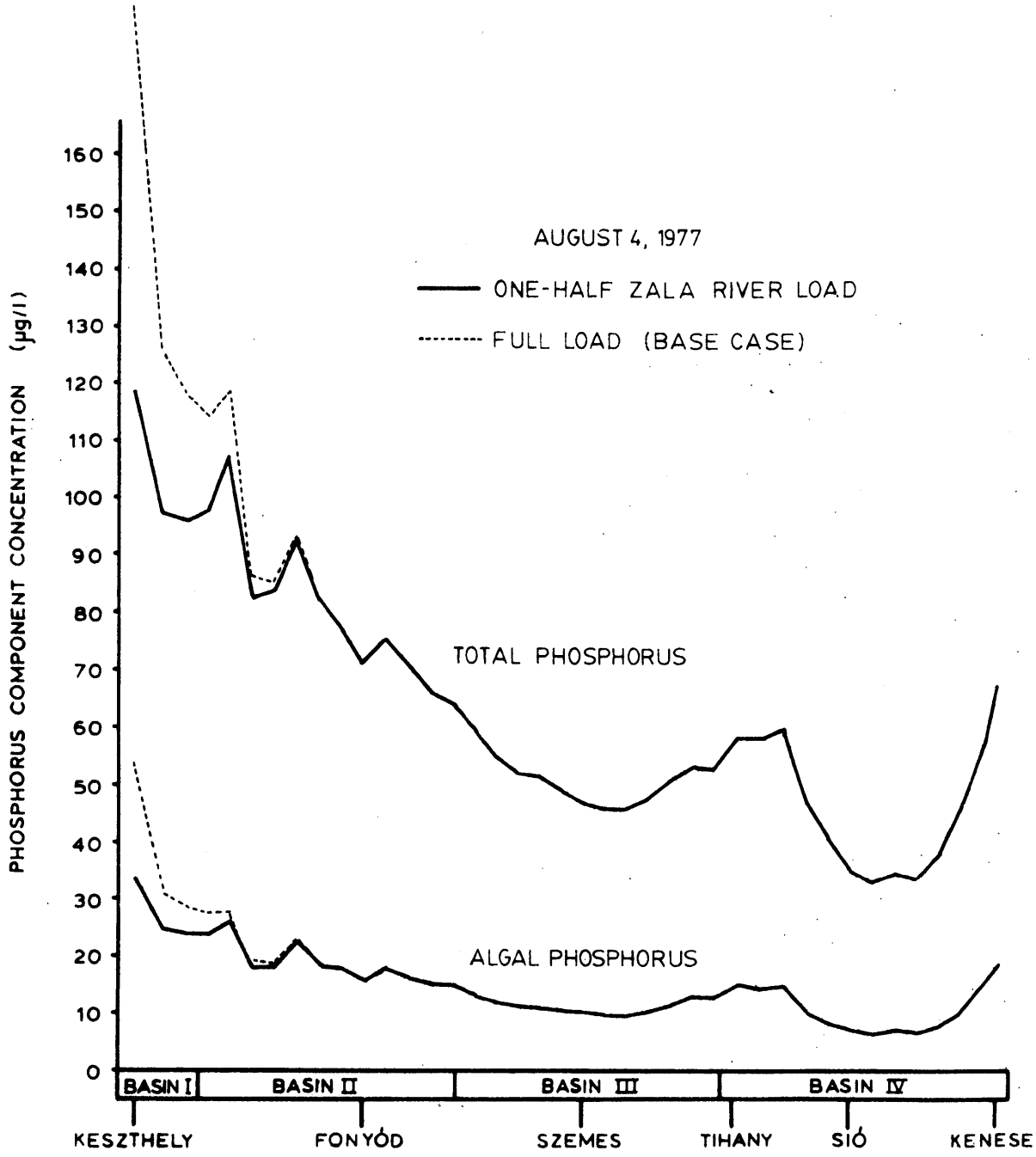

Figure 6.19

Predicted water quality profile for August 4, 1977
with reduced and full Zala River load

of the distribution, as well as the response to loading changes, are strongly affected by hydrodynamic influences.

- A reduction in loading, as would be likely in prognostic simulations, can be masked if incorrect hydrodynamics are employed in the model.

6.4.2 Results with the Four-Box Model

Comparison with the Forty-Grid Model

The discussion of multiple-box models in Chapter 2 makes clear that there are several impediments to their use as successful models of lake water quality. The model hydrodynamics are clouded by the hidden influence of implicit dispersion, to the point that mixing becomes a parameter of the model to be determined by calibration along with a multitude of biogeochemical model constants. In this section, we will use the base case forty-grid finite difference model as a comparison standard against which to evaluate the four-box model predictions, with particular attention to the problems in capturing hydrodynamic influences.

Let us begin with a preliminary analysis based on the conceptual models of Section 2.5.4. From Equation 2.9, we can compute the Peclet Number of the forty-grid model as an analog of the dispersed flow reactor. In applying Equation 2.9, we employ the following parameter values: Q = 10.4 m^3/s (annual average hydrologic flow), L = 65 km (Keszthely to Siófok distance), A = 24,000 m^2 (average over the lake) and D = 1 m^2/s (determined in Section 6.4.1). The computed Peclet Number is roughly 30, implying rather small longitudinal mixing. From Figures 2.10 and 2.11, the tanks-in-series model (with no exchange flow) with roughly equivalent mixing should consist of seventeen or eighteen tanks. The use of only four boxes -- in fact, of essentially three boxes (see Figure 2.11) -- in the Balaton model necessarily implies considerably greater mixing. Using Equation 2.14, a three-box model is equivalent to a Peclet Number of 4.75, or using the parameters above, a dispersion coefficient of about 7 m^2/s. If we also add the influence of the exchange flow employed by van Straten (an average of 23 m^3/s between boxes 2, 3 and 4) the Peclet Number from Equations 2.15 and 2.16 is about 1.1. For this situation, the equivalent dispersion is about 30 m^2/s. Thus, both with and without exchange flow, the four-box Lake Balaton model includes much greater dispersion than determined in the forty-grid model.

In Figure 6.20 we compare four-box model predictions with the forty-grid base case simulation. The loss of spatial detail in the four-box model is, of course, immediately obvious: local concentration peaks cannot be predicted and only a rough outline of the concentration profile along the lake is possible. Also evident are considerably lower predictions for Keszthely Bay as a result of the greater mixing in the four-box model. Addition of exchange flows between the boxes only decreases the Keszthely Bay concentrations further. The predictions at Keszthely are particularly important, since this is the location of greatest water quality problems in Balaton.

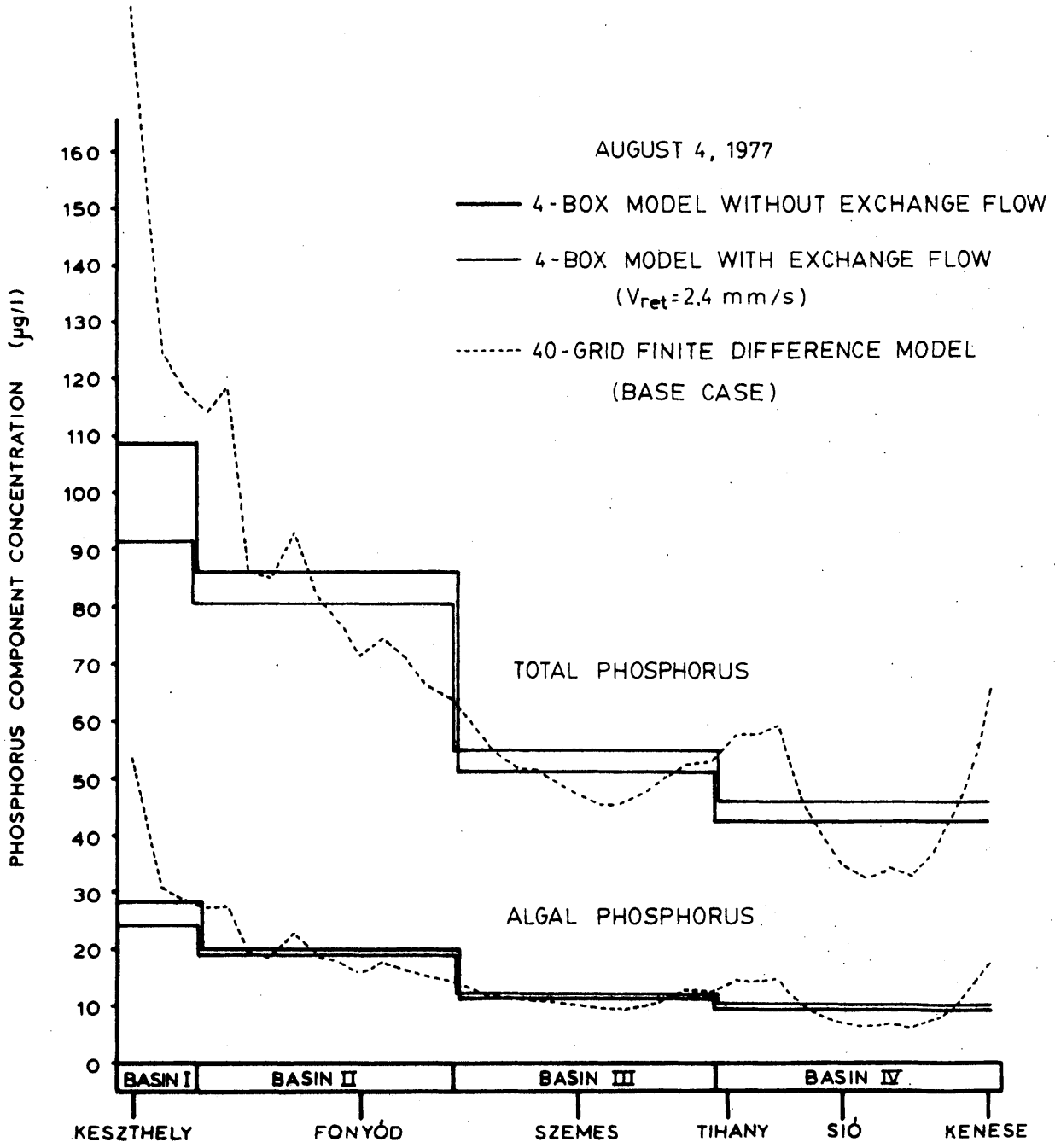

Figure 6.20

Predicted water quality profile for August 4, 1977
from four-box model and finite difference model

In time, the phosphorus constituent concentrations (Figure 6.21) behave somewhat similarly to those seen in the forty-grid model run with only hydrologic flow (Figure 6.16a). Compared with the base case simulation (Figure 6.16b), total phosphorus concentrations are higher in the spring but lower in summer, with an overall tendency to be low. Algal phosphorus concentration predictions are closer between the two models, although the summer peak is lower in the four-box results.

Returning to Figure 6.20, comparison of the four-box model without exchange flows with the base case reveals a passable ability by the four-box model to capture the lake-wide longitudinal gradients. The inclusion of a small box for Keszthely Bay is probably particularly fortunate in this respect. Were it combined with the second box, the predictions in Basins II through IV would likely change little, but concentrations in Keszthely Bay would probably be underpredicted.

Predictive Ability

In Figure 6.22 we show results of a four-box model simulation in which the Zala River nutrient load is reduced by one-half. This is the same simulation as reported above for the forty-grid model and we have included its predictions, shown originally in Figure 6.19, in Figure 6.22 as well. This simulation may be viewed as a test of the model used in a predictive mode.

The relative comparison of four-box and forty-grid results differs little from full-load to half-load. In the half-load runs, concentrations are again underpredicted for total phosphorus and, to a lesser degree, for algal phosphorus. The loss of spatial detail remains considerable and this becomes increasingly important as the Zala River load decreases. As seen in the forty-grid predictions in Figure 6.22, the local peaks immediately east of Keszthely Bay assume greater significance as the Keszthely Bay water quality improves. Szigliget Bay is already considered an area of relatively low water quality and predictions of its response to loading changes would be valuable. The four-box model cannot supply this information to any detail however. Particularly for local water quality problems outside of Keszthely Bay, the four-box model is ineffective.

Conclusions

Evaluation of the results from the four-box model leads to the following conclusions:

- Predictions by the four-box model are low in Keszthely Bay and are unable to show spatial detail in the phosphorus concentration distribution. The box model predictions are only able to capture the broadest trends in the lake-wide concentration distribution.

- The four-box model includes far greater mixing than that determined by the calculation of dispersion coefficients for the forty-grid model. This is due to the dispersion implicit in the box formulation. Additional dispersion via an exchange flow should certainly not be included.

Key: 1 Total algal phosphorus
2 Detrital phosphorus
3 Dissolved inorganic phosphorus
4 Total phosphorus

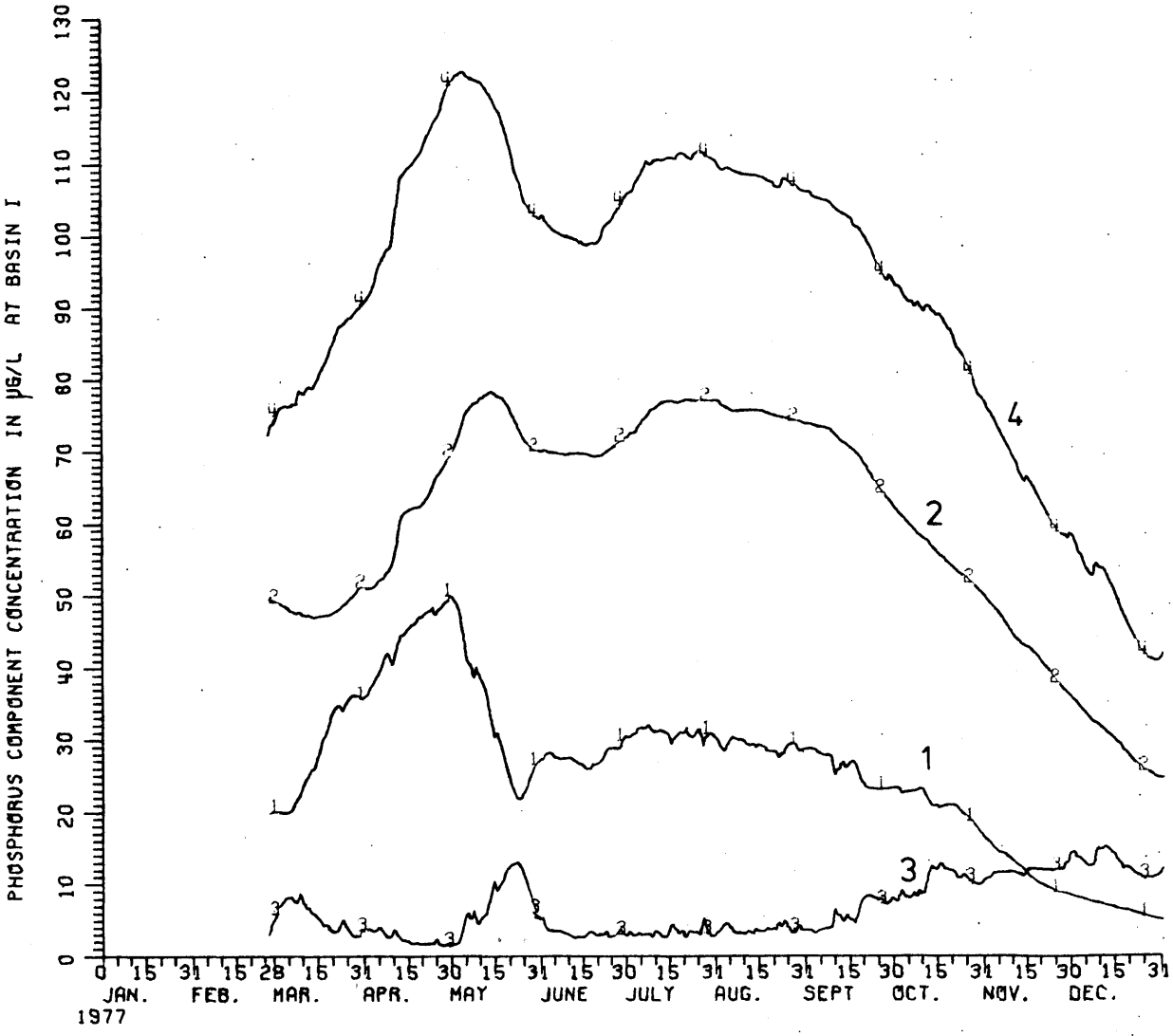

Figure 6.21

Predicted phosphorus concentrations versus time
for Keszthely Bay from four-box model

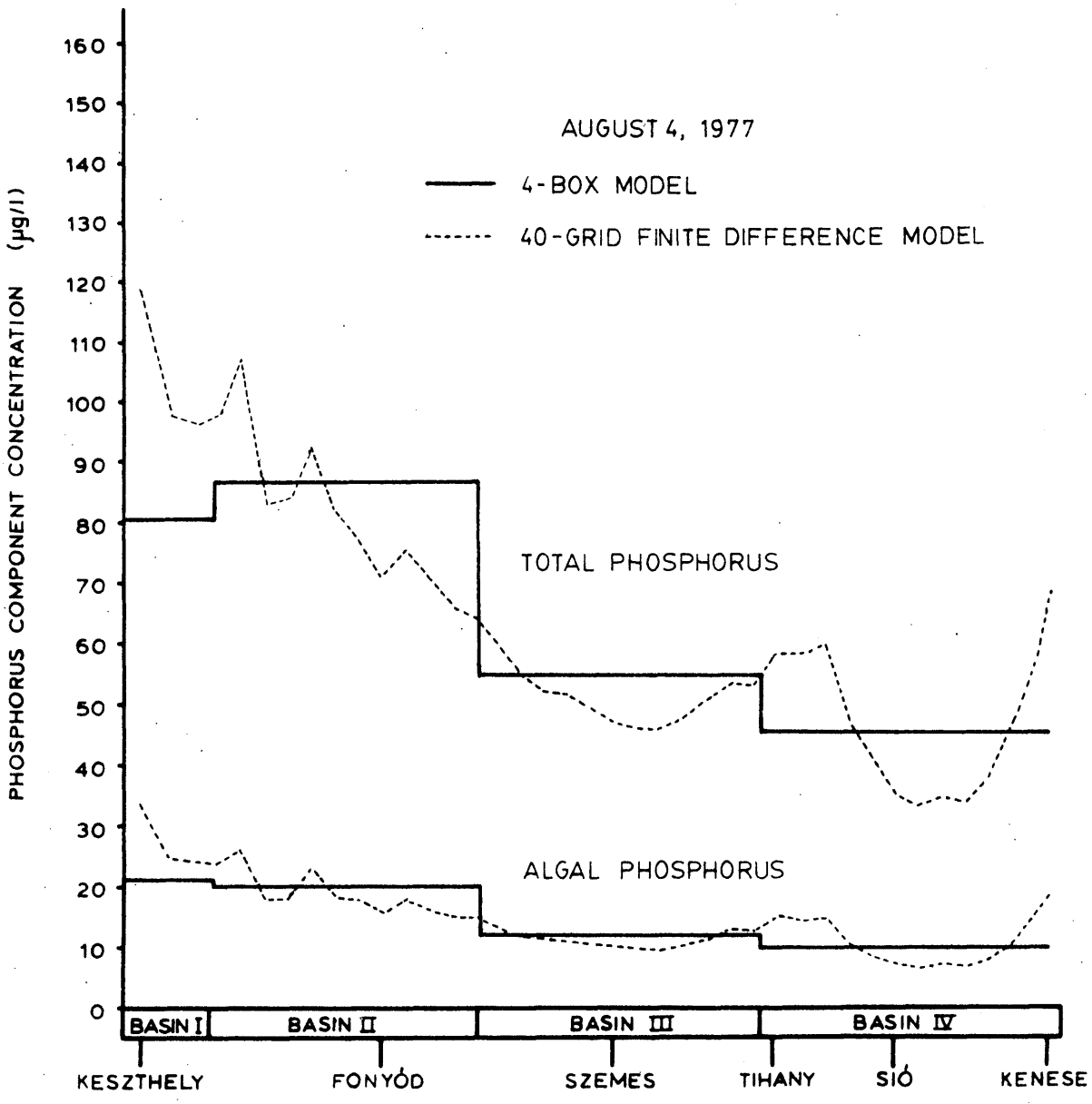

Figure 6.22

Predicted water quality profile for August 4, 1977
with reduced Zala River load from four-box model
and finite difference model

- The loss of spatial detail in the four-box model reduces its effectiveness as a predictive tool. Particularly if local problems are of concern, the more detailed finite difference model should be used.

6.4.3 Summary of Results

The model evaluations show the results to be significantly sensitive to the model formulation and to the model hydrodynamics. The results most similar in character to observations in the lake are produced by the forty-grid model with the dispersion coefficient computed as a function of time and space by the hydrodynamic component. The four-box model is able to show only a rough outline of the concentration distribution in the lake, and its predictions tend to be low.

The simulations have also shown that the hydrodynamic component can influence the model results on a par with biogeochemical influences. Thus, calibration of the biogeochemical model component can be invalidated by improper or incorrect hydrodynamics. This can be a particular problem with box models where artificial mixing is an implicit consequence of the model formulation.

7 CONCLUSIONS AND RECOMMENDATIONS

7.1 Conclusions on the Use of Lake Water Quality Models

In this report we have offered the proposition that lake water quality modeling can be improved if the influence of lake hydrodynamics is properly incorporated in the model. This proposition is a challenge to the school of thought that biogeochemistry alone dominates lake water quality and that a state-of-the-art water quality model can employ a highly complex and sophisticated biogeochemical model in the framework of a multiple-box formulation.

We have supported this idea in a theoretical analysis of the properties of the tanks-in-series reactor, equivalent to the multiple-box model. That analysis shows that multiple-box models carry within their formulation a large implicit dispersion, controllable only if the fundamental character of the model is changed by varying the number of boxes. Further mixing can be added to the multiple-box models by incorporating an equal but opposite exchange flow between the boxes. However, this exchange flow cannot be determined directly from observation or simulation of the lake hydrodynamics. Rather, it is a model-dependent parameter which will vary as the number of boxes or the box sizes vary. It must thus be determined by calibration, compounding the already difficult problem of biogeochemical model calibration. In short, use of box models is confounded by their confusion of hydrodynamics and biogeochemistry.

In contrast to the multiple-box model, there are higher dimensional finite difference models which seek to closely approximate the continuum solution of the mass conservation equations. In these models artificial dispersion is reduced to an insignificant level, thus allowing the explicit specification of the dispersion coefficient, D, as the determinant of the mixing properties of the model. A one-dimensional model is developed in this thesis for application to Lake Balaton in Hungary.

Application of the developed model and comparison with results from a four-box model of Lake Balaton further supports our proposition. The simulations illustrate that hydrodynamic mixing can significantly affect the model predictions, to a degree comparable to that of the biogeochemical model. Comparison of available field data with model results shows that the finite difference model employing a dispersion coefficient computed from simulated lake hydrodynamics is best able to capture the character of the observed water quality in the lake. The box model is found to underpredict the concentration of phosphorus as a consequence of too large an implicit dispersion and a lack of spatial detail.

Our conclusion is unequivocal: the multiple-box model is in fact a "black-box" model, based largely on empiricism rather than physics. In contrast, the finite difference model permits a rational and direct determination of mixing in the model, correctly isolating the influence of hydrodynamics from biogeochemistry. As a consequence, this model can be more soundly calibrated and more effectively used as a predictive tool than the box model. In sum, the directness and clarity of the finite dif-

ference model approach recommends its use over the box model formulation.

In the remainder of this chapter, we expand upon our experience to suggest a rational procedure for the development of linked hydrodynamic and biogeochemical water quality models. We go on to summarize the major findings of our work, with special attention to our model development and what it has revealed about the character of Lake Balaton. Finally, we close with recommendations for future research.

7.2 Recommendations for Design of Lake Water Quality Models

7.2.1 Introduction

In this section we will review the assumptions and structure of the Lake Balaton water quality model as an example of rational model design. In a sense, this will be a repetition of the process described in Section 5.1, but with new insight gained from the results of our work. Further, the implications of the analysis as a general process for lake water quality model design will be discussed.

Our analysis of the model structure and assumptions will be organized around a length and time scale diagram, as used previously in Chapter 5. Our procedure will be to gather as exhaustively as possible the various length and time scales which appear in the model. The majority of these are explicit in the model formulation and can be determined directly from the model parameters. Others are implicit in our modeling decisions and will be more subtle in their influence -- it is these length and time scales which we particularly wish to uncover and scrutinize. For all of these length and time scales, we will seek as accurate quantification as realistic, to refine the approximate definitions made in Section 5.1.

7.2.2 Detailed Length and Time Scale Analysis

Physical Processes

The physical processes with the most impact on lake water quality are those associated with the advective and dispersive terms of the equations of motion. Long-term advection may be characterized by the hydraulic residence times, given by Baranyi (1973a) as 14 months, 4 years, 6 years and 9 years for the four Balaton basins defined in Chapter 4. For the entire lake, a residence time of about 5 years may be computed from data in van Straten et al. (1979). This last residence time may be viewed as the endpoint of a continuous relation between length and time defined by the hydrologic through-flow. Using the long-term hydrologic flow and average cross-sectional area to find an average through-flow velocity, U, we define the linear length-time relation $x = Ut$ indicated as hydrologic flow in Figure 7.1.

Mixing times may be computed to characterize dispersion. The mean lateral mixing time can be estimated as the average lake half-width, 4 km, divided by a characteristic transverse velocity, roughly 3 cm/sec from our model results. This yields about one and one-half days as the mean lateral mixing time, shown in Figure 7.1 as one point in the continuum of mixing time-transverse distance relations. The vertical mixing time is given by H^2/A_V, equal to about two hours using parameter values from Table 5.2. Again, a continuous relation between length and time is shown in Figure 7.1.

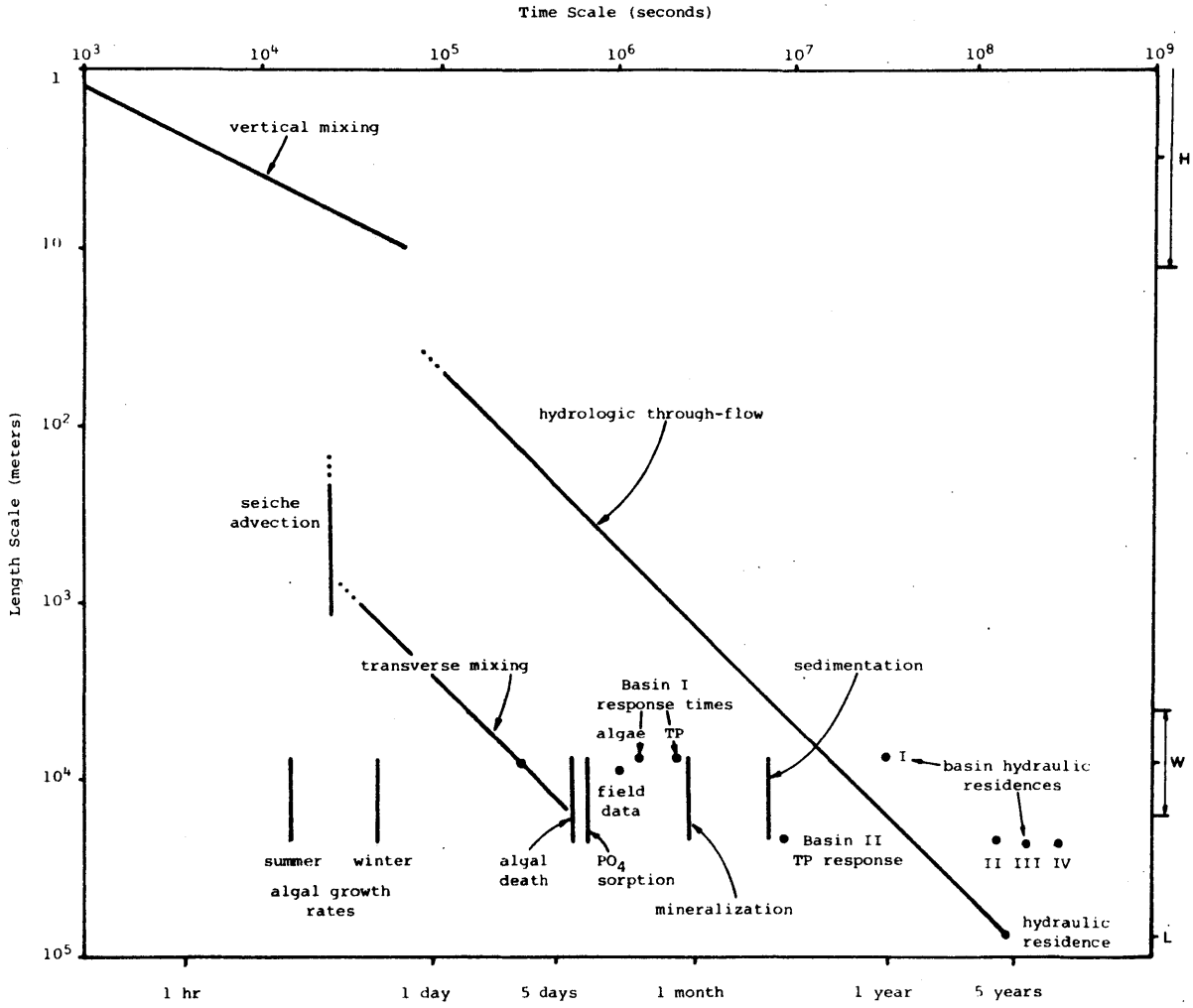

Figure 7.1

Detailed length and time scale analysis for linked water quality model of Lake Balaton

Other physical length and time scales will also influence water quality. Most obvious is the uni-nodal longitudinal seiche period, 8.5 hours in the circulation model simulations. This is also the averaging period for the dispersion coefficient in the method of Holley et al. (1970). For water quality, the length scale associated with the seiche period is the seiche excursion, which can be seen in Section 6.2 to be on the order of a few hundred meters.

The paragraphs above have dealt primarily with the time scales of the physical processes. The length scales are, however, quite obvious as the length, width and depth of the lake and the lengths of the four lake basins. The length and time scales are used together to plot the domains of the physical processes in Figure 7.1.

Biological Processes

To define the time scales of the biological processes, we can draw upon the various model rate constants given in Table 5.3, taking the inverse of a rate constant as the time scale of the process. From the rate constants defined in Table 5.3, we can determine that the shortest growth time for summer algae is roughly 0.2 day and for winter algae, 0.5 day. (Under the typically less than ideal conditions algae experience in the lake, maximum growth rates will not be achieved and growth times will be longer.) The mortality rate determines a life span on the order of 8 days for both algal varieties. Mineralization responds on a scale of about 30 days at 25 C, while sorption/desorption requires only 6 days. Finally, settling of detritus proceeds very slowly, requiring time periods of roughly eighty days.

Length scales for the biological processes are less obviously defined. Although the individual cells clearly experience very small distances, homogeneity of populations and environmental conditions is reasonably expected over much wider areas. For lack of better information, we have assumed length scales on the order of the lake width to be representative. The biological processes are also included in Figure 7.1.

Field Data

The dependency of the modeling process upon availability of field data was stressed in Section 5.1. The frequency of sampling in both time and space suggest time and length scales to be considered in our analysis. For the phosphorus components, measurements are made every other week at nine stations along the 75 km length of the lake. These time and length scales for field data are so indicated in Figure 7.1.

Modeling Decisions

In the preliminary model design process, described in Section 5.1, a less detailed space and time scale analysis led us to a general outline of the model characteristics. Can we not determine specific aspects of the model structure and linkage using the detailed information of Figure 7.1? To a reasonable degree, we can.

We go into this analysis with some preconceptions of various aspects of the model, and we will examine these first. Implicit in the selection of a one-dimensional model is the assumption that mixing in the vertical and lateral directions will be sufficiently rapid to allow variations in those directions to be neglected. There is clearly no difficulty posed by the vertical mixing scale for this assumption. For lateral mixing, the problems are minor. At its very fastest rate, algal growth will proceed somewhat faster than lateral mixing, thus leading to lateral concentration variations. The discrepancy between growth and mixing is small however, particularly since light, temperature and nutrient limitations will prevent the fastest growth rates from being achieved on all but rare occasions. Therefore, this is an occasional and not terribly serious mismatch in time scales.

The lateral mixing time also exceeds the longitudinal seiche period. Thus, transport by the seiche could interact with, for example, shoreline nutrient discharges to violate the assumed one-dimensionality. This might happen if the seiche acted to carry away an influent nutrient discharge as a nearshore plume before it could be mixed laterally. The short length scale of the seiche excursion shows this will not be a problem, however, except very locally. The decision to average out seiche advective transport is thus sound.

One of the most pertinent modeling decisions is the choice of the spatial increment, Δx. The obvious suggestion for Δx is that used in the linked hydrodynamic circulation model, 1900 meters. For that value of Δx to be consistent in the water quality model depends to a great degree upon the time scales it implies for longitudinal advection and mixing. Advection due to hydrologic through-flow will traverse 1900 meters in about 4×10^6 seconds -- well above the time necessary for cross-sectional mixing, and thus within the limits posed by the one-dimensional assumption. Time scales for longitudinal mixing may also be determined from the selected grid size if a dispersion coefficient, D, is known. To not violate the one-dimensional assumption, the longitudinal mixing time, equal to $(\Delta x)^2/D$, should not be significantly less than the transverse mixing time. Using the average transverse mixing time as a guide, a choice of Δx = 1900 meters is consistent if the dispersion coefficient is less than about 22 m^2/s. As we have seen in Chapter 6, dispersion in Lake Balaton is generally much lower than this, so that the time for longitudinal mixing will safely exceed that for lateral mixing. A final matter concerning the choice of Δx is its magnitude relative to the seiche excursion. The decision to average out seiche advection implicitly defines the excursion as the minimum length scale realistic for the model. The typical seiche excursion is smaller than 1900 meters by about five times, so again this particular choice of Δx is realistic.

Time scales must also be chosen for the 1-D water quality model, although we have considerably less latitude here than we had in selecting the space scale. Having fixed Δx and solution procedures, accuracy and stability characteristics of the numerical solution will largely dictate the computational time steps to be used in the fractional step solution. The minimum time steps can be found analytically (Verboom and Vreugdenhil, 1975) or by trial and error, for example successively halving the time

step until the solution no longer changes as Δt changes. To a large extent, the computational time steps reflect the speed of the physical processes being modeled and thus should not differ drastically from the time scales found in Figure 7.1. For the linked finite difference model of Lake Balaton, the following time steps were determined by trial and error: advection - 8.5 hours (the seiche period), dispersion - 4.25 hours, and reaction - 2.125 hours. The integral relation of the time steps is a requirement of the fractional time step method (see Appendix B).

At a broader level, the time scale question affects our treatment of the model results. The scale analysis can offer insights into the consistency of the model in its temporal characteristics, and suggest those time ranges at which model results cannot be expected to be very realistic. A crucial question for the model concerns its ability to capture the lake's behavior on the time scales of loading changes -- this is the model's goal as a tool for water quality management. Some feeling for the important time scales in this behavior is supplied by van Straten (1981). He constructs analytical models of the lake phosphorus cycle that are simple enough to be solved analytically. Analysis of the solutions identifies the lake response times as approximate functions of loss and reaction rates. The response time is determined as the time scale in which the lake concentration changes as the result of a step change in input loading. van Straten gives results for total phosphorus responses in Basins I and II as 25 and 75 days respectively, and for algal phosphorus in Basin I as 15 days. Though clearly based on very approximate methods, van Straten's estimates of system response times are nevertheless useful as indicators of the order of magnitude of the time to respond to changes in loading. Length scales to accompany the time estimates may be determined from the sizes of Basins I and II, to allow plotting of the loading response on the length and time scale diagram. This is done in Figure 7.1, and shows good consistency between the loading response times and the model time scales.

In summary, the collection of model length and time scales in Figure 7.1 shows a comforting degree of consistency between the various model components. There are no glaring incompatibilities, and van Straten's basin response estimates lie right in the middle of the various time and length scales.

7.2.3 Discussion and Conclusions

The previous section suggests a method of greater generality for modeling decisions than its use above. In particular, the selection of the model space increment, Δx, appears as the major decision made. In selecting Δx, we follow a procedure in which Δx is suggested and then justified with the biological and physical properties of the lake. What of the converse process -- given no preconception of a grid size, can a time and length scale analysis specify one? Such a process, if possible, is of a generality which transcends the specific case of Lake Balaton. Indeed, we will see that this process is central to model identification and definition.

Examination of Figure 7.1, rather than simply suggesting a grid size, reveals three alternative ranges of spatial representation, as we show in Figure 7.2. The range of shortest space scales are those less than the lake depth. Selection of such a scale implies that the model must necessarily include both the longitudinal and lateral dimensions as well, unless a very local area is of interest. If somewhat longer space scales are employed, variations with depth become negligible. However, the associated time scales for longitudinal advection are still less than or comparable to transverse mixing time scales, and a grid of length Δx cannot be assumed fully-mixed laterally. These conditions define the regime for 2-D modeling, as indicated in Figure 7.2. The next range is that in which we have chosen to operate, where the transverse mixing time is so much shorter than the longitudinal advection and dispersion times that a 1-D simplification is permissible. The spatial increment we have selected is near the lower limit of the 1-D range and much greater spatial detail is not reasonable in a 1-D model. A larger grid size is entirely possible, and we show a rough upper limit to the range for the 1-D model.

Between the ranges defined above we have shown ranges where consistent modeling is not possible due to conflicting scale requirements for the important processes. Consider, for example, a one-dimensional model with Δx = 67 meters. This is the grid size suggested in Section 5.5.2 by numerical modeling requirements when seiche advection is included. According to those findings, 67 meters is the maximum grid spacing able to capture the influence of seiche oscillation properly. However, consider the implications of the cross-sectional mixing time for such a model, as shown in Figure 7.3. Longitudinal mixing times are included in Figure 7.3 for a family of reasonable values for the dispersion coefficient in Lake Balaton. Only at the very smallest values of dispersion does a one-dimensional assumption approach rationality for Δx = 67 m. In all other cases, the grid will mix much faster longitudinally than it will laterally -- thus deviating from the assumption of one-dimensionality. Larger values of Δx will approach one-dimensionality, but will run afoul of the seiche excursion requirements. Hence, there is no suitable model in the range above 67 meters until Δx becomes sufficiently larger than the seiche excursion to allow neglect of seiche advection.

Figure 7.2 suggests the possibility of a two-dimensional model of Lake Balaton's water quality. Such a model could afford certain conveniences not possible with the one-dimensional model. Most significantly, it eliminates the necessity for computing the one-dimensional dispersion coefficient. There are, however, practical complications in using a two-dimensional model due to the length scale for seiche advection. As we have shown in Figure 7.2, there are only certain ranges of allowable Δx values. A grid size below 67 meters is permitted, but would be prohibitively expensive for computation. Above roughly 1100 meters, a two-dimensional model may be employed instead of the simpler one-dimensional model also possible in that range. However, at this length scale, seiche advection must necessarily be averaged out for either the one or two-dimensional model. An effective diffusion coefficient would thus be required in the two-dimensional model to account for the effects of this temporal averaging. This would lead to essentially similar calculations as required to compute the one-dimensional dispersion coefficient,

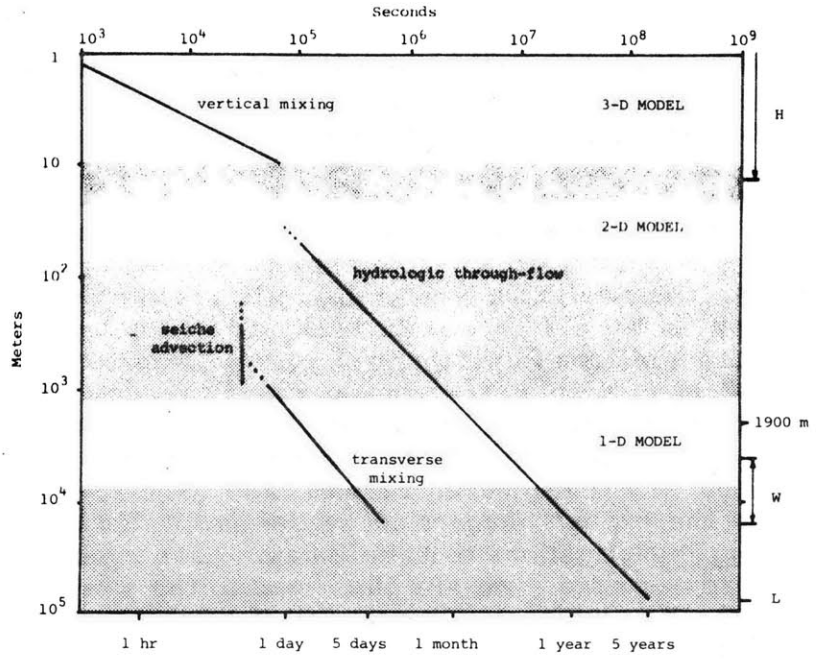

Figure 7.2

Modeling alternatives determined
from length and time scale analysis

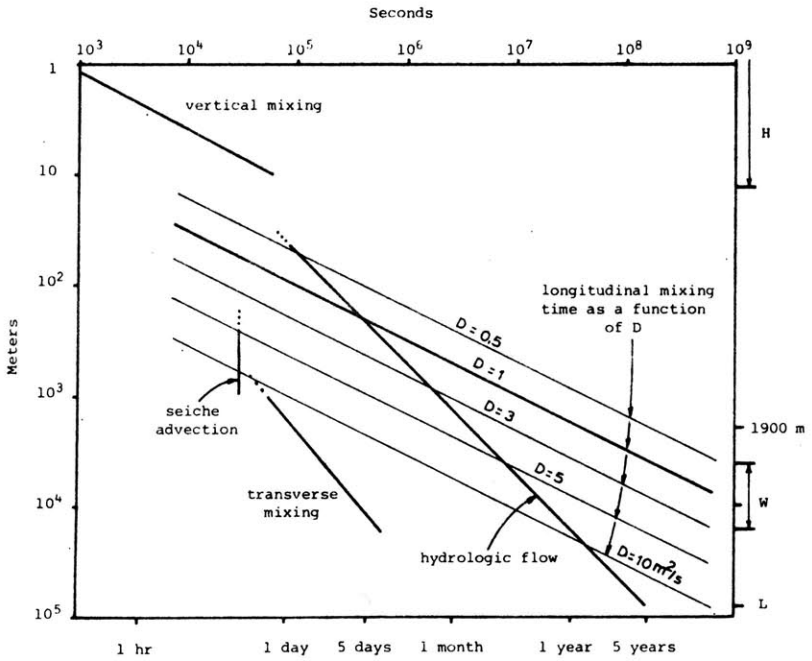

Figure 7.3

Longitudinal advection and dispersion
length and time scales

eliminating much of the advantage sought from the two-dimensional model. In short, two-dimensional modeling of Lake Balaton offers no practical advantage over one-dimensional modeling at longer length scales, and it is computationally infeasible at short grid sizes.

Finally, there is the range of Δx larger than about 8000 meters. Box models, such as the four-box Lake Balaton models, fall within this range. However, Figure 7.3 illustrates an inconsistency in these models due to a mismatch of mixing and advective time scales. To assume that each box in a box model behaves as a fully-mixed tank, the time scale for mixing should be less than the time for through-flow. However, this assumption becomes less valid in Balaton as the length scale increases. For example, the twenty kilometer length scale of Basins II, III and IV in the four-box Balaton model is reasonable only if the dispersion coefficient exceeds 10 m^2/s. Conversely, the box model carries approximately this level of dispersion due to the implicit dispersion we defined in Section 2.5. However, our modeling investigations of Lake Balaton have revealed much less dispersion to be appropriate. We are thus lead to the same conclusion as in Section 2.5: the box model is a reasonable formulation only if the size of the box (and its accompanying implicit dispersion) fortuitously reflect the mixing processes within the actual lake. Our determination of the dispersion coefficient, as reported in Section 6.2, shows that dispersion will be much less than that implied by the box models, and thus the box models are inappropriate.

Although the analysis performed above was done for the specific case of Lake Balaton, we believe the method of analysis to be applicable to lake modeling in general. That is, a thorough and careful analysis of model space and time scales will identify the alternative model structures feasible for a problem as well as indicate the ranges of space and time scales where one should not model. The alternative model structures arise in those "windows" of length and time scale space where underlying processes can be safely averaged or neglected without incurring fundamental inconsistencies with the processes retained. These windows will differ from application to application, but the method to discover them -- careful delineation of time and space scales -- is general.

7.2.4 Implications for Data Collection

In the length and time scale analysis presented above, the available field data are accepted as a given. However, the length and time scale analysis can be used profitably in the converse process: to design a field data collection program based upon the lake characteristics and the likely modeling format.

There are many issues to be addressed in a comprehensive field data program. Not the least consideration is the fact that the program must serve many different modeling, management and analysis purposes. We will ignore this complexity here, and examine only those data necessary for water quality modeling. Even within this single discipline, the data collection program has many facets which must be considered. We will concentrate here on the issues of spatial coverage, and frequency and duration in time.

The spatial coverage of the program should be no less than that necessary to support the selected modeling scheme. Better still, it should be sufficiently comprehensive for at least an initial period to permit an appropriate modeling scheme to be selected. Consider this in the context of Figure 7.2. For each of the modeling regimes shown, there is an appropriate spatial scale for the data collection program. This is the lower space scale delimiting the regime -- a sufficient quantity of data should be collected at this spatial increment to permit evaluation of the modeling alternative. For example, in Lake Balaton such data exist in sufficient quantity for the 1-D model only. Lateral transects of algal concentration would be necessary to evaluate the need for 2-D modeling; a considerably greater quantity (duration) of such data would be needed to calibrate and verify a 2-D model. Clearly, a well-designed data program would supply data at various increments over the different dimensions to examine alternative models. Limited funding, manpower and equipment would constrain the coverage of the data program; however the program should be designed to maintain a continuous base level supplemented with occasional detailed samplings. For example, a basically longitudinal sampling network could be established for phosphorus measurements (as done in Balaton) but enough resources should be reserved for occasional detailed sampling transects made between and lateral to the regular stations.

The sampling frequency and duration can similarly be planned using the space and time scale analysis as a guide. As above, the program must strike a compromise between all possibly useful data and the limitations of finite resources. Sufficient frequency must be achieved within the program to analyze the various possible influences, and sufficient duration is needed to identify trends over time. The question of frequency is probably most troublesome. For example, consider the data required to properly evaluate the influence of seiche advection. As indicated in Figure 7.1, data measurements at roughly hourly intervals at a number of locations would be necessary to detect the influence of the seiche. This would be a substantial exercise to conduct for one or two days -- it would be virtually impossible to continue for any length of time. Accordingly, our recommendation for the treatment of temporal scales follows that made above the spatial scales: establish a base sampling frequency but supplement the base program with occasional periods of intensive measurements. These intensive periods should be designed to analyze the processes identified in Figure 7.1. For example, sampling at a single station at a frequency of one hour could be conducted over a few days to investigate the dynamics of algal growth. Daily sampling at a number of stations across the lake would be needed to investigate transverse mixing, and the more extensive program outlined above would be necessary to look at longitudinal advection and mixing. Careful design of a field data program would maintain continuous bi-weekly sampling as a base, but reserve resources to permit occasional intensive measurement periods. The intensive measurements investigate the transient processes identified above, while the base sampling rate is designed to observe changes due to nutrient loading as characterized by the basin response times in Figure 7.1.

Finally, the duration of the program must be determined. For Balaton, the hydraulic residence times in Figure 7.1 are long, mandating a program continuing for decades. In general, data collection lasting over a few

hydraulic residence times is the minimum necessary to track long-term trends. To investigate individual phenomena identified in Figure 7.1, the same general rule can be followed: the program will be most useful if it lasts long enough to observe at least several repetitions of the process. The information in Figure 7.1 lends naturally to the determination of the necessary program duration.

This brief analysis has led to a general recommendation for field data collection planning and shown by example how space and time scales of specific processes may be drawn from the space and time scale analysis to plan specific measurements. Our general recommendation is to design a base program with a frequency and spatial detail that will show the transient response of lake basins. Beyond this base level, occasional supplementary measurements should be planned to investigate particular shorter scale phenomena. The design of these intensive supplementary programs can be based upon the specific information found in Figure 7.1.

7.3 Conclusions from the Lake Balaton Model

An indication of how much we have learned about Lake Balaton is the degree to which our conception of the lake has changed in the course of this research. As this study was begun, it was thought that the dominant longitudinal gradient observed in phosphorus concentration was largely determined by the hydrologic through-flow combined with loss mechanisms. The model has demonstrated that it is, in fact, more immediately due to the distribution of nutrient inflows. Concerning modeling of the lake, as we began to study the lake's seiche motion, we hypothesized that the lake behaved and could be modeled much as an estuary. However, the seiche excursion in the lake is so much shorter than the estuarine tidal excursion that a practical distinction arises. Not only does it become very difficult from a computational standpoint to model the seiche advection, from a practical point of view it becomes unnecessary: the seiche excursion is too short to materially affect the predicted water quality. Our view of mixing in the lake has changed considerably as well. The lake is commonly believed to be quite well-mixed, at least within the defined basins. However, our calculations have shown, with the support of field data, that the mixing is in fact fairly weak, that nutrients introduced to the lake will be transported away fairly slowly.

What we have learned about the lake's water quality is that there are many processes which materially influence it. Clearly, the dominant influence is the spatial distribution of the inflowing nutrient loads. Lesser, but nevertheless important factors are biogeochemical reaction, hydrologic advection, and dispersive mixing. None of these three factors can be singled out as dominating the others: all must be considered important. Finally, we determined the back-and-forth seiche advection to be a minor influence which could be neglected so long as its influence on dispersion was captured.

7.4 Recommendations for Future Research

The findings of this study suggest an immediate path for continuing research. This is the recalibration of the biogeochemical model within the framework of the one-dimensional finite difference model. Our findings have made clear that the change from a four-box model is accompanied by changes in hydrodynamic transport which can alter the calibration. A suggestion for this future work would be to investigate the coarser grid suggested in Section 7.2.3 as a means to lower computation costs while still operating in an acceptable range of space and time scales. Also worthwhile may be the disaggregation of tributary nutrient inflows from monthly data to daily data by correlation with the daily Zala River data. The importance of the nutrient loading to the model results suggests the greater temporal detail may change the character of the results.

Data needs suggest longer range goals for the research as well. Perhaps the greatest limitation on this study was the lack of basic data. To unequivocally verify the circulation model much more information on water motion in the lake is necessary and better resolution of the spatial wind field is essential. To confirm the dispersion coefficient calculation, field data on the origin and fate of tracer constituents are required. To corroborate the predicted water quality profiles, measurements with greater spatial resolution must be taken. To validate the biogeochemical model calibration and formulation, many more data in time and space are needed

The lack of data leaves many gaps which can be filled by future research. Here we recommend two which we see as particularly necessary. First is the crucial need to resolve uncertainties in the biogeochemical model -- most specifically the part of the model dealing with sediment interaction. To do so requires basic experimentation to determine if sediments are a source of phosphorus which can be utilized by phytoplankton. Chapter 2 suggests possible contributing factors in such phosphorus release: disruption of the sediments by wind action and chemical modification during intermittent anoxic conditions. A second research need is an independent test of the model linkage mechanism. This would entail gathering data on a conservative substance measured in Lake Balaton to be used as a tracer in model simulation tests. van Straten et al. (1979) show data from the lake for a number of conservative substances, however none show distinct gradients within the lake and we do not know if data for any of these substances has been taken for the Zala River or other tributaries. Baranyi (1973b) reports on studies using tritium as a tracer, and the original references and data from that work may be helpful.

APPENDIX A FIELD STUDIES OF LAKE BALATON CURRENTS

A.1 Introduction

Field studies were made as a part of this research on four different days, July 11, 1980 and August 11, 12 and 15, 1980. The measuring program sought a qualitative picture of the vertical velocity profile at various locations in the lake and under various wind conditions. A map showing the approximate locations of the measuring stations is included as Figure A.1.

The basic tool for the measurements was a Marsh-McBirney Model 201 Electromagnetic Current Meter. This instrument consists of a sensor probe which is attached by 12 meters of cable to an electronic processor with a visually read panel meter. The processor and panel meter are housed together in a portable electronics case. When the probe is immersed, water flowing past it interacts with the probe's magnetic field to induce a small voltage in the water about the probe. This voltage, which is related to the water velocity, is sensed by electrodes on the probe and then processed to produce a velocity read-out.

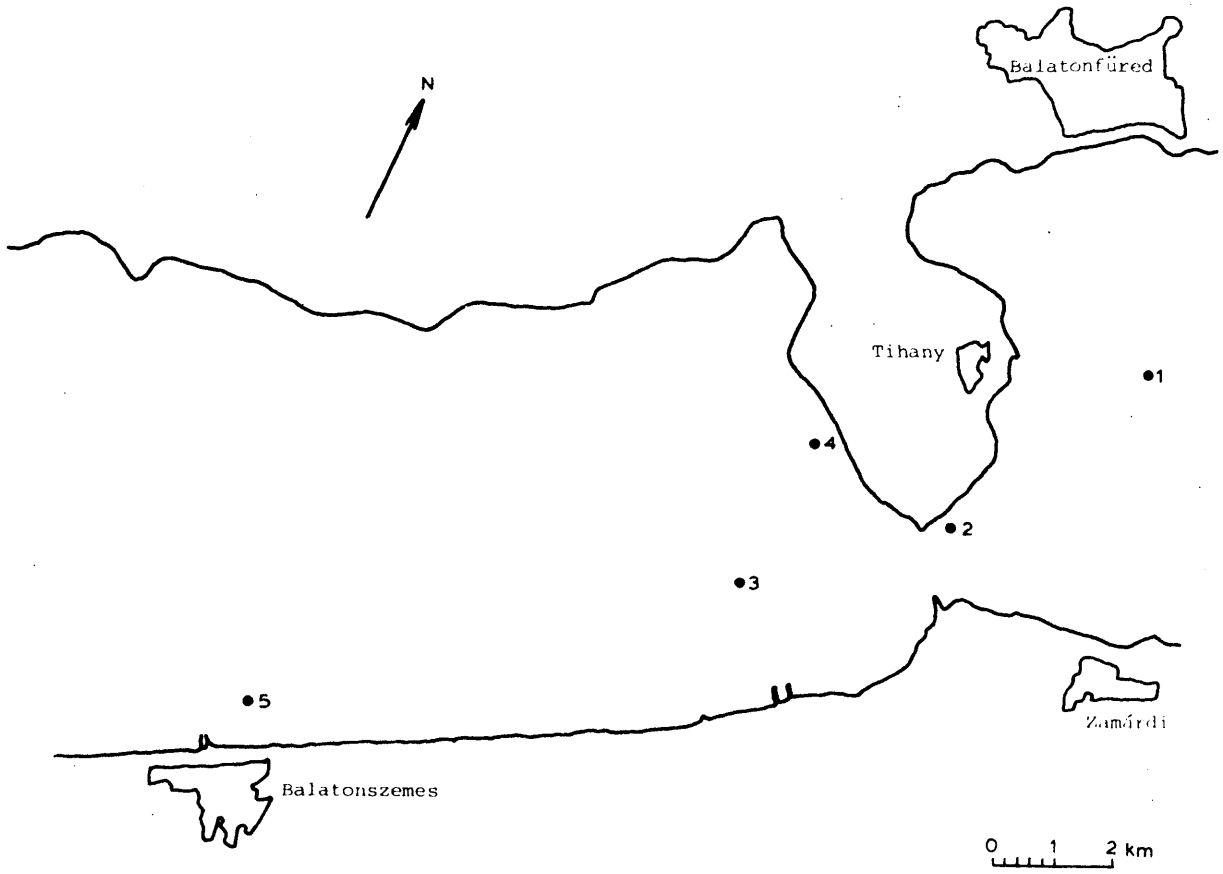

Figure A.1

Approximate location of measurement stations

A.2 Measurement Results

The following describes the conditions and results for each study day in chronological order. At the end of this Appendix, a list of all collected data is included as Table A.1.

July 11

These studies were made with the assistance of the Hungarian Academy of Sciences Biological Institute at Tihany. The Institute's research boat, the Loczy Lajos, was used to make measurements at Stations 1 through 4 about the peninsula of Tihany. Since this was the first use of the current meter in Lake Balaton the studies were intended to test the utility of the meter as well as gather some data.

Wind conditions were variable, but generally light during the morning. During the first two sets of measurements, the winds were from the east and quite light. Later, as we proceeded to Station 3, the winds shifted to the north and grew stronger, almost stormy. These winds died out by the time of our final measurements, however. Stations 3 and 4 were in the wind shadow of the hills on the western side of the Tihany Peninsula during the north winds.

The measurement apparatus consisted of a 5 meter iron pipe, roughly 2 cm in diameter, to which the current meter probe was attached at the end. Tape strips were positioned at one half meter intervals from the probe to mark the length of the pipe, and cross marks were also placed to show the direction in which the probe was pointed. The pipe was lowered into the water to various depths and the velocity was read from the read-out meter on the boat. Since the probe only senses current velocity in a single direction, the pipe was rotated until the direction of maximum velocity was found. The speed was then recorded, along with the direction as estimated by comparing the directional tape marks on the pipe with a compass. The meter velocity reading was quite steady and showed no large influence due to boat motion. The boat was anchored at each stop.

The single exception to this procedure was made at Station 4 during the readings beginning at 1215. Here, the probe was moved about two meters from the end of the pipe and the pipe was pushed into the lake bottom to remain stationary for about 15 minutes at a depth of 2.5 meters. During that time the current reading remained essentially constant. The readings at 2, 1.5 and 0.5 meters were then made in the fashion described above.

The data collected are shown in Figures A.2 through A.5 following the text of this Appendix. With the exception of the nearly constant profile in the Strait of Tihany (Station 2), the currents were variable in both speed and direction. At Station 3 at 1245 hours, for example, the current appeared particularly transient, shifting direction and varying speed considerably at the 2.5 meter depth. The Station 3 measurements at 1130 hours are clearly unreasonable physically -- most likely they reflect unsteady conditions and measurement error.

August 11 and 12

These studies were made using the Biological Institute's research boat in the same fashion as reported above. The only significant change in procedure was the use of VITUKI's stream gaging rod rather than an iron pipe for holding the current meter velocity probe. The metal gaging rod was scored at 10 cm intervals, enabling more accurate depth placement of the probe.

The procedure used in these studies was to position the boat (with three anchors) and remain in place for repeated measurements. On the 11th the wind was very light at first, but accelerated by mid-afternoon to 3.5 m/s. Wind direction was generally from the east with the exception of a brief period around 1500 hours when the wind came from SSW. Six profiles at Station 1 and two at Station 3 are included as Figures A.6 and A.7.

One variation on the measurement procedure was employed at Station 1 to evaluate the steadiness of the current. The probe was aligned with the approximate wind direction (80 degrees) and held stationary at four depths for 2 or 3 minute durations. During these periods, readings were made continuously at an interval of about 3 seconds (the time to read aloud and write down a measurement). The results are shown in Figures A.8 and A.9.

Measurements were made only on the morning on August 12 and, as we typically found in the morning, winds were light. Three profiles at Station 3 were taken and are included as Figure A.10.

August 15

Using the VITUKI research boat, László Somlyódy made measurements off Balatonszemes on the 15th. The VITUKI boat is larger than the Biological Institute's and proved less suited for the measurements. Keeping the boat stationary was particularly troublesome and prevented taking useful measurements during the morning. By afternoon, a procedure was devised to collect useful data and three detailed profiles were made under fairly brisk onshore winds. The collected data are given in Figures A.11 and A.12.

A.3 Conclusions

The collected data lead to the following conclusions:

- Strong, unidirectional currents were found in Tihany Strait, in agreement with Muszkalay's (1973) earlier measurements.

  This conclusion is qualified by the fact that it is based upon a single measured profile.

- Currents in other parts of the lake are highly transient, apparently responding to an unsteady turbulent transport of wind shear vertically into the water column, as well as to other apparently strong influences such as seiching.

  The continuous measurements made at Station 1, shown in Figure A.8, are particularly revealing in this respect. Visual inspection of Figure A.8 indicates increasing unsteadiness with depth - compare, for example, the trace for 0.5 meter with that for 2.5 meters. This is confirmed by the statistics plotted in Figure A.9. The mean velocity falls more or less into the type of profile predicted by theory. The increasing standard deviation with depth confirms our observation that unsteadiness increases with depth. Significantly, these measurements indicate a fundamental difficulty in accurately measuring the velocity profile with a single meter in the relatively slow procedure used in our studies.

- The currents rarely, if ever, behave as predicted by theoretical arguments such as Plate's (1970).

  Few of the profiles conform with classic theory in which the surface current aligns with the wind and in which there is a return current along the bottom in the reverse direction. The series of six consecutive profiles at Station 1 on August 11 under progressively stronger winds could be expected to show the development of such a flow profile. But, as seen in Figure A.6 such is not the case with any consistency. In general, the profiles show unidirectional flow, implying that seiche motion or horizontal flow gyres dominate the flow, preventing establishment of vertical return circulation. Only a synoptic measurement program would be able to prove or disprove this hypothesis, however.

Table A.1

Collected current data

Date, Station	Hour	Depth (m)	Current Measurement Speed (cm/sec)	Direction * (degrees)	Wind at Szemes Speed (km/hr)	Direction	Comments
July 11, 1980							
1	1015	3	10.5	180			light wind
(depth		2	2.5	300			from east
3.5 m)		1	17	30			
2	1045	5	16	230			light wind
(depth		4.5	18.5	230			from east
10.6 m)		4	18.5	230			
		3.5	20.5	230			
		3	16	230			
		2.5	15	230			
		2	15	230			
		1.5	12.5	230			
		1	17	230			
		0.5	18	220			
3	1130	3.5	13.5	230			north wind-
(depth		3	8.5	100			increasing in
3.9 m)		2.5	15	260			speed during
		2	20.5	270			measurements
		1.5	15.5	80			
		1	14.5	270			
		0.5	variable 25 max.				
4	1145	3	9.5	230			north wind-
(depth							now decreasing
3.3 m)		2.5	14	230	highly variable		
		2	12	230	readings		
		1.5	13	230			
		1	10	70			
		0.5	5 to 10	230			
4	1215	2.5	4	180			north wind
		2	3.5	230			
		1.5	1	230			
		0.5	5	20			

* Direction from which current flows in degrees counterclockwise from magnetic north

Date, Station	Hour	Depth (m)	Current Measurement Speed (cm/sec)	Direction * (degrees)	Wind at Szemes Speed (km/hr)	Direction	Comments
3	1245	3.5	14.5	230			north wind
		2.5	10	230	sequential readings		
		2.5	3-5	20	made in roughly		
		2.5	5-6	230	ten minutes		
		1.5	14	120			
August 11, 1980							
1	1130	3.5	0	-	0.5	S	observed wind
(depth		3	3	320	at 1100		from east to
3.8 m)		2	7	320			northeast
		1	5	320			
		0.5	4	120			
1	1155	3.5	0	-	3.0	S	
(depth		3	0	-	at 1200		
3.8 m)		2	0	-			
		1	0-4	180			
		0.5	7	180			
1	1445	3.4	6	130	10.5	-	observed wind from
(depth		3	6	130	at 1500		approx. 210 deg.
3.9 m)		2	6	150			
		1	5	270			
1	1515	3.4	6.5	145	10.5	-	
(depth		3	7.5	80	at 1500		
3.9 m)		2	2.0	90			
	1530	1	5.5	260			
1	1530	3.4	6.5	80	13.0	-	observed wind
(depth		3	2.5	80	at 1600		from east
3.9 m)		2	variable	-			increasing
	1540	1	2.5	100			wind speed
1	1545	3.7	variable-	60	13.0	-	
(depth			approx. 6		at 1600		
4.2 m)		1.5	5-6	60			
	1615	0.5	12	30			
3	1650	3.2	3.5	100	7.0	-	observed wind
(depth		2.2	4	90	at 1700		from east
3.7 m)		1.2	6.5	90			
	1700	0.2	11	90			

Date, Station	Hour	Depth (m)	Current Measurement Speed (cm/sec)	Direction * (degrees)	Wind at Szemes Speed (km/hr)	Direction	Comments
3 (depth 3.7 m)	1702	3.2	variable 7 max.	-	7.0 at 1700	-	
		2.2	5	90			
		1.2	5	70			
	1715	0.2	8	70			
August 12, 1980							
3 (depth 4 m)	1015	3.5	2	320	1.5 at 1000	-	observed wind from 280 deg.
		2.5	3	300			
		1.5	3	320			
	1030	0.25	7	310			
3 (depth 4 m)	1115	3.5	3.5	170	5.0 at 1100	-	
		2.5	3	180			
		1.5	3	180			
	1125	0.25	7	310			
3 (depth 4 m)	1142	3.5	3.5	180	5.5 at 1200	-	
		2.5	3	190			
		1.5	3	230			
		0.25	7.5	310			
August 15, 1980							
5 (depth 3.5 m)	1300	0.1	7	330	18.0 at 1300	-	observed wind from NNW
		0.3	7	330			
		0.5	4-5	330			
		0.7	7	330			
		1.0	5	330			
		1.5	0	-			
		2.0	5	330			
		2.5	4	330			
		3.0	2	330			
		3.3	0	-			

Date, Station	Hour	Depth (m)	Current Measurement Speed (cm/sec)	Direction * (degrees)	Wind at Szemes Speed (km/hr)	Direction	Comments
5 (depth 3.5 m)	1425	0.3	6	285	17.0 at 1400	-	
		0.5	8	285			
		0.7	8	285			
		1.0	8	285			
		1.2	6	285			
		1.5	6	285			
		2.0	2	285			
		2.5	3	285			
		2.7	7	240			
		3.0	5	240			
		3.3	2.5	240			
5 (depth 3.5 m)	1555	0.3	4.5	310	7.0 at 1600	-	
		0.5	3	310			
		1.0	8	240			
		1.5	0	-			
		2.0	5-6	240			
		2.5	5	240			
		3.0	1	40			
		3.3	1	40			

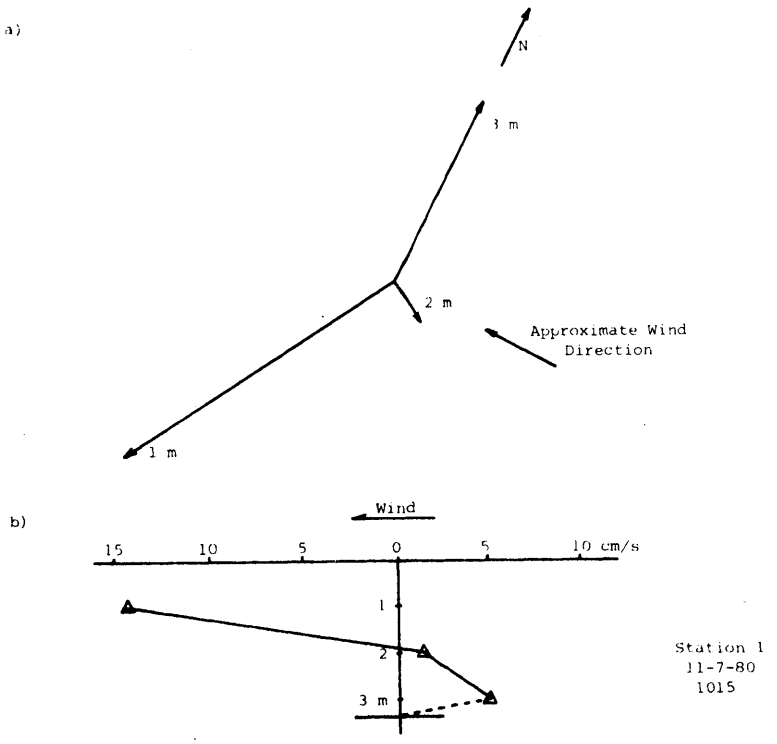

Figure A.2

Current measurements at Station 1, 11 July 1980

a) Current vector diagram
b) Velocity component along lake longitudinal axis versus depth

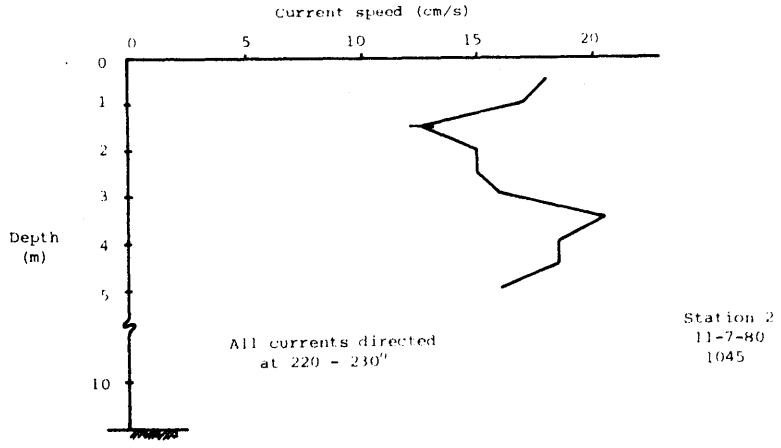

Figure A.3

Current measurements at Station 2, 11 July 1980

Velocity profile in Tihany Strait

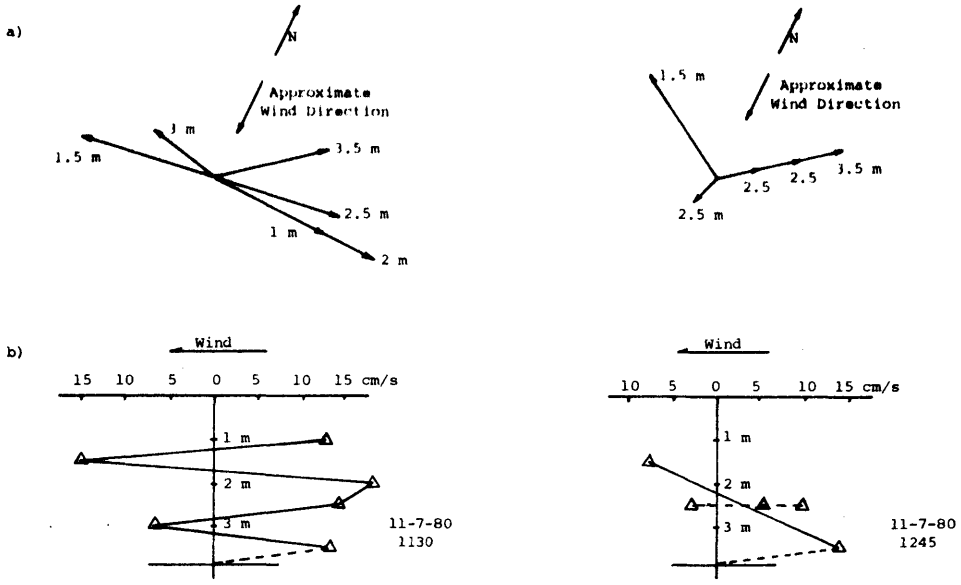

Figure A.4

Current measurements at Station 3, 11 July 1980

a) Current vector diagrams
b) Longitudinal velocity profiles

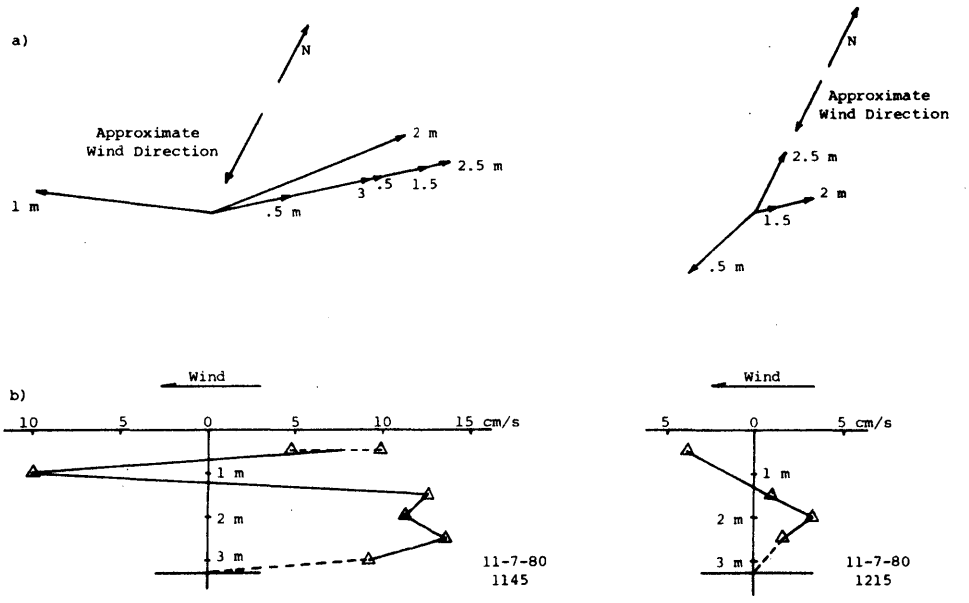

Figure A.5

Current measurements at Station 4, 11 July 1980

a) Current vector diagrams
b) Longitudinal velocity profiles

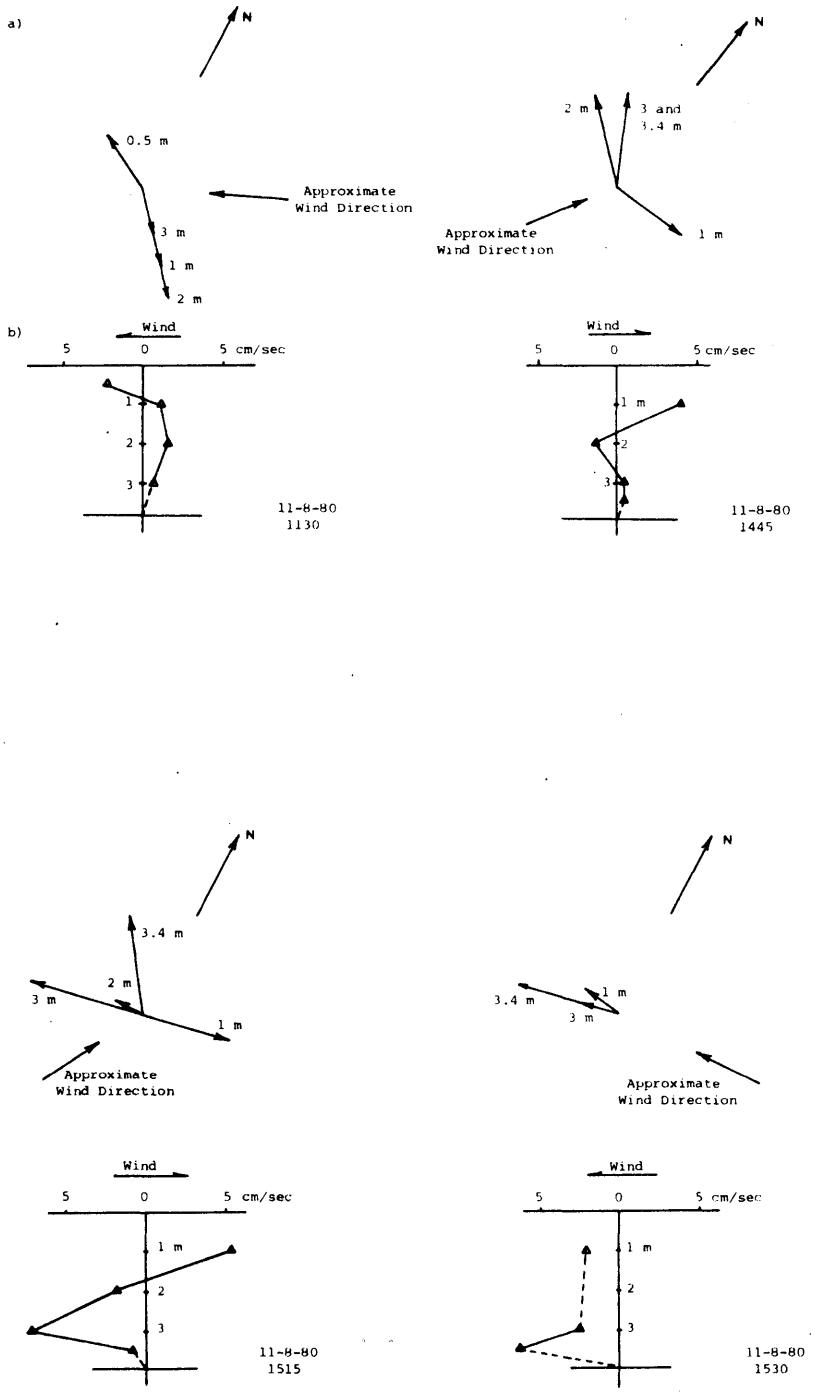

Figure A.6

Current measurements at Station 1, 11 August 1980

a) Current vector diagrams
b) Longitudinal velocity profiles

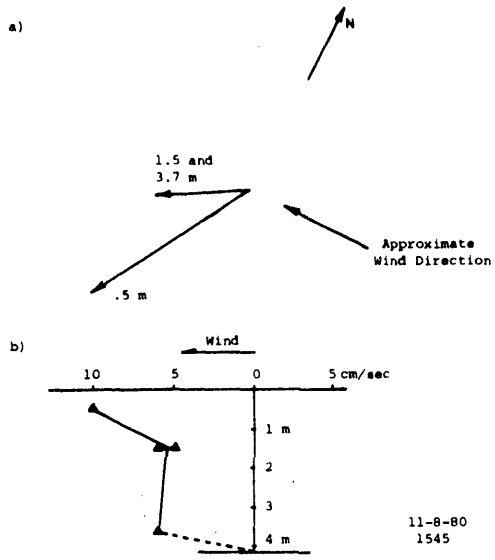

Figure A.6 Current measurements at Station 1, 11 August 1980 continued

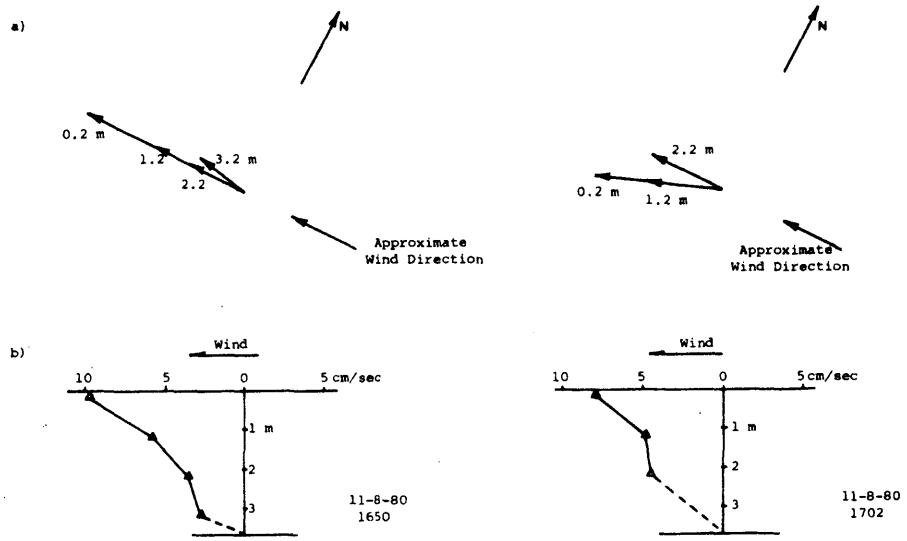

Figure A.7

Current measurements at Station 3, 11 August 1980

a) Current vector diagrams
b) Longitudinal velocity profiles

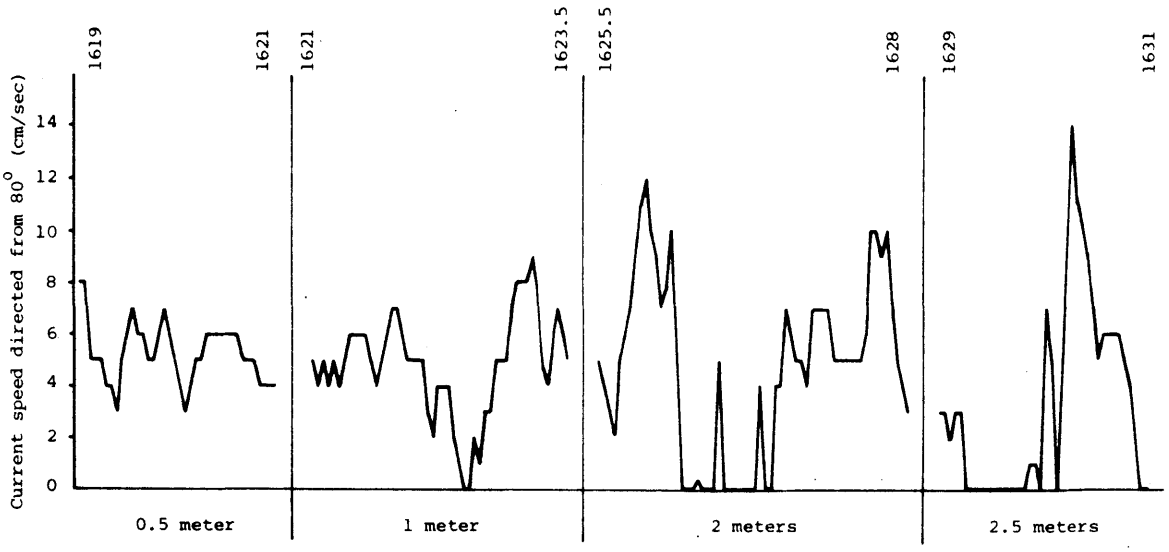

Figure A.8

Continuous measurements at Station 1
11 August 1980 1619 to 1631 hours

Measurement interval is approximately 3 seconds

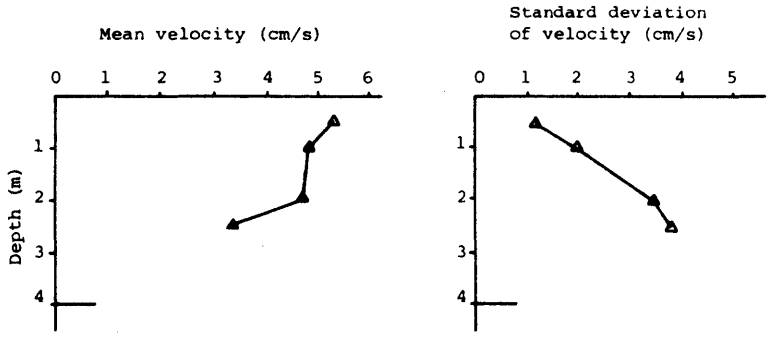

Figure A.9

Temporal statistics of continuous measurements
at Station 1, 11 August 1980

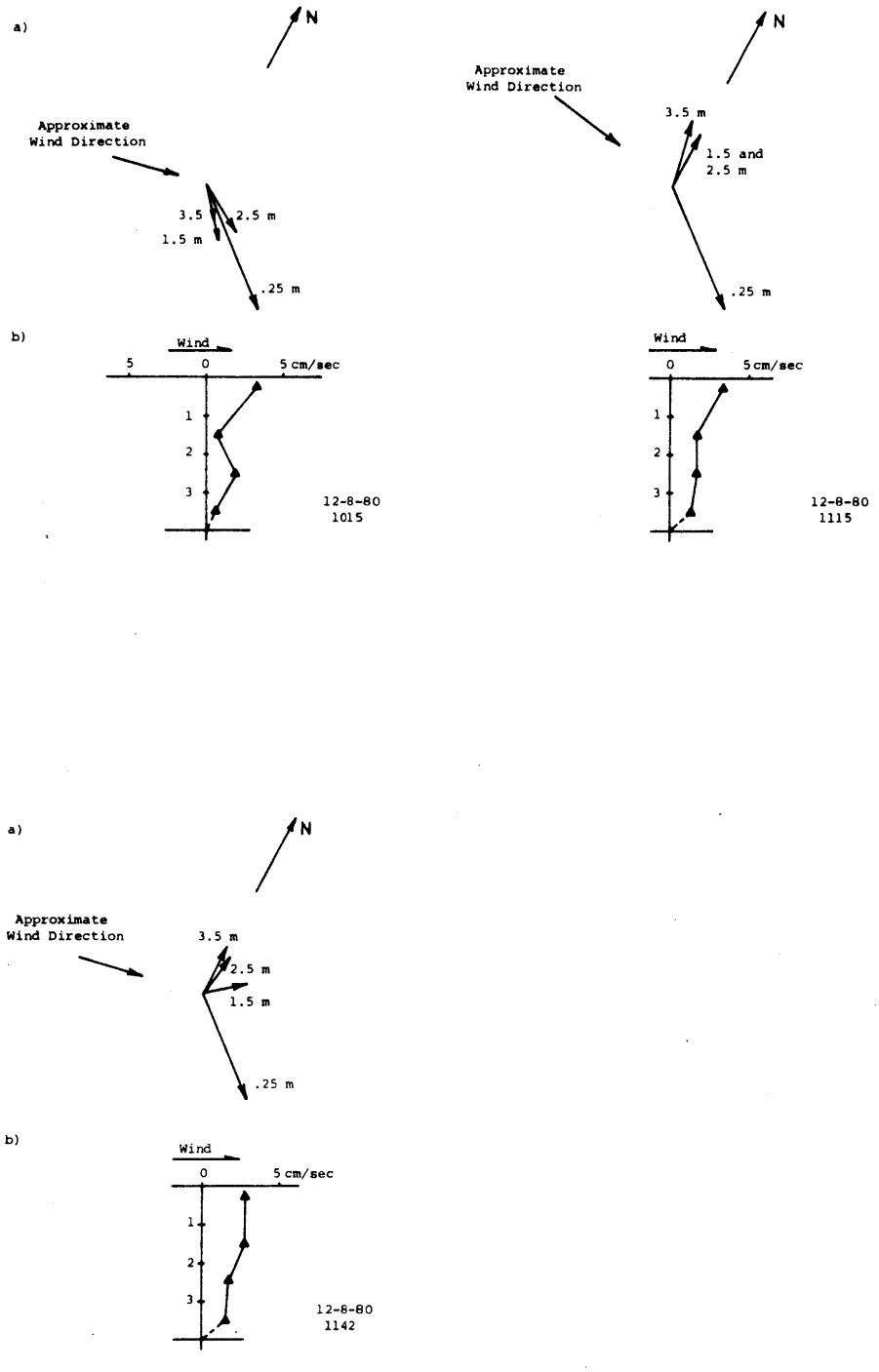

Figure A.10

Current measurements at Station 3, 12 August 1980

a) Current vector diagrams
b) Longitudinal velocity profile

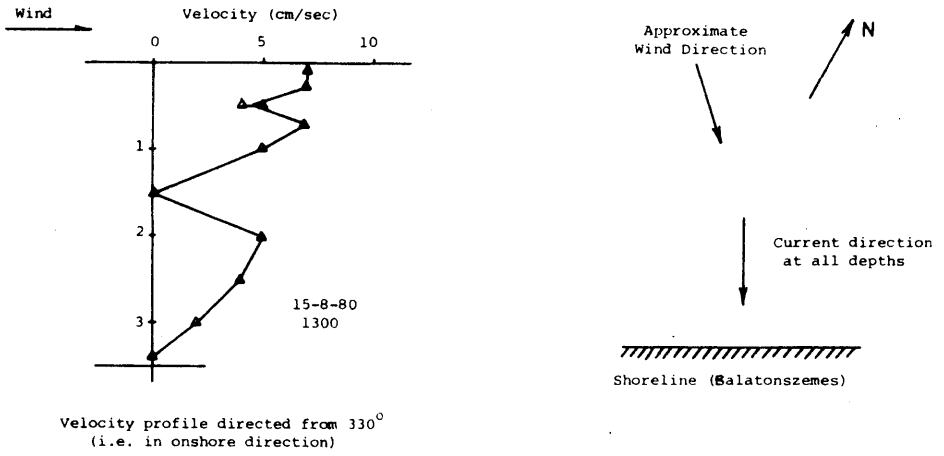

Figure A.11

Current measurements at Station 5, 15 August 1980, 1300 hours

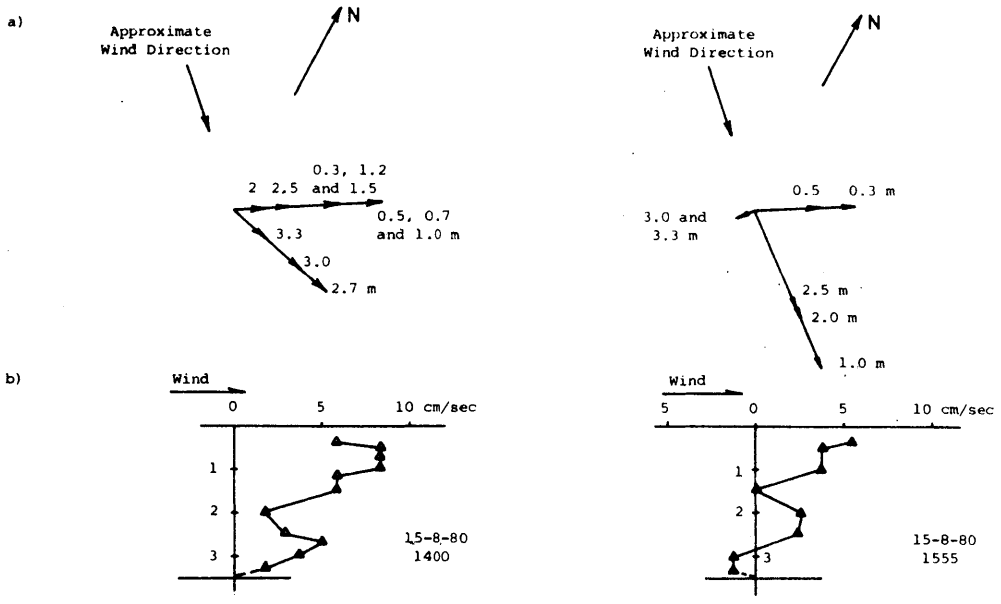

Figure A.12

Current measurements at Station 5, 15 August 1980

a) Current vector diagrams
b) Longitudinal velocity profile

APPENDIX B A FRACTIONAL STEP METHOD USING MIXED TIME STEPS

The fractional step method (or time splitting) is a numerical method to solve equations of the form:

$$\frac{\partial c}{\partial t} = Lc \qquad \text{(B.1)}$$

where L is a differential operator in one or more space variables.

The key element of the method is to decompose the operator L into a summation series of component operators, $L = L_1 + L_2 + \ldots L_k$. Justification for such a procedure arises by considering a finite difference representation of the time integration required to solve Equation B.1. We assume a temporal discretization into intervals of length Δt counted by the index n and determine the unknown $c(t+\Delta t)$ by Taylor expansion about the known value $c(t)$:

$$\begin{aligned} c(t+\Delta t) &= c(t) + \Delta t \left.\frac{\partial c}{\partial t}\right|_t + \frac{(\Delta t)^2}{2!} \left.\frac{\partial^2 c}{\partial t^2}\right|_t \\ &\quad + \frac{(\Delta t)^3}{3!} \left.\frac{\partial^3 c}{\partial t^3}\right|_t + \cdots \\ &= \left[1 + \Delta t \frac{\partial}{\partial t} + \frac{(\Delta t)^2}{2!} \frac{\partial^2}{\partial t^2} + \frac{(\Delta t)^3}{3!} \frac{\partial^3}{\partial t^3} + \cdots\right] c(t) \end{aligned} \qquad \text{(B.2)}$$

where the term in brackets is a differential operator in time. This equals exactly:

$$c(t+\Delta t) = \exp\left(\Delta t \frac{\partial}{\partial t}\right) c(t) \qquad (B.3)$$

From Equation B.1, $\partial/\partial t = L$ and thus,

$$c(t+\Delta t) = \exp(\Delta t L)\, c(t) \qquad (B.4)$$

Clearly, if $L = L_1 + L_2 + \ldots + L_k$, then

$$c(t+\Delta t) = \exp(\Delta t L_1) \exp(\Delta t L_2) \cdots \exp(\Delta t L_k)\, c(t) \qquad (B.5)$$

The notion of fractional steps derives from the solution of Equation B.5 in a step-wise fashion. For simplicity, consider two terms only, $L = L_1 + L_2$. Then,

$$c(t+\Delta t) = \exp(\Delta t L_1) \exp(\Delta t L_2)\, c(t) \qquad (B.6)$$

We may solve this in two steps:

$$\begin{aligned} c^* &= \exp(\Delta t L_2)\, c(t) \\ c(t+\Delta t) &= \exp(\Delta t L_1)\, c^* \end{aligned} \qquad (B.7)$$

where the intermediate solution, c^*, has no physical significance. In practice, $\exp(\Delta t L_1)$ and $\exp(\Delta t L_2)$ are replaced by finite difference

approximations accurate to some power of Δt. The advantage of the method, aside from the convenience involved in separating a complex operation into a series of simpler steps, owes to its consistency, stability and accuracy characteristics. It can be demonstrated that the method preserves the consistency and stability of the individual steps if the operators L_1 and L_2 commute (that is, if $L_1L_2 = L_2L_1$). If L_1 and L_2 do not commute (the usual case) Equation B.7 must be alternated with:

$$c^{**} = \exp(\Delta t L_1)\, c(t+\Delta t)$$

$$c(t+2\Delta t) = \exp(\Delta t L_2)\, c^{**} \qquad \text{(B.8)}$$

This is the same process as equation B.7 with the order of the operations reversed. This preserves the accuracy of the individual steps to order $(\Delta t)^2$. Thus, consistency and stability, as well as accuracy to order $(\Delta t)^2$, may be guaranteed if the individual steps are consistent and stable, and accurate to order $(\Delta t)^2$.

Time splitting methods have received wide usage in two-dimensional problems where $L = L_x + L_y$ separates operations into the two directional components. The alternating direction implicit (A.D.I.) and locally one-dimensional (L.O.D.) techniques are examples of time splitting applied in this fashion (Verboom and Vreugdenhill, 1975 and Gourlay and Mitchell, 1969a, 1969b, and 1972). Verboom (1976) has illustrated an application to the one-dimensional advection diffusion equation. This is an example of the fractional step method where the operator L is split not according to coordinate directions but simply into convenient step operations.

Here we consider an extension to Verboom's method to increase the efficiency and decrease the cost of the solution. The problem to be solved is represented by a set of coupled advection - diffusion - reaction equations in one dimension:

$$\frac{\partial \underline{\underline{P}}}{\partial t} = -U \frac{\partial \underline{\underline{P}}}{\partial x} + \frac{1}{A} \frac{\partial}{\partial x}\left(DA \frac{\partial \underline{\underline{P}}}{\partial x}\right) + \underline{\underline{N}}\,\underline{P} \qquad \text{(B.9)}$$

where
- $\underline{P}$ is a vector of reactant concentrations,
- $\underline{U}$ is the advective velocity,
- A is the cross-sectional area,
- D is the longitudinal dispersion coefficient, and,

$\underline{N}$ is a reaction vector specifying the interaction of the various reactants.

For simplicity the following analysis will employ the analogous equation for one constituent,

$$\frac{\partial c}{\partial t} = Lc = L_a c + L_d c + L_r c \qquad \text{(B.10)}$$

where L is an operator in x which is subdivided into three separate operators:

L_a for advection,

L_d for dispersion, and

L_r for reaction.

Suppose finite difference approximations to solve the three operations in time are developed so that the L_a operation is limited by stability or accuracy requirements to a time step Δt, while the L_d operation is limited to $\ell\Delta t$, $\ell > 1$, and the L_r is limited to $k\Delta t$, $k > 1$. Suppose for now k exceeds ℓ and is an integral multiple of ℓ such that $k = 2m\ell$. The solution method we propose would then be to solve for $c(t+k\Delta t)$ as a function of $c(t)$ as follows:

$$c(t+k\Delta t) = \exp(k\Delta t L_r) \left\{ [\exp(\Delta t L_a)]^{\ell} \exp(\ell\Delta t L_d) \exp(\ell\Delta t L_d) [\exp(\Delta t L_a)]^{\ell} \right\}^{m} c(t) \qquad \text{(B.11a)}$$

This is alternated with:

$$c(t+2k\Delta t) = \left\{ \text{expression above} \right\}^{m} \exp(k\Delta t L_r)\, c(t+k\Delta t) \qquad \text{(B.11b)}$$

The steps in this solution are:

1) Solve for advection ℓ times sequentially
2) Solve for dispersion over one time step of length $\ell\Delta t$
3) Repeat 2
4) Repeat 1
5) Repeat the sequence 1-4 another (m-1) times
6) Solve for reaction over one time step of length $k\Delta t$

This sequence must then be followed by:

7) Repeat 6
8) Repeat the sequence 1-4 m times.

It can be shown (after considerable algebra) that this procedure preserves the accuracy of the individual steps to order $(\Delta t)^2$. That stability is preserved is easily shown. A scheme will be stable if it solves

$$c(t+\Delta t) = \exp(\Delta tL)\, c(t)$$

such that

$$c(t+\Delta t) \leq |\exp(\Delta tL)\, c(t)|$$

or

$$|\exp(\Delta tL)| \leq 1 \qquad \text{(B.12)}$$

In our proposed method, $\exp(\Delta tL)$ is given by Equation B.11. A sufficient condition for Equation B.12 is:

$$\exp(k\Delta tL_r) < 1,$$

$$\exp(\Delta tL_a) < 1, \text{ and}$$

$$\exp(\ell\Delta tL_d) < 1.$$

This is simply a statement of the stability of the individual steps. The property that the characteristics of the individual steps is preserved is extremely useful. With this property, more troublesome components

(e.g., the advective term in Equation B.10) may be treated with higher accuracy than less difficult terms. The accuracy of the individual treatments carries through to the scheme as a whole.

Advantages of the mixed time-step fractional step method include those of the single time-step version:

1. The ability to break a complex problem into a number of simpler steps.
2. The ability to develop individual solution schemes appropriate to each of the steps.
3. The ability of the scheme to preserve the accuracy (to order $(\Delta t)^2$), stability and consistency of the individual steps.

The mixed time step scheme adds a further advantage:

4. Computational requirements are greatly reduced for some parts of the solution.

APPENDIX C CLOSURE OF 3-D CIRCULATION MODEL STUDY

In previous work (Shanahan, Harleman and Somlyódy, 1981) a three-dimensional circulation model was developed and applied to Lake Balaton. Since publication of that report, additional study has revealed significant flaws in the model and its results which should be clarified.

The problem arises due to an error in the model computer program with insidious consequences. The error, which was inherited from the precursor program, affects simulations using only particular forms of the vertical eddy viscosity -- namely those with zero slope at the surface and consisting of more than one linear segment. For these particular cases, a special form of the Galerkin statement is required since the eddy viscosity function parameter α goes to zero. (See Appendix B of Shanahan et al.) Failure to program this special form for one term of the statement, a term derived from the vertical momentum transport term in the governing equation, led to a misaccounting of the momentum transport. The result of this error was an effective, but artificial, non-linear friction at the bottom boundary.

Although the model, including this error, was able to be calibrated, the inappropriateness of this eddy viscosity is clear. This is suggested in Section 3.6.1, where the inseparability of the eddy viscosity and bottom friction choices is discussed. The 3-D circulation model employed as its bottom friction a linear law in which the velocity at the bottom has a significant finite value. Such a bottom friction formulation must necessarily be accompanied by a constant viscosity near the bottom. Otherwise, a steep velocity profile will be specified which, on top of the already finite bottom velocity, will lead to far too large velocities in the interior of the flow. The error contained in the program prevented this from happening in our earlier results.

Correction of the program error eliminated the artificial non-linear bottom friction, leaving only the linear friction relation. Unfortunately, this proved inadequate in Lake Balaton where friction is such an important influence: it was simply impossible to achieve simulation behavior with the damping characteristics of the actual lake. Further, the Galerkin formulation proved incompatible with an explicitly non-linear friction law without creating an unreasonably expensive program to execute. The 3-D model was thus abandoned, the apparently successful calibration being considered fortuitous at best, without sufficient theoretical backing to be reliable.

APPENDIX D DISPERSION RELATIONS IN THE 1-D MODEL

D.1 Derivation of the 1-D Dispersion Equation

In this section we proceed from the three-dimensional equations of conservation of mass to derive the analogous equation for one dimension. Holley and Harleman (1965) give a similar derivation, however the derivation presented here employs the equations of continuity (conservation of mass of water) and the kinematic boundary condition to achieve the same results in a more direct fashion.

We begin with the 3-D conservation of mass equation:

$$\frac{\partial c}{\partial t} + u\frac{\partial c}{\partial x} + v\frac{\partial c}{\partial y} + w\frac{\partial c}{\partial z} = \frac{\partial}{\partial x}\left(\varepsilon_x \frac{\partial c}{\partial x}\right) + \frac{\partial}{\partial y}\left(\varepsilon_y \frac{\partial c}{\partial y}\right) + \frac{\partial}{\partial z}\left(\varepsilon_z \frac{\partial c}{\partial z}\right)$$

where the notation is that used in Chapter 5. To make the equation one-dimensional, we must integrate it over the cross-sectional area. For any function ϕ of y and z, the integration is:

$$\int_A \phi dA = \int_{z_1(x,t)}^{z_2(x,t)} dz \int_{y_1(x,t)}^{y_2(x,t)} dy\ \phi$$

where z_1 and z_2 are the surface and bottom vertical coordinates, and
y_1 and y_2 are the lateral coordinates of the right and left banks.

Before integrating, we add:

$$c\left(\frac{\partial u}{\partial x} + \frac{\partial v}{\partial y} + \frac{\partial w}{\partial z}\right) = 0$$

to Equation D.1. The expression above is derived from the continuity equation. Equation D.1 thus becomes:

$$\frac{\partial c}{\partial t} + \frac{\partial (uc)}{\partial x} + \frac{\partial (vc)}{\partial y} + \frac{\partial (wc)}{\partial z} =$$

$$\frac{\partial}{\partial x}\left(\varepsilon_x \frac{\partial c}{x}\right) + \frac{\partial}{\partial y}\left(\varepsilon_y \frac{\partial c}{\partial y}\right) + \frac{\partial}{\partial z}\left(\varepsilon_z \frac{\partial c}{\partial z}\right) \qquad \text{(D.2)}$$

We now integrate the left-hand side of Equation D.2 term-by-term.

Term 1:

$$\iint_A \frac{\partial c}{\partial t}\, dA = \frac{\partial}{\partial t}(A\bar{c}) + \int_{y_1}^{y_2} \left(c(z_1) \frac{dz_1}{dt} - c(z_2) \frac{dz_2}{dt} \right) dy$$

where we define the overbar to denote a cross-sectional average, as in:

$$\frac{1}{A} \iint_A c\, dA = \bar{c}$$

Term 2:

$$\iint_A \frac{\partial (uc)}{\partial x}\, dA = \frac{\partial}{\partial x} \iint_A uc\, dA + \int_{y_1}^{y_2} \left(c(z_1)u(z_1)\frac{dz_1}{dx} - c(z_2)u(z_2)\frac{dz_2}{dx} \right) dy$$

Term 3:

$$\iint_A \frac{\partial (vc)}{\partial y}\, dA = \int_{z_1(y_2)}^{z_2(y_2)} v(y_2)c(y_2)\, dz - \int_{z_1(y_1)}^{z_2(y_2)} v(y_1)c(y_1)\, dz$$

$$+ \int_{y_1}^{y_2} \left(c(z_1)v(z_1)\frac{dz_1}{dy} - c(z_2)v(z_2)\frac{dz_2}{dy} \right) dy$$

Term 4:

$$\iint_A \frac{\partial (wc)}{\partial z}\, dA = \int_{y_1}^{y_2} \left(w(z_2)c(z_2) - w(z_1)c(z_1) \right) dy$$

In arriving at these integrals, we make repeated use of Liebnitz's rule in the manner described by Holley and Harleman (1965). If we gather together the expressions above, we have:

$$\frac{\partial}{\partial t}(\overline{Ac}) + \frac{\partial}{\partial x}\left(\iint_A ucdA \right) + \int_{y_1}^{y_2} \left(c(z_1)\left[\frac{dz_1}{dt} + u(z_1)\frac{dz_1}{dx} + v(z_1)\frac{dz_1}{dy} - w(z_1) \right] - \right.$$

$$\left. c(z_2)\left[\frac{dz_2}{dt} + u(z_2)\frac{dz_2}{dx} + v(z_2)\frac{dz_2}{dy} - w(z_2) \right] \right) dy$$

By the kinematic boundary condition, the two bracketed terms are zero, so that the integration of the left-hand side reduces to:

$$\frac{\partial}{\partial t}(\overline{Ac}) + \frac{\partial}{\partial x}\left(\iint_A ucdA \right)$$

We now integrate the right-hand side terms:

Term 5:

$$\iint_A \frac{\partial}{\partial x}\left(\varepsilon_x \frac{\partial u}{\partial x} \right) dA = \frac{\partial}{\partial x}\left(\iint_A \varepsilon_x \frac{\partial c}{\partial x}\, dA \right) + \int_{y_1}^{y_2} \left[\left(\varepsilon_x \frac{\partial c}{\partial x} \right)_{z_1} \frac{dz_1}{dx} - \left(\varepsilon_x \frac{\partial c}{\partial x} \right)_{z_2} \frac{dz_2}{dx} \right] dy$$

Since the bracketed term is small, this equals to good approximation:

$$\iint_A \frac{\partial}{\partial x}\left(\varepsilon_x \frac{\partial u}{\partial x} \right) dA = \frac{\partial}{\partial x}\left(\iint_A \varepsilon_x \frac{\partial c}{\partial x}\, dA \right)$$

Terms 6 and 7:

By Stoke's Theorem:

$$\iint_A \left[\frac{\partial}{\partial y} \left(\varepsilon_y \frac{\partial c}{\partial y} \right) + \frac{\partial}{\partial z} \left(\varepsilon_z \frac{\partial c}{\partial z} \right) \right] dA = \oint_B \left[\varepsilon_y \frac{\partial c}{\partial y} dz - \varepsilon_z \frac{\partial c}{\partial z} \right] dy$$

where B denotes the boundary of the cross-section.

The right-hand integral is the dispersive flux across the boundary, which is zero, so Terms 6 and 7 drop out of the equation.

The one-dimensional equation of mass conservation is thus:

$$\frac{\partial}{\partial t} (A\bar{c}) + \frac{\partial}{\partial x} \left(\iint_A ucdA \right) = \frac{\partial}{\partial x} \left(\iint_A \varepsilon_x \frac{\partial c}{\partial x} dA \right) \qquad (D.3)$$

We define u and c as the sum of a cross-sectional average and a derivative function, as for example:

$$c(x, y, z, t) = \bar{c}(x, t) + c''(x, y, z, t)$$

where,

$$\bar{c} = \frac{1}{A} \iint_A cdA$$

and,

$$\iint_A c''dA = 0$$

Substituting these expressions into Equation D.3, using the fact that

$$\iint_A c''\bar{u}dA = \iint_A \bar{c}u''dA = 0$$

and assuming

$$\iint_A \varepsilon_x'' \frac{\partial c''}{\partial x} dA \simeq 0$$

the equation becomes:

$$\frac{\partial}{\partial t}(A\bar{c}) + \frac{\partial}{\partial x}(A\overline{uc}) = \frac{\partial}{\partial x}(AE\frac{\partial \bar{c}}{\partial x}) - \frac{\partial}{\partial x}\left(\iint_A u''c''dA\right) \qquad (D.4)$$

where $E = \frac{1}{A}\iint_A \varepsilon_x dA$

By one-dimensional continuity

$$\frac{\partial A}{\partial t} + \frac{\partial(A\bar{u})}{\partial x} = 0$$

so Equation D.4 simplifies still further to:

$$\frac{\partial \bar{c}}{\partial t} + \bar{u}\frac{\partial \bar{c}}{\partial x} = \frac{1}{A}\left(\frac{\partial}{\partial x}(AE\frac{\partial \bar{c}}{\partial x})\right) - \frac{1}{A}\frac{\partial}{\partial x}\left(\iint_A u''c''dA\right) \qquad (D.5)$$

The last term in this expression is the longitudinal dispersion arising from deviations in the cross-sectional concentration and velocity distributions. By analogy with Fickian diffusion, it is assumed to take the form:

$$-\frac{1}{A}\frac{\partial}{\partial x}\left(\iint_A u''c''dA\right) = \frac{1}{A}\frac{\partial}{\partial x}\left(DA\frac{\partial \bar{c}}{\partial x}\right)$$

or

$$DA\frac{\partial \bar{c}}{\partial x} = -\iint_A u''c''dA \qquad (D.6)$$

where D is the longitudinal dispersion coefficient.

Therefore, we have

$$\frac{\partial \bar{c}}{\partial t} + \bar{u}\frac{\partial \bar{c}}{\partial x} = \frac{1}{A}\left(\frac{\partial}{\partial x}\left(A(D+E)\frac{\partial \bar{c}}{\partial x}\right)\right)$$

Usually, D is much larger than E, so that

$$\frac{\partial \bar{c}}{\partial t} + \bar{u}\frac{\partial \bar{c}}{\partial x} = \frac{1}{A}\left(\frac{\partial}{\partial x}\left(AD\frac{\partial \bar{c}}{\partial x}\right)\right) \qquad (D.7)$$

This is the one-dimensional equation for conservation of mass in its most common form.

D.2 Equation for the Dispersion Coefficient

In this section, we follow a derivation similar to Fischer's (1967) to derive an expression for the one-dimensional dispersion coefficient. We begin by returning to the original equation of three-dimensional mass conservation, Equation D.1, and transform to a moving coordinate system. Using the relations $\tau = t$ and $\xi = x - ut$, Equation D.1 becomes:

$$\frac{\partial c}{\partial \tau} + u'' \frac{\partial c}{\partial \xi} + v \frac{\partial c}{\partial y} + w \frac{\partial c}{\partial z} =$$

$$\frac{\partial}{\partial \xi}\left(\varepsilon_x \frac{\partial c}{\partial \xi}\right) + \frac{\partial}{\partial y}\left(\varepsilon_y \frac{\partial c}{\partial y}\right) + \frac{\partial}{\partial z}\left(\varepsilon_z \frac{\partial c}{\partial z}\right) \qquad \text{(D.8)}$$

If we make the assumption that c varies only slowly with z, a reasonable assumption for a shallow lake, and integrate Equation D.8 over the lake depth, we have:

$$\frac{\partial c}{\partial \tau} + \frac{q''}{h}\frac{\partial c}{\partial \xi} + \frac{V}{h}\frac{\partial c}{\partial y} = \frac{\partial}{\partial \xi}\left(\bar{E}_x \frac{\partial c}{\partial \xi}\right) + \frac{\partial}{\partial y}\left(\bar{E}_y \frac{\partial c}{\partial y}\right) \qquad \text{(D.9)}$$

where h is the lake depth,

$$q'' = \int_{-h}^{0} u''dz \qquad V = \int_{-h}^{0} v dz$$

$$\bar{E}_x = \frac{1}{h}\int_{-h}^{0} \varepsilon_x dz$$

Equation D.9 can be made non-dimensional using the following scaling quantities:

$$c^* = \frac{c}{C} \qquad \tau^* = \frac{\tau}{T}$$

$$\xi^* = \frac{\xi}{L} \qquad y^* = \frac{Y}{W} \qquad h^* = \frac{h}{H}$$

$$u^* = \frac{q''}{Hu_d} \qquad v^* = \frac{V}{Hv_d}$$

$$E_x^* = \frac{\overline{E}_x}{E} \qquad E_y^* = \frac{\overline{E}_y}{E}$$

where

C	is a reference concentration,
T	is a reference time period,
L	is the lake length (75 km),
W	is the lake width (8 km),
H	is the mean lake depth (3 m),
E	is a reference dispersion coefficient, and
u_d, v_d	are reference velocities.

We define the reference velocity u_d as the root-mean-square fluctuation velocity:

$$u_d = \sqrt{\overline{(u'')^2}}$$

where the overbar indicates a cross-sectional average. The value of u_d in Lake Balaton is very roughly 0.1 m/s. The lateral velocity v_d may be taken as the average lateral velocity over the cross-section, $\bar{v} \simeq 3$ cm/sec. The reference dispersion will be assumed to be 1 m^2/sec. Selection of a reference time is based upon a typical water quality transport time or residence time. The smallest applicable time is the time for lateral transport, $T \simeq W/\bar{v} \simeq 3$ days. Substitution of the scaling quantities into Equation D.9 leads to the following non-dimensional equation with indicated order-of-magnitude for each term:

$$\left[\frac{L}{u_d T}\right]\frac{\partial c^*}{\partial \tau^*} + u^*\frac{\partial c^*}{\partial \xi^*} + \left[\frac{L}{W}\frac{\bar{v}}{u_d}\right]v^*\frac{\partial c^*}{\partial y^*} = \left[\frac{E}{u_d L}\right]\frac{\partial}{\partial \xi^*}\left(E_x^*\frac{\partial c^*}{\partial \xi^*}\right) + \left[\frac{EL}{u_d W^2}\right]\frac{\partial}{\partial y^*}\left(E_y^*\frac{\partial c^*}{\partial y^*}\right)$$

$$3 \qquad 1 \qquad 3 \qquad 1 \times 10^{-4} \qquad 0.01$$

The scaling analysis establishes that the lateral advective term, , will dominate lateral diffusion, , in Lake Balaton. This is a significant departure from stream and estuarine situations where the reverse is usually assumed. As a result of this scaling analysis, it is justified to replace Equation D.9 with the simplified equation,

$$\frac{\partial c}{\partial \tau} + u''\frac{\partial c}{\partial \xi} = -v\frac{\partial c}{\partial y} \qquad \text{(D.10)}$$

The derivation continues following Fischer's (1967) general development, adapted to the form of Equation D.10. First, c is replace by $\bar{C} + c''$ in Equation D.10:

$$\frac{\partial \bar{c}}{\partial \tau} + \frac{\partial c''}{\partial \tau} + u''\frac{\partial \bar{c}}{\partial \xi} + u''\frac{\partial c''}{\partial \xi} = -v\frac{\partial \bar{c}}{\partial y} - v\frac{\partial c''}{\partial y}$$

This can be simplified by assuming, as Fischer,

$$\frac{\partial c''}{\partial \tau} \ll \frac{\partial \bar{c}}{\partial \tau} ,$$

$$u''\frac{\partial c''}{\partial \xi} \ll u''\frac{\partial \bar{c}}{\partial \xi} , \text{ and}$$

$$\frac{\partial \bar{c}}{\partial \tau} \ll u''\frac{\partial \bar{c}}{\partial \xi} .$$

Finally, by definition $\frac{\partial \bar{c}}{\partial y} = 0$.

The remaining equation is:

$$u'' \frac{\partial \bar{c}}{\partial \xi} = -v \frac{\partial c''}{\partial y} \qquad \text{(D.11)}$$

We integrate D.11 over the depth, assuming c'' varies slowly with z to get:

$$q'' \frac{\partial \bar{c}}{\partial \xi} = -V \frac{\partial c''}{\partial y} \qquad \text{(D.12)}$$

Solving for c'':

$$c''(y) = -\frac{\partial \bar{c}}{\partial \xi} \int_0^y \frac{q''}{V} dy \qquad \text{(D.13)}$$

By definition (Equation D.6)

$$DA \frac{\partial \bar{c}}{\partial x} = -\iint_A u''c''dA$$

Substituting Equation D.13 for c'' and rearranging:

$$D = \frac{1}{A} \iint_A u'' \left(\int_0^y \frac{q''}{V} dy \right) dA$$

Recognizing that only u" is a function of z, this can be simplified to the following expression for the dispersion coefficient D:

$$D = \frac{1}{A} \int_0^b dy\, q'' \int_0^y dy\, \frac{q''}{V} \qquad \text{(D.14)}$$

where b is the lake width.

This expression is directly analogous to that of Fischer (1967), but it proceeds from the assumption that advection rather than diffusion dominates lateral mixing.

We can construct a non-dimensional version of Equation D.14 in the same fashion as Fischer (1969) employing the following definitions:

$$f(y) = \frac{q''}{h\sqrt{\overline{(u'')^2}}}$$

$$y^* = \frac{y}{b}$$

$$g = \frac{V}{h\sqrt{\overline{v^2}}}$$

Substituting into Equation D.14 and gathering terms:

$$D = \frac{b\overline{u''^2}}{\sqrt{\overline{v^2}}} I \qquad \text{(D.15)}$$

where the term I is defined by the non-dimensional velocity distributions f and g:

$$I = \int_0^1 dy^* \, f(y^*) \int_0^y dy^* \, \frac{f(y^*)}{g(y^*)} \qquad \text{(D.16)}$$

The value of I is approximately 0.1 for typical velocity profiles.

APPENDIX E

INPUT DATA TO THE WATER QUALITY MODEL

GRID AND SECTION PROPERTIES FOR THE 40-GRID MODEL

GRID NUMBER	VOLUME (MIL M**3)	LENGTH (M)	SURFACE AREA (MIL SQ M)	DEPTH (M)
1	23.10	2900.	12.	1.88
2	26.50	1900.	12.	2.25
3	24.20	1900.	11.	2.18
4	25.30	1900.	11.	2.39
5	38.60	1900.	12.	3.27
6	54.20	1900.	16.	3.43
7	62.50	1900.	19.	3.36
8	58.40	1900.	20.	2.96
9	51.20	1900.	16.	3.26
10	44.60	1900.	15.	2.97
11	36.10	1900.	11.	3.37

SECTION NUMBER	SECTION AREA (K SQ M)	TOP WIDTH (M)
2	14.15	6200.
3	13.84	6100.
4	11.64	5200.
5	15.39	5200.
6	25.56	7700.
7	31.51	9300.
8	34.19	10700.
9	27.32	9600.
10	26.60	9100.
11	20.37	6600.

GRID AND SECTION PROPERTIES FOR THE 40-GRID MODEL

GRID NUMBER	VOLUME (MIL M**3)	LENGTH (M)	SURFACE AREA (MIL SQ M)	DEPTH (M)
12	33.90	1900.	12.	2.85
13	32.90	1900.	11.	2.96
14	33.70	1900.	11.	3.15
15	35.70	1900.	12.	3.00
16	34.30	1900.	10.	3.36
17	35.20	1900.	10.	3.52
18	42.40	1900.	12.	3.45
19	52.40	1900.	15.	3.56
20	57.40	1900.	16.	3.59
21	54.80	1900.	16.	3.51

SECTION NUMBER	SECTION AREA (K SQ M)	TOP WIDTH (M)
12	17.58	5700.
13	18.11	6300.
14	16.50	5800.
15	19.05	6500.
16	18.77	6000.
17	17.32	5200.
18	19.77	5800.
19	24.91	7100.
20	30.30	8300.
21	30.13	8600.

GRID AND SECTION PROPERTIES FOR THE 40-GRID MODEL

GRID NUMBER	VOLUME (MIL M**3)	LENGTH (M)	SURFACE AREA (MIL SQ M)	DEPTH (M)
22	50.20	1900.	14.	3.56
23	48.30	1900.	13.	3.63
24	48.10	1900.	14.	3.56
25	47.60	1900.	14.	3.31
26	36.40	1900.	14.	2.56
27	21.30	1900.	7.	2.92
28	20.90	1900.	9.	2.37
29	44.60	1900.	16.	2.88
30	55.60	1900.	16.	3.47
31	62.20	1900.	16.	3.86

SECTION NUMBER	SECTION AREA (K SQ M)	TOP WIDTH (M)
22	27.66	8000.
23	25.33	7300.
24	25.48	7200.
25	25.38	7200.
26	25.02	7600.
27	16.55	7200.
28	4.30	1800.
29	21.02	7300.
30	27.35	8400.
31	31.69	9600.

GRID AND SECTION PROPERTIES FOR THE 40-GRID MODEL

GRID NUMBER	VOLUME (MIL M**3)	LENGTH (M)	SURFACE AREA (MIL SQ M)	DEPTH (M)
32	65.10	1900.	16.	4.04
33	68.00	1900.	18.	3.78
34	74.70	1900.	19.	3.95
35	87.40	1900.	23.	3.85
36	98.40	1900.	24.	4.12
37	99.40	1900.	28.	3.61
38	80.90	1900.	21.	3.83
39	47.00	1900.	15.	3.18
40	13.90	1500.	5.	2.78

SECTION NUMBER	SECTION AREA (K SQ M)	TOP WIDTH (M)
32	33.92	9400.
33	34.65	9200.
34	36.92	9500.
35	41.96	10600.
36	50.10	12500.
37	53.55	13900.
38	51.69	14300.
39	33.68	9300.
40	16.87	5400.

MONTHLY FLOW AND LOADING DATA FOR THE 40-GRID MODEL

	JAN.	FEB.	MAR.	APR.	MAY	JUNE	JULY	AUG.	SEPT	OCT.	NOV.	DEC.	
GRID 1													
INFLOW	15.4	20.2	11.6	12.9	5.0	2.8	2.4	2.4	2.1	3.6	5.1	5.6	CMS
OUTFLOW	0.0	0.0	0.0	0.0	0.0	0.0	0.0	0.0	0.0	0.0	0.0	0.0	CMS
FACE 2													
MEAN FLOW	15.7	20.1	11.8	12.4	4.9	2.8	2.3	2.3	2.1	3.5	4.9	5.5	CMS
GRID 2													
INFLOW	0.0	0.0	0.0	0.0	0.0	0.0	0.0	0.0	0.0	0.0	0.0	0.0	CMS
OUTFLOW	0.0	0.0	0.0	0.0	0.0	0.0	0.0	0.0	0.0	0.0	0.0	0.0	CMS
FACE 3													
MEAN FLOW	16.0	20.1	12.0	11.9	4.8	2.7	2.2	2.2	2.1	3.4	4.8	5.5	CMS
GRID 3													
INFLOW	0.0	0.0	0.0	0.0	0.0	0.0	0.0	0.0	0.0	0.0	0.0	0.0	CMS
OUTFLOW	0.0	0.0	0.0	0.0	0.0	0.0	0.0	0.0	0.0	0.0	0.0	0.0	CMS
FACE 4													
MEAN FLOW	16.3	20.0	12.1	11.4	4.6	2.7	2.1	2.1	2.1	3.3	4.7	5.5	CMS
GRID 4													
INFLOW	0.0	0.0	0.0	0.0	0.0	0.0	0.0	0.0	0.0	0.0	0.0	0.0	CMS
OUTFLOW	0.0	0.0	0.0	0.0	0.0	0.0	0.0	0.0	0.0	0.0	0.0	0.0	CMS
FACE 5													
MEAN FLOW	16.6	19.9	12.3	11.0	4.5	2.6	2.0	2.0	2.1	3.3	4.5	5.4	CMS
GRID 5													
INFLOW	3.4	4.4	2.6	2.8	1.1	0.6	0.5	0.5	0.5	0.8	1.1	1.2	CMS
OUTFLOW	0.0	0.0	0.0	0.0	0.0	0.0	0.0	0.0	0.0	0.0	0.0	0.0	CMS
FACE 6													
MEAN FLOW	20.3	24.3	15.0	13.3	5.5	3.2	2.5	2.5	2.6	4.0	5.5	6.6	CMS
GRID 6													
INFLOW	0.0	0.0	0.0	0.0	0.0	0.0	0.0	0.0	0.0	0.0	0.0	0.0	CMS
OUTFLOW	0.0	0.0	0.0	0.0	0.0	0.0	0.0	0.0	0.0	0.0	0.0	0.0	CMS
FACE 7													
MEAN FLOW	20.7	24.2	15.2	12.6	5.3	3.1	2.3	2.3	2.6	3.9	5.3	6.5	CMS

MONTHLY FLOW AND LOADING DATA FOR THE 40-GRID MODEL

	JAN.	FEB.	MAR.	APR.	MAY	JUNE	JULY	AUG.	SEPT	OCT.	NOV.	DEC.	
GRID 7													
INFLOW	0.0	0.0	0.0	0.0	0.0	0.0	0.0	0.0	0.0	0.0	0.0	0.0	CMS
OUTFLOW	0.0	0.0	0.0	0.0	0.0	0.0	0.0	0.0	0.0	0.0	0.0	0.0	CMS
FACE 8													
MEAN FLOW	21.2	24.1	15.5	11.8	5.2	3.1	2.2	2.2	2.6	3.7	5.1	6.4	CMS
GRID 8													
INFLOW	5.4	7.1	4.1	4.5	1.8	1.0	0.8	0.8	0.7	1.3	1.8	2.0	CMS
OUTFLOW	0.0	0.0	0.0	0.0	0.0	0.0	0.0	0.0	0.0	0.0	0.0	0.0	CMS
FACE 9													
MEAN FLOW	27.1	31.1	19.9	15.5	6.7	4.0	2.9	2.9	3.3	4.9	6.6	8.3	CMS
GRID 9													
INFLOW	0.0	0.0	0.0	0.0	0.0	0.0	0.0	0.0	0.0	0.0	0.0	0.0	CMS
OUTFLOW	0.0	0.0	0.0	0.0	0.0	0.0	0.0	0.0	0.0	0.0	0.0	0.0	CMS
FACE 10													
MEAN FLOW	27.5	31.0	20.1	14.9	6.6	3.9	2.8	2.8	3.3	4.7	6.4	8.3	CMS
GRID 10													
INFLOW	1.0	1.3	0.7	0.8	0.3	0.2	0.2	0.2	0.1	0.2	0.3	0.4	CMS
OUTFLOW	0.0	0.0	0.0	0.0	0.0	0.0	0.0	0.0	0.0	0.0	0.0	0.0	CMS
FACE 11													
MEAN FLOW	28.9	32.1	21.1	15.0	6.7	4.1	2.8	2.8	3.5	4.9	6.6	8.5	CMS
GRID 11													
INFLOW	0.0	0.0	0.0	0.0	0.0	0.0	0.0	0.0	0.0	0.0	0.0	0.0	CMS
OUTFLOW	0.0	0.0	0.0	0.0	0.0	0.0	0.0	0.0	0.0	0.0	0.0	0.0	CMS
FACE 12													
MEAN FLOW	29.2	32.1	21.2	14.6	6.6	4.0	2.7	2.7	3.5	4.8	6.4	8.5	CMS
GRID 12													
INFLOW	1.1	1.4	0.8	0.9	0.3	0.2	0.2	0.2	0.1	0.3	0.4	0.4	CMS
OUTFLOW	0.0	0.0	0.0	0.0	0.0	0.0	0.0	0.0	0.0	0.0	0.0	0.0	CMS
FACE 13													
MEAN FLOW	30.6	33.4	22.2	15.0	6.8	4.2	2.8	2.8	3.6	4.9	6.6	8.8	CMS
GRID 13													
INFLOW	0.0	0.0	0.0	0.0	0.0	0.0	0.0	0.0	0.0	0.0	0.0	0.0	CMS
OUTFLOW	0.0	0.0	0.0	0.0	0.0	0.0	0.0	0.0	0.0	0.0	0.0	0.0	CMS

MONTHLY FLOW AND LOADING DATA FOR THE 40-GRID MODEL

	JAN.	FEB.	MAR.	APR.	MAY	JUNE	JULY	AUG.	SEPT	OCT.	NOV.	DEC.	
FACE 14													
MEAN FLOW	30.9	33.4	22.4	14.5	6.7	4.1	2.7	2.7	3.6	4.9	6.5	8.8	CMS
GRID 14													
INFLOW	0.4	0.5	0.3	0.3	0.1	0.1	0.1	0.1	0.0	0.1	0.1	0.1	CMS
OUTFLOW	0.0	0.0	0.0	0.0	0.0	0.0	0.0	0.0	0.0	0.0	0.0	0.0	CMS
FACE 15													
MEAN FLOW	31.5	33.8	22.8	14.4	6.7	4.1	2.7	2.7	3.7	4.9	6.5	8.9	CMS
GRID 15													
INFLOW	0.0	0.0	0.0	0.0	0.0	0.0	0.0	0.0	0.0	0.0	0.0	0.0	CMS
OUTFLOW	0.0	0.0	0.0	0.0	0.0	0.0	0.0	0.0	0.0	0.0	0.0	0.0	CMS
FACE 16													
MEAN FLOW	31.8	33.7	23.0	13.8	6.6	4.1	2.6	2.6	3.7	4.8	6.3	8.8	CMS
GRID 16													
INFLOW	0.3	0.3	0.2	0.2	0.1	0.0	0.0	0.0	0.0	0.1	0.1	0.1	CMS
OUTFLOW	0.0	0.0	0.0	0.0	0.0	0.0	0.0	0.0	0.0	0.0	0.0	0.0	CMS
FACE 17													
MEAN FLOW	32.3	34.0	23.3	13.6	6.6	4.1	2.5	2.5	3.7	4.8	6.3	8.9	CMS
GRID 17													
INFLOW	0.0	0.0	0.0	0.0	0.0	0.0	0.0	0.0	0.0	0.0	0.0	0.0	CMS
OUTFLOW	0.0	0.0	0.0	0.0	0.0	0.0	0.0	0.0	0.0	0.0	0.0	0.0	CMS
FACE 18													
MEAN FLOW	32.6	33.9	23.5	13.2	6.5	4.1	2.5	2.5	3.7	4.7	6.2	8.8	CMS
GRID 18													
INFLOW	0.0	0.0	0.0	0.0	0.0	0.0	0.0	0.0	0.0	0.0	0.0	0.0	CMS
OUTFLOW	0.0	0.0	0.0	0.0	0.0	0.0	0.0	0.0	0.0	0.0	0.0	0.0	CMS
FACE 19													
MEAN FLOW	32.9	33.8	23.7	12.7	6.4	4.0	2.4	2.4	3.7	4.6	6.0	8.8	CMS
GRID 19													
INFLOW	0.5	0.7	0.4	0.4	0.2	0.1	0.1	0.1	0.1	0.1	0.2	0.2	CMS
OUTFLOW	0.0	0.0	0.0	0.0	0.0	0.0	0.0	0.0	0.0	0.0	0.0	0.0	CMS

MONTHLY FLOW AND LOADING DATA FOR THE 40-GRID MODEL

	JAN.	FEB.	MAR.	APR.	MAY	JUNE	JULY	AUG.	SEPT	OCT.	NOV.	DEC.	
FACE 20													
MEAN FLOW	33.8	34.5	24.3	12.5	6.4	4.1	2.3	2.3	3.8	4.6	6.0	8.9	CMS
GRID 20													
INFLOW	0.5	0.6	0.3	0.4	0.1	0.1	0.1	0.1	0.1	0.1	0.1	0.2	CMS
OUTFLOW	0.0	0.0	0.0	0.0	0.0	0.0	0.0	0.0	0.0	0.0	0.0	0.0	CMS
FACE 21													
MEAN FLOW	34.7	35.0	24.9	12.2	6.4	4.1	2.3	2.3	3.8	4.6	6.0	9.0	CMS
GRID 21													
INFLOW	0.0	0.0	0.0	0.0	0.0	0.0	0.0	0.0	0.0	0.0	0.0	0.0	CMS
OUTFLOW	0.0	0.0	0.0	0.0	0.0	0.0	0.0	0.0	0.0	0.0	0.0	0.0	CMS
FACE 22													
MEAN FLOW	35.1	34.9	25.1	11.5	6.2	4.0	2.1	2.1	3.8	4.5	5.8	8.9	CMS
GRID 22													
INFLOW	0.0	0.0	0.0	0.0	0.0	0.0	0.0	0.0	0.0	0.0	0.0	0.0	CMS
OUTFLOW	0.0	0.0	0.0	0.0	0.0	0.0	0.0	0.0	0.0	0.0	0.0	0.0	CMS
FACE 23													
MEAN FLOW	35.5	34.8	25.3	10.9	6.1	4.0	2.0	2.0	3.8	4.4	5.6	8.9	CMS
GRID 23													
INFLOW	0.3	0.4	0.2	0.3	0.1	0.1	0.1	0.1	0.0	0.1	0.1	0.1	CMS
OUTFLOW	0.0	0.0	0.0	0.0	0.0	0.0	0.0	0.0	0.0	0.0	0.0	0.0	CMS
FACE 24													
MEAN FLOW	36.2	35.1	25.8	10.7	6.0	4.0	2.0	2.0	3.9	4.4	5.5	8.9	CMS
GRID 24													
INFLOW	0.0	0.0	0.0	0.0	0.0	0.0	0.0	0.0	0.0	0.0	0.0	0.0	CMS
OUTFLOW	0.0	0.0	0.0	0.0	0.0	0.0	0.0	0.0	0.0	0.0	0.0	0.0	CMS
FACE 25													
MEAN FLOW	36.5	35.0	26.0	10.1	5.9	3.9	1.9	1.9	3.9	4.3	5.4	8.9	CMS
GRID 25													
INFLOW	0.0	0.0	0.0	0.0	0.0	0.0	0.0	0.0	0.0	0.0	0.0	0.0	CMS
OUTFLOW	0.0	0.0	0.0	0.0	0.0	0.0	0.0	0.0	0.0	0.0	0.0	0.0	CMS

MONTHLY FLOW AND LOADING DATA FOR THE 40-GRID MODEL

	JAN.	FEB.	MAR.	APR.	MAY	JUNE	JULY	AUG.	SEPT	OCT.	NOV.	DEC.	
FACE 26													
MEAN FLOW	36.9	35.0	26.2	9.5	5.7	3.9	1.8	1.8	3.9	4.2	5.2	8.8	CMS
GRID 26													
INFLOW	0.4	0.6	0.3	0.4	0.1	0.1	0.1	0.1	0.1	0.1	0.1	0.2	CMS
OUTFLOW	0.0	0.0	0.0	0.0	0.0	0.0	0.0	0.0	0.0	0.0	0.0	0.0	CMS
FACE 27													
MEAN FLOW	37.7	35.4	26.7	9.2	5.7	3.9	1.7	1.7	4.0	4.2	5.1	8.9	CMS
GRID 27													
INFLOW	0.0	0.0	0.0	0.0	0.0	0.0	0.0	0.0	0.0	0.0	0.0	0.0	CMS
OUTFLOW	0.0	0.0	0.0	0.0	0.0	0.0	0.0	0.0	0.0	0.0	0.0	0.0	CMS
FACE 28													
MEAN FLOW	37.9	35.4	26.8	8.9	5.7	3.9	1.7	1.7	4.0	4.1	5.1	8.9	CMS
GRID 28													
INFLOW	0.0	0.0	0.0	0.0	0.0	0.0	0.0	0.0	0.0	0.0	0.0	0.0	CMS
OUTFLOW	0.0	0.0	0.0	0.0	0.0	0.0	0.0	0.0	0.0	0.0	0.0	0.0	CMS
FACE 29													
MEAN FLOW	38.1	35.3	26.9	8.5	5.6	3.9	1.6	1.6	4.0	4.1	4.9	8.9	CMS
GRID 29													
INFLOW	0.0	0.0	0.0	0.0	0.0	0.0	0.0	0.0	0.0	0.0	0.0	0.0	CMS
OUTFLOW	0.0	0.0	0.0	0.0	0.0	0.0	0.0	0.0	0.0	0.0	0.0	0.0	CMS
FACE 30													
MEAN FLOW	38.5	35.2	27.2	7.9	5.4	3.8	1.5	1.5	4.0	4.0	4.8	8.8	CMS
GRID 30													
INFLOW	0.0	0.0	0.0	0.0	0.0	0.0	0.0	0.0	0.0	0.0	0.0	0.0	CMS
OUTFLOW	0.0	0.0	0.0	0.0	0.0	0.0	0.0	0.0	0.0	0.0	0.0	0.0	CMS
FACE 31													
MEAN FLOW	38.9	35.1	27.4	7.2	5.2	3.7	1.3	1.3	4.0	3.9	4.6	8.7	CMS
GRID 31													
INFLOW	0.2	0.2	0.1	0.1	0.0	0.0	0.0	0.0	0.0	0.0	0.0	0.1	CMS
OUTFLOW	0.0	0.0	0.0	0.0	0.0	0.0	0.0	0.0	0.0	0.0	0.0	0.0	CMS

MONTHLY FLOW AND LOADING DATA FOR THE 40-GRID MODEL

	JAN.	FEB.	MAR.	APR.	MAY	JUNE	JULY	AUG.	SEPT	OCT.	NOV.	DEC.	
FACE 32													
MEAN FLOW	39.5	35.2	27.8	6.6	5.1	3.7	1.2	1.2	4.0	3.8	4.4	8.7	CMS
GRID 32													
INFLOW	0.2	0.2	0.1	0.1	0.0	0.0	0.0	0.0	0.0	0.0	0.0	0.1	CMS
OUTFLOW	0.0	0.0	0.0	0.0	0.0	0.0	0.0	0.0	0.0	0.0	0.0	0.0	CMS
FACE 33													
MEAN FLOW	40.1	35.3	28.1	6.1	5.0	3.7	1.1	1.1	4.0	3.7	4.3	8.7	CMS
GRID 33													
INFLOW	0.0	0.0	0.0	0.0	0.0	0.0	0.0	0.0	0.0	0.0	0.0	0.0	CMS
OUTFLOW	44.5	35.0	30.7	0.0	3.6	3.2	0.0	0.0	4.1	2.7	2.5	8.2	CMS
FACE 34													
MEAN FLOW	-3.9	0.2	-2.3	5.3	1.2	0.4	1.0	1.0	-0.1	0.9	1.5	0.4	CMS
GRID 34													
INFLOW	0.0	0.0	0.0	0.0	0.0	0.0	0.0	0.0	0.0	0.0	0.0	0.0	CMS
OUTFLOW	0.0	0.0	0.0	0.0	0.0	0.0	0.0	0.0	0.0	0.0	0.0	0.0	CMS
FACE 35													
MEAN FLOW	-3.4	0.1	-2.0	4.5	1.0	0.3	0.8	0.8	-0.1	0.7	1.3	0.3	CMS
GRID 35													
INFLOW	0.0	0.0	0.0	0.0	0.0	0.0	0.0	0.0	0.0	0.0	0.0	0.0	CMS
OUTFLOW	0.0	0.0	0.0	0.0	0.0	0.0	0.0	0.0	0.0	0.0	0.0	0.0	CMS
FACE 36													
MEAN FLOW	-2.9	0.0	-1.7	3.6	0.8	0.3	0.7	0.7	-0.1	0.6	1.0	0.2	CMS
GRID 36													
INFLOW	0.0	0.1	0.0	0.0	0.0	0.0	0.0	0.0	0.0	0.0	0.0	0.0	CMS
OUTFLOW	0.0	0.0	0.0	0.0	0.0	0.0	0.0	0.0	0.0	0.0	0.0	0.0	CMS
FACE 37													
MEAN FLOW	-2.2	-0.1	-1.3	2.6	0.6	0.2	0.5	0.5	-0.1	0.4	0.7	0.2	CMS
GRID 37													
INFLOW	0.4	0.5	0.3	0.3	0.1	0.1	0.1	0.1	0.1	0.1	0.1	0.1	CMS
OUTFLOW	0.0	0.0	0.0	0.0	0.0	0.0	0.0	0.0	0.0	0.0	0.0	0.0	CMS

MONTHLY FLOW AND LOADING DATA FOR THE 40-GRID MODEL

	JAN.	FEB.	MAR.	APR.	MAY	JUNE	JULY	AUG.	SEPT	OCT.	NOV.	DEC.	
FACE 38													
MEAN FLOW	-1.1	0.2	-0.6	1.7	0.4	0.2	0.3	0.3	0.0	0.3	0.5	0.2	CMS
GRID 38													
INFLOW	0.0	0.0	0.0	0.0	0.0	0.0	0.0	0.0	0.0	0.0	0.0	0.0	CMS
OUTFLOW	0.0	0.0	0.0	0.0	0.0	0.0	0.0	0.0	0.0	0.0	0.0	0.0	CMS
FACE 39													
MEAN FLOW	-0.5	0.1	-0.3	0.8	0.2	0.1	0.2	0.2	0.0	0.1	0.2	0.1	CMS
GRID 39													
INFLOW	0.0	0.0	0.0	0.0	0.0	0.0	0.0	0.0	0.0	0.0	0.0	0.0	CMS
OUTFLOW	0.0	0.0	0.0	0.0	0.0	0.0	0.0	0.0	0.0	0.0	0.0	0.0	CMS
FACE 40													
MEAN FLOW	-0.1	0.0	-0.1	0.2	0.1	0.0	0.0	0.0	0.0	0.0	0.1	0.0	CMS
GRID 40													
INFLOW	0.0	0.0	0.0	0.0	0.0	0.0	0.0	0.0	0.0	0.0	0.0	0.0	CMS
OUTFLOW	0.0	0.0	0.0	0.0	0.0	0.0	0.0	0.0	0.0	0.0	0.0	0.0	CMS

GRID AND SECTION PROPERTIES FOR THE 4-BOX MODEL

GRID NUMBER	VOLUME (MIL M**3)	LENGTH (M)	SURFACE AREA (MIL SQ M)	DEPTH (M)
1	82.00	7000.	38.	2.16
2	413.00	22000.	144.	2.87
3	600.00	23000.	186.	3.23
4	802.00	23000.	228.	3.52

SECTION NUMBER	SECTION AREA (K SQ M)	TOP WIDTH (M)
2	15.40	5200.
3	17.30	5200.
4	4.30	1800.

MONTHLY FLOW AND LOADING DATA FOR THE 4-BOX MODEL

	JAN.	FEB.	MAR.	APR.	MAY	JUNE	JULY	AUG.	SEPT	OCT.	NOV.	DEC.	
GRID 1													
INFLOW	15.4	20.2	11.6	12.9	5.0	2.8	2.4	2.3	2.1	3.6	5.1	5.6	CMS
OUTFLOW	0.0	0.0	0.0	0.0	0.0	0.0	0.0	0.0	0.0	0.0	0.0	0.0	CMS
FACE 2													
MEAN FLOW	17.1	19.7	10.7	11.5	8.2	6.3	6.6	3.6	3.6	4.6	6.5	5.3	CMS
GRID 2													
INFLOW	0.0	0.0	0.0	0.0	0.0	0.0	0.0	0.0	0.0	0.0	0.0	0.0	CMS
OUTFLOW	0.0	0.0	0.0	0.0	0.0	0.0	0.0	0.0	0.0	0.0	0.0	0.0	CMS
FACE 3													
MEAN FLOW	30.2	31.0	19.5	13.4	10.4	8.1	7.6	4.2	5.1	6.0	8.1	8.1	CMS
GRID 3													
INFLOW	0.0	0.0	0.0	0.0	0.0	0.0	0.0	0.0	0.0	0.0	0.0	0.0	CMS
OUTFLOW	0.0	0.0	0.0	0.0	0.0	0.0	0.0	0.0	0.0	0.0	0.0	0.0	CMS
FACE 4													
MEAN FLOW	37.7	34.1	25.2	8.2	7.9	6.4	4.7	2.6	4.9	4.8	6.1	8.5	CMS
GRID 4													
INFLOW	0.0	0.0	0.0	0.0	0.0	0.0	0.0	0.0	0.0	0.0	0.0	0.0	CMS
OUTFLOW	44.5	35.0	30.7	0.0	3.6	3.2	0.0	0.0	4.1	2.7	2.5	8.2	CMS

REFERENCES

Abbott, M.B., "Computational Hydraulics: A Short Pathology," Journal of Hydraulic Research, 14:4, 271, 1976.

Abbott, M.B. and C.H. Rasmussen, "On the Numerical Modeling of Rapid Expansions and Contractions that are Two-Dimensional in Flow," Hydraulic Engineering for Improved Water Management, 17th Congress, International Association for Hydraulic Research, Baden-Baden, Paper A104, Volume 2, page 229, Germany, August, 1977.

Babajimopoulus, C. and K.W. Bedford, "Formulating Lake Models which Preserve Spectral Statistics," ASCE, Journal of the Hydraulics Division, 106:HY1, 1, January 1980.

Banks, R.B., "Some Features of Wind Action on Shallow Lakes," ASCE, Journal of the Environmental Engineering Division, 101:EE5, 813, October 1975.

Baranyi, S., "Method of Determining the Turnover Time of the Water Resources of Lakes with an Outlet," Hydrology of Lakes Symposium, Helsinki, IAHS-AISH Publication 109, page 54, July 1973 a.

Baranyi, S., "The Use of Tritium Measurement in the Investigation of Lake Balaton," Hydrology of Lakes Symposium, Helsinki, IAHS-AISH Publication 109, page 28, July 1973 b.

Bedford, K.W. and I.S. Rai, "Efficient Pressure Solutions for Circulation Prediction," ASCE, Journal of the Hydraulics Division, 104: HY6, 899, June 1978.

Bella, D.A. and W.J. Grenney, "Finite-Difference Convection Errors," ASCE, Journal of the Sanitary Engineering Division, 96:SA6, 1361, December 1970.

Bengtsson, L., "Mathematical Models of Wind Induced Circulation in a Lake," Hydrology of Lakes Symposium, IAHS-AISH Publication 109, Helsinki, 1973.

Bhomik, N.G. and J.B. Stall, "Circulation Patterns in the Fox Chain of Lakes in Illinois," Water Resources Research, 14:4, 633, August 1978.

Bonham-Carter, G. and J.H. Thomas, "Numerical Calculation of Steady Wind-Driven Currents in Lake Ontario and Rochester Embayment," Proceedings of the 16th Conference on Great Lakes Research, page 640, 1973.

Boyce, F.M., A.S. Fraser, E. Halfon, D. Hyde, D.C.L. Lam, W.M. Schertzer, A.H. Al-Shaarawi, T.J. Simons, K. Wilson and D. Warry, "Assessment of Water Quality Capability for Lake Ontario," Scientific Series No. 111, Inland Waters Directorate, National Water Research Institute, Canada Centre for Inland Waters, Burlington, Ontario, 1979.

Brown, R.T., "Effects of Data Variability and Model Structure on Reservoir Ecosystem Simulation," Ph.D. Thesis, Department of Civil Engineering, Massachusetts Institute of Technology, Cambridge, Massachusetts, April 3, 1978.

Bryan, K., "A Numerical Method for the Circulation of the World Ocean," Journal of Computational Physics, 4:3, 347, October 1969.

Bye, J.A.T., "Wind-Driven Circulation in Unstratified Lakes," Limnology and Oceanography, 10, 451, 1965.

Chatwin, P.C., "On the Longitudinal Dispersion of Passive Contaminant in Oscillatory Flow in Tubes," Journal of Fluid Mechanics, 71:3, 513, 1975.

Chen, C.W., M. Lorenzen and D.J. Smith, "A Comprehensive Water Quality-Ecological Model for Lake Ontario," NTIS Report No. PB 258 064, Great Lakes Environmental Research Laboratory, National Oceanic and Space Administration, October 1975.

Chen, C.W. and D.J. Smith, "Preliminary Insights into a Three-Dimensional Ecological-Hydrodynamic Model," in Perspectives on Lake Ecosystem Modeling edited by D. Scavia and A. Robertson, Ann Arbor Science Publishers, Inc., Ann Arbor, Michigan, 1979.

Cheng, R.T., T.M. Powell and T.M. Dillon, "Numerical Models of Wind-Driven Circulation in Lakes," Applied Mathematical Modeling, 1, 141, December 1976.

Cheng, R.T. and C. Tung, "Wind Driven Circulation by the Finite Element Method," Proceedings of the 13th Conference on Great Lakes Research, page 891, 1970.

Csáki, P. and T. Kutas, "The BEM Modeling Approach II: Model Development in the Lake Balaton Ecosystem," Proceedings of the Second Joint MTA/IIASA Task Force Meeting on Lake Balaton Modeling, August 27-30, 1979, Veszprém, Hungary, edited by G. van Straten, S. Herodek, J. Fischer and I. Kovács, Hungarian Academy of Sciences, Veszprém, Hungary, Volume I, page 94, 1980.

Dailey, J.E. and D.R.F. Harleman, "Numerical Model for Prediction of Transient Water Quality in Estuary Networks," Report Number 158, Ralph M. Parsons Laboratory for Water Resources and Hydrodynamics, Department of Civil Engineering, Massachusetts Institute of Technology, Cambridge, Massachusetts, October 1972.

Deardroff, J.W., "On the Magnitude of the Subgrid Scale Eddy Coefficient," Journal of Computational Physics, 7:1, 120, February 1971.

DiToro, D.M. and J.P. Connolly, "Mathematical Models of Water Quality in Large Lakes, Part 2: Lake Erie," Report EPA-600/3-80-065, United States Environmental Protection Agency, July 1980.

DiToro, D.M. and W.F. Matystik, Jr., "Mathematical Models of Water Quality in Large Lakes, Part 1: Lake Huron and Saginaw Bay," Report EPA-600/3-80-056, United States Environmental Protection Agency, July 1980.

Dobolyi, E., "Data on the Bottom Sediment in Lake Balaton," Proceedings of the Second Joint MTA/IIASA Task Force Meeting on Lake Balaton Modeling, August 27-30, 1979, Veszprém, Hungary, edited by G. van Straten, S. Herodek, J. Fischer and I. Kovács, Hungarian Academy of Sciences, Veszprém, Hungary, Volume II, page 66, 1980.

Dobolyi, E. and S. Herodek, "On the Mechanism Reducing the Phosphate Concentration in the Water of Lake Balaton," Internationale Revue des gesamten Hydrobiologie, 65:3, 339, 1980.

Edinger, J.E. and E.M. Buchak, "Reservoir Longitudinal and Vertical Implicit Hydrodynamics," in Environmental Effects of Hydraulic Engineering Works, Proceedings of an International Symposium held at Knoxville, Tennessee, September 12-14, 1978, edited by E.E. Driver and W.O. Wunderlich, Tennessee Valley Authority, Knoxville, Tennessee, 1979.

Engelund, F., "Effect of Lateral Wind on Uniform Channel Flow," Progress Report 45, Institute of Hydrodynamic and Hydraulic Engineering, Technical University of Denmark, page 33, April 1978.

Entz, B., "Regional and Circadian Oxygen Determination in Lake Balaton Concerning the Eutrophication of the Lake," Annales Instituti Biologici (Tihany), 43, 69, 1976.

Fischer, H.B., "A Note on the One-dimensional Dispersion Model," International Journal of Air and Water Pollution, 10, 443, June/July 1966.

Fischer, H.B., "The Mechanics of Dispersion in Natural Streams," ASCE, Journal of the Hydraulics Division, 93:HY6, 187, November 1967.

Fischer, H.B., "Cross-Sectional Time Scales and Dispersion in Estuaries," 13th Congress of the IAHR, Kyoto, Japan, Paper C19, Volume 3, page 173, August 31-September 5, 1969.

Ford, D.E. and K.W. Thornton, "Time and Length Scales for the One-Dimensional Assumption and Its Relation to Ecological Models," Water Resources Research, 15:1, 113, February 1979.

Gallagher, R.H., J.A. Liggett and S.T.K. Chan, "Finite Element Shallow Lake Circulation," ASCE, Journal of the Hydraulics Division, 99:HY7, 1083, July, 1973.

Gedney, R.T. and W. Lick, "Wind-Driven Currents in Lake Erie," Journal of Geophysical Research, 77:15, 2714, May 20, 1972.

Golterman, H.L., "Natural Phosphate Sources in Relation to Phosphate Budgets: A Contribution to the Understanding of Eutrophication," Water Research, 7:1/2, 3, January/February 1973.

Gourlay, A.R. and A.R. Mitchell, "The Equivalence of Certain Alternating Direction and Locally One-Dimensional Difference Methods," SIAM Journal of Numerical Analysis, 6:1, 37, March 1969 a.

Gourlay, A.R. amd A.R. Mitchell, "A Classification of Split Difference Methods for Hyperbolic Equations in Several Space Dimensions," SIAM Journal of Numerical Analysis, 6:1, 62, March 1969 b.

Gourlay, A.R. amd A.R. Mitchell, "On the Structure of Certain Alternating Direction Implicit (A.D.I.) and Locally One-Dimensional (L.O.D.) Difference Methods," Journal of the Institute of Mathematics and its Applications, 9:1, 80, February 1972.

Győrke, O., "Studies into the Factors Affecting the Morphological Processes in Shallow Lakes by Means of a Hydraulic Model," Fundamental Tools to be Used in Environmental Problems, 16th Congress, IAHR, São Paulo, Brazil, Paper B4, Volume 2, page 24, July 27-August 1, 1975.

Hamblin, P. F. and J.R. Salmon, "On the Vertical Transfer of Momentum in a Lake," Memoires Societe Royale des Sciences de Liege, 6e serie, tome VII, page 211, 1975.

Hamvas, F., "Investigations into the Erosion of Shore at Lake Balaton," Hydrology of Lakes and Reservoirs, Symposium of Garda, IAHS-AISH Publication Number 70, page 473, October 1966.

Haq, A. and W. Lick, "On the Time-Dependent Flow in a Lake," Journal of Geophysical Research, 80:3, 431, January 20, 1975.

Harleman, D.R.F., "One-Dimensional Models," in "Estuarine Modeling: An Assessment," edited by G.H. Ward and W.H. Espey, Report 16070 DZV 02/71, United States Environmental Protection Agency, February 1971.

Harleman, D.R.F. and P. Shanahan, "Aspects of Wind-Driven Circulation and Mixing in Eutrophication Studies of Lake Balaton," Proceedings of the Second Joint MTA/IIASA Task Force Meeting on Lake Balaton Modeling, August 27-30, 1979, Veszprém, Hungary, edited by G. van Straten, S. Herodek, J. Fischer and I. Kovács, Hungarian Academy of Sciences, Veszprém, Hungary, Volume I, page 50, 1980.

Herodek, S. and P. Csáki, "The BEM Modeling Approach I: Ecological Aspects of the Lake Balaton Eutrophication Model," Proceedings of the Second Joint MTA/IIASA Task Force Meeting on Lake Balaton Modeling, August 27-30, 1979, Veszprém, Hungary, edited by G. van Straten, S. Herodek, J. Fischer and I. Kovács, Hungarian Academy of Sciences, Veszprém, Hungary, Volume I, page 81, 1980.

Hicks, B.B., R.L. Drinkrow, and G. Grauze, "Drag and Bulk Transfer Coefficients Associated with a Shallow Water Surface," Boundary Layer Meteorology, 6, 287, 1974.

Hinwood, J.B. and I.G. Wallis, "Classification of Models of Tidal Waters," ASCE, Journal of the Hydraulics Division, 101:HY10, 1313, October 1975.

Hollan, E. and T.J. Simons, "Wind-Induced Changes of Temperature and Currents in Lake Constance," Archiv für Meteorologie, Geophysik und Bioklimatologie, Series A, 27, 333, 1978.

Holley, E.R. and D.R.F. Harleman, "Dispersion of Pollutants in Estuary Type Flows," Report Number 74, Hydrodynamics Laboratory, Department of Civil Engineering, Massachusetts Institute of Technology, Cambridge, Massachusetts, January 1965.

Holley, E.R., D.R.F. Harleman and H.B. Fischer, "Dispersion in Homogeneous Estuary Flow," ASCE, Journal of the Hydraulics Division, 96:HY8, 1691, August 1970.

Holly, F.M., "Two-Dimensional Mass Dispersion in Rivers," Hydrology Paper Number 78, Colorado State University, Fort Collins, Colorado, September 1975.

Hornbeck, R.W., Numerical Methods, Quantum Publishers, New York, 1975.

Hsu, S.A., "Wind Stress on Nearshore and Lagoonal Waters of a Tropical Island," Limnology and Oceanography, 20:1, 113, January 1975.

Hutchinson, G.E., A Treatise on Limnology, Volume 1, Part 1 - Geography and Physics of Lakes, John Wiley and Sons, Inc., New York, 1975.

Jolánkai, G. and A. Szöllősi-Nagy, "A Simple Eutrophication Model for the Bay of Keszthely, Lake Balaton," Modelling the Water Quality of the Hydrologic Cycle Symposium, Baden, Austria, IAHS-AISH Publication Number 125, page 137, September 1978.

Jolánkai, G. and L. Somlyódy, "Nutrient Loading Estimate for Lake Balaton," Collaborative Paper CP-81-21, International Institute of Applied Systems Analysis, Laxenburg, Austria, April 1981.

Jørgensen, S.E., "A Eutrophication Model for a Lake," Ecological Modeling, 2:2, 147, June 1976.

Jørgensen, S.E., "Examination of a Lake Model," Ecological Modeling, 4:2, 253, 1978.

Jørgensen, S.E., L. Kamp-Nielson and O.S. Jacobsen, "A Submodel for Anaerobic Mud-Water Exchange of Phosphate," Ecological Modeling, 1:2, 133, July 1975.

Kenney, B.C., "Lake Surface Fluctuations and the Mass Flow Through the Narrows of Lake Winnipeg," Journal of Geophysical Research, 84:C3, 1225, March 20, 1979.

Kizlauskas, A.G. and P.L. Katz, "A Two-Layer Finite-Difference Model for Flows in Thermally Stratified Lake Michigan," Proceedings of the 16th Conference on Great Lakes Research, page 743, 1973.

Koutitas, C.G., "Numerical Solution of the Complete Equations for Nearly Horizontal Flows," Advances in Water Resources, 1:4, 213, 1978.

Kutas, T. and S. Herodek, "The BEM Modeling Approach III: Recent Results in Simulating the Balaton Ecosystem," Proceedings of the Second Joint MTA/IIASA Task Force Meeting on Lake Balaton Modeling, August 27-30, 1979, Veszprém, Hungary, edited by G. van Straten, S. Herodek, J. Fischer and I. Kovács, Hungarian Academy of Sciences, Veszprém, Hungary, Volume I, page 103, 1980.

Lam, D.C.L. and E. Halfon, "Model of Primary Production, including Circulation Influences in Lake Superior," Applied Mathematical Modelling, 2:1, 30, March 1978.

Lam, D.C.L. and T.J. Simons, "Numerical Computations of Advective and Diffusive Transports of Chloride in Lake Erie, 1970," Journal of the Fisheries Research Board of Canada, 33:3, 537, 1976.

Lean, D.R.S., "Movements of Phosphorus Between its Biologically Important Forms in Lake Water," Journal of the Fisheries Research Board of Canada, 30:10, 1525, 1973.

Lean, G.H. and T.J. Weare, "Modeling Two-Dimensional Circulating Flow," ASCE, Journal of the Hydraulics Division, 105:HY1, 17, January 1979.

Leendertse, J.J., "A Water-Quality Simulation Model for Well-Mixed Estuaries and Coastal Seas: Volume I, Principles of Computation," Memorandum RM-6230-RC, Rand Corporation, Santa Monica, California, February 1970.

Leendertse, J.J., "Digital Techniques: Finite Differences," in "Estuarine Modeling: An Assessment," edited by G.H. Ward and W.H. Espey, Report 16070 DZV 02/71, United States Environmental Protection Agency, February 1971.

Leonov, A. "Mathematical Modeling of Phosphorus Transformation in Relation to Eutrophication of Lake Balaton," Proceedings of the Second Joint MTA/IIASA Task Force Meeting on Lake Balaton Modeling, August 27-30, 1979, Veszprém, Hungary, edited by G. van Straten, S. Herodèk, J. Fischer and I. Kovács, Hungarian Academy of Sciences, Veszprém, Hungary, Volume I, page 111, 1980 a.

Leonov, A.V., "Mathematical Modeling of Phosphorus Transformation in the Lake Balaton Ecosystem," Working Paper WP-80-149, International Institute of Applied Systems Analysis, Laxenburg, Austria, October 1980 b.

Levenspeil, O. and K.B. Bischoff, "Patterns of Flow in Chemical Process Vessels," Advances in Chemical Engineering, edited by T.B. Drew, J.W. Hoopes, Jr. and T. Vermeulen, Academic Press, New York, Volume 4, page 95, 1963.

Lick, W., "Numerical Modeling of Lake Currents," Annual Review of Earth and Planetary Sciences, Volume 4, page 49, 1976.

Lien, S.L. and J.A. Hoopes, "Wind Driven, Steady Flows in Lake Superior," Limnology and Oceanography, 23:1, 91, January 1978.

Liggett, J.A., "Cell Method for Computing Lake Circulation," ASCE, Journal of the Hydraulics Division, 96:HY3, 725, March 1970.

Lijklema, L., "Sediment-Water Exchange Processes in (Shallow) Lakes," Proceedings of the Second Joint MTA/IIASA Task Force Meeting on Lake Balaton Modeling, August 27-30, 1979, Veszprém, Hungary, edited by G. van Straten, S. Herodek, J. Fischer and I. Kovács, Hungarian Academy of Sciences, Veszprém, Hungary, Volume II, page 13, 1980.

Lindijer, G.J.H., "Three-Dimensional Circulation Models for Shallow Lakes and Seas; General Formulation and Stationary Models," Report R 900-I, Delft Hydraulics Laboratory, Netherlands, July 1976.

Lindijer, G.J.H., "Three-Dimensional Circulation Models for Shallow Lakes and Seas; Semi-Analytical Steady State Analysis of Wind-Driven Current Including the Effect of a Depth-Dependent Turbulent Exchange Coefficient," Report R 900-II, Delft Hydraulics Laboratory, Netherlands, March 1979.

Liu, H. and H.J. Perez, "Wind-Induced Circulation in Shallow Water," ASCE, Journal of the Hydraulics Division, 97:HY7, 923, July 1971.

Madsen, O.S., "A Realistic Model of the Wind-Induced Ekman Boundary Layer," Journal of Physical Oceanography, 7:2, 248, March 1977.

McRoy, C.P., R.J. Barsdate and M. Nebert, "Phosphorus Cycling in an Eelgrass *(Zostera Marina L.)* Ecosystem," Limnology and Oceanography, 17:1, 58, January 1972.

Müller, G., "High-magnesian Calcite and Protodolomite in Lake Balaton (Hungary) Sediments," Nature, 226:5246, 749, May 23, 1970.

Müller, G., "Aragonite Precipitation in a Freshwater Lake," Nature Physical Science, 229:1, 18, January 4, 1971.

Murray, S.P., "Trajectories and Speeds of Wind-Driven Currents near the Coast," Journal of Physical Oceanography, 5:2, 347, April 1975.

Murthy, C.R. and A. Okubo, "Interpretation of Diffusion Characteristics of Oceans and Lakes Appropriate for Numerical Modeling," Symposium on Modeling of Transport Mechanisms in Ocean and Lakes, Manuscript Report Series Number 43, Marine Sciences Directorate, Department of Fisheries and Environment, Ottawa, Canada, page 129, 1977.

Murty, T.S. and D.B. Rao, "Wind-Generated Circulations in Lakes Erie, Huron, Michigan and Superior," Proceedings of the 16th Conference on Great Lakes Research, page 927, 1970.

Muszkalay, L., "La Mesure des Dénivellations Longitudinales et Transversales de la Nappe D'Eau du Lac Balaton," ("Measurement of Longitudinal and Transverse Water Surface Denivellations in Lake Balaton" - in French), Hydrology of Lakes and Reservoirs, Symposium of Garda, Volume 1, IAHS-AISH Publication Number 70, page 100, October 1966.

Muszkalay, L., "A Balaton Vizének Jellemző Mozgásai," ("Characteristic Water Motions in Lake Balaton" - in Hungarian), VITUKI (Research Center for Water Resources Development), Budapest, Hungary, 1973.

Najarian, T.O. and D.R.F. Harleman, "A Real Time Model of Nitrogen-Cycle Dynamics in an Estuarine System," Report Number 204, Ralph M. Parsons Laboratory for Water Resources and Hydrodynamics, Department of Civil Engineering, Massachusetts Institute of Technology, Cambridge, Massachusetts, July 1975.

Nelson, S.M., "Application of a Numerical Model for Three-Dimensional Sheared Flows," M.S. Thesis, Department of Civil Engineering, Massachusetts Institute of Technology, Cambridge, Massachusetts, September 1979.

Neumann, G. and W.J. Pierson, Principles of Physical Oceanography, Prentice-Hall Incorporated, Englewood Cliffs, New Jersey, 1966.

Orlob, G.T., "Mathematical Modeling of Surface Water Impoundments," Resource Management Associates, Inc., Lafayette, California, June 1977.

Otsuki, A. and R.G. Wetzel, "Coprecipitation of Phosphate with Carbonates in a Marl Lake," Limnology and Oceanography, 17:5, 763, September 1972.

Ottesen-Hansen, N.-E., "Effect of Wind Stress on Stratified Deep Lake," ASCE, Journal of the Hydraulics Division, 101:HY8, 1037, August 1975.

Parker, F.L., B.A. Benedict, and C. Tsai, "Evaluation of Mathematical Models for Temperature Prediction in Deep Reservoirs," Report EPA-660/3-75-038, United States Environmental Protection Agency, June 1975.

Paskausky, D.F., "Winter Circulations in Lake Ontario," Proceedings of the 14th Conference on Great Lakes Research, 593, 1971.

Paul, J.F., W.L. Richardson, A.B. Gorstko, and A.A. Matveyev, "Results of a Joint U.S.A./U.S.S.R. Hydrodynamic and Transport Modeling Project," Report EPA-600/3-79-015, United States Environmental Protection Agency, February 1979.

Plate, E.J., "Water Surface Velocities Induced by Wind Shear," ASCE, Journal of the Engineering Mechanics Division, 96:EM3, 295, June 1970.

Platzman, G.W., "The Dynamical Prediction of Wind Tides on Lake Erie," Meteorological Monographs, 4:26, September 1963.

Quinlan, A.V., "Design and Analysis of Mass Conservative Models of Ecodynamic Systems," Ph.D. Thesis, Department of Civil Engineering, Massachusetts Institute of Technology, Cambridge, Massachusetts, February 1975.

Richardson, W.L., "An Evaluation of the Transport Characteristics of Saginaw Bay Using a Mathematical Model of Chloride," in Modeling Biochemical Processes in Aquatic Ecosystems, edited by R.P. Canale, Ann Arbor Science Publishers, Inc., Ann Arbor, Michigan, 1976.

Ruggles, K.W., "The Vertical Mean Wind Profile Over the Ocean for Light to Moderate Winds," Journal of Applied Meteorology, 9:3, 389, June 1970.

Seki, H., M. Takahashi, Y. Hara and S. Ichimura, "Dynamics of Dissolved Oxygen During Algal Bloom in Lake Kasumigaura, Japan," Water Research, 14:2, 179, 1980.

Shanahan, P., D.R.F. Harleman and L. Somlyódy, "Modeling Wind-Driven Circulation in Lake Balaton," Collaborative Paper CP-81-7, International Institute of Applied Systems Analysis, Laxenburg, Austria, March 1981.

Shemdin, O.H., "Modeling of Wind Induced Current," Journal of Hydraulic Research, 11:3, 281, 1973.

Sheng, Y.P., W. Lick, R.T. Gedney and F.B. Molls, "Numerical Computation of Three-Dimensional Circulation in Lake Erie: A Comparison of a Free-Surface Model and a Rigid-Lid Model," Journal of Physical Oceanography, 8:4, 713, July 1978.

Sibul, O., "Laboratory Study of Wind Tides in Shallow Water," Technical Memorandum Number 61, Beach Erosion Board, United States Army Corps of Engineers, August 1955.

Simons, T.J., "Development of Numerical Models of Lake Ontario," Proceedings of the 14th Conference on Great Lakes Research, page 654, 1971.

Simons, T.J., "Development of Numerical Models of Lake Ontario: Part II," Proceedings of the 15th Conference on Great Lakes Research, page 655, 1972.

Simons, T.J., "Analysis and Simulation of Spatial Variations of Physical and Biochemical Processes in Lake Ontario," Journal of Great Lakes Research, 2:2, 215, December 1976.

Simons, T.J., "Hydrodynamic Models of Lakes and Shallow Seas," Unpublished Draft Report, Canada Centre for Inland Waters, Burlington, Ontario, Canada, February 1979.

Simons, T.J. and D.C.L. Lam, "Some Limitations of Water Quality Models for Large Lakes: A Case Study of Lake Ontario," Water Resources Research, 16:1, 105, February 1980.

Somlyódy, L., "Hydrodynamical Aspects of the Eutrophication Modeling in the Case of Lake Balaton," Collaborative Paper CP-79-1, International Institute for Applied Systems Analysis, Laxenburg, Austria, February 1979.

Somlyódy, L., "Preliminary Study of Wind Induced Interaction Between Water and Sediment for Lake Balaton (Szemes Basin)," Proceedings of the Second Joint MTA/IIASA Task Force Meeting on Lake Balaton Modeling, August 27-30, 1979, Veszprém, Hungary, edited by G. van Straten, S. Herodek, J. Fischer and I. Kovács, Hungarian Academy of Sciences, Veszprém, Hungary, Volume II, page 26, 1980.

Stefan, H.G. and A.C. Demetracopoulos, "Cells-In-Series Simulation of Riverine Transport," ASCE, Journal of the Hydraulics Division, 107:HY6, 675, June 1981.

Stolzenbach, K.D., O.S. Madsen, E.E. Adams, A.M. Pollack and C.K. Cooper, "A Review and Evaluation of Basic Techniques for Predicting the Behavior of Surface Oil Slicks," Report Number 222, Ralph M. Parsons Laboratory for Water Resources and Hydrodynamics, Massachusetts Institute of Technology, Cambridge, Massachusetts, February 1977.

Stone, H.L. and P.L.T. Brian, "Numerical Solution of Convective Transport Problems," Journal of the American Institute of Chemical Engineers, 9:5, 681, September 1963.

Stumm, W. and J.J. Morgan, Aquatic Chemistry: An Introduction Emphasizing Chemical Equilibrium in Natural Waters, Wiley-Interscience, New York, 1970.

Stumm, W. and E. Stumm-Zollinger, "The Role of Phosphorus in Eutrophication," in Water Pollution Microbiology, edited by R. Mitchell, Wiley-Interscience, New York, 1972.

Su, C.-L., J.H. Pohl and G. Shih, "Wind-Driven Circulations in Lake Okeechobee," Finite Elements in Water Resources, Proceedings of the First International Conference on Finite Elements in Water Resources held at Princeton University, edited by W.G. Gray, G.F. Pinder and C.A. Brebbia, Pentech Press, London, page 4.113, July 1976.

Sundermann, J. "Numerical Modeling of Circulation in Lakes," Hydrodynamics of Lakes, Proceedings of a Symposium 12-13 October, 1978, Lausanne, Switzerland, edited by W.H. Graf and C.H. Mortimer, Elsevier Scientific Publishing Company, New York, page 1, 1979.

Thomann, R.V., Systems Analysis and Water Quality Management, McGraw-Hill Book Company, New York, 1972.

Thomann, R.V., D.M. DiToro, R.P. Winfield and D.J. O'Connor, "Mathematical Modeling of Phytoplankton in Lake Ontario: 1. Model Development and Verification," Report EPA-660/3-75-005, United States Environmental Protection Agency, March 1975.

Thomann, R.V., R.P. Winfield and J.J. Segna, "Verification Analysis of Lake Ontario and Rochester Embayment Three Dimensional Eutrophication Models," Report EPA-600/3-79-094, United States Environmental Protection Agency, August 1979.

Thomas, H.A. Jr. and J.E. McKee, "Longitudinal Mixing in Aeration Tanks," Sewage Works Journal, 16:1, 42, January 1944.

Thomas, J.H., "A Theory of Steady Wind-Driven Current in Shallow Water with Variable Eddy Viscosity," Journal of Physical Oceanography, 5:1, 136, January 1975.

Tóth, L., "Reeds Control Eutrophication of Balaton Lake," Water Research, 6:12, 1533, December 1972.

Tuan, V.A., N.C. Thanh and B.N. Lohani, "Hydraulic Model for Biological Reactors: Application to Activated Sludge," Journal Water Pollution Control Federation, 52:7, 1931, July 1980.

Van Dorn, W.G., "Wind Stress on an Artificial Pond," Journal of Marine Research, 12:3, 249, 1953.

van Straten, G., "Analysis of Model and Parameter Uncertainty in Simple Phytoplankton Models of Lake Balaton," Second ISEM Meeting, Liege, Belgium, April 1980. (Also published as Working Paper WP-80-139, International Institute of Applied Systems Analysis, Laxenburg, Austria, September 1980.)

van Straten, G., "Aspects of Nutrient Loading in Relation to Lake Balaton Eutrophication Modeling," paper delivered at Man and Biosphere, 5th Conference, Amsterdam, May 11-14, 1981.

van Straten, G., G. Jolánkai and S. Herodek, "Review and Evaluation of Research on the Eutrophication of Lake Balaton -- A Background Report for Modelling," Collaborative Paper CP-79-13, International Institute for Applied Systems Analysis, Laxenburg, Austria, August 1979.

van Straten, G. and L. Somlyódy, "Lake Balaton Eutrophication Study: Present Status and Future Program," Working Paper WP-80-187, International Institute for Applied Systems Analysis, Laxenburg, Austria, December 1980.

Verboom, G.K., "The Advection-Dispersion Equation for an An-Isotropic Medium Solved by Fractional-Step Methods," in Mathematical Models for Environmental Problems, edited by C.A. Brebbia, John Wiley and Sons, 1976.

Verboom, G.K. and C.B. Vreugdenhil, "Basic Aspects of Mathematical Models," Chapter 9 in European Course on Heat Disposal from Power Generation in the Water Environment, Delft Hydraulics Laboratory, Delft, The Netherlands, June 23-27, 1975.

Wallsten, M., "Effects of Growth of *Elodea Canadensis* Michx. in a Shallow Lake (Lake Tämnaren, Sweden)," in Shallow Lakes: Contributions to their Limnology, Developments in Hydrobiology, Volume 3, edited by M. Dokulil, H. Metz and D. Jewson, Dr. W. Junk Publishers b.v., The Hague, 1980.

Wang, M.-P., "The Hydrothermal-Biochemical Coupling of Lake Eutrophication Models," Sc.D. Thesis, Department of Civil Engineering, Massachusetts Institute of Technology, Cambridge, Massachusetts, September 1980.

Wetzel, R.G., Limnology, W.B. Saunders Company, Philadelphia, 1975.

Wilson, B.W., "Note on Surface Wind Stress over Water at Low and High Wind Speeds," Journal of Geophysical Research, 65:10, 3377, October 1960.

Witten, A.J. and J.H. Thomas, "Steady Wind-Driven Currents in a Large Lake with Depth-Dependent Eddy Viscosity," Journal of Physical Oceanography, 6:1, 85, January 1976.

Wu, J. "Wind Stress and Surface Roughness at Air-Sea Interface," Journal of Geophysical Research, 74:2, 444, January 15, 1969.

Zvirin, Y. and R. Shinnar, "A Comparison of Lumped-Parameter and Diffusional Models Describing the Effects of the Outlet Boundary Conditions on the Mixing in Flow Systems," Water Research, 10:9, 765, 1976.